

**HYDROTHERMAL ALTERATION CHARACTERIZATION
AND STABLE ISOTOPE GEOCHEMISTRY AS VECTORS
TOWARDS ORE NEAR STOCKTON, UTAH**

by
Stephanie M. Murillo Maikut

Submitted as partial fulfillment of the
Requirements for the Degree of
Master of Science in Geology
February 22, 2008.

Department of Earth and Environmental Science
New Mexico Institute of Mining and Technology
Socorro, NM

ABSTRACT

The Stockton Mining District, Utah, an area of current mineral exploration shares many geological characteristics with the nearby Bingham Canyon Porphyry Cu-Au-Mo Deposit. Stable isotopes, petrographic analysis and fluid inclusions are used in this study to guide exploration and to aid in a better understanding of the area.

Fluids play a major role in the formation of ore deposits of hydrothermal origin, not only do they cause mineral deposits but they also cause mineralogical and isotopic changes in the host rocks. This change depends on temperature and on the chemical composition of both the host rocks and the fluids circulating through them. Areas with the highest fluid flow (higher water/rock ratio) feature rocks with the largest isotopic shift from their original values. Stable isotopes can be used to map "cryptic" alteration, helping to determine areas altered by fluids even though this alteration may not be visible in hand specimens or thin sections and this enables stable isotopes to be used as an exploration tool in mineralized areas.

Hydrothermal alteration in the analyzed samples seems to be strongly controlled by lithology; the main alteration assemblage in igneous rocks is K-silicate constructive, characterized by the presence of hydrothermal biotite. This alteration usually has an incipient to weak phyllic overprint. Sedimentary rocks have been mainly altered to quartz, carbonate and calc-silicate minerals, which include diopside, actinolite, tremolite, garnet, epidote and zoisite. Hydrothermal magnetite, indicating early hydrothermal

alteration is present in igneous rocks from drill holes SD-16, SD-21 and SD-22 where it is spatially associated to hydrothermal biotite, and in sedimentary rocks from drill holes SD-14 and SD-23; where calc-silicate minerals occur.

Carbon ($\delta^{13}\text{C}$) and oxygen ($\delta^{18}\text{O}$) stable isotopes were analyzed on limestones from Stockton, to determine how stable isotopes vary locally around mineralized zones. A total of 150 samples were collected across two spatial scales encompassing both district wide variations and local variations around individual mineralized bodies. Thin calcite veins are very common in these limestones; in some cases these veins were thick enough to allow them to be sampled and they were analyzed separately from the rock samples.

The sampled limestones have $\delta^{18}\text{O}$ values that vary from 1.7 to 26.1 ‰. Limestone $\delta^{13}\text{C}$ values range from -10.9 to 5‰. The veins are usually lighter than their host rock suggesting that they are of diagenetic. Two trends are seen in the isotopic composition of the limestones, including both altered and unaltered values. We believe that at least two processes are needed to account for the distribution seen in the data. Possible processes are: hydrothermal alteration (accounting for the low oxygen values) and contact metamorphism (which could be responsible for the low carbon values.). Both carbon and oxygen show regional isotopic patterns.

A preliminary fluid inclusion study demonstrated that brine fluids are present in samples from drill holes SD SD-16, SD-21 and SD-23, and in one outcrop sample. Opaque daughters are present in inclusions from all samples, except the one collected at surface; some of these have triangular shapes, which are characteristic of chalcopyrite, suggesting the presence of fluids with a high copper content. Microthermometric studies

are needed to better understand the fluid inclusions present in the igneous and sedimentary rocks of the Stockton area.

Overall the Stockton prospect area has many lithological and alteration characteristics common of porphyry Cu deposits, these include a strong K-silicate constructive alteration with a phyllic overprint, and the presence halite daughter minerals within fluid inclusions.

ACKNOWLEDGMENTS

I would like to thank Kennecott Exploration, especially Dave Andrews and Joey Wilkins for this thesis project, which was a great experience. Joey I learned a lot from you and had a really great time out in the field mapping and sampling.

I would like to acknowledge the Don Yardley Fellowship in Economic Geology.

Thanks to Andrew Campbell and Bill Chavez, for being excellent professors and advisors, I really enjoyed all your classes, and hope some day I can be half as good a professor as you both are. Thanks to my other committee member Dave Norman, for his insight, I really enjoyed the trip to Mexico.

I would like to thank all the friends I made here in Socorro, thanks for making Socorro fun and for putting up with me for two whole years, I will miss you.

Thanks to the University of Costa Rica for having a job for me when I return back home, I really wish to go home and pass on what I have learned to the new generations of geologists.

Thanks to my parents, Andrea Maikut and Miguel Angel Murillo Monge, and the rest of my family back home in Costa Rica for being supportive and for encouraging me to follow my dreams. I love you all.

Finally I would like to thank my boyfriend, Douglas, for his support, for insisting that I follow my dreams and for being patient and waiting for me for two years; I could not have done this without you.

TABLE OF CONTENTS

	Page
TITLE PAGE	i
ABSTRACT	
ACKNOWLEDGMENTS	ii
LIST OF TABLES	vi
LIST OF FIGURES	vii
LIST OF PHOTOS	x
LIST OF ABBREVIATIONS	xiii
LIST OF APPENDICES	xiv
INTRODUCTION	1
Present study	1
Location	2
BACKGROUND	3
Geology	3
Mining History	4
METHODS	7
Petrographic analysis methodology	7
Stable isotopes methodology	9

Fluid inclusion methodology	11
RESULTS	14
Petrography	14
Drill hole samples	14
Field samples	36
Stable isotopes	39
Veins	40
Rocks	41
Petrographic analysis of isotope samples	47
Transects	51
Spatial distribution	60
Fluid Inclusions	63
Comparison to Bingham	69
STABLE ISOTOPES: A VECTOR TOWARDS ORE	72
Brief overview of other studies done on hydrothermal systems	73
Carlin-Type gold deposits	73
Skarn deposits	74
DISCUSSION AND CONCLUSIONS	77
Petrography analysis and comparison to Bingham	77
Rock types	77
Alteration	77
Sulfides	80
Stable isotopes	82

Fluid inclusions	84
Hydrothermal alteration and sulfide zonation based on petrographic analysis	85
Exploration conclusions	86
REFERENCES	88
APPENDIX A: Petrography of drill core samples	92
APPENDIX B: Petrography of field samples	161
APPENDIX C: Limestone descriptions	165
APPENDIX D: Fluid inclusion descriptions	172
APPENDIX E: Stable isotope data	185

LIST OF TABLES

	Page
Table 1: Values of $\delta^{18}\text{O}$ and $\delta^{13}\text{C}$ obtained for duplicate samples using different sample sizes.	12
Table 2: Stable isotope samples selected for petrography analysis.	47

LIST OF FIGURES

	Page
Figure 1: Location of the study area.	2
Figure 2: Stratigraphic column, taken from Hintze (1988). Thicknesses are given in feet.	5
Figure 3: Sampled drill holes. (Drill holes STK-034 and 04RDYR01 are located south of this area).	8
Figure 4: Calcite veins cutting limestones.	10
Figure 5: Location of drill holes sampled for fluid inclusions and location of sample SM-23/05/06-8 collected at the surface.	13
Figure 6: South-north transect, includes drill holes SD-14, SD-23, SD-16 and SD-21.	34
Figure 7: East-west transect, includes drill holes SD-22, SD-16, SD-15 and SD-26.	35
Figure 8: $\delta^{13}\text{C}$ vs. $\delta^{18}\text{O}$ diagram. Includes all the analyzed samples (vein samples are shown as triangles and rock samples are shown as squares)	40
Figure 9: $\delta^{13}\text{C}$ vs. $\delta^{18}\text{O}$ diagram. Compares calcite veins to their host rocks.	41
Figure 10: $\delta^{13}\text{C}$ vs. $\delta^{18}\text{O}$ diagram. Isotope values divided into three main groups.	42
Figure 11: $\delta^{13}\text{C}$ vs. $\delta^{18}\text{O}$ diagram. Compares luminescent (CL) calcite with nonluminescent (NL). Oxygen and carbon isotope values are given relative to PDB (Grossman, et al., 1993).	43
Figure 12: $\delta^{13}\text{C}$ vs. $\delta^{18}\text{O}$ diagram. Red box represents the luminescent or diagenetically altered samples from figure 11.	44

Figure 13: $\delta^{13}\text{C}$ vs. $\delta^{18}\text{O}$ diagram. The two red lines show the two main hypothesized paths to explain the trends in the data. A: hydrothermal alteration. B: decarbonation by contact metamorphism.	45
Figure 14: $\delta^{13}\text{C}$ vs. $\delta^{18}\text{O}$ diagram. A: batch volatilization. B: rayleigh volatilization. Modified after Valley (1986).	46
Figure 15: Transects sampled around the mines: Bullion, Galena King, Ben Harrison, Prize, Argent and Calumet.	52
Figure 16: $\delta^{13}\text{C}$ vs. $\delta^{18}\text{O}$ diagram. Each transect is highlighted in a different color.	53
Figure 17: A: Distance vs. $\delta^{13}\text{C}$. B: Distance vs. $\delta^{18}\text{O}$ diagrams. Transect near the Calumet mine.	54
Figure 18: A: Distance vs. $\delta^{13}\text{C}$. B: Distance vs. $\delta^{18}\text{O}$ diagrams. Transect near the Calumet mine.	55
Figure 19: A: Distance vs. $\delta^{13}\text{C}$. B: Distance vs. $\delta^{18}\text{O}$ diagrams. Argent Mine Transect.	56
Figure 20: A: Distance vs. $\delta^{13}\text{C}$. B: Distance vs. $\delta^{18}\text{O}$ diagrams. Ben Harrison Mine Transect.	57
Figure 21: A: Distance vs. $\delta^{13}\text{C}$. B: Distance vs. $\delta^{18}\text{O}$ diagrams. Galena King Mine Transect.	58
Figure 22: A: Distance vs. $\delta^{13}\text{C}$. B: Distance vs. $\delta^{18}\text{O}$ diagrams. Prize Mine Transect.	59
Figure 23: Map showing some major structures in the area and the sampled transects.	61
Figure 24: Regional isotopic pattern.	62
Figure 25: Location of fluid inclusion samples in the alteration profile. Fluid inclusion samples are highlighted in green.	70
Figure 26: Fluid inclusion study done in quartz veins present in the QMP orebody of the Bingham Canyon deposit (Redmond, et al., 2004).	71

Figure 27: Sample location and oxygen isotope data from carbonate rocks.
Heavy line represents the pit outline
(After Arehart & Donelick, 2006). 74

Figure 28: Sample location and carbon isotope data from carbonate rocks.
Heavy line represents the pit outline
(After Arehart & Donelick, 2006). 75

LIST OF PHOTOS

	Page
Photo 1: Altered hornblende, sample SD-21-1581 ft. (f.o.v. = 1.8 mm long).	16
Photo 2: Sphene, sample SD-23-2270.5 ft. (f.o.v. = 0.9 mm long).	16
Photo 3: Volcanic rock with abundant plagioclase phenocrysts from sample 04RDYR01-1896.5 ft. (f.o.v. = 1.8 mm long).	18
Photo 4: Hydrothermal biotite replacing magmatic biotite in sample SD-16-2629 ft. (f.o.v. = 0.9 mm long).	20
Photo 5: Biotite (brown) replacing hornblende (green), sample SD-21-1592.5 ft. (f.o.v. = 0.9 mm long).	20
Photo 6: Parallel magnetite veins, sample SD-22-1270 ft. (f.o.v. = 1.8 mm long).	21
Photo 7: Magnetite being replaced by specular hematite (blue), sample SD-21-1961.5 ft. (f.o.v. = 0.225 mm long).	21
Photo 8: White phyllosilicates altering biotite, sample SD-16-2185 ft. (f.o.v. = 1.8 mm long).	22
Photo 9: Bladed muscovite replacing biotite, sample SD-22-1321 ft. (f.o.v. = 0.45 mm long).	23
Photo 10: Biotite being altered to chlorite, sample SD-16-2629 ft. (f.o.v. = 0.9 mm long).	24
Photo 11: Cinnamon rutile associated with biotite, sample SD-16-2629 ft. (f.o.v. = 0.9 mm long).	24
Photo 12: Cinnamon rutile with chalcopyrite, sample SD-21-660.5 ft. (f.o.v. = 0.45 mm long).	25

Photo 13: Mafic mineral replaced by fibrous amphibole (actinolite), sample SD-21-490 ft. (f.o.v. = 0.9 mm long).	26
Photo 14: K-feldspar showing alteration to epidote and carbonate, sample SD-21-490 ft. (f.o.v. = 1.8 mm long).	26
Photo 15: Magnetite replacing specular hematite, sample SD-23-1556 ft. (f.o.v. = 0.45 mm long).	28
Photo 16: Chalcopyrite surrounding pyrite, and magnetite surrounding chalcopyrite, sample SD-23-1556 ft. (f.o.v. = 0.45 mm long).	28
Photo 17: Cluster of hydrothermal biotite and pyrite, sample SD-21-660.5 ft. (f.o.v. = 0.9 mm long).	30
Photo 18: Chalcopyrite surrounding muscovite; sample SD-23-1466 ft. (f.o.v. = 0.45 mm long).	31
Photo 19: Chalcopyrite surrounding pyrite; sample SD-22-1321 ft. (f.o.v. = 0.45 mm long).	32
Photo 20: Bornite together with chalcopyrite, sample SD-31-1760 ft. (f.o.v. = 0.225 mm long).	32
Photo 21: Chalcocite replacing chalcopyrite, sample SD-23-1556 ft. (f.o.v. = 0.45 mm long).	33
Photo 22: Marcasite surrounding chalcopyrite, sample SD-14-1346 ft. (f.o.v. = 0.45 mm long).	33
Photo 23: Hornblende replacing a clinopyroxene, sample SM-15/06/06-4 (f.o.v. = 0.9 mm long).	37
Photo 24: Diopside skarn. (f.o.v. = 0.9 mm long).	49
Photo 25: Tremolite (?) replaced by calcite and fine grain silica. (f.o.v. = 0.9 mm long).	49
Photo 26: Garnet skarn cut by calcite and quartz veins (f.o.v. = 1.8 mm long).	50
Photo 27: Possible crinoid has been replaced by chert (f.o.v. = 1.8 mm long).	50
Photo 28: Liquid + vapor + two salts (halite and sylvite), occurs together with vapor-rich fluid inclusions, sample SD-21-2130.5 ft.	64

Photo 29: Liquid + vapor + two daughters (possibly halite and sylvite), sample SM-23/05/06-8.	65
Photo 30: Liquid + vapor + two salts (halite and sylvite) + opaque daughter, sample SD-23-1448 ft.	66
Photo 31: Liquid + vapor + multiple daughters, sample SD-16-1103 ft. Opaque daughter has a triangular shape.	66
Photo 32: Liquid + vapor + multiple daughters, sample SD-13-1448 ft.	67
Photo 33: Vapor-rich with euhedral inclusion, sample SD-21-2130.5 ft.	67
Photo 34: Vapor-rich inclusion with halite daughter, sample SD-23-1448 ft.	68
Photo 35: Vapor-rich with a dark daughter, sample SD-21-2130.5 ft.	68
Photo 36: Vapor-rich fluid inclusion + halite + opaque daughter, sample SD-21-1633 ft.	69

LIST OF ABBREVIATIONS

br: bornite

co: covellite

dg: digenite

f.o.v: field of view

marc: marcasite

mo: molybdenite

po: pyrrhotite

tetra: tetrahedrite

Tr: trace

ND: not determined

NA: non applicable

LIST OF APPENDICES

	Page
Appendix A: PETROGAPHY OF DRILL CORE SAMPLES	92
Appendix B: PETROGRAPHY OF FIELD SAMPLES	161
Appendix C: LIMESTONE DESCRIPTIONS	165
Appendix D: FLUID INCLUSION DESCRIPTIONS	172
Appendix E: STABLE ISOTOPE DATA	185

This Thesis is accepted on behalf of the faculty
of the Institute by the following committee:

Andrew Currell 2/21/08
Academic Adviser

Research Advisor

William X. King 21 February, 2008
Committee Member

David L. Norman 22 Feb, 2008
Committee Member

Committee Member

Date

I release this document to New Mexico Institute of Mining and Technology

[Signature]
Students Signature

22 Feb 2008

Date

INTRODUCTION

Present study

This study forms part of an exploration campaign taking place in the Stockton area, Utah, by Rio Tinto. Petrographic and geochemical exploration techniques will be used to aid in the exploration and to help direct drilling in the area.

One of the main attractions that lead to the continued interest in exploration in this area, are the similarities it shares with Bingham Canyon, which is the richest mining district in Utah (Stokes, 1986). Another detail that brought attention to this area was the existence of numerous old workings, demonstrating a continuous interest. The prospect area is relatively close to the Bingham Canyon Porphyry. These two areas share many lithological characteristics, including similar ages for the intrusions.

The oldest igneous phase in the Bingham mine area, corresponds to an equigranular monzonite phase intruded at 39.8 ± 0.4 Ma. It is believed that mineralization started after the emplacement of this intrusion and is related to the formation of the quartz monzonite porphyry. However the date of the quartz monzonite porphyry can not be determined due to strong hydrothermal alteration. Copper mineralization probably ended before the intrusion of the quartz latite porphyry plugs which are located in the central pit, at 38.8 ± 0.3 Ma (Warnaars, et al., 1978). A quartz monzonite porphyry in the Stockton area has been dated at 39.4 ± 0.26 Ma ((Davies, 1996), which falls within the range of the Bingham mine igneous rocks.

The present study will encompass an oxygen and carbon stable isotope analysis of carbonate rocks, as well as the examination of carefully selected petrographic samples and fluid inclusion samples. Stable isotopes and alteration analysis of petrographic

samples will be used as vector toward ore and to better understand the prospect. A brief fluid inclusion study will help to determine the presence of porphyry like fluids and to compare the results to fluid inclusion studies done in the Bingham porphyry system.

Location

The study area is located southwest of Salt Lake City, Utah, approximately 13 miles southwest from the Bingham Canyon Cu-Mo-Au Porphyry (Figure 1). Both Bingham and the prospect area form part of the Oquirrh Mountain Range (Davies, 1996).

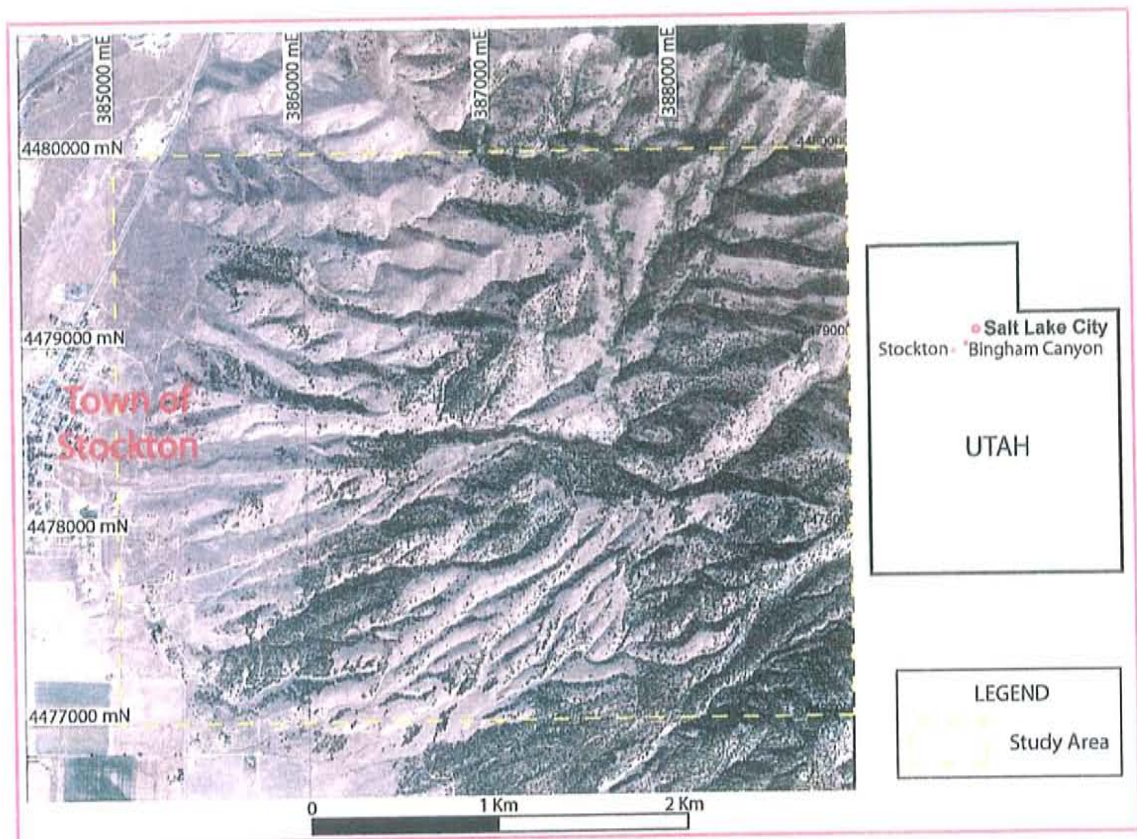


Figure 1: Location of the study area.

BACKGROUND

Geology

Most of the Oquirrh Mountains are composed of Pennsylvanian age marine strata that form part of the Oquirrh Group (Figure 2)(Hintze, 1988). The Oquirrh group is the thickest stratigraphic unit in the Oquirrh Mountains; it is composed of intercalated limestones and sandstones (or quartzites). Few quartzites are present at the base, these become more abundant and thicker towards the top. Silica cemented sandstones are more abundant than lime cemented sandstones (Gilluly, 1932).

Intrusive and extrusive igneous rocks are present in the Stockton area. Intrusive rocks are the most abundant; these are mainly quartz monzonite porphyries and include many dikes, sills and small stocks. Most of these seem to have intruded along earlier north trending faults (Gilluly, 1932).

The intrusive rocks are of Oligocene Age. A K-feldspar phenocryst from a quartz monzonite porphyry, taken from drill hole SD-16 at a depth of 2550 ft, was dated at 39.4 ± 0.26 Ma using the Ar^{40}/Ar^{39} method (Davies, 1996).

Quaternary deposits occupy a large area of the Stockton quadrangle, these include: alluvium, talus deposits, glacial moraines and sediments from Lake Bonneville (Gilluly, 1932).

Structure

The geologic structure of the Oquirrh Range is similar to others in the Basin and Range Province. Strata has been folded and later cut by normal faults (Gilluly, 1932).

The Stockton area is cut by many faults; these are considered of "economic importance" because of their close association to mineralization. Two main systems

occur, with at least two periods of faulting in each one. The most important system economically speaking has faults that strike mainly N 10°-30° E, this system is known as the north-south system by previous authors (Gilluly, 1932). The second system closely follows the attitude of the sedimentary rocks in the area; faults strike close to east and dip north. Evidence suggests that the east-west fault system was the first one to form (Gilluly, 1932).

Sedimentary rocks in the area strike mainly west-northwest and dip north-northeast, except for in the area of the Ben Harrison mine where they go from vertical to slightly overturned (Davies, 1996).

Mining History

The Oquirrh Mountains have been of interest to miners since the 1800's. Gold was first discovered in Bingham Canyon in 1863 (Stokes, 1988). The Stockton mining district, also known as Rush Valley was formed in June 12, 1864. It originally formed part of the West Mountain Bingham District (Gilluly, 1932). Most of the exploited lead-silver-zinc-copper deposits in the Stockton quadrangle correspond to bedded replacement bodies. There seems to be both lithological and structural control because most deposits are located at the intersection between fissures and favorable beds (Gilluly, 1932).

Old mine workings and prospects are abundant in the area; these include adits, shafts and dumps. The main ore minerals found in the dumps left by these past activities are galena and sphalerite. Copper sulfides and oxides are also sometimes present. Mineralized bodies include mantos, mentioned above, and veins; the first follow stratigraphy and the veins cut through it, mainly with a north south orientation, following existing structures.

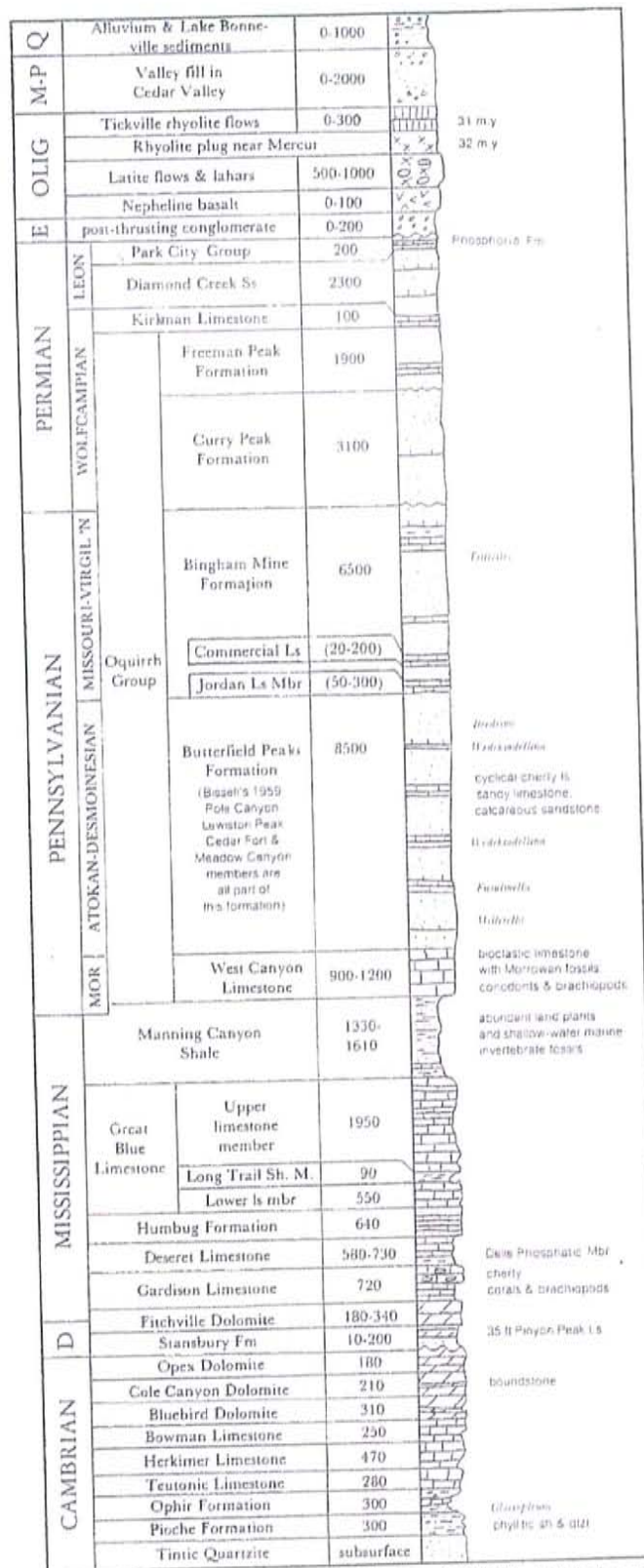


Figure 2: Stratigraphic column, taken from Hintze (1988). Thicknesses are given in feet.

Hypogene minerals that are the most abundant in these bedded deposits are: galena, sphalerite, chalcopyrite, microscopic argentite, tennantite, pyrite and pyrrhotite. Oxidation minerals include: cerussite, plumbo-jarosite, anglesite, jarosite, "limonite", aurichalcite, smithsonite, clamine, hydrozincite, malachite, azurite, pyrolite, psilomelane, and wad. There was little migration of the metals during the oxidation of the sulfides, which is expected due to the abundance of carbonate present in the wall-rocks (Gilluly, 1932).

Typical ore from Stockton was 6-20% lead, 2-12% zinc and 2-8 ounces of silver (Gilluly, 1932). Through 1927 production was divided among: lead (75%), silver (16%), zinc (5%), gold (3%) and copper (1%) (Moore, et al., 1966).

METHODS

Petrographic Analysis Methodology

Petrography samples were collected from drill holes and outcrops to characterize the types and spatial variation of rock types, alteration assemblages and mineral associations. Depending on the mineralogic characteristics of the rock and on the abundance of opaque minerals, either a thin section or a polished thin section was prepared, and one sample was made into a polished slab. Together these total 61 samples, of which 49 were taken from drill core and 12 were collected from outcrops. Most of the outcrop samples fall within the location figure shown in figure 1, but there are two samples (SM-15/06/06-4 and SM-15/06/06-5) which are located approximately 1.2 Km to the east of this area, the coordinates of these samples are 386287mE / 4478715mN and 386846mE / 4478816mN respectively.

Polished thin sections were prepared by Quality Thin Section in Tucson, Arizona; thin sections were prepared by Thomas Parkhill in Albuquerque, New Mexico and the polished slab was made at the New Mexico Institute of Mining and Technology.

Sampling of drill holes was mainly done on two major transects (Figure 3) one with north-south orientation and the other with east-west orientation. The north-south transect comprises drill holes SD-21, SD-16, SD-23 and SD-14, and the east-west transect comprises holes SD-22, SD-16, SD-15 and SD-26. Other drill holes outside of these transects were also sampled, these are: SD-18, SD-19, SD-31, STK-034 and 04RDYR01. The last two drill holes are located south of the area shown in figure 3. Two drill hole samples (one from SD-14 and one from SD-15) were also analyzed for oxygen and carbon stable isotopes.

Drill hole sample descriptions are found in appendix A and include: rock type or protolith, alteration minerals and assemblage, vein types and ore minerals; if possible, the paragenetic sequence of mineral formation was also ascertained. Outcrop sample descriptions are found in appendices B and C. Pictures and sketches to illustrate important observations are shown in appendixes A, B and C.

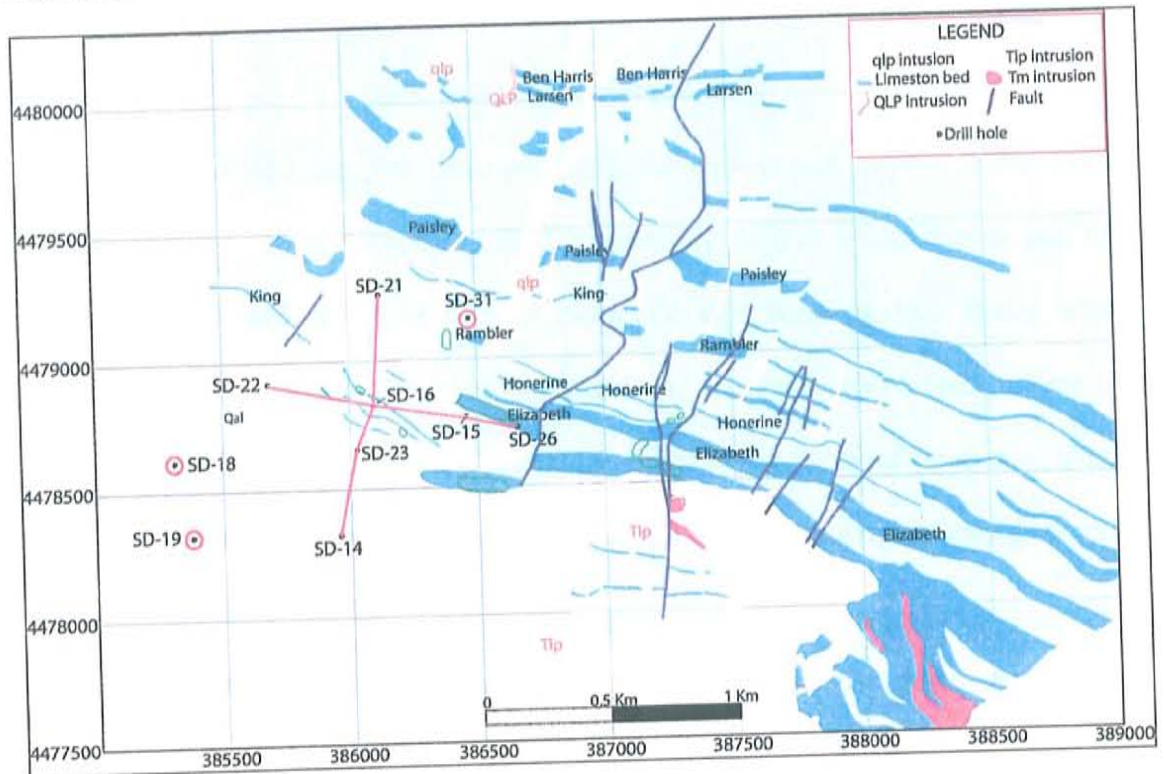


Figure 3: Sampled drill holes. (Drill holes STK-034 and 04RDYR01 are located south of this area).

Outcrop samples include intrusive and sedimentary rocks; the first were collected to compare the hydrothermal alteration signatures at topographically higher elevations with alteration observed from the drill hole samples at depth.

Most of the outcrop sedimentary rocks were sampled for oxygen and carbon stable isotope analyses (Appendix C); of these, samples that were analyzed petrographically were carefully selected to encompass all the major differences; these

differences include white limestones, gray limestones, limestones cut by abundant calcite veins, limestones with scarce veins, coarse limestones and fine-grain limestones. The main reason for describing these samples was to have a detailed petrographic description of the rocks to help explain variations seen in the isotopic analyses. The remaining sedimentary rock sampled was collected from a dump rich in copper oxides; the purpose of this sample was to determine the host rock.

Stable Isotopes Methodology

A total of 150 samples were collected for carbon and oxygen stable isotope analyses; of these 148 correspond to field samples and two to core samples, one from drill hole SD-14 and one from SD-15. Sampling was done on two spatial scales; regionally to encompass district wide variations, and locally around known mineralized bodies to determine how the isotopic signature varies in the surrounding area of mantos or veins which are usually mineralized with lead and zinc; for example detailed sampling was done in the vicinity of the Argent Mine.

Most of the stable isotope samples correspond to limestones, which vary in color from dark gray to white and also vary in quartz content "sandy limestones" and grain size. Petrographic analysis shows that one of the "white limestones" is actually a chert, possibly a silicified limestone. The sample from drill hole SD-14 corresponds to a garnet skarn which has recrystallized carbonate.

It is very common to find calcite veins cutting the limestones (Figure 4), with most veins usually very narrow (sub-millimeter scale); although in some cases they are wide enough to provide samples that were analyzed separately from their host rock. This was done for a total of 14 veins. Vein density was determined for each outcrop in which

an isotope sample was collected; and was done by counting how many veins intersected a meter-long line.

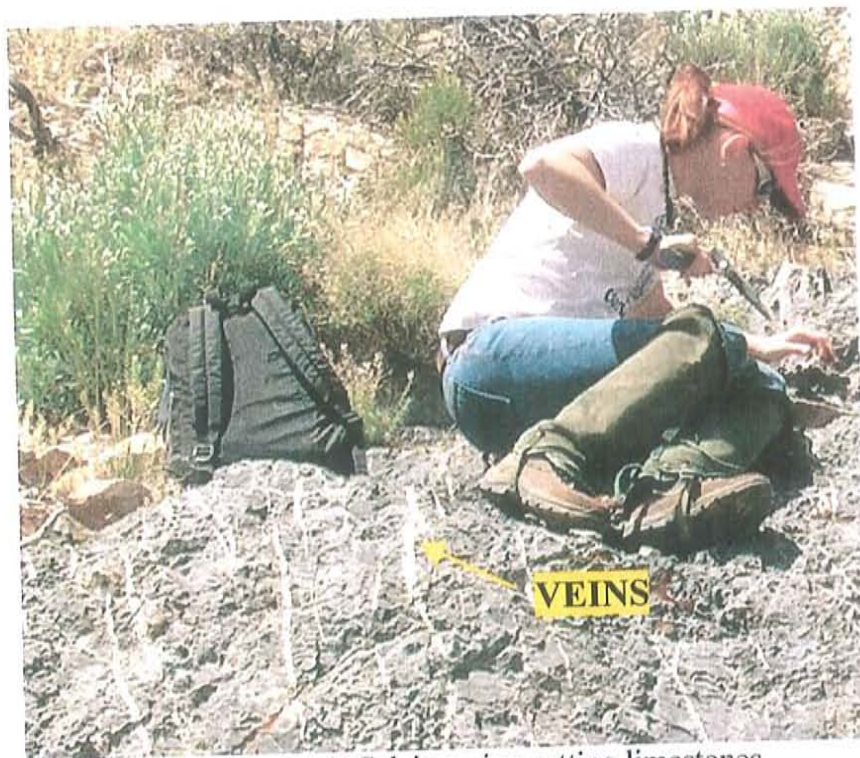


Figure 4: Calcite veins cutting limestones.

Because only a very small amount of sample is needed when analyzing for carbon and oxygen isotopes, samples were collected by hand drilling each rock. Some samples had very noticeable heterogeneities, such as patches with different colors or crystallinity; in these cases, both areas were drilled and analyzed separately to determine whether visible differences also yielded differences in isotopic composition.

Samples were analyzed in continuous flow mode with gas bench in a Finnigan MAT Delta Plus XP with an autosampler. Analysis was done using the standard technique of acidification with 100% phosphoric acid. The reaction between the phosphoric acid and the carbonate took place at a constant temperature of 45°C and each sample was left to react for more than three hours. Mineral standards were run with

every batch of samples and were used to calibrate the data. Values of $\delta^{18}\text{O}$ are presented relative to SMOW, and values of $\delta^{13}\text{C}$ are relative to PDB.

Different weights of the same samples were analyzed to determine whether the amount of sample would have an effect on the measured isotopic value; however, it was found that generally the amount of sample does not affect the values obtained. Values of $\delta^{18}\text{O}$ and $\delta^{13}\text{C}$ for the same samples using approximately 0.5 mg and approximately 0.2 mg are shown in table 1. Every run done after this used approximately 0.2 mg of sample under the assumption that the samples were 100% carbonate. In a few cases samples with low yields, due to impurities, were re-run using a larger amount of sample.

Duplicates of samples were done to check precision; showing that 19 out of 23 duplicates have values that vary from each other from 0.0‰ to 0.4‰ and have an average difference of 0.2‰ for $\delta^{18}\text{O}$ and $\delta^{13}\text{C}$ combined.

Fluid Inclusion Methodology

Fluid inclusion samples were collected from three selected drill holes and one outcrop. Drill hole samples total seven, five of these are from drill hole SD-21, one is from SD-16 and one from SD-23 (Figure 5). The location of the sample taken at surface is shown in figure 5.

When collecting these samples, one of the main factors taken into consideration was the presence of quartz, preferably of secondary origin, which usually occurs in veins, this was done because fluid inclusions, if present, are more easily observed in clear minerals, such as quartz. If the quartz being analyzed is an alteration mineral of secondary origin, it means that the fluids that formed it are also secondary or "hydrothermal", and one of the main objectives of this part of the study is to document

the presence of “porphyry like fluids”. Thick sections for the analysis of these samples were prepared by Quality Thin Section in Tucson, Arizona. Detailed descriptions of fluid inclusions are found in Appendix D.

Sample	Weight (mg)	d13C/12C	d18O/16O	Weight (mg)	d13C/12C	d18O/16O
SM-27/05/06-8	0.46	1.5	20.3	0.21	1.4	20.0
SM-05/06/06-21	0.46	0.6	18.6	0.24	0.4	18.1
SM-27/05/06-16	0.53	4.2	24.4	0.17	4.2	24.8
SM-23/05/06-6 (B)	0.52	4.1	21.2	0.18	4.2	21.5
SM-14/06/06-11	0.5	1.7	16.1	0.24	1.5	16.4
SM-05/06/06-2 (VEIN)	0.5	3.1	24.6	0.22	3.1	24.0
SM-05/06/06-7	0.53	3.2	22.4	0.18	3.1	22.4
SM-05/06/06-7 (DUP)	0.5	3.2	22.0	0.22	2.9	22.0
SM-05/06/06-9	0.51	3.5	24.7	0.18	3.3	24.6
SM-29/05/06-6	0.47	1.5	19.5	0.19	1.4	19.5
SM-14/06/06-6	0.45	2.7	18.0	0.22	2.5	18.1
SM-27/05/06-13	0.53	3.7	21.0	0.18	3.6	20.8
SM-27/05/06-14	0.52	3.9	24.4	0.19	3.8	24.7
SM-27/05/06-15	0.5	4.7	24.9	0.2	4.5	25.4
SM-27/05/06-15 (DUP)	0.48	4.7	25.1	0.21	4.6	25.3
SM-27/05/06-18 (A)	0.48	3.3	21.4	0.2	3.1	21.3
SM-27/05/06-18 (B)	0.5	3.7	22.6	0.18	3.4	22.6
SM-27/05/06-4	0.56	2.3	13.0	0.22	2.3	13.4
SM-27/05/06-6	0.46	1.8	24.0	0.18	1.8	24.1
SM-27/05/06-7	0.52	2.0	25.1	0.22	2.0	25.5
SM-27/05/06-9	0.45	2.5	22.3	0.18	2.5	22.5
SM-27/05/06-10	0.55	2.5	19.5	0.18	2.3	19.9
SM-27/05/06-10 (DUP)	0.5	2.4	19.8	0.21	2.3	19.9
SM-07/08/06-1	0.46	1.7	11.0	0.23	1.7	10.9
SM-07/08/06-1 (VEIN A)	0.47	1.0	11.1	0.18	1.1	11.6
SM-07/08/06-1 (VEIN B)	0.48	-0.2	11.2	0.18	0.2	11.2
SM-14/06/06-1	0.49	-0.3	18.4	0.25	-0.3	18.7
SM-14/06/06-2	0.56	1.1	16.4	0.2	1.1	16.9
SM-14/06/06-3	0.51	2.5	23.5	0.23	2.3	23.3
SM-14/06/06-4	0.47	2.7	13.3	0.24	2.7	13.2
SM-14/06/06-4 (DUP)	0.45	2.7	12.9	0.21	2.5	12.9

Table 1. Values of $\delta^{18}\text{O}$ and $\delta^{13}\text{C}$ obtained for duplicate samples using different sample sizes.

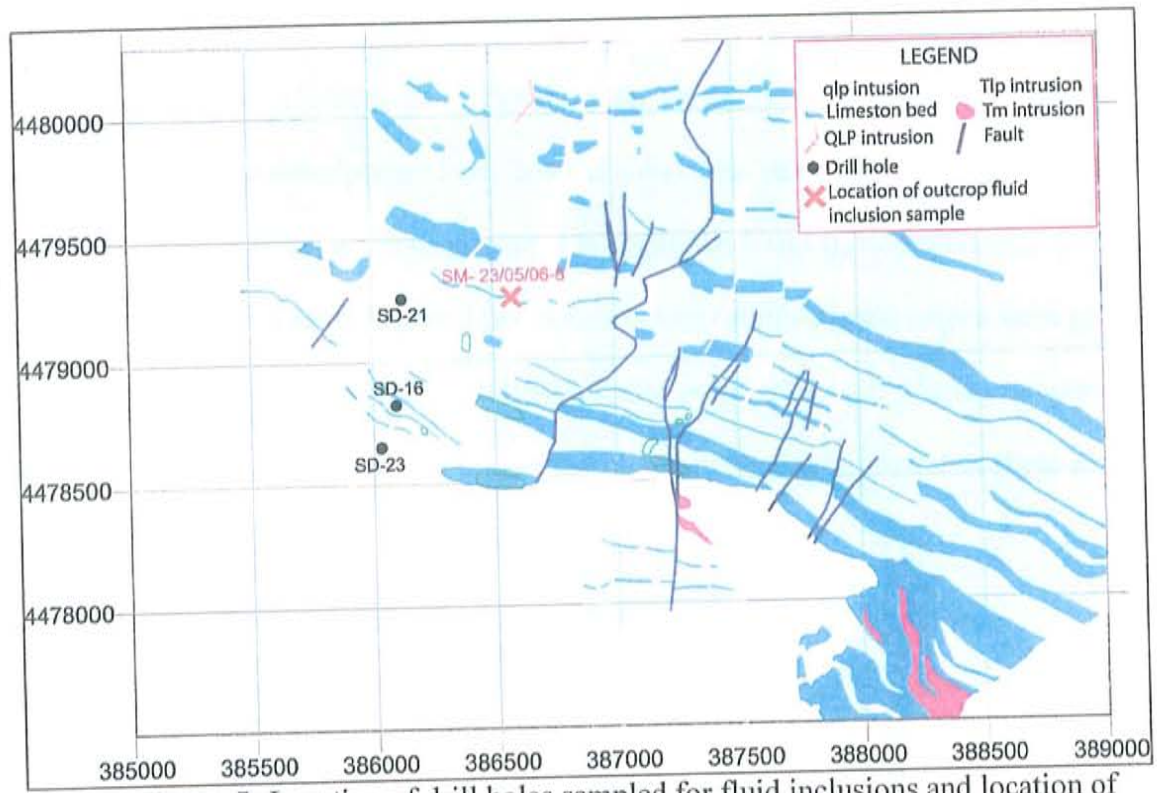


Figure 5: Location of drill holes sampled for fluid inclusions and location of sample SM-23/05/06-8 collected at the surface.

RESULTS

Petrography

Thin section descriptions have been divided into drill hole samples and field samples, with detailed descriptions presented in appendix A and B, respectively.

For all igneous rocks, mineral percentages were estimated, and names were given using the classification from Hughes (1982). Latite porphyries with quartz phenocrysts were classified as quartz-latite porphyries, the quartz phenocrysts present in these rocks are commonly quartz eyes.

Drill hole samples

Intrusive Igneous rocks

Most of the samples analyzed correspond to intrusive igneous rocks; these vary in composition from intermediate to felsic, with monzonites and latites the most abundant rock types. There are several fine-grain, equigranular igneous rock, originally logged as monzonites, which were collected from drill holes SD-15, SD-22, SD-23, SD-26 and SD-31. These "monzonites" showed variable petrographic characteristics, and were classified as biotite quartz-diorite, alkali feldspar quartz-syenite, biotite monzonite or hornblende quartz monzonite (Appendix A). Magmatic magnetite is present in most of these rocks, except for the biotite monzonite and one of the alkali feldspar quartz-syenites; total magnetite varies from <1.5 to 6 vol-% and it is more abundant in the biotite quartz-diorites.

Quartz-monzonites are the most abundant rock type, and are characterized by having a greater amount of quartz than the "monzonites" described above and by being of coarser grain. Quartz in these types of rocks is usually irregularly shaped, and zircon is

commonly present as trace microcrysts. Scarce magmatic magnetite (<1 vol-%) is sometimes present, observed only in one quartz-monzonite: SD-21-1948.5 ft. Some quartz-monzonites are weakly porphyritic.

Porphyritic rocks are divided into two main groups, with few exceptions; quartz-monzonite porphyries and quartz-latite porphyries. Both of these porphyry types have sub-equal amounts of plagioclase and K-feldspar; however, the main difference between these two types of rocks is the grain size and composition of the matrix. Quartz-latite porphyries are characterized by having a very fine grain matrix, which usually comprises quartz, in some cases with plagioclase and K-feldspars; quartz-monzonites porphyries have a coarser groundmass of quartz and K-feldspar with sub-equal amounts of each, and sometimes scarce plagioclase. In both intrusion types K-feldspars are usually the largest phenocrysts, and often have mineral inclusions of plagioclase, quartz and/or biotite.

K-feldspar, plagioclase, quartz and biotite are the main phenocrysts in both, quartz-latite porphyries and quartz-monzonite porphyries. Hornblende is more abundant in the quartz-latite porphyries (Photo 1), with only trace hornblende seen in quartz-monzonite porphyries. Sample SD-21-1852.5 ft. was logged as an "hornblende quartz-latite porphyry" due to the abundance of hornblende. Sample SD-21-660.5 ft. is a biotite quartz latite porphyry due to the abundance of biotite; in this rock, biotite is the most abundant mineral, comprising approximately 50-55 vol-% most of which seems to be of late magmatic-early hydrothermal paragenesis. Due to strong K-silicate constructive alteration, only scarce phenocrysts, besides biotite, are present, but include K-feldspar, plagioclase, hornblende, and trace quartz. The matrix of this rock type is comprises fine-grain quartz, plagioclase and K-feldspar.

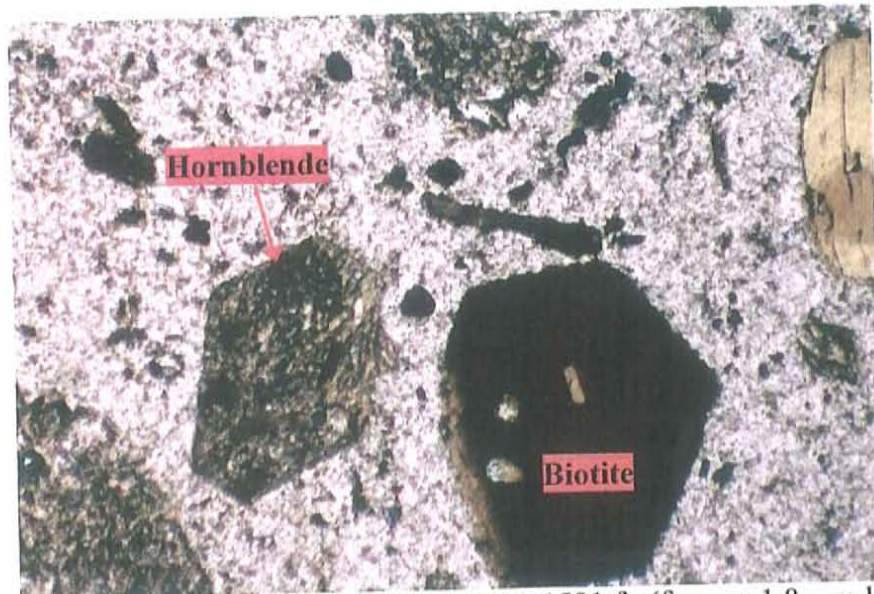


Photo 1: Altered hornblende, sample SD-21-1581 ft. (f.o.v. = 1.8 mm long).

Quartz-latitude porphyries are also characterized by rounded quartz phenocrysts or “quartz eyes” and by the presence of trace sphene (Photo 2), which does not seem to be present in the quartz monzonite porphyries.



Photo 2: Sphene, sample SD-23-2270.5 ft. (f.o.v. = 0.9 mm long).

Two porphyritic samples were not classified as quartz latite porphyry or quartz monzonite porphyries. Sample SD-21-1584.5 ft. was classified as an hornblende dacite porphyry. Biotite is the most abundant phenocryst, followed by hornblende and plagioclase, with scant quartz; no K-feldspar phenocrysts are observed. Magmatic magnetite is present, comprising <3 vol-% of this rock. The matrix is very fine grain and is composed of smectite, K-feldspar and quartz; the fine-grain texture of the groundmass suggests that this rock is probably hypabyssal.

The last drill core sample of porphyritic nature is a quartz-diorite porphyry (sample SD-21-2011 ft.). This rock comprises biotite, quartz, plagioclase and trace zircon, but no K-feldspar. The matrix is composed of quartz and plagioclase.

Two samples that have been strongly altered could not be classified into any specific igneous rock type. These correspond to SD-14-1219.5 ft. and SD-21-1899 ft. The first sample displays early K-silicate constructive alteration with strong phyllic overprint; the latter one has been biotitized. Both of these have several characteristics that indicate that they might be igneous in origin, such as the presence of relic phenocrysts.

Volcanic Igneous Rocks

Three of the described samples are of volcanic origin, and include two andesites and one biotite dacite. One of the andesites was collected from drill hole SD-18 and the other from drill hole 04RDYR01 (Appendix A). These andesites are characterized by a fine grain matrix composed mainly of plagioclase and plagioclase as the main phenocryst (Photo 3). Sample 04RDYR01-1896.5 ft. corresponds to a very fresh rock, containing clinopyroxene, hornblende and magmatic magnetite.

Plagioclase is also the most abundant phenocryst in the biotite dacite collected from drill hole SD-19; other phenocrysts include K-feldspar, quartz and biotite. The matrix is mainly composed of quartz and alteration-derived smectite. Zircon and apatite are common trace microcrysts in most igneous rocks studied.

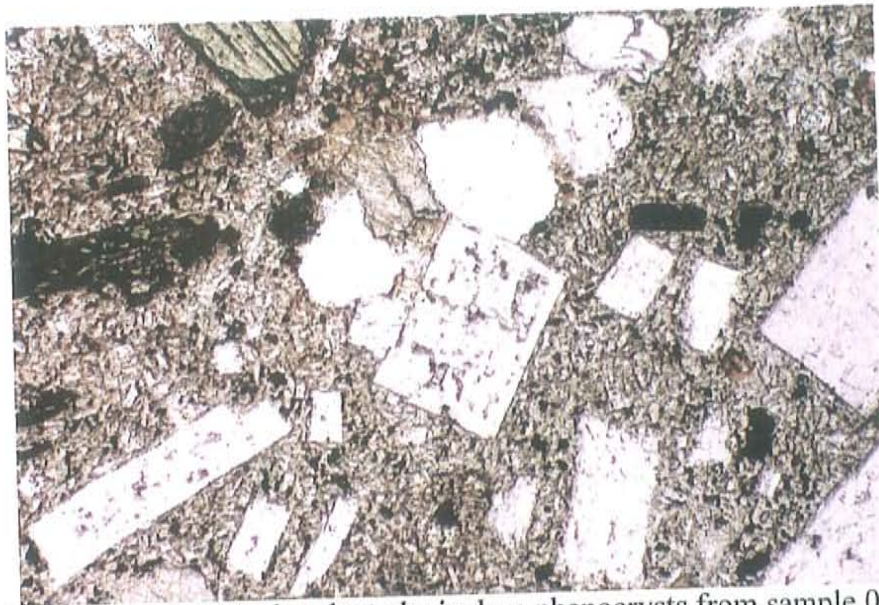


Photo 3: Volcanic rock with abundant plagioclase phenocrysts from sample 04RDYR01-1896.5 ft. (f.o.v. = 1.8 mm long).

Sedimentary Rocks

All the sedimentary rocks collected from drill holes have been altered to some extent, except for sample SD-15-72 ft. which corresponds to a fresh limestone (Appendix A). Samples that have been completely altered were probably originally carbonates. In some cases, some carbonates likely possessed an original clay content to account for the aluminum necessary to generate garnet; examples are SD-14-1124 ft., SD-23-2322.5 ft. and SD-31-1760 ft. In all of these rocks residual recrystallized carbonate is present.

Detrital quartz is still very abundant in three samples, classified as quartz arenites, these are SD-14-1266.6 ft, SD-23-885 ft and 05STK034-609 m. Other samples, such as SD-31-1430 ft., SD-31-1760 ft. and SD-31-2178 ft. may also have quartz of detrital

origin but in lesser amount, the protolith in these cases was probably a sandy limestone or lime sandstone (Appendix A).

Alteration

Alteration of Igneous rocks

Hydrothermal biotite is the most abundant alteration mineral in the igneous samples, with most Stockton igneous rocks displaying replacement to some extent by hydrothermal biotite. This mineral is characteristic of an alteration assemblage known as potassium-silicate constructive or "potassic"; muscovite, K-feldspar and biotite are the main minerals in this alteration type (Creasey, 1959); of these biotite is the most abundant in the Stockton samples. Hydrothermal K-feldspar is not usually present at Stockton, except in a few samples from drill holes SD-16 and SD-21. Hydrothermal K-feldspar is distinguished from magmatic K-feldspar by occurrence of the former in veins. Some of the K-feldspar that occurs in the matrix of quartz monzonite porphyries could also be of late magmatic-early hydrothermal origin.

Hydrothermal biotite at Stockton is generally shreddy and usually occurs in clusters, is usually fine grained, and sometimes has an olive-green pleochroism. In some cases hydrothermal biotite replaces magmatic biotite (Photo 4) and usually replaces hornblende (Photo 5).

Hydrothermal magnetite is spatially related to the K-silicate constructive alteration and is present in igneous rocks in drill holes SD-16, SD-21 and SD-22. It is common to find magnetite associated to this alteration assemblage (Beane, 1982). This was also observed in Butte Montana, here there is magnetite spatially associated with early biotite (Meyer, 1965).

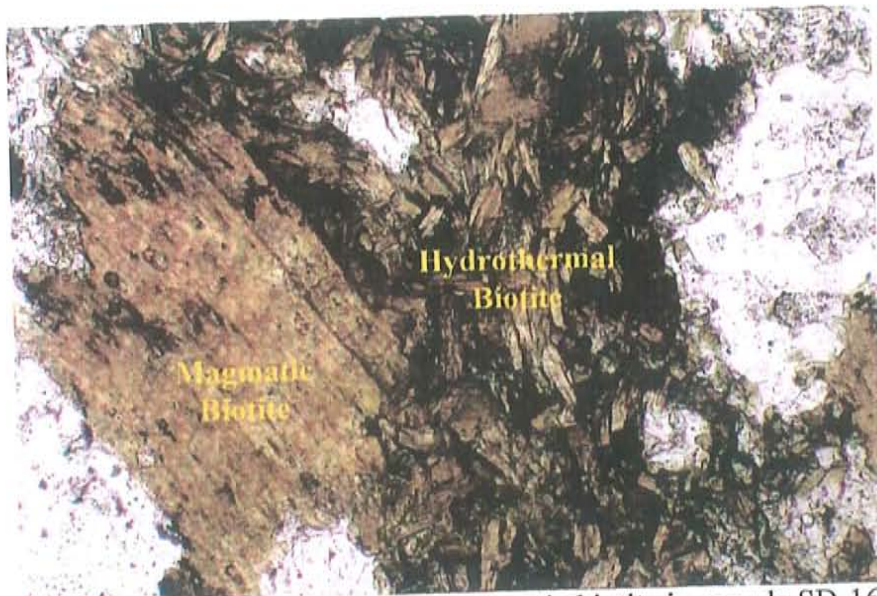


Photo 4: Hydrothermal biotite replacing magmatic biotite in sample SD-16-2629 ft. (f.o.v. = 0.9 mm long).

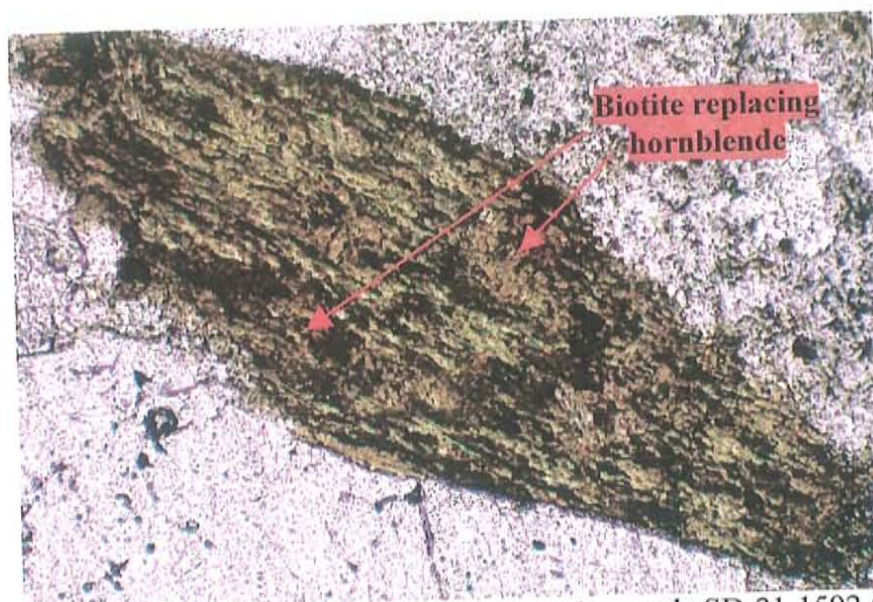


Photo 5: Biotite (brown) replacing hornblende (green), sample SD-21-1592.5 ft. (f.o.v = 0.9 mm long).

Magnetite of hydrothermal origin commonly occurs with hydrothermal biotite and sulfides, and as K-feldspar, hydrothermal magnetite is distinguished from magmatic magnetite by its occurrence in veins (Photo 6).

Magnetite in Stockton igneous rocks varies from <2 vol-% to approximately 15 vol-%. Drill hole SD-22, in the western portion of the property, has the greatest

hydrothermal magnetite content; this occurs in samples SD-22-1240 ft. and SD-22-1270 ft. (Appendix A), intervals in which sulfides are scant (<2 vol-%). Importantly hydrothermal magnetite generally shows variable replacement by specularite (Photo 7), suggesting late oxidation of the K-silicate + magnetite assemblage.



Photo 6: Parallel magnetite veins, sample SD-22-1270 ft. (f.o.v. = 1.8 mm long).

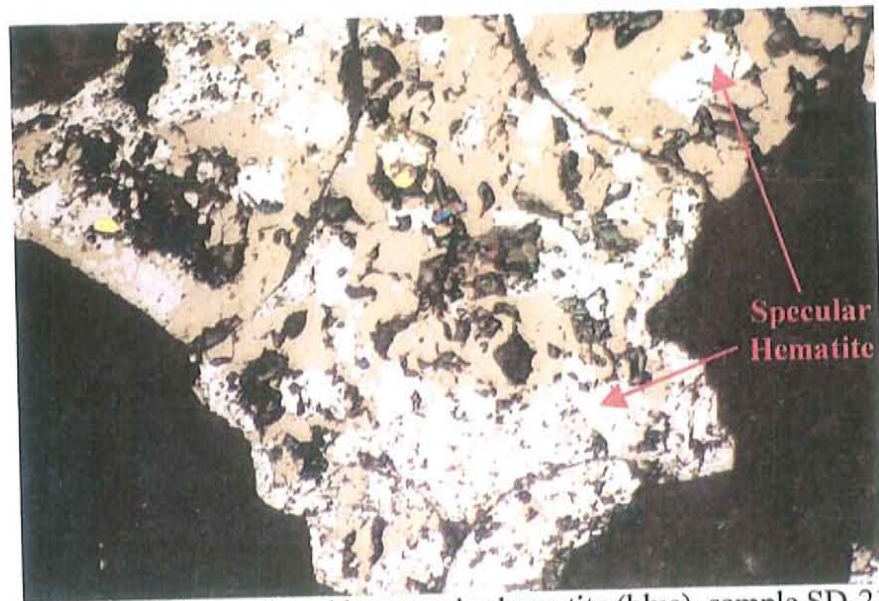


Photo 7: Magnetite being replaced by specular hematite (blue), sample SD-21-1961.5 ft. (f.o.v. = 0.225 mm long).

K-silicate constructive alteration at Stockton is usually variably overprinted by phyllic alteration, characterized by the presence of white phyllosilicates, scarce muscovite, and in some cases, scarce phengite.

Destruction of feldspars and biotite is characteristic of the phyllic alteration (Beane, 1982). In agreement with this, white phyllosilicates mainly occur as replacement of feldspars; in some samples white phyllosilicates + scarce muscovite occur as scarce patches; it is also common to find white phyllosilicates associated with carbonate such as in sample SD-16-2185 ft.; this same feature was observed in the porphyry copper deposit at El Salvador, Chile, where minor calcite occurs with sericite that alters feldspars (Gustafson and Hunt, 1975). Some white phyllosilicates directly replace both magmatic and hydrothermal biotite (Photo 8 and photo 9). White phyllosilicate veinlets are also sometimes present in the Stockton igneous rocks.

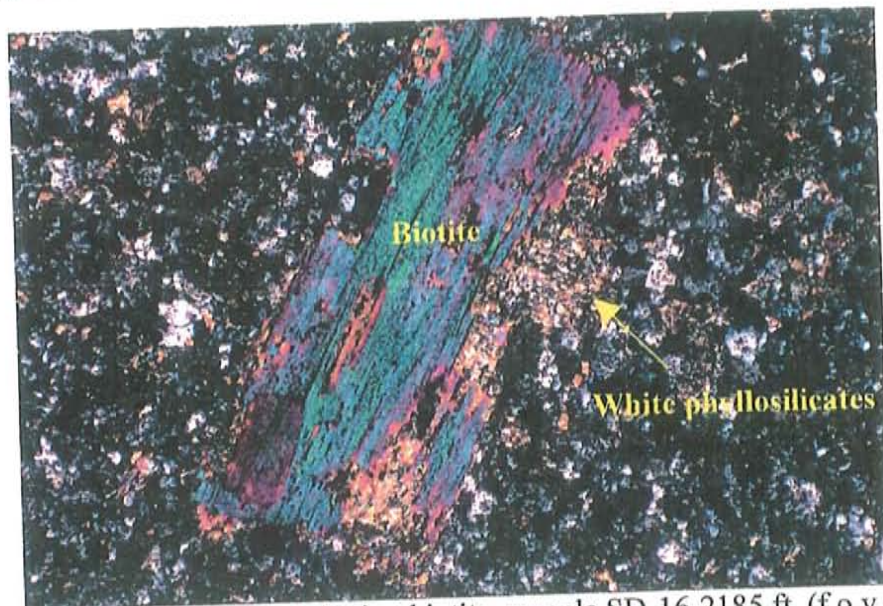


Photo 8: White phyllosilicates altering biotite, sample SD-16-2185 ft. (f.o.v. = 1.8 mm long).

QSP (quartz + "sericite" + pyrite) veins, a consequence of phyllic alteration (Beane, 1982), were only observed in sample SD-15-1230 ft. (Appendix A). Calcite is

present in one QSP vein; this is not uncommon as has been previously documented at the porphyry copper deposit at El Salvador, Chile (Gustafson and Quiroga, 1995).

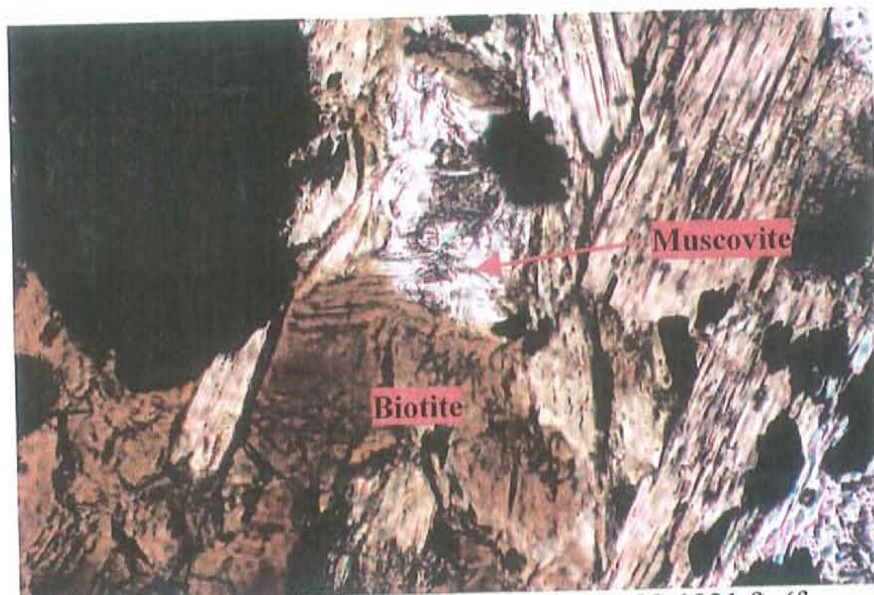


Photo 9: Bladed muscovite replacing biotite, sample SD-22-1321 ft. (f.o.v. = 0.45 mm long).

The degree of phyllic overprint varies substantially, but is usually incipient to weak, meaning that abundant biotite is as yet present. Two samples have strong phyllic overprint; are SD-14-1219.5 ft. and SD-23-1466 ft.

In some samples hydrothermal biotite has also been overprinted by patchy, late carbonate. Carbonate occurs altering phenocrysts, as scarce patches in matrix, in veins, and in clusters with other alteration minerals such as biotite. In some cases there is a spatial association between carbonate and chlorite, such as in samples SD-21-1581 ft. and SD-21-1584.5 ft.

Biotite commonly displays incipient replacement by chlorite (Photo 10); with chlorite usually <1 vol-%. Alteration-derived cinnamon rutile is present in most Stockton igneous rocks, usually comprising <2 vol-%, and occur in close spatial association with biotite (Photo 11). Scant cinnamon rutile occurs together white phyllosilicates, suggesting

probable replacement of biotite; in addition cinnamon rutile may also be associated with chalcopyrite (Photo 12).

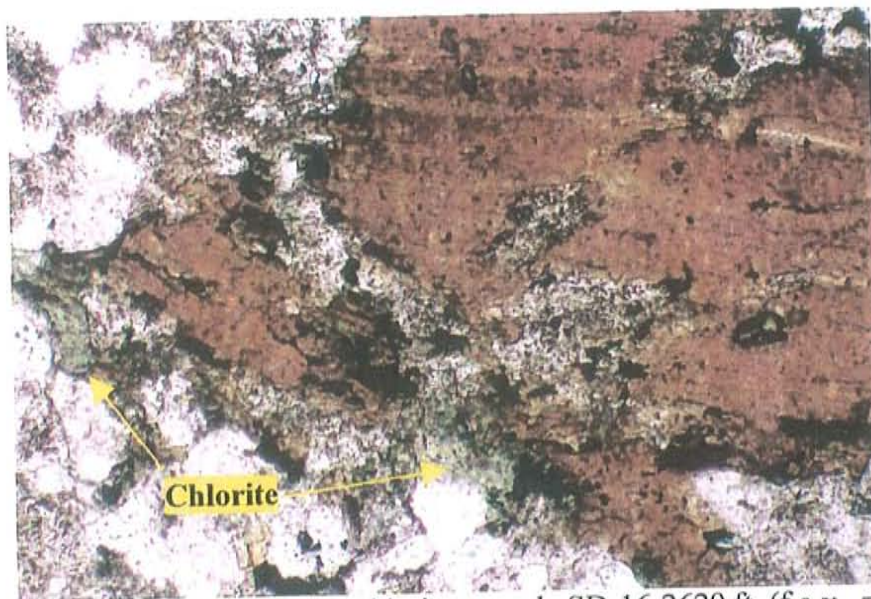


Photo 10: Biotite being altered to chlorite, sample SD-16-2629 ft. (f.o.v. = 0.9 mm long).

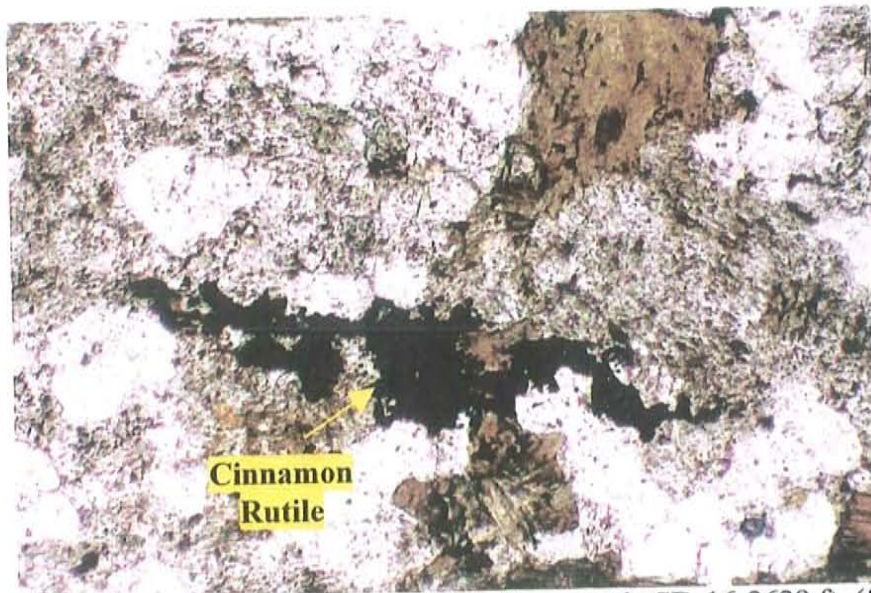


Photo 11: Cinnamon rutile associated with biotite, sample SD-16-2629 ft. (f.o.v. = 0.9 mm long).

Feldspars in Stockton igneous rocks have been replaced by a series of minerals generally represented as patches and veinlets. These alteration minerals include white

phyllosilicates, muscovite, biotite, carbonate, quartz, smectite showing greater development in plagioclase, epidote, and trace chlorite. Scant kaolinite alters plagioclase in sample SD-21-1581 ft. Kaolinite is also present in sample SD-16-1219.5 ft., where some phenocrysts have been completely replaced by white phyllosilicates, scarce biotite, scarce carbonate, trace muscovite and sometimes kaolinite, these phenocrysts were probably originally plagioclase. Sample SD-23 -1466 ft. has phenocrysts that have been replaced by white phyllosilicates, carbonate and in some cases scarce kaolinite, these were also probably originally plagioclase.

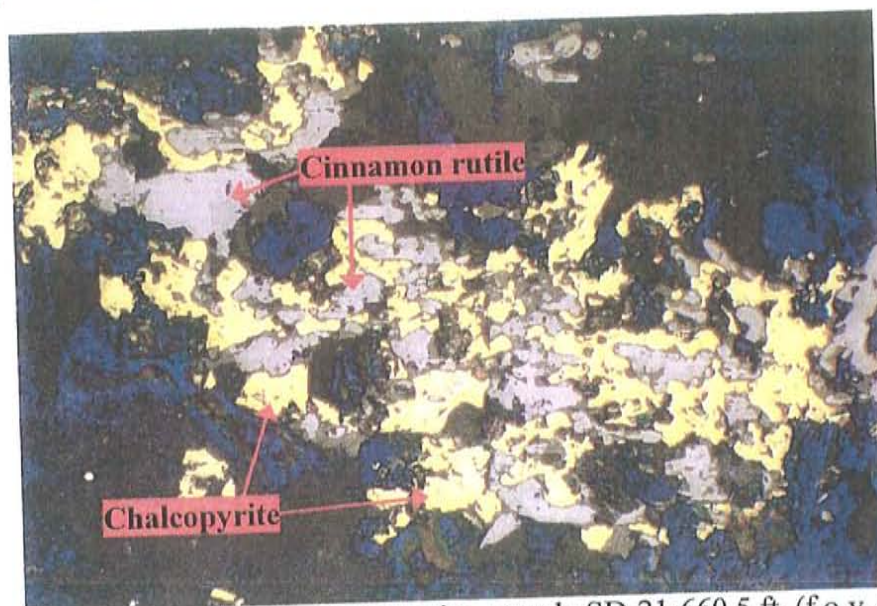


Photo 12: Cinnamon rutile with chalcopyrite, sample SD-21-660.5 ft. (f.o.v. = 0.45 mm long).

Several igneous rock units show a calc-silicate style overprint. In drill hole SD-21, sample SD-21-1584.5 ft. has actinolite, and samples: SD-21-660.5 ft., SD-21-1948.5 ft., SD-21-1961.5 and SD-21-2325.5 ft. have trace epidote. In drill hole SD-23 sample SD-23-2270.5 ft. is cut by a vein that has a halo of zoisite and scarce epidote; also in this rock scant epidote replaces plagioclase. Sample SD-31-2205 ft. has actinolite and trace epidote.

Only one igneous sample lacks biotite (SD-21-490 ft.). In this case, the main alteration minerals are actinolite (Photo 13) and carbonate, each one comprising <5 vol-%, perhaps representing calc-silicate endoskarn. Epidote (<2 vol-%) is also present and is closely associated with carbonate (Photo 14).

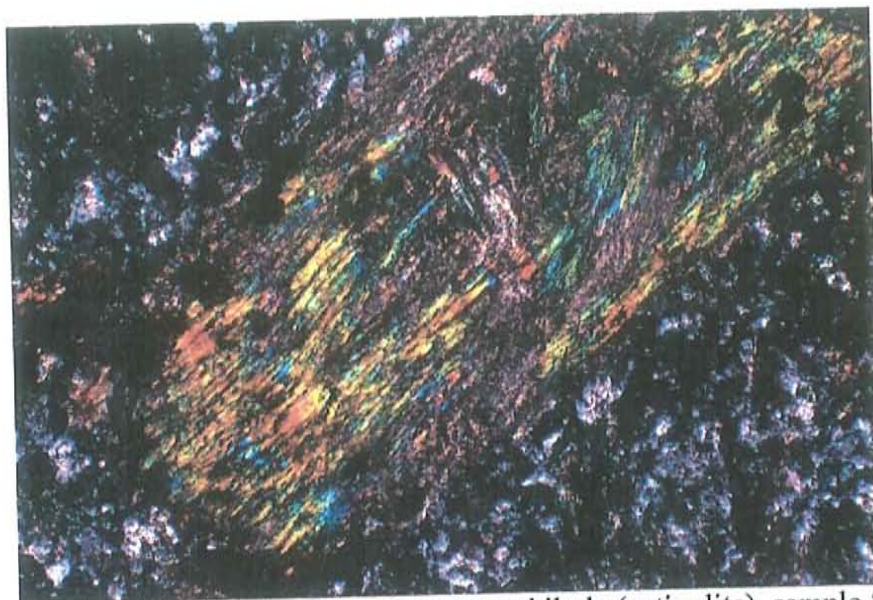


Photo 13: Mafic mineral replaced by fibrous amphibole (actinolite), sample SD-21-490 ft. (f.o.v. = 0.9 mm long).

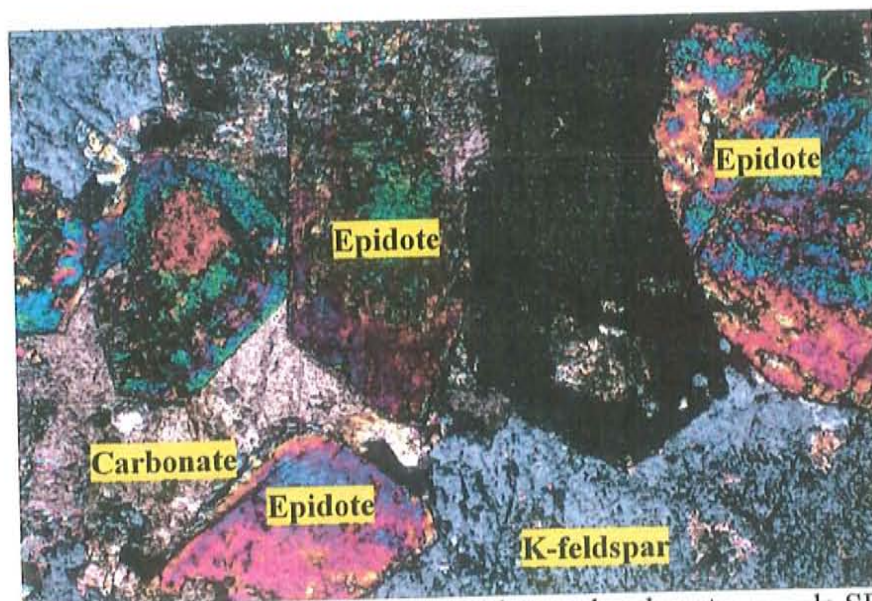


Photo 14: K-feldspar showing alteration to epidote and carbonate, sample SD-21-490 ft. (f.o.v. = 1.8 mm long).

Alteration of Sedimentary Rocks

Sedimentary rocks noted from drill holes have been mainly altered to calc-silicate minerals, plus carbonate and quartz. These calc-silicate minerals include diopside, actinolite, tremolite, garnet, epidote and zoisite, occasionally occurring with chlorite, serpentine, magnetite, specularite and smectite. Scarce chloritoid (<2 vol-%) is also present in one sample (SD-23-1556 ft.) in which it replaces amphiboles and clinopyroxenes. Trace K-feldspar is present in sample SD-31-2178 ft. In sample SD-23-2322.5 ft. serpentine replaces garnet. In the quartz arenites, alteration minerals are usually interstitial to detrital quartz grains.

Chlorite, when present, is usually associated with amphiboles, apparently replacing them. The sedimentary rock with the greatest chlorite content corresponds to SD-31-2178 ft. (Appendix A), where it comprises approximately 5 vol-% of the rock; here, chlorite replaces an amphibole (tremolite/actinolite?), and is being replaced by carbonate.

Hydrothermal magnetite is also sometimes present in sedimentary rocks, it occurs in veins in sample SD-14-1266.6 ft. and SD-23-1556 ft (Appendix A).

In Stockton igneous rocks specularite usually replaced magnetite; in sample SD-23-1566 ft. the opposite occurs, serpentine formed first but it is now being replaced by hydrothermal magnetite, together these comprise approximately <6 vol-% of the rock, the evidence that suggests that in this case specularite formed first is that these minerals are bladed, a common feature of specular hematite (Photo 15). Also in this sample magnetite surround chalcopyrite and pyrite, possibly replacing them (Photo 16), indicating that this hydrothermal alteration was a late feature in this rock.

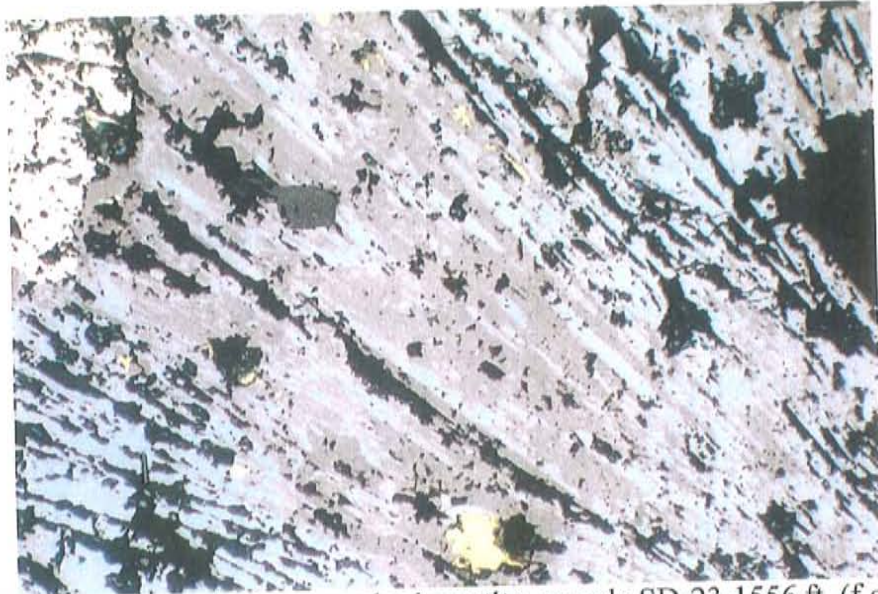


Photo 15: Magnetite replacing specular hematite, sample SD-23-1556 ft. (f.o.v. = 0.45 mm long).



Photo 16: Chalcopyrite surrounding pyrite, and magnetite surrounding chalcopyrite, sample SD-23-1556 ft. (f.o.v. = 0.45 mm long).

As with igneous rocks, carbonate also seems to be a late alteration feature in sedimentary rocks. In some samples carbonate is sometimes poikilotopic, and surrounds other minerals, for example in sample SD-23-2322.5 ft. diopside is surrounded by poikilotopic calcite, indicating that the calcite had to form after the diopside. Other

examples that indicate that carbonate was one of the last minerals to form include sample SD-21-548 ft., where carbonate replaces tremolite and diopside, with a stronger replacement of tremolite, and sample SD-31-2178 in which carbonate replaces an amphibole and chlorite (Appendix A).

Sample SD-21-885 ft. corresponds to a sedimentary rock, apparently a quartz arenite, in which hydrothermal biotite is the most abundant alteration mineral, comprising approximately 15 vol-% of the rock, it is followed in abundance by carbonate and quartz which comprise 5-10 vol-% each and by white phyllosilicates; the total amount of white phyllosilicates is <7 vol-%. In this sample the alteration assemblage is classified as K-silicate constructive with a phyllic overprint. Cinnamon rutile (<2 vol-%) and trace epidote are also present. Cinnamon rutile in this sample is mainly associated with biotite and carbonate and scarce occurs with white phyllosilicates.

Sulfides

Overall, pyrite is the most abundant sulfide, followed by chalcopyrite. Other sulfides which are only present in scarce samples, include marcasite, bornite, digenite, chalcocite, idaite, covellite, pyrrhotite, trace molybdenite and trace sphalerite; except for marcasite all the other sulfides only occur in scarce to trace amounts. Sulphosalts include enargite in sample 05STK034-566.6 m and what appears to be trace tetrahedrite in sample SD-14-1219.5 ft.

Sulfides are spatially associated with hydrothermal biotite; in the Stockton samples it is very common to find sulfides, mainly pyrite and chalcopyrite in clusters with hydrothermal biotite (Photo 17).

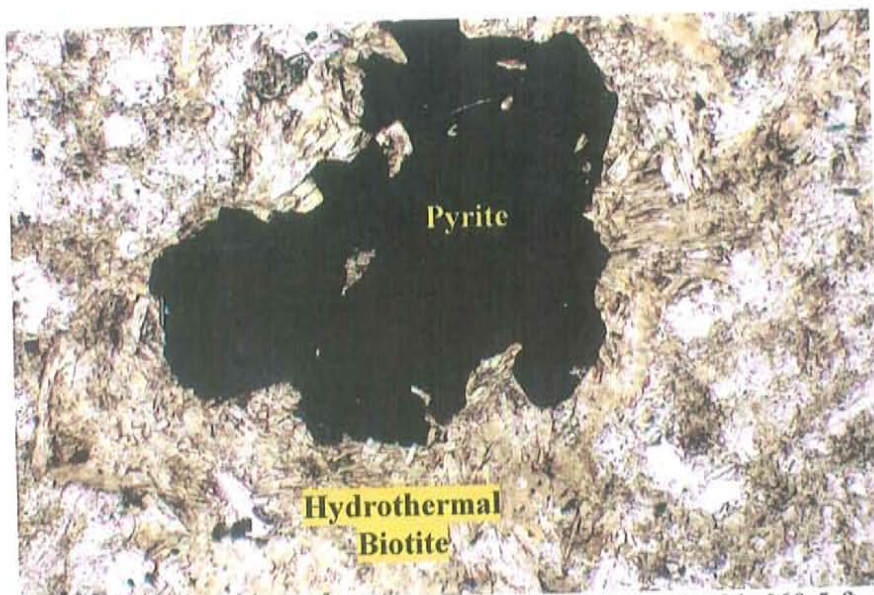


Photo 17: Cluster of hydrothermal biotite and pyrite, sample SD-21-660.5 ft. (f.o.v. = 0.9 mm long).

In three samples sulfides are associated to phyllic alteration; these are SD-14 - 1219.5 ft., SD-15-1230 ft. and SD-23-1466 ft. In the first sample pyrite is the most abundant sulfide followed by chalcopyrite and bornite with sub-equal amounts, scarce digenite, scarce tetrahedrite and trace covellite are also present, these last three minerals were not observed in any other sample.

In SD-15-1230 ft. most sulfides occur in a QSP vein. In SD-23-1466 ft. chalcopyrite is more abundant than pyrite, in this case there is chalcopyrite associated with hydrothermal biotite, but the greatest concentration in the rock occurs together with white phyllosilicates + carbonate + silica + cinnamon rutile + muscovite. In this sample there were probably two pulses of copper introduction, one related to the K-silicate constructive alteration and one associated to the phyllic overprint. In this sample it is also common to find chalcopyrite associated with euhedral muscovite (Photo 18).



Photo 18: Chalcopyrite surrounding muscovite; sample SD-23-1466 ft. (f.o.v. = 0.45 mm long).

In the Stockton samples, pyrite was the first mineral to form and is commonly surrounded by chalcopyrite (Photo 19). Bornite and idaite, when present, occur together with chalcopyrite, indicating that these three are possibly coeval (Photo 20). Digenite and tetrahedrite seem to have formed after bornite (apparently replacing it?); this relationship is only based on one sample, SD-14-1219.5 ft. Chalcocite is also only present in one sample (SD-23-1556 ft.); in which it replaces chalcopyrite (Photo 21). Marcasite surrounds chalcopyrite in sample SD-14-1346 ft. (Photo 22), indicating that it formed later.

Pyrrhotite occurs in one sample SD-21-2011 ft., where it is spatially associated with chalcopyrite and magnetite. Pyrrhotite and chalcopyrite occur as small blebs inside of magnetite and probably formed by exsolution. Enargite surrounds pyrite in sample 05-STK-034-566.6 m., indicating that it formed later.

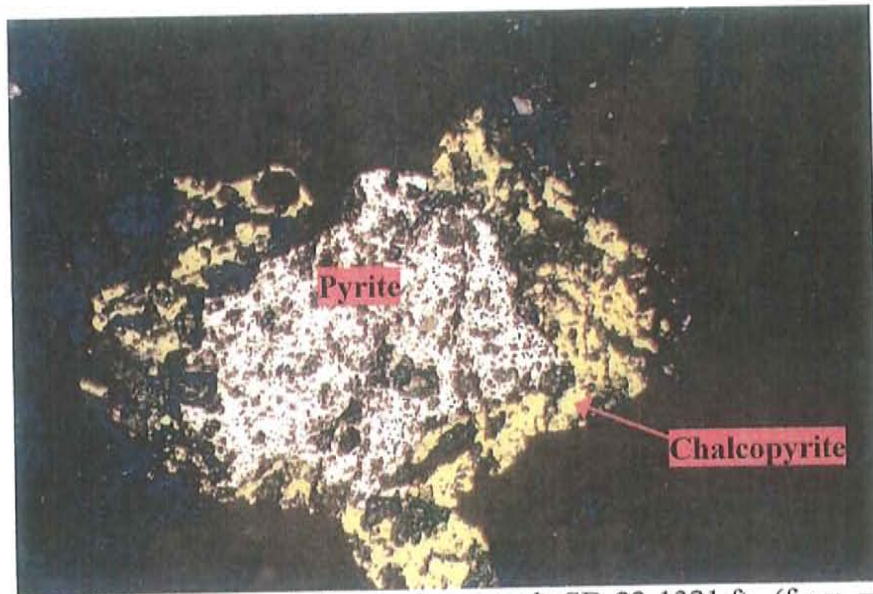


Photo 19: Chalcopyrite surrounding pyrite; sample SD-22-1321 ft. (f.o.v. = 0.45 mm long).

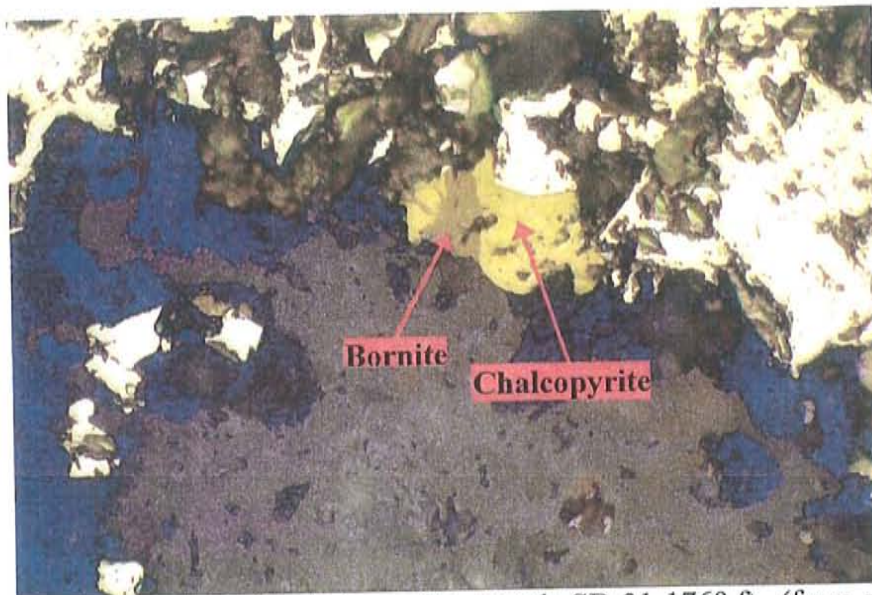


Photo 20: Bornite together with chalcopyrite, sample SD-31-1760 ft. (f.o.v. = 0.225 mm long).

The relationship of covellite, molybdenite and sphalerite to other sulfides could not be determined due to the fact that each only occurs in one sample and in trace amounts.

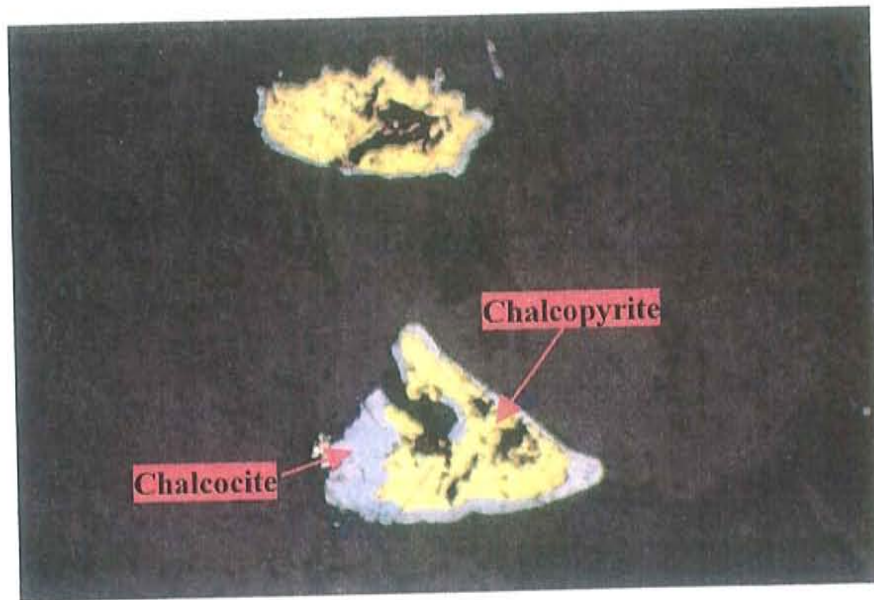


Photo 21: Chalcocite replacing chalcopyrite, sample SD-23-1556 ft. (f.o.v. = 0.45 mm long).

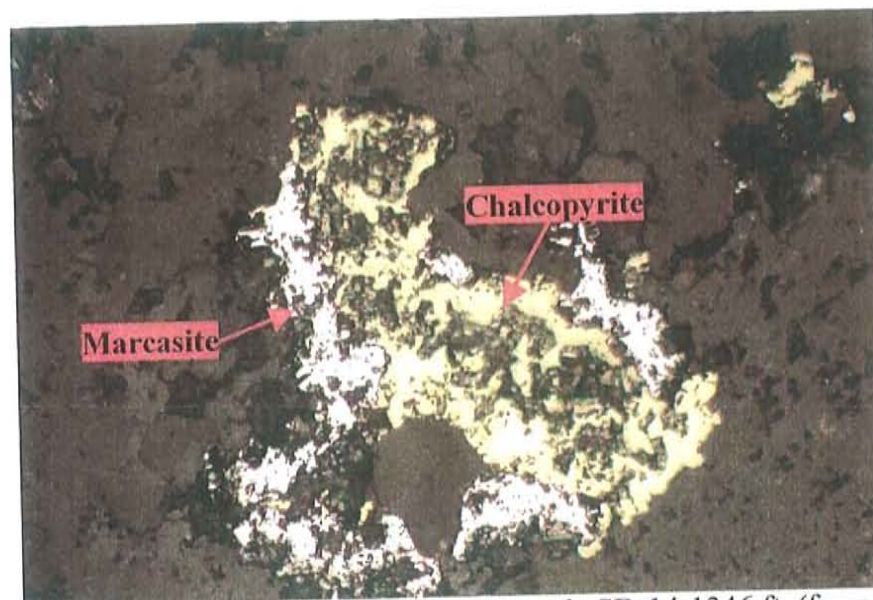


Photo 22: Marcasite surrounding chalcopyrite, sample SD-14-1346 ft. (f.o.v. = 0.45 mm long).

Sedimentary rocks with the greatest percentage of sulfides occur in drill holes SD-14, SD-23 and SD-31. Of these sample SD-23-1556 ft. has the greatest abundance with sulfides comprising approximately 10 vol-% of the rock (pyrite>chalcopyrite).

Profiles

Two profiles one with a north-south orientation, and one with an east-west orientation, were constructed to determine the spatial variation of the alteration (Figure 6 and Figure 7). The location of sulfides and sulfosalts, other than pyrite and chalcocopyrite are also indicated in these profiles, excluding samples SD-31-1760 ft. which has trace bornite and idaite and sample 05STK 034-566.6 m. which has enargite, marcasite and trace sphalerite.

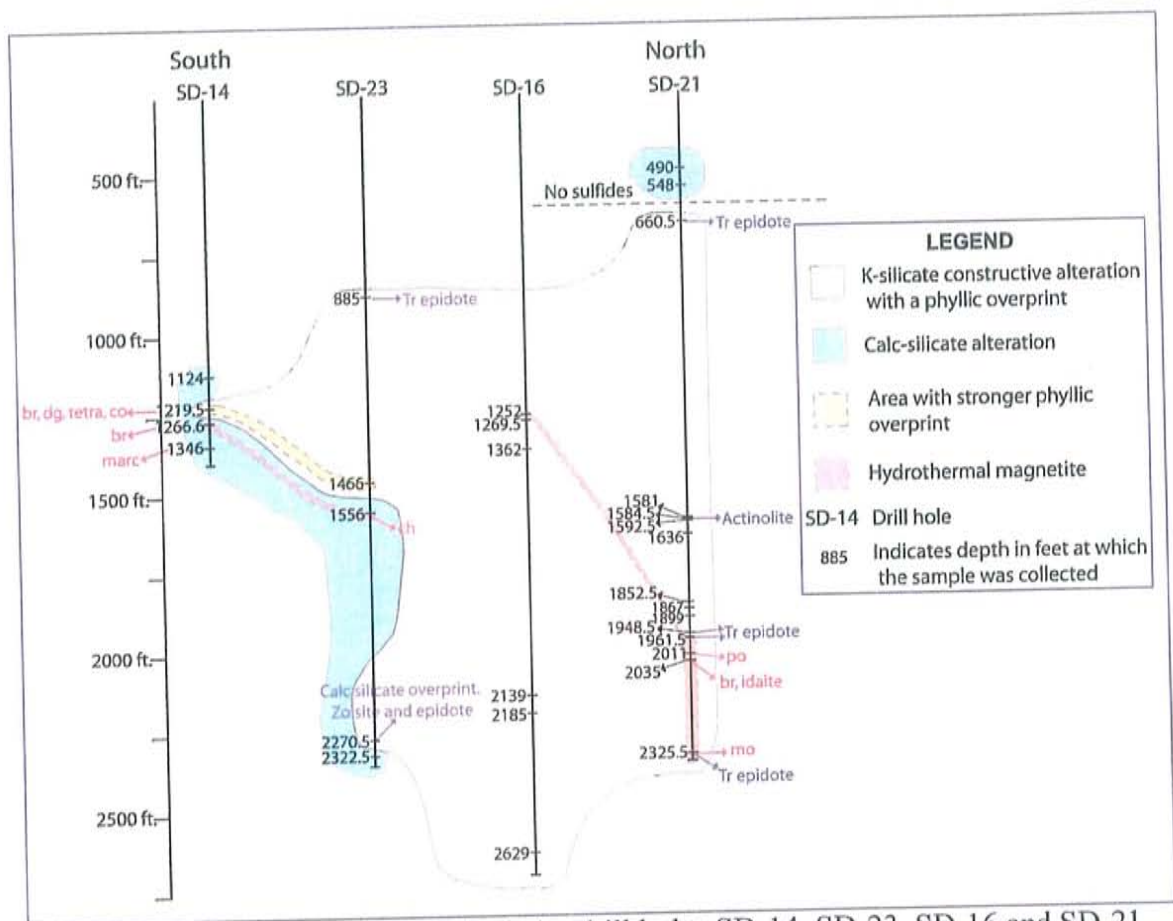


Figure 6: South-north transect, includes drill holes SD-14, SD-23, SD-16 and SD-21.

Based on sample descriptions and on spatial variations, it can be concluded that alteration in the drill holes is mainly lithologically controlled. Igneous rocks are characterized by having been altered hydrothermally; the main alteration assemblage is

K-silicate constructive with a phyllic overprint. And sedimentary rocks have been mainly altered to calc-silicate minerals.

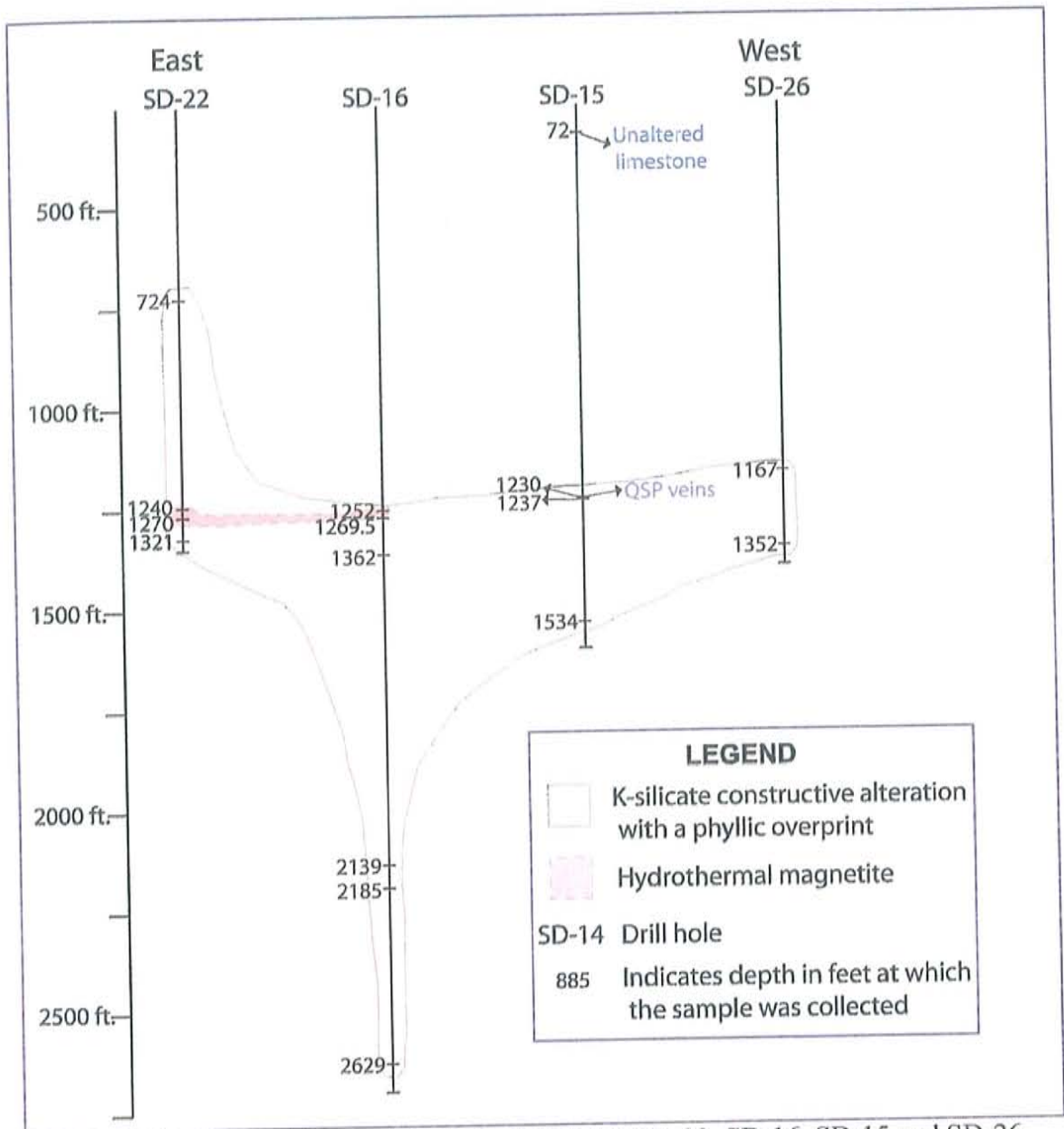


Figure 7: East-west transect, includes drill holes SD-22, SD-16, SD-15 and SD-26.

Exceptions to this rule occur near the contact between sedimentary and igneous rocks; it can be expected for fluids that precipitated calc-silicate minerals to also affect igneous rocks that are relatively close, as well as for hydrothermal fluids that formed K-

silicate minerals to also alter sedimentary rocks in the surrounding area; such is the case of sample SD-23-885 ft. which corresponds to a sedimentary rock in which hydrothermal biotite is the main alteration mineral and sample SD-21-490 ft., an igneous rock that has actinolite as the most abundant alteration mineral.

There also seems to be a weak calc-silicate overprint at the bottom of drill hole SD-21, characterized by the presence of actinolite and trace epidote.

Two samples (SD-14-1219.5 ft. and SD-23-1466 ft.) have a stronger phyllic overprint than the rest of the samples, in both cases white phyllosilicates are more abundant than hydrothermal biotite. The location of these samples is shown in figure 6.

Hydrothermal magnetite is concentrated in two main areas, possibly associated to fractures, these areas comprise drill holes SD-14, SD-15, SD-21, SD-22 and SD-23 (Figure 6 and 7), it is mostly associated with the K-silicate constructive alteration, except for two samples, SD-14 -1266.6 ft. and SD-23-1566 ft., both of sedimentary origin (Figure 7).

Field samples

Igneous rocks

Sample SM--29/05/06-1 was classified as a monzodiorite; magmatic minerals present in this rocks include, plagioclase, K-feldspar, hornblende, biotite, magnetite, quartz and clinopyroxene, possibly augite. Trace zircon is also present. Sample SM-15/06/06-4 is similar to the previous rocks, but due to its abundant hornblende (7-10 vol-%) it was classified as a hornblende monzodiorite, this rock also has trace amount of apatite and rutile (Appendix B). In both of these rocks, there are clinopyroxenes that have been altered to hornblende (Photo 23) and biotite, indicating a possible hydration of the

rocks, biotite also replaces hornblende. Both samples present a weak K-silicate constructive alteration, based on the presence of K-feldspar overgrowths around plagioclase phenocrysts. Sample SM-29/05/06-1 also has shreddy biotite, of late magmatic-early hydrothermal appearance.

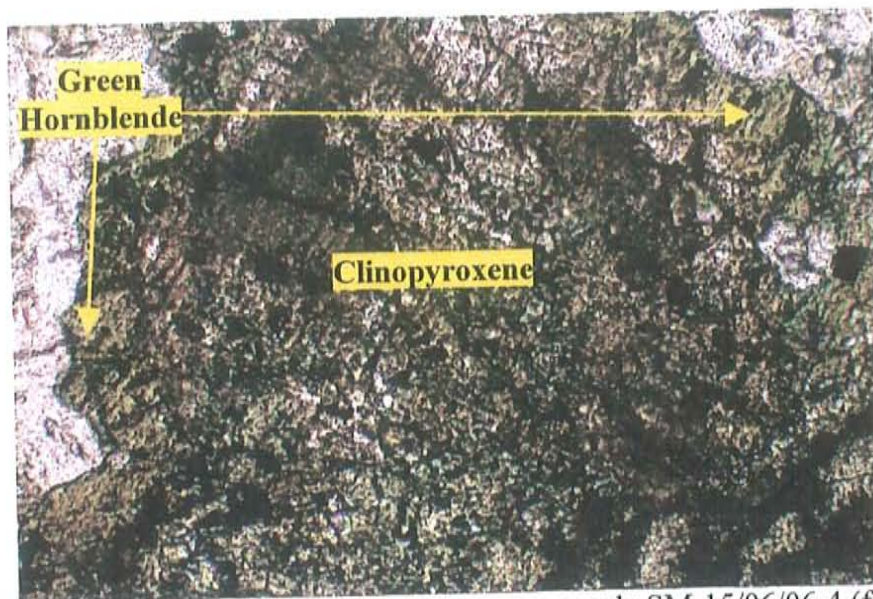


Photo 23: Hornblende replacing a clinopyroxene, sample SM-15/06/06-4 (f.o.v. = 0.9 mm long).

In sample SM-15/06/06-4, there is a weak phyllic overprint of the K-silicate constructive alteration, evidenced by the presence of trace muscovite replacing biotite and of white phyllosilicates altering feldspars, the total alteration to white phyllosilicates varies from 0 to <5 vol-%, and is weaker in K-feldspars than in plagioclase.

Other alteration minerals in samples SM--29/05/06-1 and SM-15/06/06-4 include actinolite, which comprises <1 to 1 vol-% and chlorite with <1.5 vol-%. Actinolite replaces biotite, hornblende and augite; and chlorite replaces hornblende and biotite. Both the monzo-diorite and the hornblende monzo-diorite lack sulfides.

Samples SM-29/05/06-11 and SM-15/06/06-4 are classified as quartz-lathite porphyries. Alteration minerals in these samples include white phyllosilicates, muscovite,

chlorite and scarce to trace carbonate. Abundant iron oxides and hydroxides, apparently hematite and goethite are present in both samples. Chlorite is more abundant in sample SM-29/05/06-11 comprising approximately <5 vol-%.

White phyllosilicates + muscovite comprise approximately 8-10 vol-%, the lack of white phyllosilicate veins and the fact that they occur in abundance everywhere throughout the sample suggests a weathering origin rather than a hydrothermal origin. The presence of abundant hematite and goethite are also a consequence of weathering of the rocks.

No residual mafic minerals are present in these quartz-latite porphyries; they have all been replaced by alteration minerals. Pyrite, identified by its cubic shape, was present in both samples (SM-29/05/06-11 and SM-15/06/06-4) but has now been replaced by hematite and goethite. K-feldspar overgrowths around "quartz eyes" are present in both quartz latite porphyries, indicating a weak K-silicates constructive alteration.

The K-silicate alteration observed in outcrop igneous samples is different from the one present in drill hole samples, it is characterized by the occurrence of K-feldspar overgrowths around other phenocrysts and not by hydrothermal biotite, which as mentioned before is very abundant in the drill hole samples. Also the alteration of field samples is not as strong as the one observed in the drill holes, indicating a weakening of the K-silicate assemblage towards shallower levels. Another important difference between that the field samples lack copper sulfides, indicating that ore bearing fluids did not reach surface levels.

Sedimentary rock

Sample SM-18/07/06-2, was classified as a chert (Appendix B). This rock shares many similarities with sample SM-06/06/06-13 (Appendix C), and the protolith was probably also a limestone, although the evidence is not as clear. Azurite and malachite are present in the rock, indicating the presence of copper. Submillimeter scale carbonate veinlets cut the rock. Unlike drill hole sedimentary rocks this sample has not experienced a calc-silicate alteration.

Stable Isotopes

The isotopic composition of carbonate rocks and veins obtained for $\delta^{13}\text{C}$ range from -10.9 to 5 ‰, and the $\delta^{18}\text{O}$ values range from 1.7 to 26.1 ‰ (Figure 8, Appendix E). Based on their characteristics rocks samples were divided into four groups: gray and dark gray limestones, skarn, coarse limestones and white limestones.

Sedimentary rocks in the study area are of Pennsylvanian age (Davies, 1996). Unaltered limestone isotope composition for this area were taken from two studies done on Pennsylvanian brachiopods. One study focused on brachiopods found in shales from Texas (Grossman, et al., 1991) and the other on late Pennsylvanian brachiopods from Kansas and New Mexico (Grossman et al., 1993). The range of $\delta^{13}\text{C}$ and $\delta^{18}\text{O}$ values was taken from these articles and these are represented as the “unaltered limestone” box (Figure 8).

When comparing the values obtained for the analyzed samples to the ones expected for unaltered limestones of that age, it is clear that all samples have experienced some degree of alteration (Figure 8).

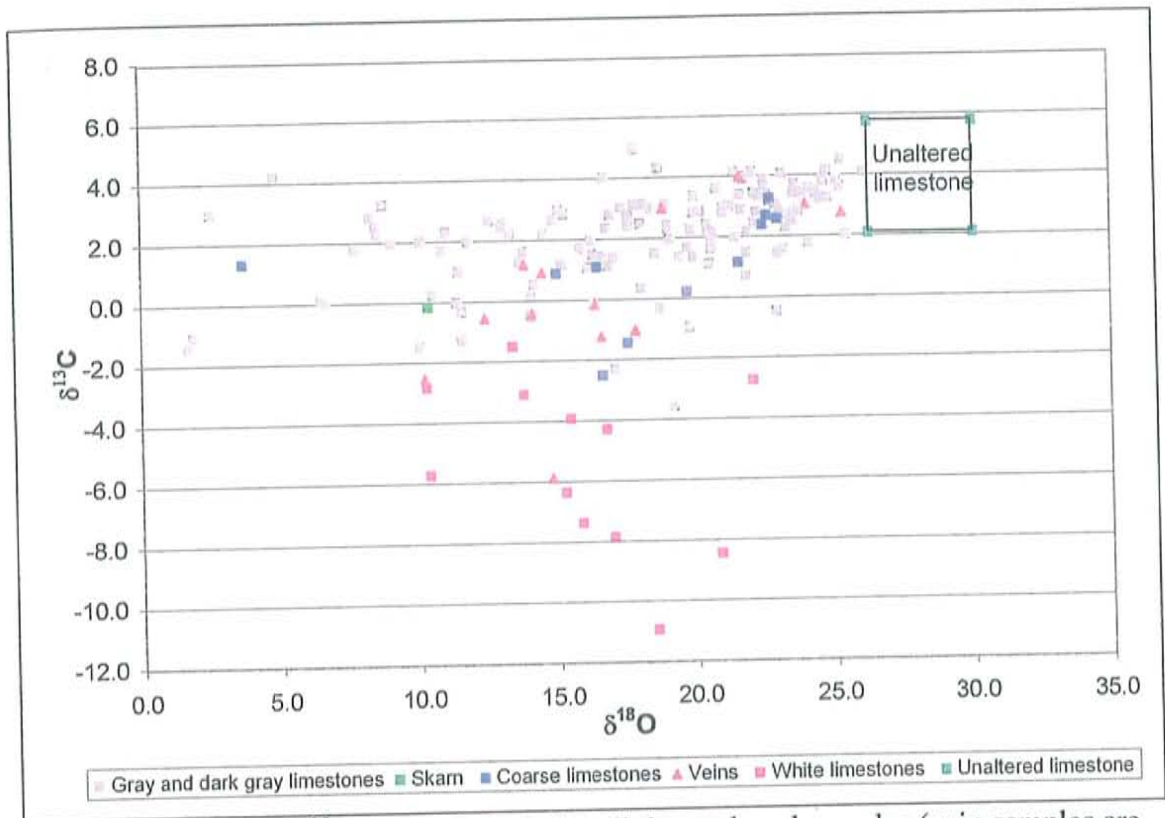


Figure 8: $\delta^{13}\text{C}$ vs. $\delta^{18}\text{O}$ diagram. Includes all the analyzed samples (vein samples are shown as triangles and rock samples are shown as squares)

Veins

Overall veins are usually lighter in $\delta^{13}\text{C}$ and $\delta^{18}\text{O}$ than their host rock (Figure 9), suggesting either a diagenetic or a hydrothermal origin, since both of these processes can cause these low $\delta^{13}\text{C}$ and $\delta^{18}\text{O}$ values.

Vein density varies widely from outcrop to outcrop; the highest density determined was of 70 veins in a meter which corresponds to sample SM-14/05/06-5 (which was also analyzed petrographically, Appendix C), taken 2.5 m away from a contact with a quartz latite porphyry. There are some few cases where no veins were observed. No direct relationship was found between the amount of veins and the isotopic signature of the rock.

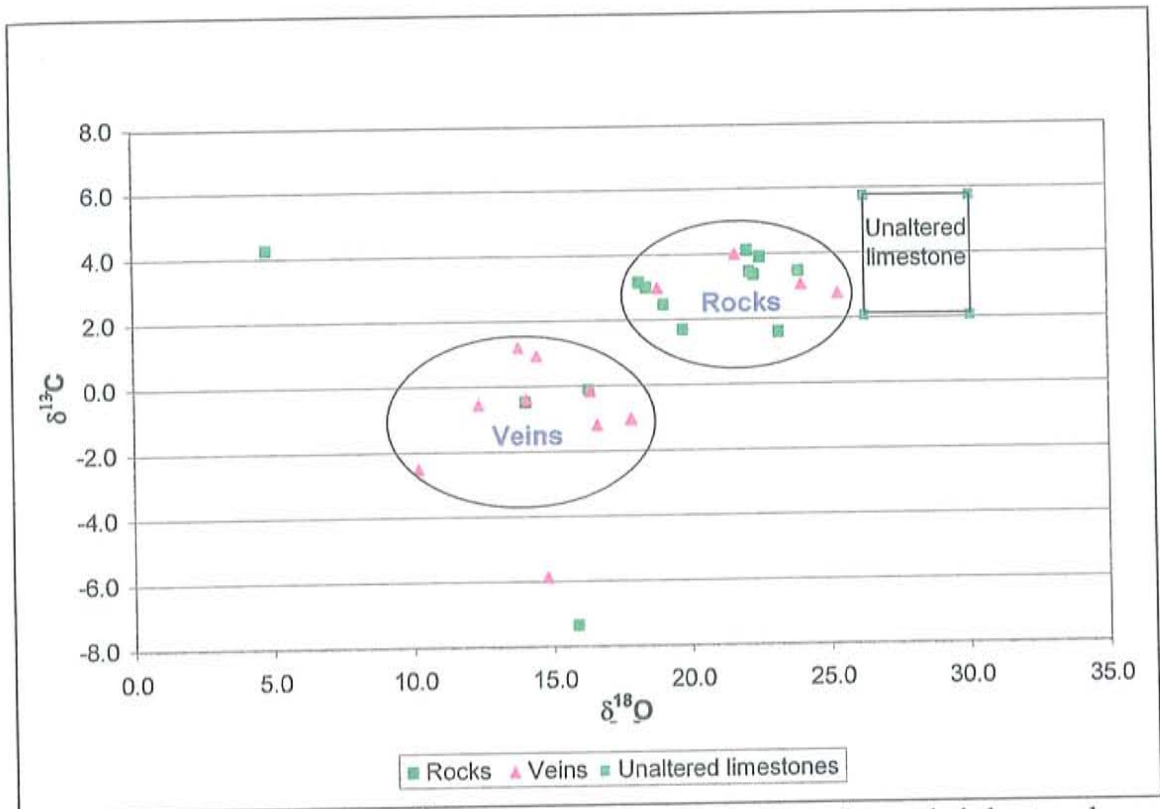


Figure 9: $\delta^{13}\text{C}$ vs. $\delta^{18}\text{O}$ diagram. Compares calcite veins to their host rocks.

Rocks

It was mentioned previously that all the samples have been altered to some extent, based on this they can be divided into three groups (Figure 10); group one corresponds to the least altered samples, group two has the ones with the lowest $\delta^{13}\text{C}$ and group three includes the samples with the that have been mainly depleted in $\delta^{18}\text{O}$.

It is believed that all analyzed samples have been diagenetically altered. A study conducted on Pennsylvanian brachiopods from New Mexico and Kansas, demonstrated that diagenetically altered shells are depleted in $\delta^{13}\text{C}$ and $\delta^{18}\text{O}$ compared to unaltered shells. When the matrix incorporates Mn due to diagenesis, it becomes luminescent, and when compared to nonluminescent calcite, it is shown that the diagenetically altered

calcite of brachiopods is lighter in both isotopes than the nonluminescent calcite (Figure 11).

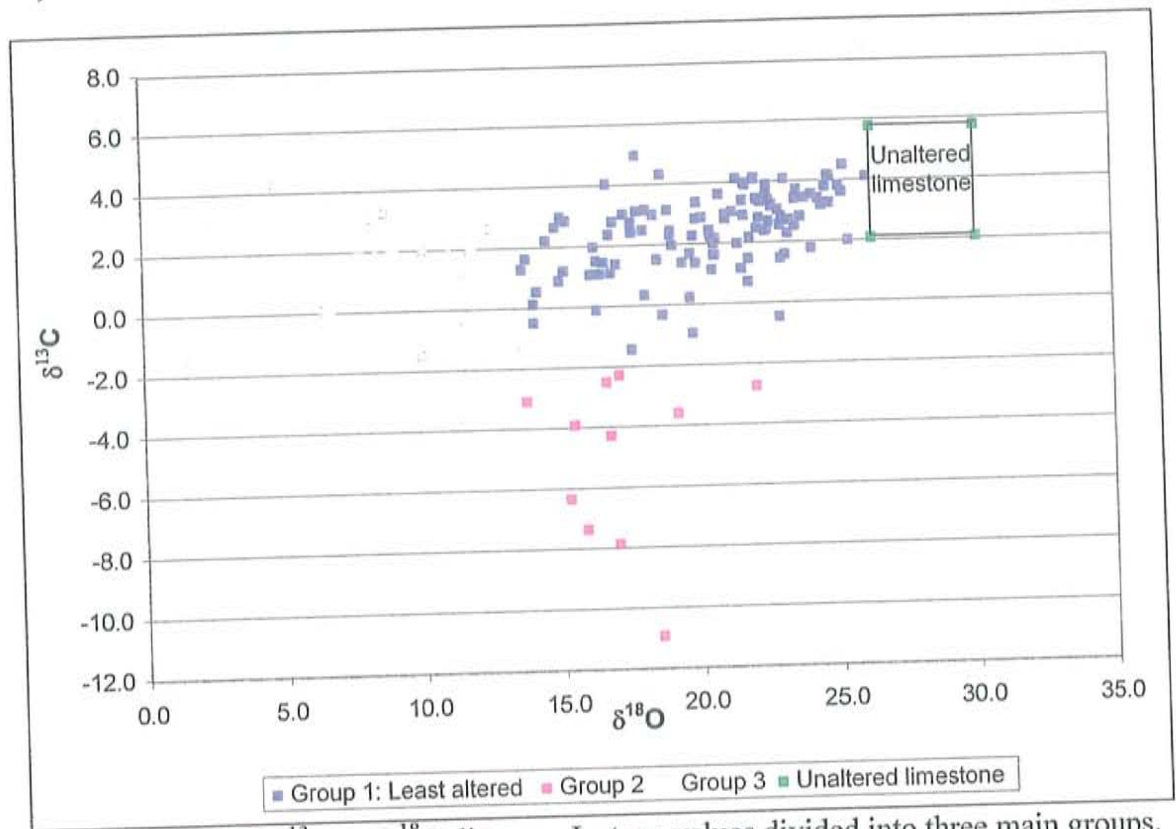


Figure 10: $\delta^{13}\text{C}$ vs. $\delta^{18}\text{O}$ diagram. Isotope values divided into three main groups.

The isotopic shift observed in figure 11, is similar to the one observed for some of the least altered samples or “group one”. When plotting the diagenetically altered values from figure 11, on figure 10, is supports the idea that samples from “group one” have been diagenetically altered (Figure 12).

From group one the composition evolved following two main trends (Figure 13), suggesting that two major processes are responsible for these depletions. Diagenesis has affected all the samples lowering both carbon and oxygen values, ($\delta^{18}\text{O}$ has a greater shift), but other processes, superimposed on top of the diagenetic alteration have depleted some specific samples to a greater extent.

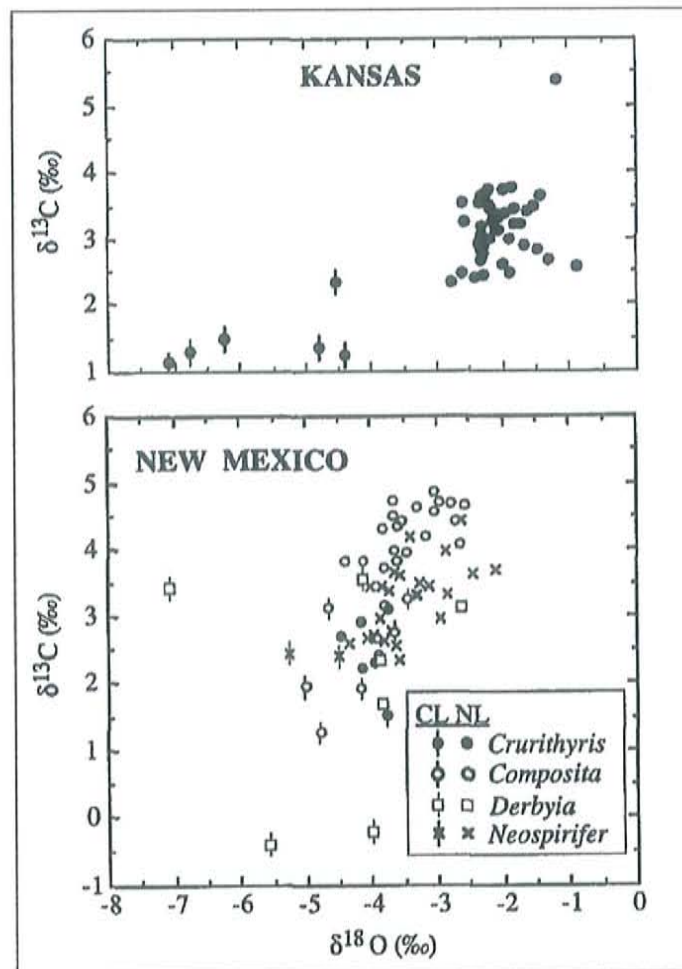


Figure 11: $\delta^{13}\text{C}$ vs. $\delta^{18}\text{O}$ diagram. Compares luminescent (CL) calcite with nonluminescent (NL). Oxygen and carbon isotope values are given relative to PDB (Grossman, et al., 1993).

The lower $\delta^{18}\text{O}$ values are interpreted as a consequence of hydrothermal alteration. Hydrothermal fluids, which are mainly water, would have a stronger effect on the $\delta^{18}\text{O}$ of the carbonates than on the $\delta^{13}\text{C}$. Because carbon is not a main component in these fluids it is not expected to find a big shift in the $\delta^{13}\text{C}$ values. Rocks that have been most shifted away from their original values are the ones that have experienced a higher fluid flow (Arehart and Donelick, 2006), based on this the rocks with lower $\delta^{18}\text{O}$ values indicate higher water/rock ratios.

It is possible that some of the samples from group one, have also been affected by superimposed hydrothermal alteration, but in figure 10 the limit between diagenesis and hydrothermal alteration can not be easily determined, and since this isotopic study is being used as an exploration tool, it is better to look for the most anomalous cases thus only the lower $\delta^{18}\text{O}$ values, which as mentioned above indicate higher water/rock ratios, will be considered as hydrothermally altered.

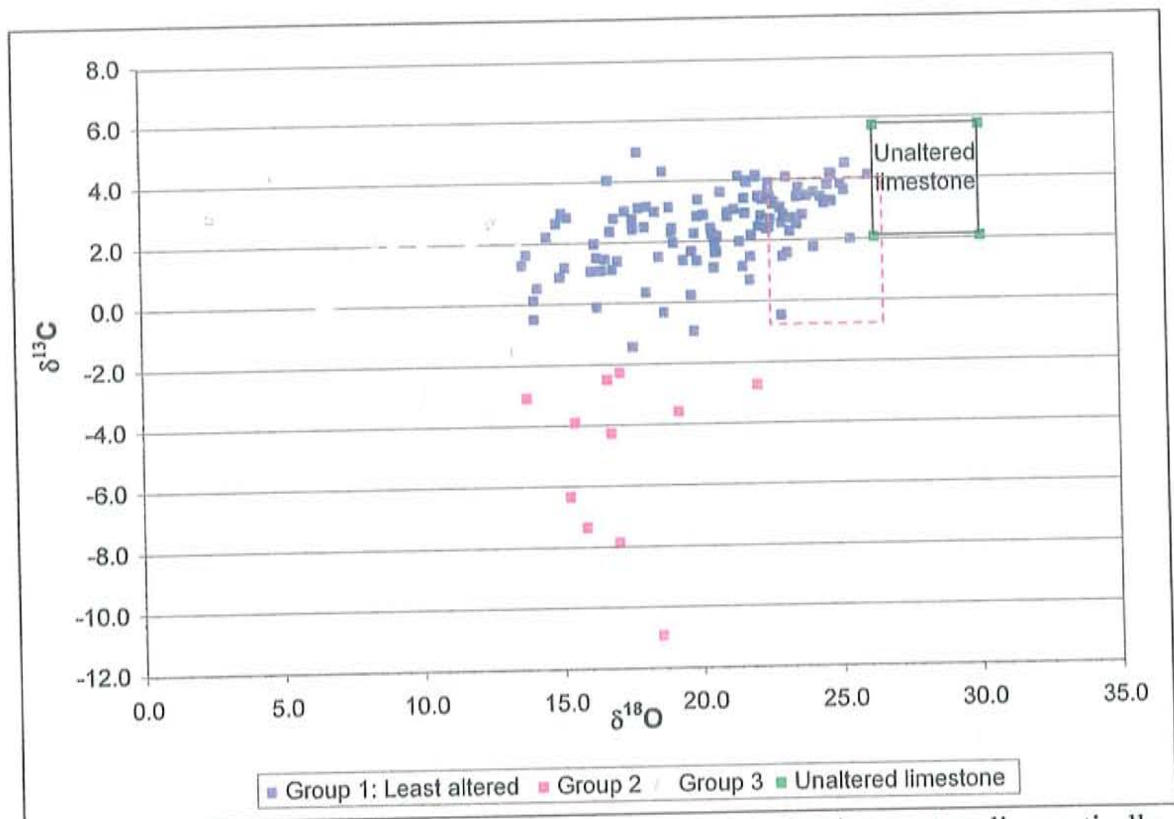


Figure 12: $\delta^{13}\text{C}$ vs. $\delta^{18}\text{O}$ diagram. Red box represents the luminescent or diagenetically altered samples from figure 11.

Water with a low $\delta^{18}\text{O}$ such as meteoric water influence is necessary to account for the lowest values seen in the data. These values could not be reached only by the interaction with magmatic fluids.

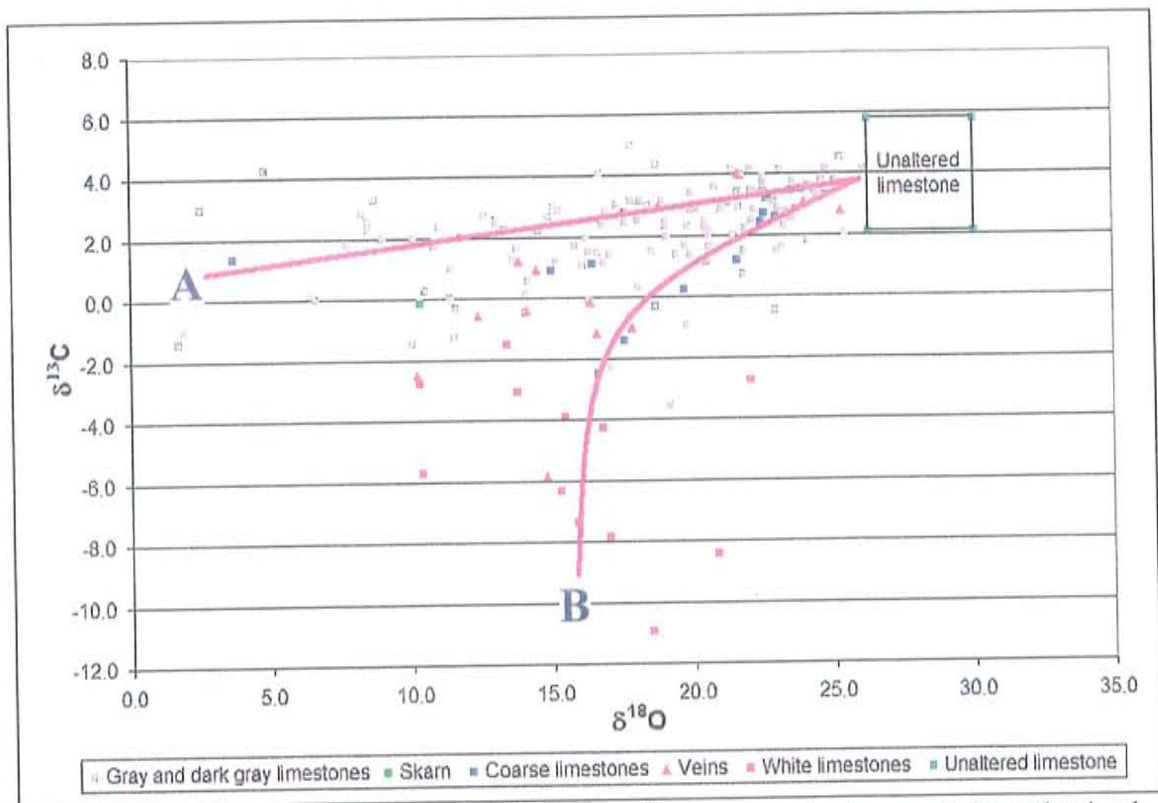


Figure 13: $\delta^{13}\text{C}$ vs. $\delta^{18}\text{O}$ diagram. The two red lines show the two main hypothesized paths to explain the trends in the data. A: hydrothermal alteration. B: decarbonation by contact metamorphism.

Samples lying along the second path with low $\delta^{13}\text{C}$ values are believed to have been caused by contact metamorphism. During metamorphism “volatile” elements are lost; in carbonate rocks, decarbonation (loss of CO_2) can occur, changing the isotopic composition of the remaining carbonate. In a closed system, the fluids have time to evolve and equilibrate with the rock before they escape (“batch volatilization”) on the other hand if the system is open the volatiles will escape before they equilibrate with the rock (“rayleigh volatilization”), when these two scenarios are represented in a $\delta^{13}\text{C}$ vs. $\delta^{18}\text{O}$ diagram (Figure 14), the batch volatilization plots as a straight line and the rayleigh volatilization forms a curve in which the $\delta^{13}\text{C}$ shift is bigger (Valley, 1986). The pattern observed in the analyzed data correlates better with a rayleigh process.

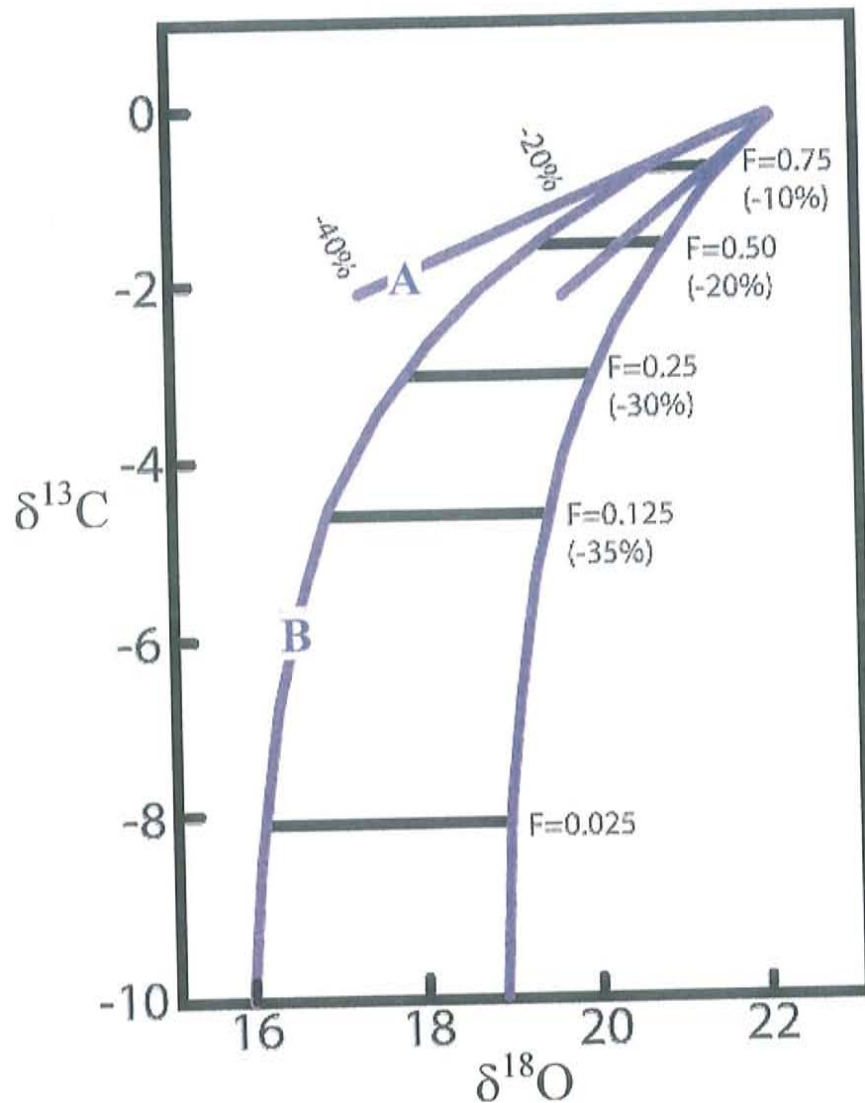


Figure 14: $\delta^{13}\text{C}$ vs. $\delta^{18}\text{O}$ diagram. A: batch volatilization. B: rayleigh volatilization. Modified after Valley (1986).

The CO_2 lost during the formation of calc-silicate minerals has heavier $\delta^{13}\text{C}$ and $\delta^{18}\text{O}$ values than the carbonate rocks, thus the rock becomes lighter (Shieh and Taylor, 1969), $\delta^{13}\text{C}$ is affected more than $\delta^{18}\text{O}$ because a greater percentage of the carbon in the rocks is lost. Most of the samples with low $\delta^{13}\text{C}$ correspond to white limestones. The calcite vein that has the lowest $\delta^{13}\text{C}$ belongs to a white limestone (sample: SM-03/06/06-3), probably the vein was also affected when the rock underwent contact metamorphism.

Petrographic analysis of isotope samples

Wide variations were observed in the 9 samples (Table 2) analyzed petrographically (detailed descriptions of these are given in Appendix C); when possible limestones were classified under Dunham (1962) and Folk (1962).

SAMPLE	$\delta^{13}\text{C}$	$\delta^{18}\text{O}$	Description
* SM-13/01/06-9	-0.1	10.4	Garnet skarn
* SM-29/05/06-4	4.1	22.1	Gray
* SM-30/05/06-1	-3.9	15.5	White
* SM-03/06/06-3	-5.7	10.4	White
* SM-05/06/06-5	2.7	22.6	Gray, coarse
* SM-05/06/06-10	3.4	20.0	Gray
* SM-06/06/06-13	-10.9	18.5	White
* SM-14/06/06-15	1.7	20.6	Dark gray
* SM-07/08/06-1	1.7	10.9	Dark gray
SM-07/08/06-1 (White A)	0.3	10.5	
SM-07/08/06-1 (White B)	0.0	11.4	

Table 2: Stable isotope samples selected for petrography analysis

SM-07/08/06-1, SM-29/5/06-4 and SM-14/06/06-15 correspond to fine grain micritic limestones; these are rich in organic material (which gives them a dark gray color) and iron, suggesting that they formed in reducing environments. Iron occurred mainly as pyrite but has now been replaced by iron oxides, especially hematite. All of these are cut by coarsely crystalline calcite veins (spary), which vary in size from sub-millimeter to millimeter scale.

SM-07/08/06-1 has laminations probably of microbial origin and was classified as a boundsonte/biolithite, these laminations are not as clear in the other two dark gray samples so they were classified as packstone-wackstone/biomicrites. SM-29/05/06-4 is the least altered having higher $\delta^{13}\text{C}$ and $\delta^{18}\text{O}$ values, SM-14/06/06-15 has a lower $\delta^{13}\text{C}$ value but it is still weakly altered when compared to the bulk of samples. SM-07/08/06-1 which was collected from drill hole SD-15 from a depth of 72ft. has a lower $\delta^{18}\text{O}$

suggesting hydrothermal alteration and higher water to rock ratios, this sample is also characterized by the presence of white areas, believed to be the result of bleaching possibly caused by oxidizing fluids, these bleached areas were analyzed separately for a total of 2 samples (labeled White A and White B in Table 2).

SM-30/05/06-1 has been completely recrystallized to poikilotopic calcite; trace submillimeter scale calcite veins cut the rock. This sample is characterized by having a very low $\delta^{13}\text{C}$ value.

Samples SM-05/06/06-5 and SM-05/06/06-10 both correspond to sandy limestones; the first one was classified as a packstone-grainstone/bioesparite and the second one which is finer grain as a packstone/biomicroite. These two samples have also been recrystallized, but to a lesser degree when compared to SM-30/05/06-1, in this case recrystallization affected mainly the matrix, making it coarser; some fossils have been preserved. In both samples chert (fine grain silica) is present in scarce amounts and it seems to be either replacing grains or filling spaces.

As with the previous two samples SM-03/06/06-3 also corresponds to a sandy limestone. Minerals present in this sample include quartz, carbonate, diopside (Photo 24) and fine grain silica. Diopside is pretty abundant, comprising approximately 25 vol-% of the rock. Another mineral, possibly tremolite, has now been completely replaced carbonate and fine grain silica; this mineral is only identified due to the presence of rectangular outlines (Photo 25). This sample gave a low $\delta^{13}\text{C}$ value, which is the consequence of the decarbonation process that affected this sample during the formation of calc-silicate minerals such as diopside.

Sample SM-13/01/06-9 corresponds to a garnet skarn (Photo 26), this sample was collected from drill hole SD-14 from a depth of 1124 ft. Carbonate has been recrystallized and it comprises less than 40% of the sample. The $\delta^{13}\text{C}$ value of this sample is low but not as low as it would be expected for a skarn sample that underwent a decarbonation process.

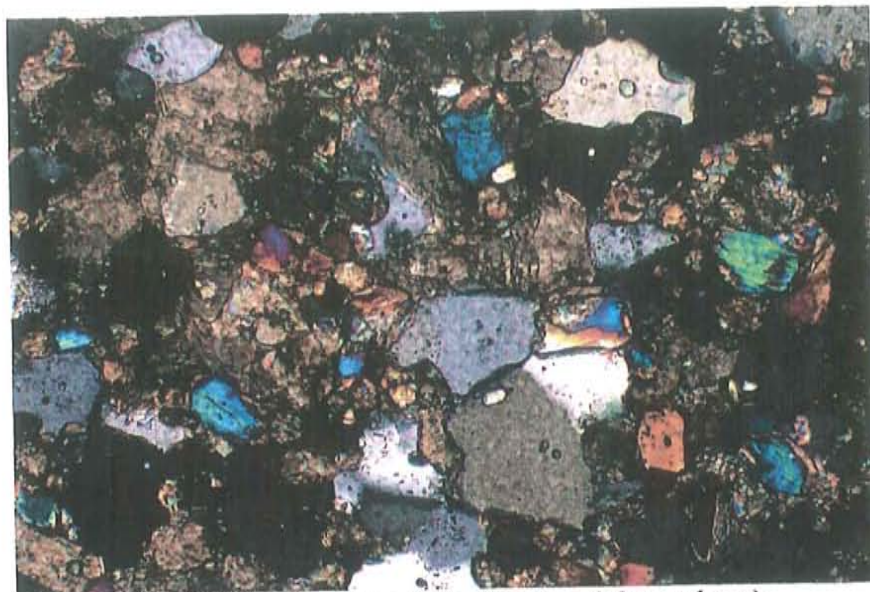


Photo 24: Diopside skarn. (f.o.v. = 0.9 mm long)



Photo 25: Tremolite (?) replaced by calcite and fine grain silica. (f.o.v. = 0.9 mm long).

The last sample (SM-06/06/06-13) corresponds to a possible fine grain sandy limestone that has now been replaced by chert. Evidence that suggests that it was limestone is the presence of outlines of possible fossils, one of these appears to have been an echinoderm (Photo 27); these are now filled with chert. Detrital quartz is still present. Submillimeter scale calcite veins cut the rock. This sample yielded the lowest $\delta^{13}\text{C}$ value of all the analyzed values.



Photo 26: Garnet skarn cut by calcite and quartz veins (f.o.v. = 1.8 mm long).



Photo 27: Possible crinoid has been replaced by chert (f.o.v. = 1.8 mm long).

Transects

All the sampled transects are located in the vicinity of an old mine (Argent, Bullion, Ben Harrison, Price, Calumet and Galena King, Figure 15). Most of the samples collected on these transects plot within the least altered group (Figure 16). Diagrams of distance vs. $\delta^{13}\text{C}$ and distance vs. $\delta^{18}\text{O}$ were done for each transect specifically (Figures 17 to 22).

Samples of the transect located near the Calumet Mine are characterized by having very low $\delta^{13}\text{C}$ values (Figure 17), these samples are located near a major intrusion. The two lowest $\delta^{13}\text{C}$ values correspond to white limestones. Some of the values seem to be controlled by structures, for example lower $\delta^{13}\text{C}$ and $\delta^{18}\text{O}$ values are seen on a sample obtained from one shaft, but this is not observed on samples recollected in the outcrop of another shaft. Samples from the Bullion transect have low $\delta^{18}\text{O}$ values characteristic of hydrothermal alteration. (Figure 18).

The Argent, Ben Harrison, Galena King and Price transects (Figures 19 to 22) are characterized by having mostly samples that belong to the least altered group. Lower $\delta^{13}\text{C}$ and $\delta^{18}\text{O}$ values are usually located near structures (structure controlled), such as intrusions and ore bodies (mantos and veins). For example in the Argent transect (Figure 19), the lowest $\delta^{13}\text{C}$ and $\delta^{18}\text{O}$ values correspond to a sample that was taken right next to the mine, also there is a sample with relatively low $\delta^{13}\text{C}$ and $\delta^{18}\text{O}$ values that is located near a quartz latite porphyry intrusion. Another good example is in the Prize transect where the lowest $\delta^{13}\text{C}$ and $\delta^{18}\text{O}$ values are from a sample taken close to a manto.

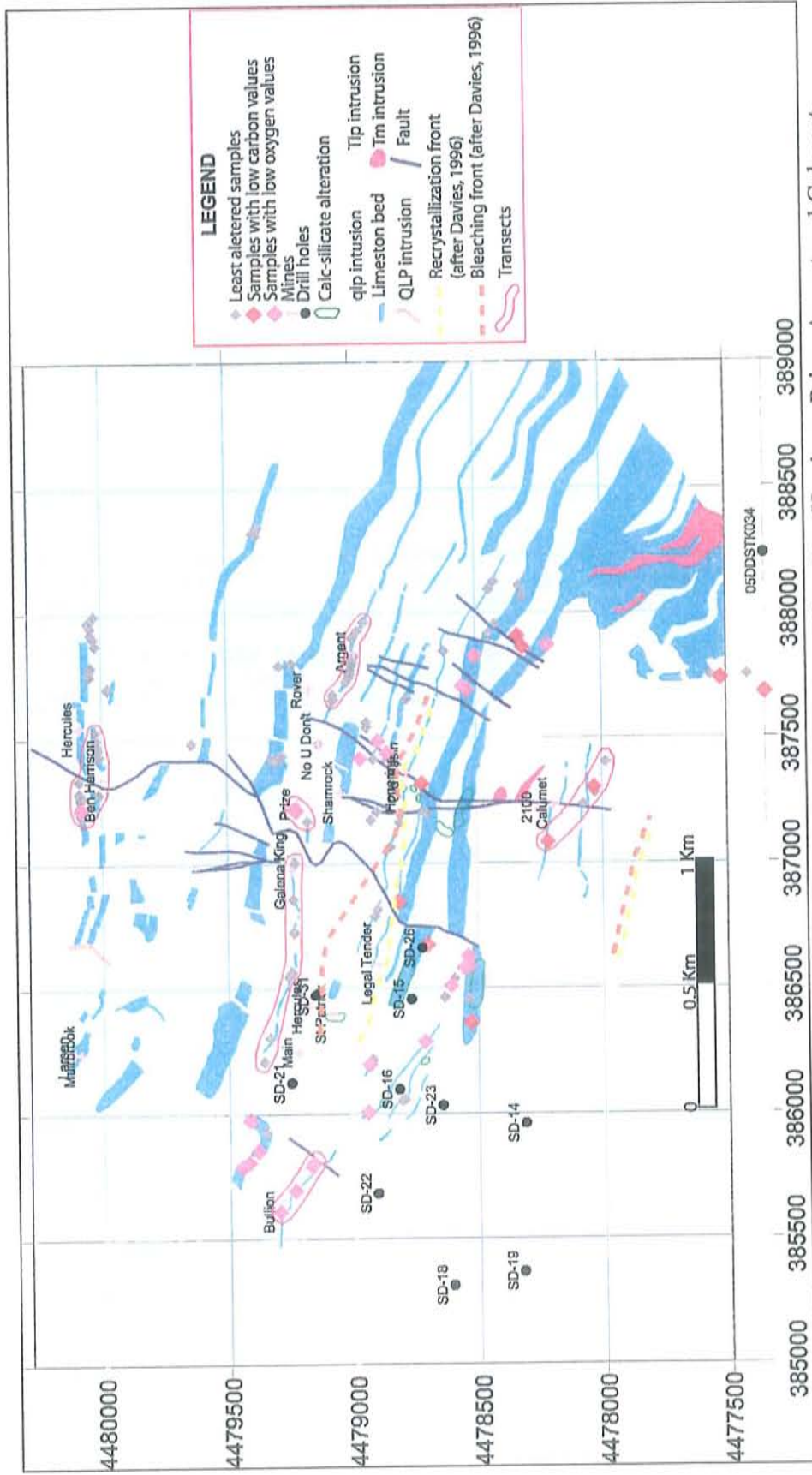


Figure 15: Transects sampled around the mines: Bullion, Galena King, Ben Harrison, Prize, Argent and Calumet.

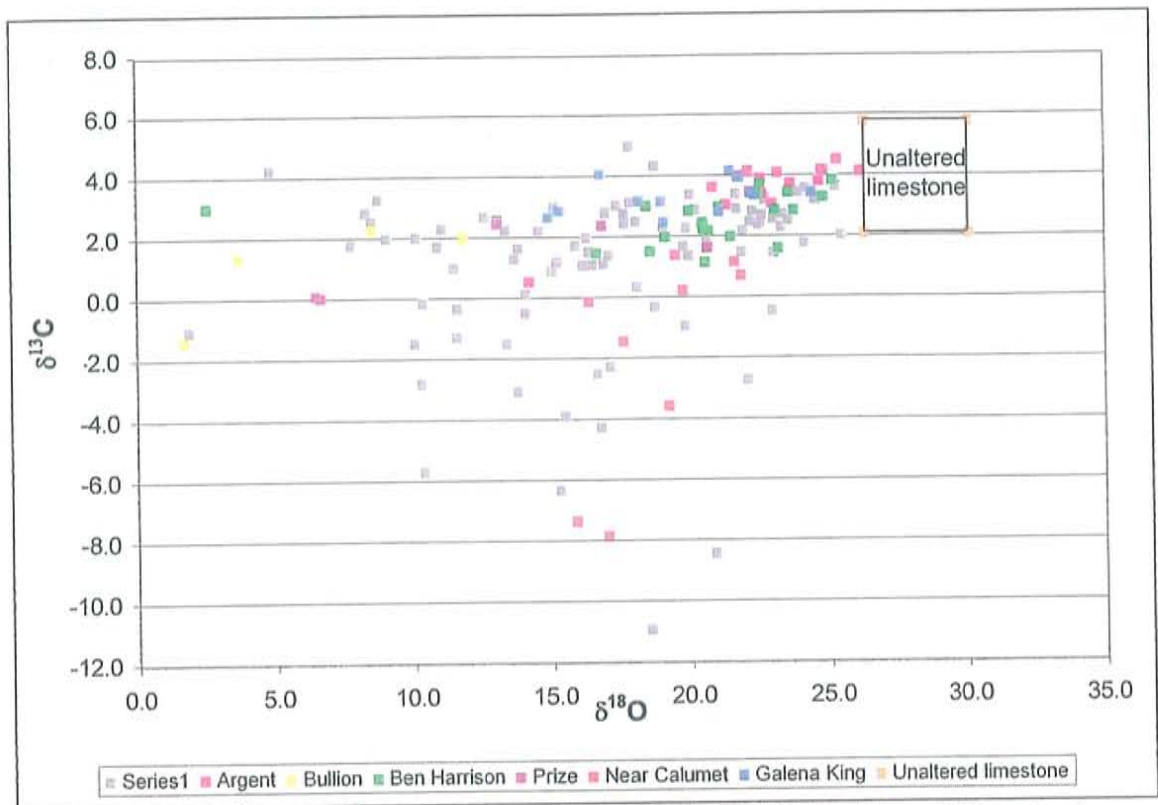


Figure 16: $\delta^{13}\text{C}$ vs. $\delta^{18}\text{O}$ diagram. Each transect is highlighted in a different color.

In these transects again it is shown that veins are commonly lighter than their host rocks; suggesting that they precede the contact metamorphism and hydrothermal alteration. If the veins formed before these processes, it is expected that when hydrothermal fluids and contact metamorphism lowered the isotopic composition of the rocks they also affected the veins present in the rocks.

There are other samples that fall outside of the transects that were also collected next to some main structure such as an ore bodies (veins or mantos), faults or intrusions (Figure 23). This part of the study shows that in most areas the fluid flow is structurally controlled.

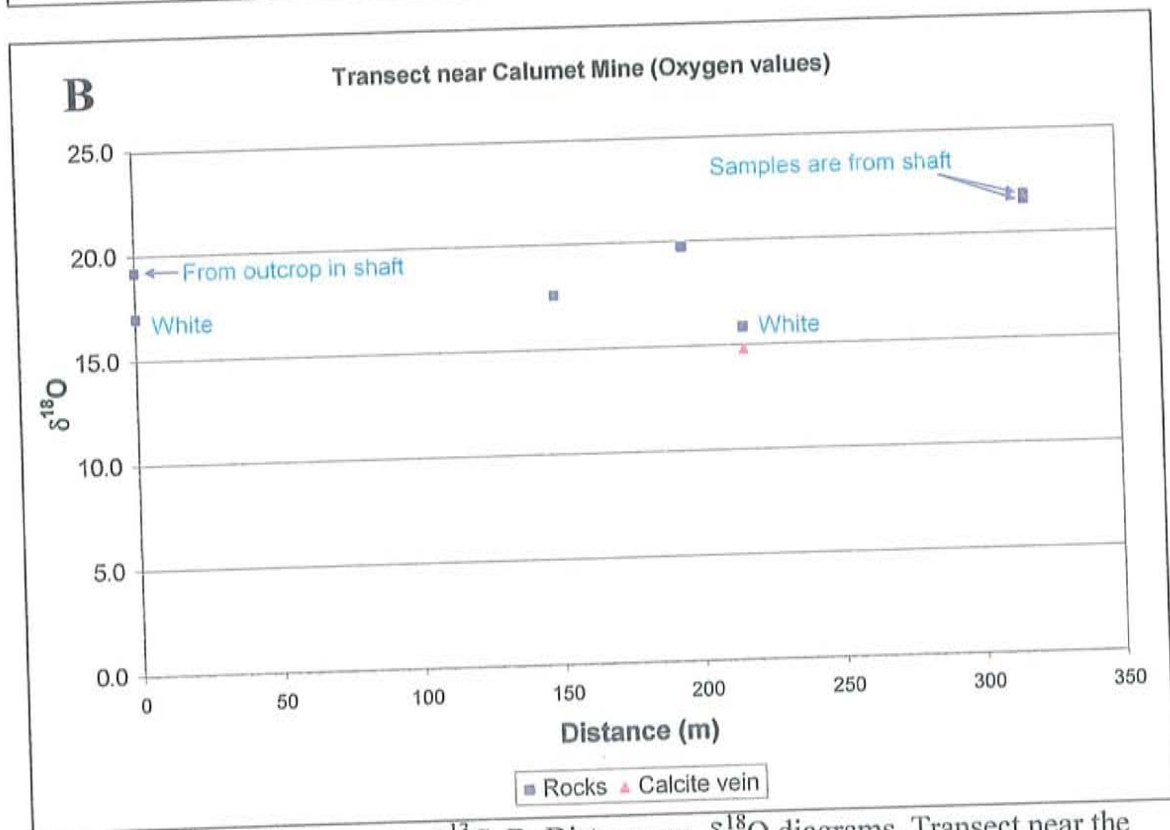
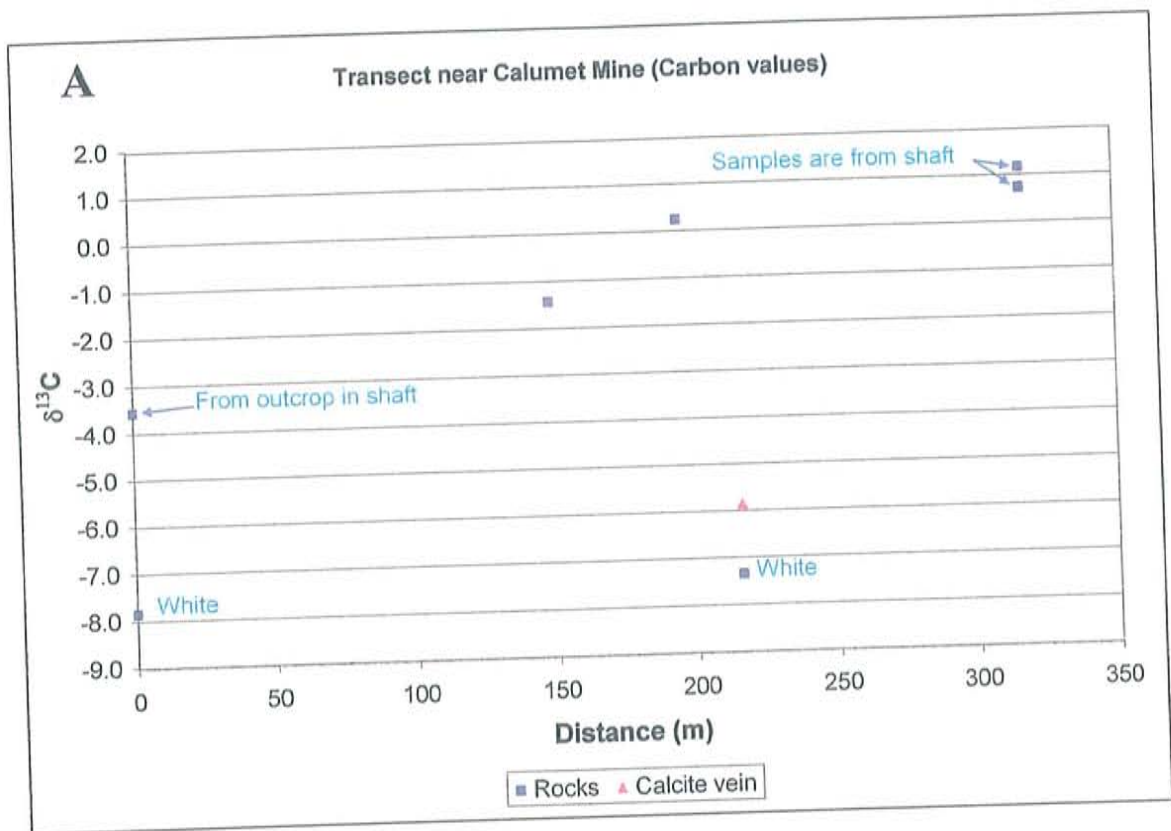


Figure 17: A: Distance vs. $\delta^{13}\text{C}$. B: Distance vs. $\delta^{18}\text{O}$ diagrams. Transect near the Calumet mine.

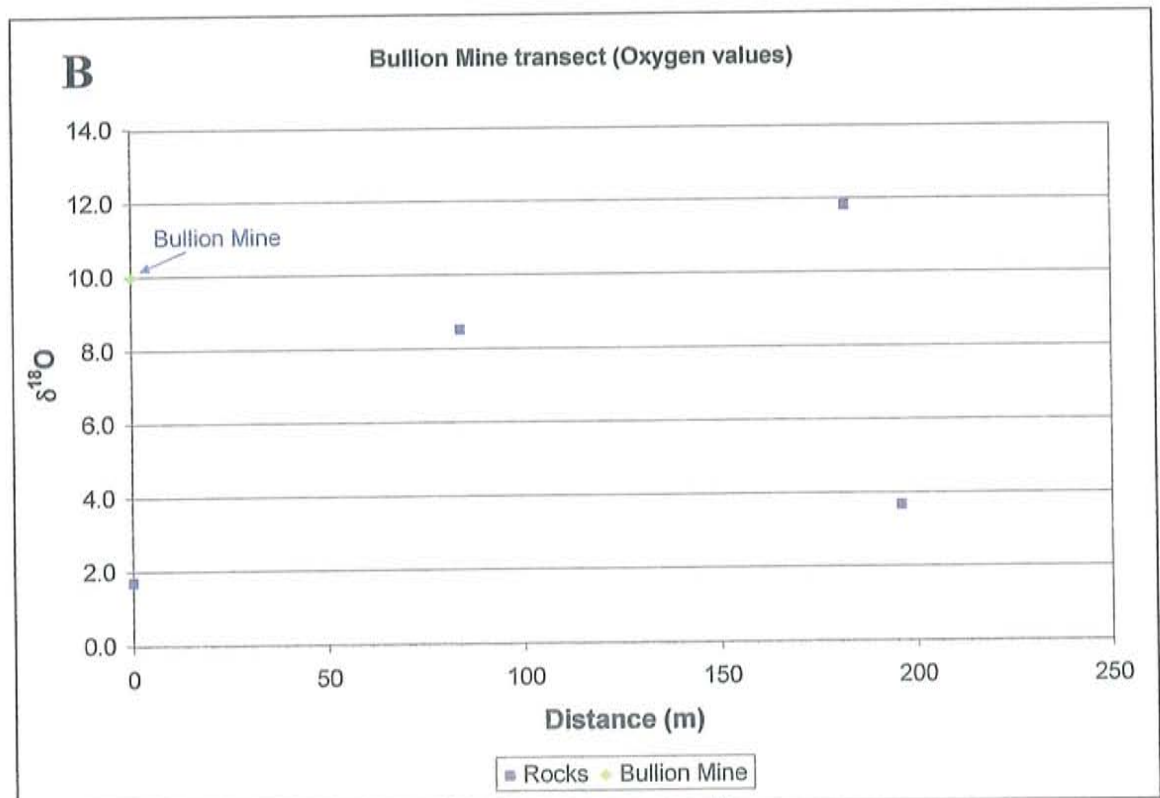
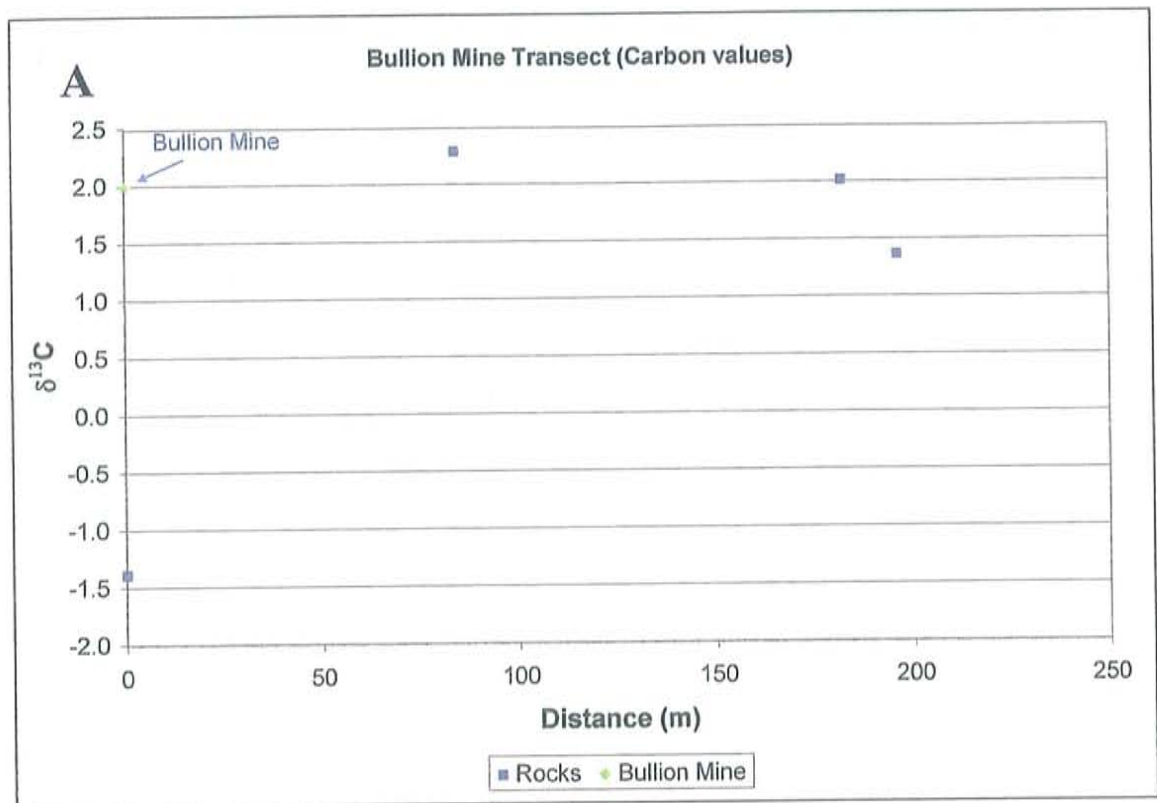


Figure 18: A: Distance vs. $\delta^{13}\text{C}$. B: distance vs. $\delta^{18}\text{O}$ diagrams. Bullion Transect

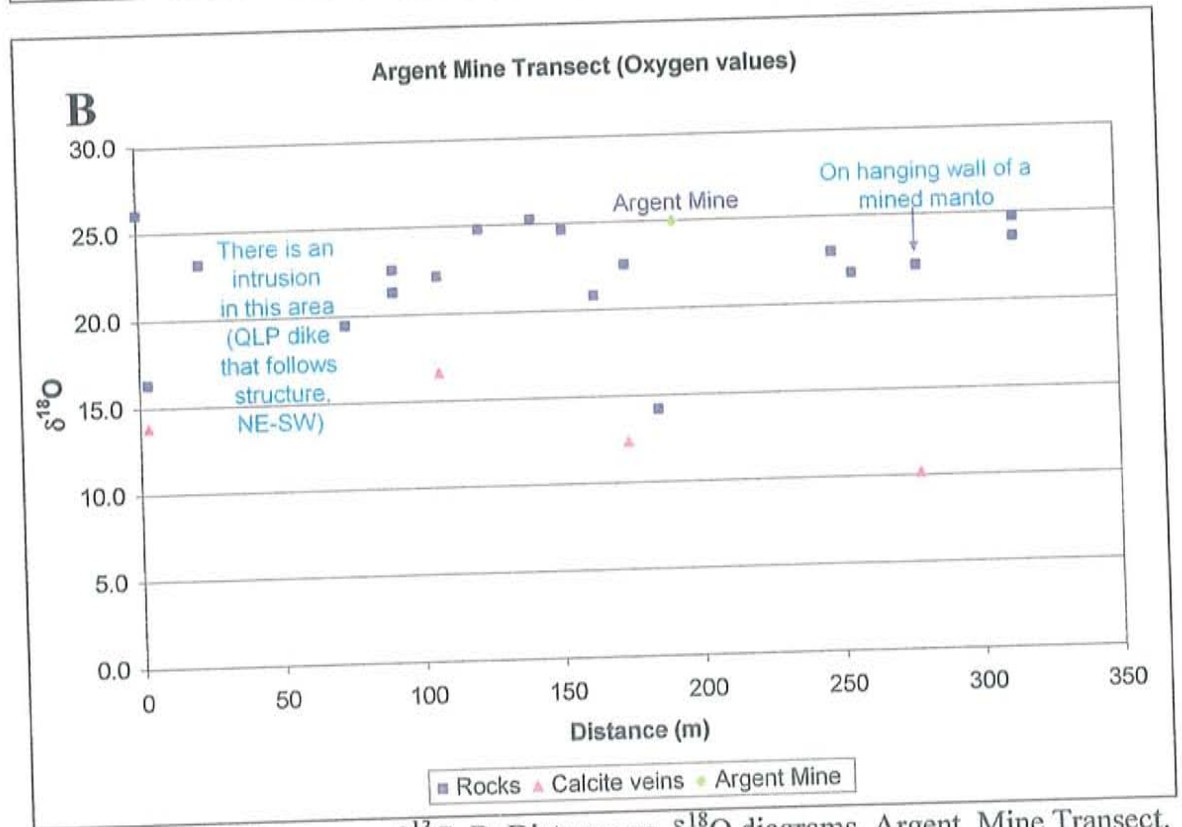
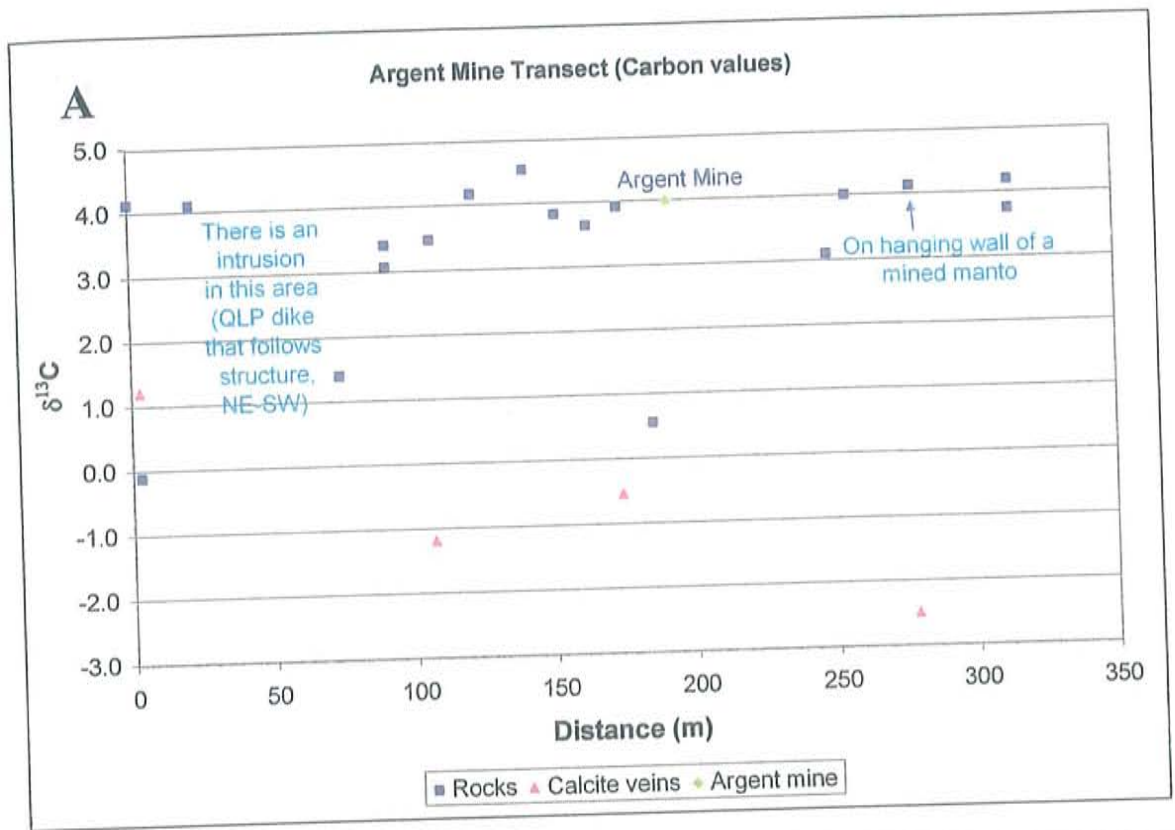


Figure 19: A: Distance vs. $\delta^{13}\text{C}$. B: Distance vs. $\delta^{18}\text{O}$ diagrams. Argent Mine Transect.

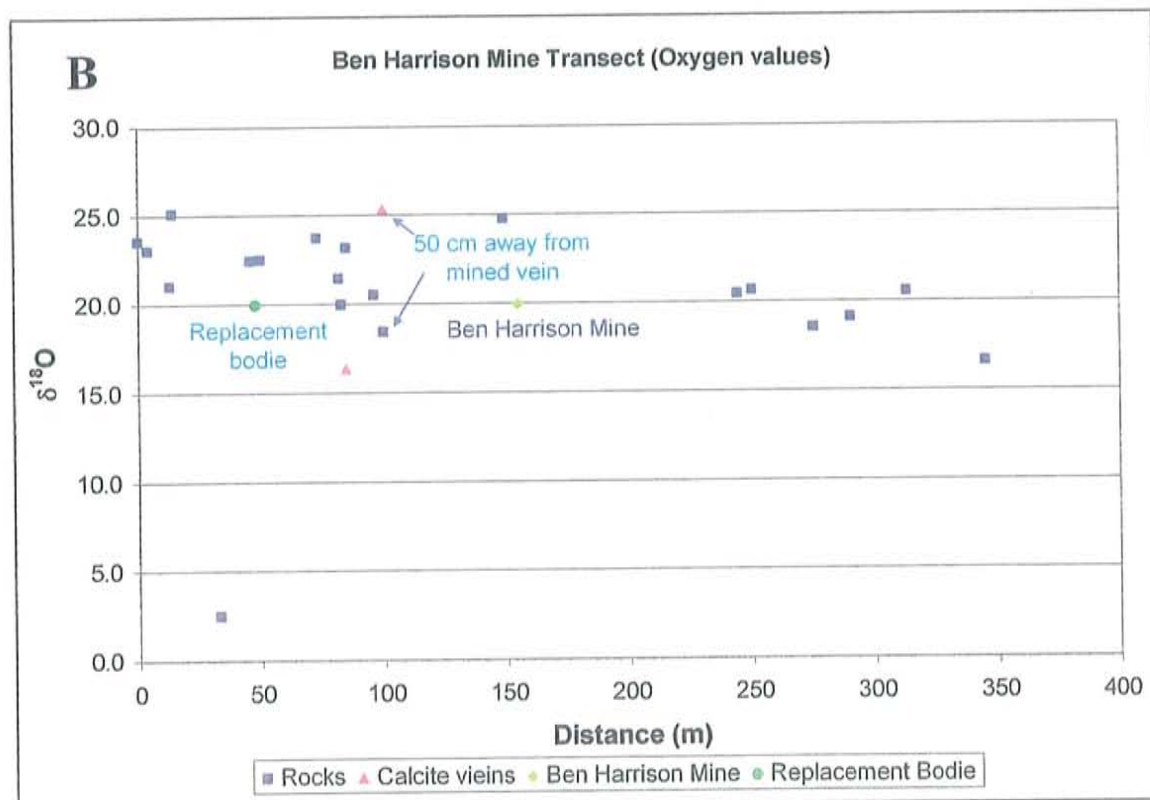
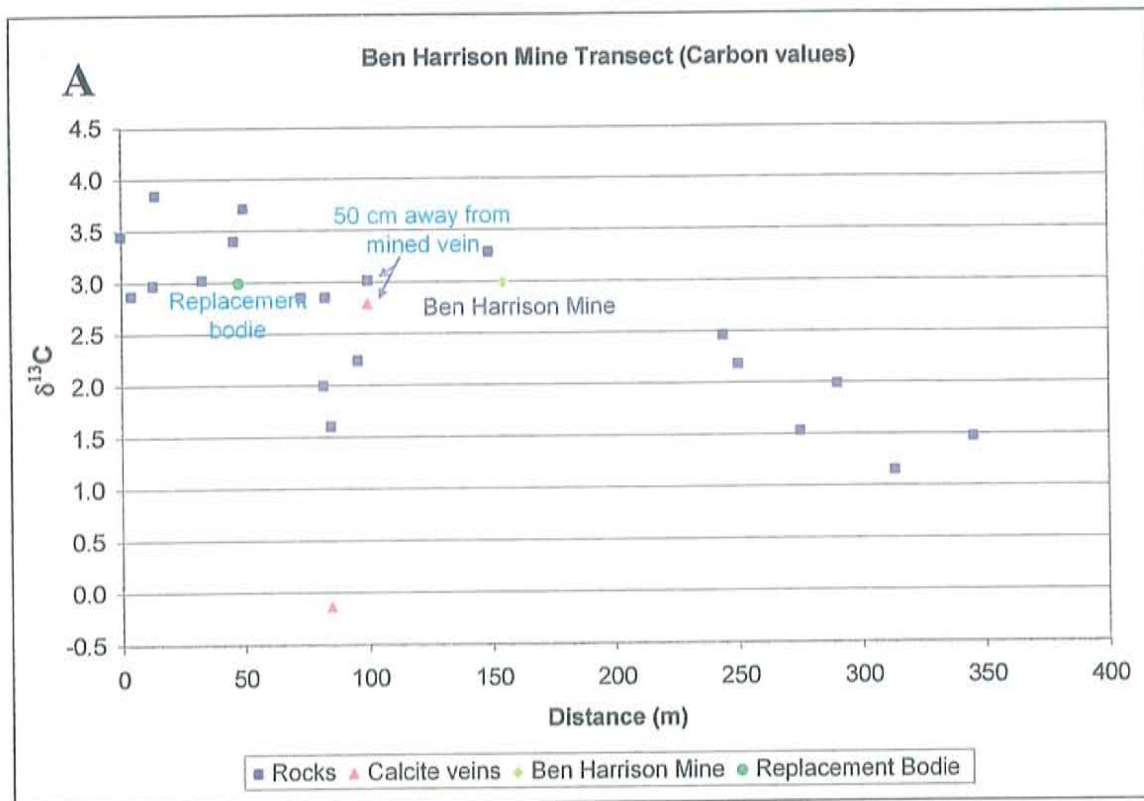


Figure 20: A: Distance vs. $\delta^{13}\text{C}$. B: Distance vs. $\delta^{18}\text{O}$ diagrams. Ben Harrison Mine Transect.

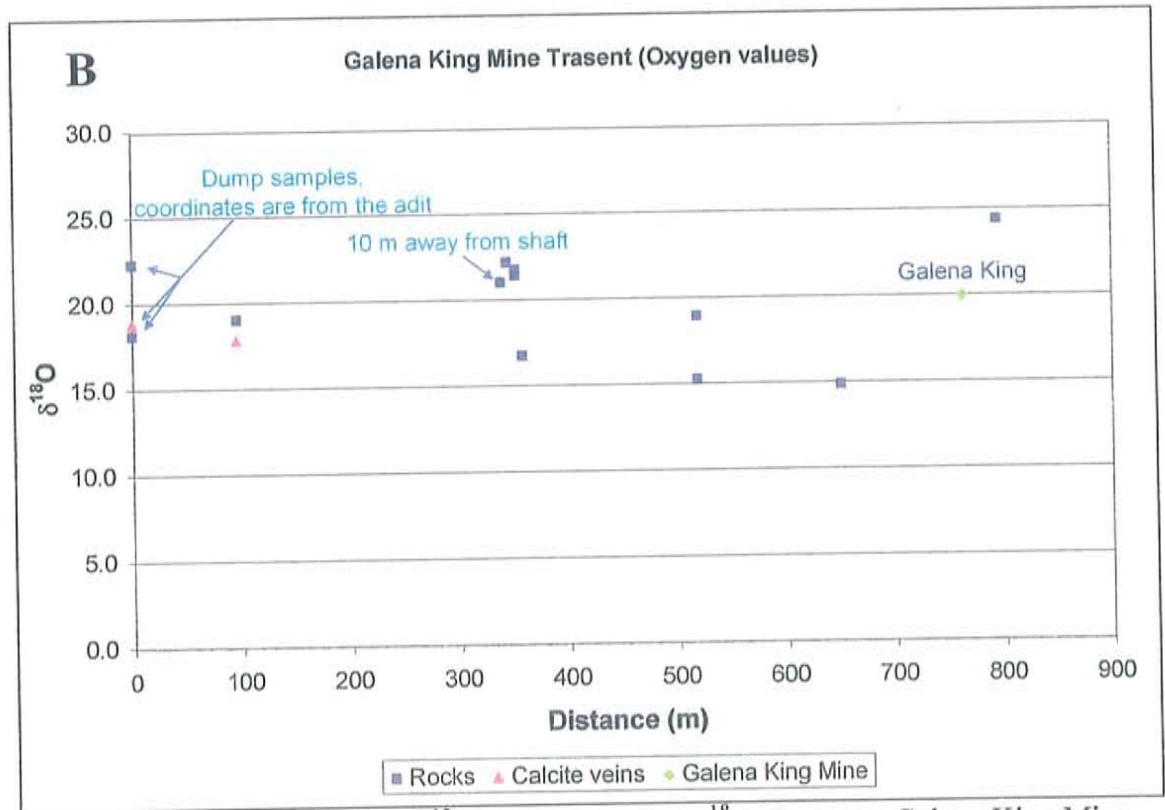
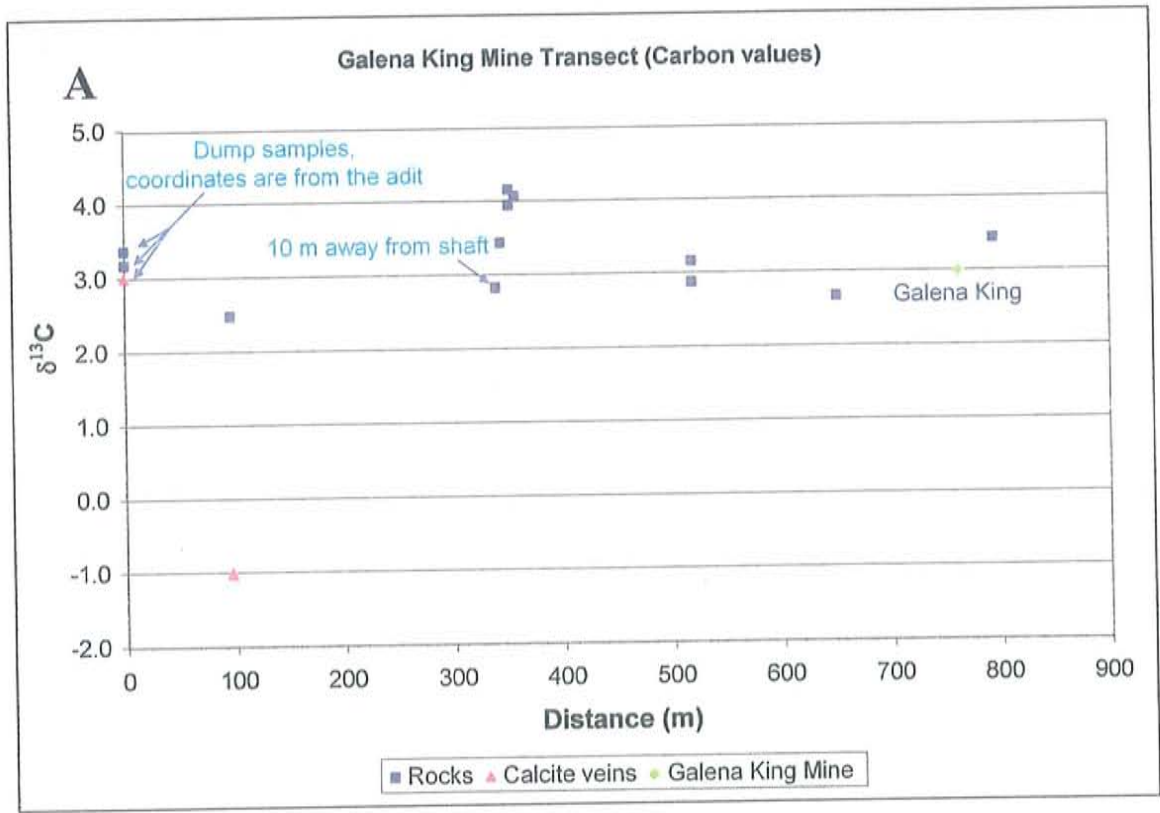


Figure 21: A: Distance vs. $\delta^{13}\text{C}$. B: Distance vs. $\delta^{18}\text{O}$ diagrams. Galena King Mine Transect.

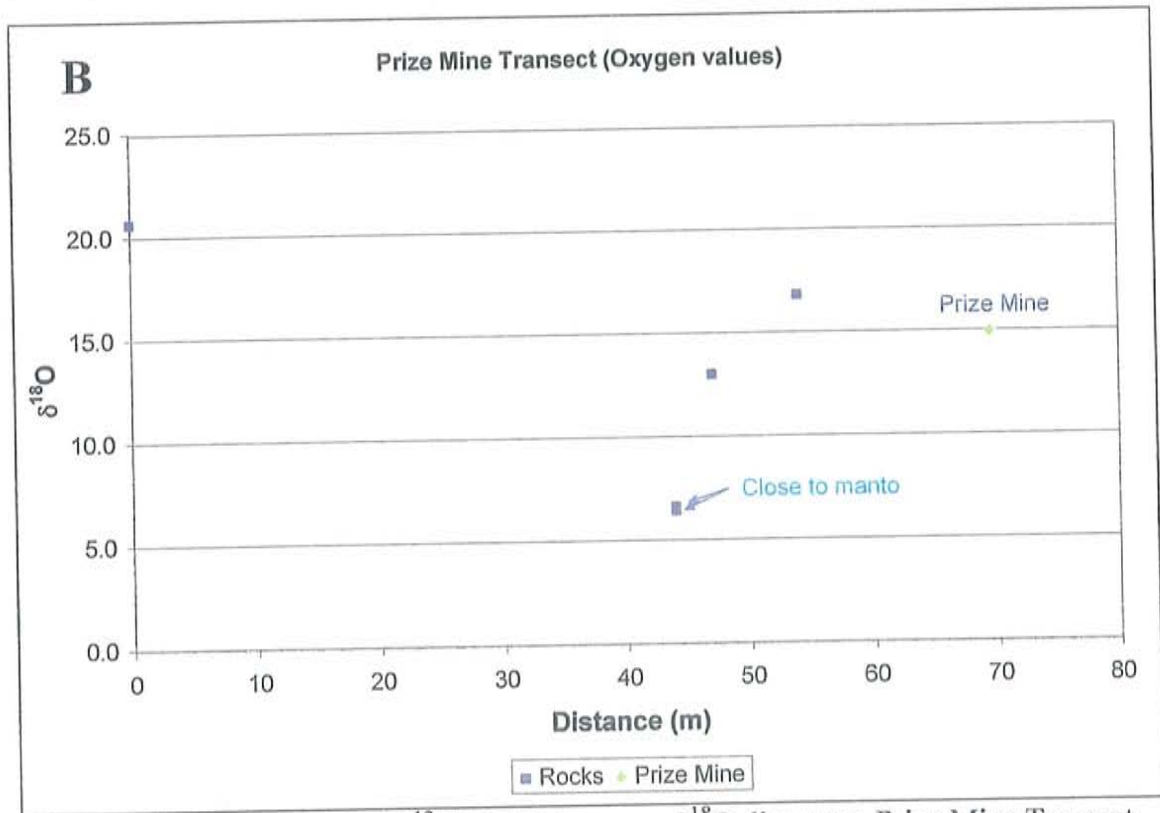
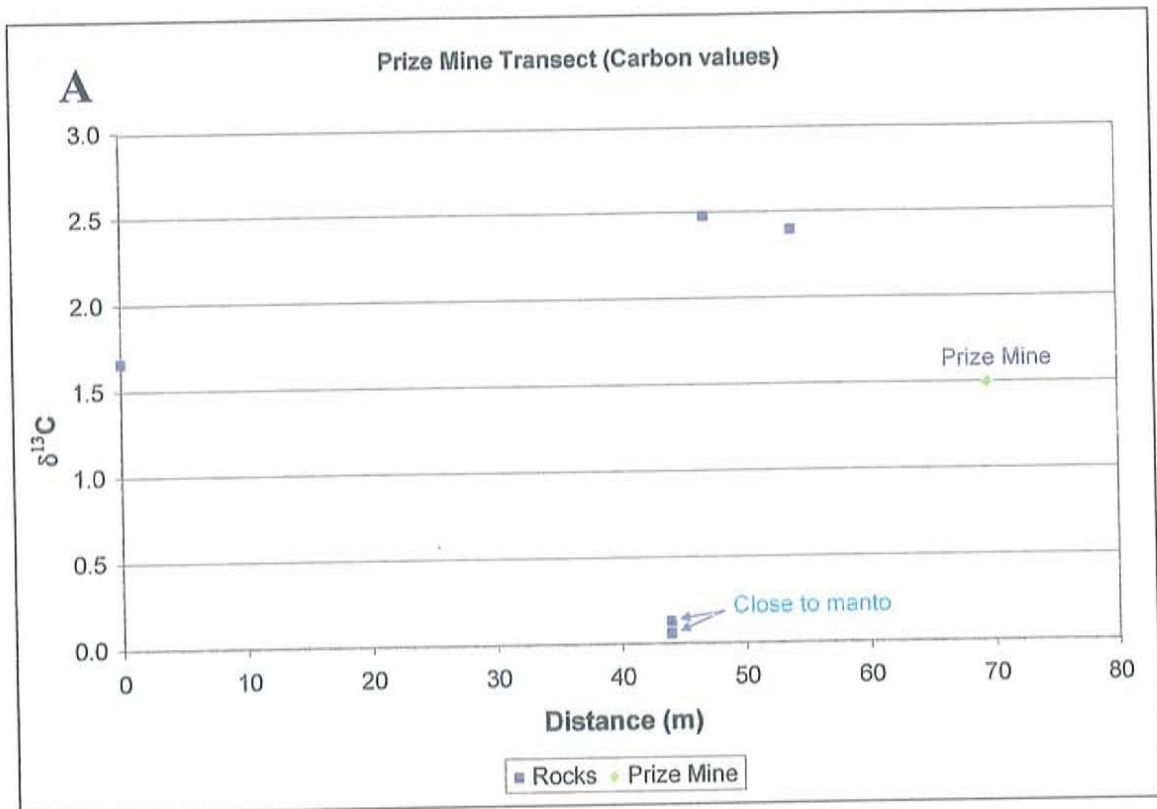


Figure 22: A: Distance vs. $\delta^{13}\text{C}$. B: Distance vs. $\delta^{18}\text{O}$ diagrams. Prize Mine Transect.

Spatial distribution

The least altered samples occur everywhere in the map, which is expected considering that presumably all samples have been diagenetically altered, but there are certain areas with a bigger concentration of samples that have been altered by either hydrothermal fluids or contact metamorphism (Figure 24).

Sample SM-15/06/06/-1 was collected approximately 1 km southeast of the map shown figure 24 (coordinates for this sample are: 389521mE / 4476694mN), and it was taken near a contact with a Monzonite sill; $\delta^{13}\text{C}$ and $\delta^{18}\text{O}$ values obtained fall in the least altered group.

There are two areas that have experienced a greater fluid flow (lowest $\delta^{18}\text{O}$ values) causing a more pervasive alteration, one is centered on drill hole SD-16 and one is located west of the Argent Mine, which encompasses the Prize and Shamrock mines. Samples from the Bullion transect are located in one of the areas that has been affected by pervasive fluid flow.

Around drill hole SD-16, samples with low $\delta^{18}\text{O}$ are from the King and Paisley limestone, in this case fluid flow followed stratigraphy. On the other hand near the Prize and Shamrock mines, samples that have been depleted in oxygen do not follow any specific bed; instead it appears that fluid flow was controlled by the abundant faults in the area, these faults strike northeast (Figure 24). These faults form part of the north-south system are considered to be of economic importance due to their close association with mineralization (Gilluly, 1932).

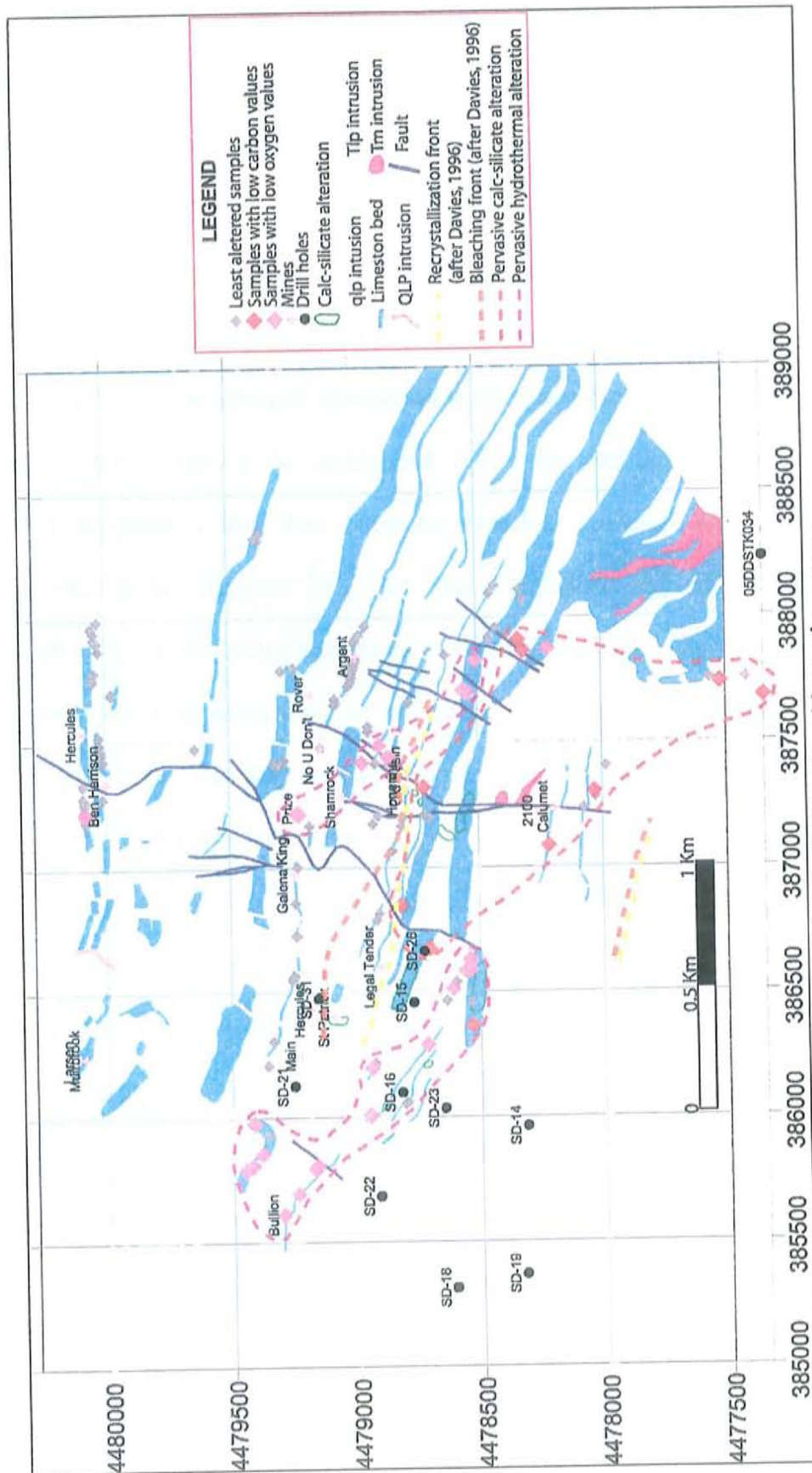


Figure 24: Regional isotopic pattern.

Low $\delta^{13}\text{C}$ samples are all located in the south part of the map; these fall near the greater concentration of areas that have been mapped as having calc-silicate alteration. Also one of the biggest intrusive bodies in the area is located in the vicinity of the Calumet mine (Davies, 1996), were some of the low $\delta^{13}\text{C}$ samples plot.

There is a zonation of the metamorphism in the area, this is possibly a consequence of the proximity to a "large intrusive mass" which occurs beneath the sedimentary cover, the strongest metamorphic alteration corresponds to skarn, which is located in the center, it is surrounded by a recrystallized zone ("intermediate metamorphic grade"), and then an outer bleached corresponding to the "lowest metamorphic grade" (Figure 24). The skarn alteration has calc-silicate minerals associated to it; the recrystallization alteration is mainly textural, almost no new minerals are formed, except for some silicification, and the bleached rocks are identified by their hardness and the fact that they are less reactive to acid when compared to the rocks that have not been altered (Davies, 1996).

Samples with low $\delta^{13}\text{C}$ values fall within these alteration zones, this correlates well with the assumption that these low values are a consequence of contact metamorphism. The southern limits of the recrystallization and bleached zones could not be exactly determined due to the alluvial cover in that area (Davies, 1996).

Fluid Inclusions

The goal of this study is to document the types of fluid inclusions that occur in the samples from Stockton. The inclusions will be described in terms of types and number of phases present in the inclusion at room temperature. This only a preliminary fluid inclusion study, as was envisioned for this thesis and microthermometric studies are

necessary to more completely understand the fluid inclusions in the igneous and sedimentary rocks of the Stockton area.

Six of the seven drill hole samples analyzed correspond to intrusive igneous rocks, only one collected from drill hole SD-21 at 137 ft. is of sedimentary origin. Sample SM-23/05/06-8 taken from an outcrop corresponds to a quartzite breccia.

In all the samples, fluid inclusions are found in quartz, and except for one sample it corresponds to vein quartz; this exception is sample SD-21-2130.5 ft. where inclusions occur in magmatic quartz, but the presence of halite bearing inclusions (Photo 28) suggests alteration by hydrothermal fluids (Appendix D).

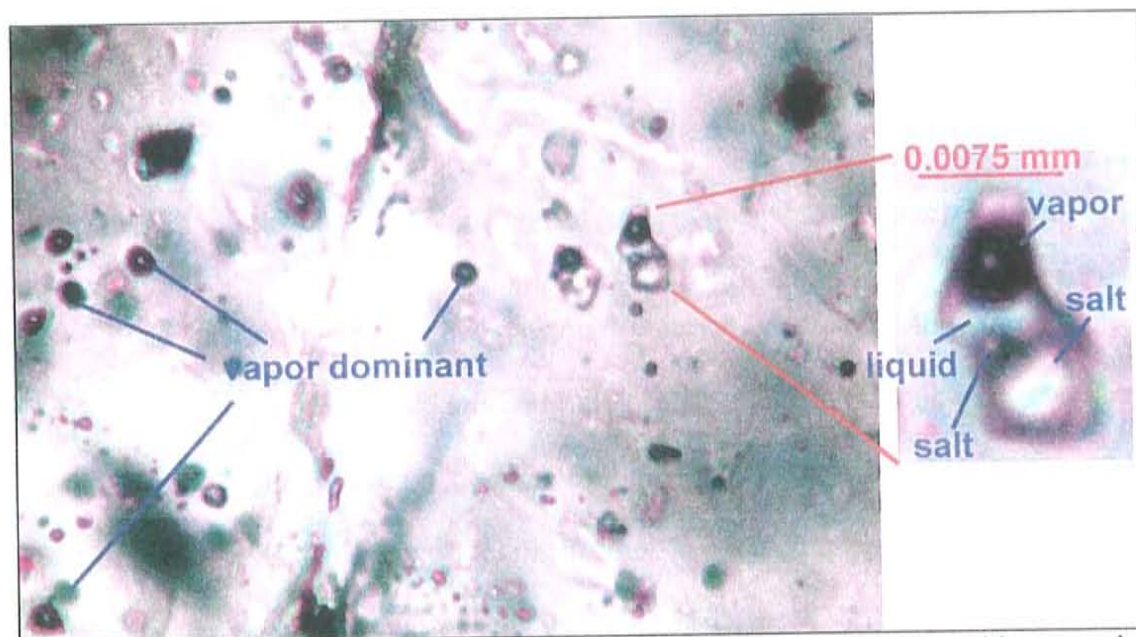


Photo 28: Liquid + vapor + two salts (halite and sylvite), occurs together with vapor-rich fluid inclusions, sample SD-21-2130.5 ft.

Inclusions that contain salt daughters, “brine inclusions” are present in all the analyzed samples, including the one collected at surface (Photo 29). When only one salt “daughter” is present, it is probably halite. A second salt “daughter” is also sometimes present, and possibly corresponds to sylvite (Photo 29 and photo 30).

Inclusions with multiple daughters, sometimes including opaques, were also observed in samples SD-16-1103 ft. (Photo 31), SD-21-1633 ft., and SD-23-1448 ft. (Photo 32).



Photo 29: Liquid + vapor + two daughters (possibly halite and sylvite), sample SM-23/05/06-8.

Fluid inclusions with opaque daughters were observed in all the samples except for SM-23/05/06-8, collected at surface. Some opaque daughters have a triangular shape (Photo 31) and a yellow color under reflected light, these are possibly chalcopyrite; if this is the case the fluids that formed these inclusions had a high copper content. Triangular shaped opaques were observed in samples SD-16-1103 ft., SD-21-1002 ft., SD-21-1633 ft. and SD-23-1448 ft. Due to the limited amount of samples a good correlation between the copper grade and the presence of triangular opaques could not be determined, although there is one sample (SD-23-1448 ft.) that correlates with a very high copper grade (1.48%).

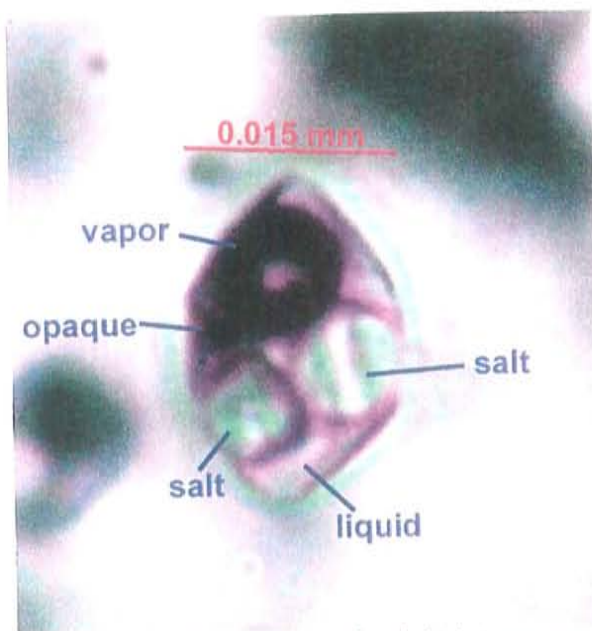


Photo 30: Liquid + vapor + two salts (halite and sylvite) + opaque daughter, sample SD-23-1448 ft.

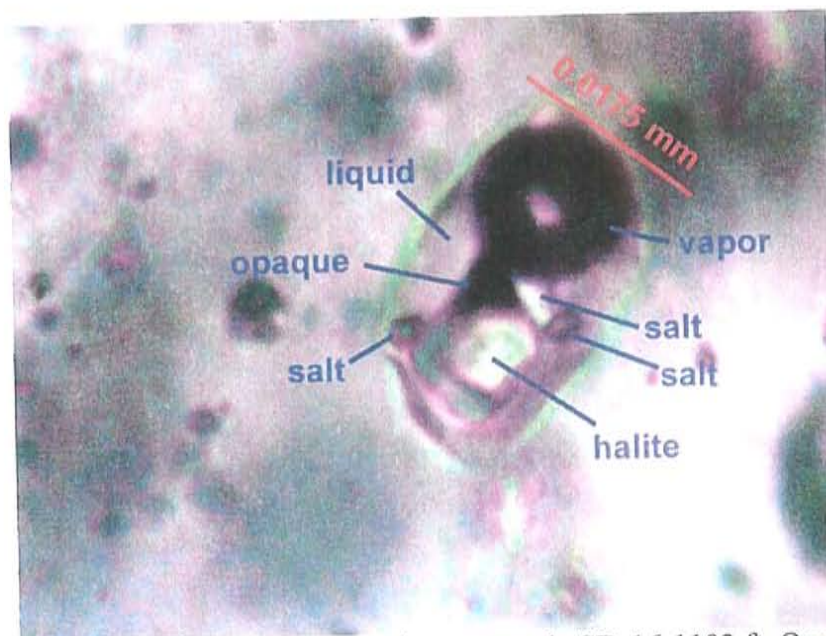


Photo 31: Liquid + vapor + multiple daughters, sample SD-16-1103 ft. Opaque daughter has a triangular shape.

Vapor-rich inclusions are present in all the samples and are overall the most abundant type; and are usually characterized by having a euhedral shape (Photo 33). These inclusions sometimes have a halite daughter (Photo 34), an opaque daughter (Photo 35) or both (Photo 36).



Photo 32: Liquid + vapor + multiple daughters, sample SD-13-1448 ft.



Photo 33: Vapor-rich with euhedral inclusion, sample SD-21-2130.5 ft.

Even though secondary fluid inclusions are also present in the analyzed samples, which are identified due to the fact that they have a linear nature, presumably following fractures, only inclusions that appeared primary in origin are described herein, and it is assumed that these formed by the same fluids that precipitated the quartz. Some

inclusions in fractures could also be pseudosecondary, meaning they formed in fractures while the crystal was still growing (Guilbert and Parks, 1986), but since these can not be easily differentiated from the secondary inclusions they were not taken into consideration.

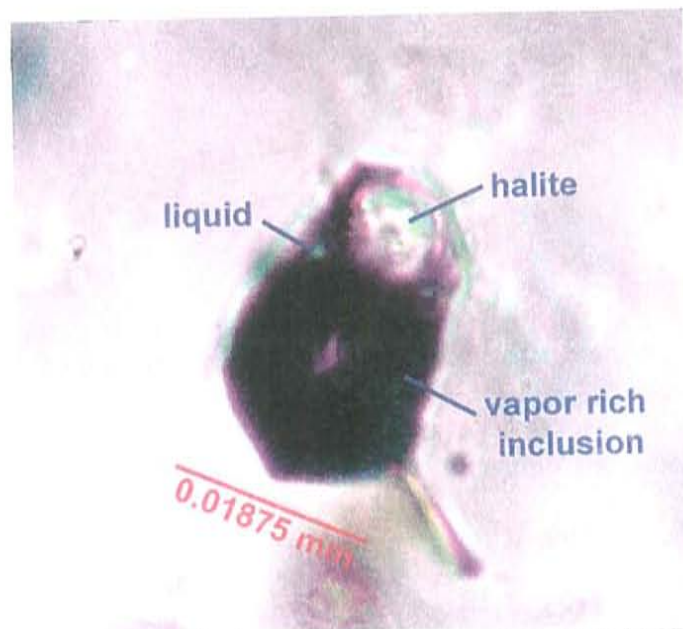


Photo 34: Vapor-rich inclusion with halite daughter, sample SD-23-1448 ft.



Photo 35: Vapor-rich with a dark daughter, sample SD-21-2130.5 ft.

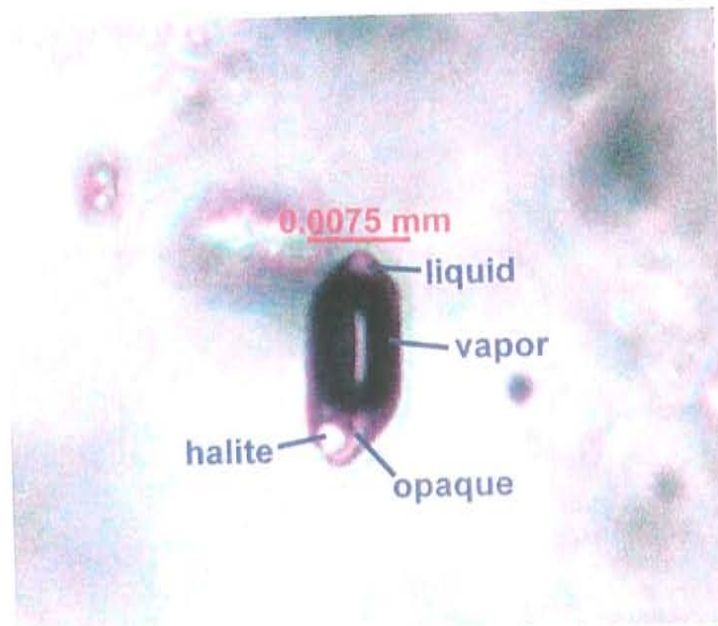


Photo 36: Vapor-rich fluid inclusion + halite + opaque daughter, sample SD-21-1633 ft.

All the igneous fluid inclusion samples fall within the area defined as having predominantly K-silicate constructive alteration with a phyllic overprint (Figure 25). Sample SD-21-137 ft., which corresponds to a sedimentary rock, is not shown in the profile. The locations where triangular opaques were observed are also shown in figure 25.

Comparison to Bingham

Fluid inclusions found in quartz veins in the QMP, which contains the highest copper grade of the Bingham orebody, include brine inclusions, vapor-rich inclusions and critical-type inclusions, these have been documented by Redmond et al. (2004) (Figure 26). Brine inclusions and vapor-rich inclusions are more common in veins present at higher elevations, whereas the critical type inclusions are only present at greater depths; the upper limit of these types of inclusion is shown in figure 26. Critical-type fluid inclusions are CO₂ rich inclusions and usually contain an opaque daughter, possibly chalcopyrite (Redmond, et al., 2004).

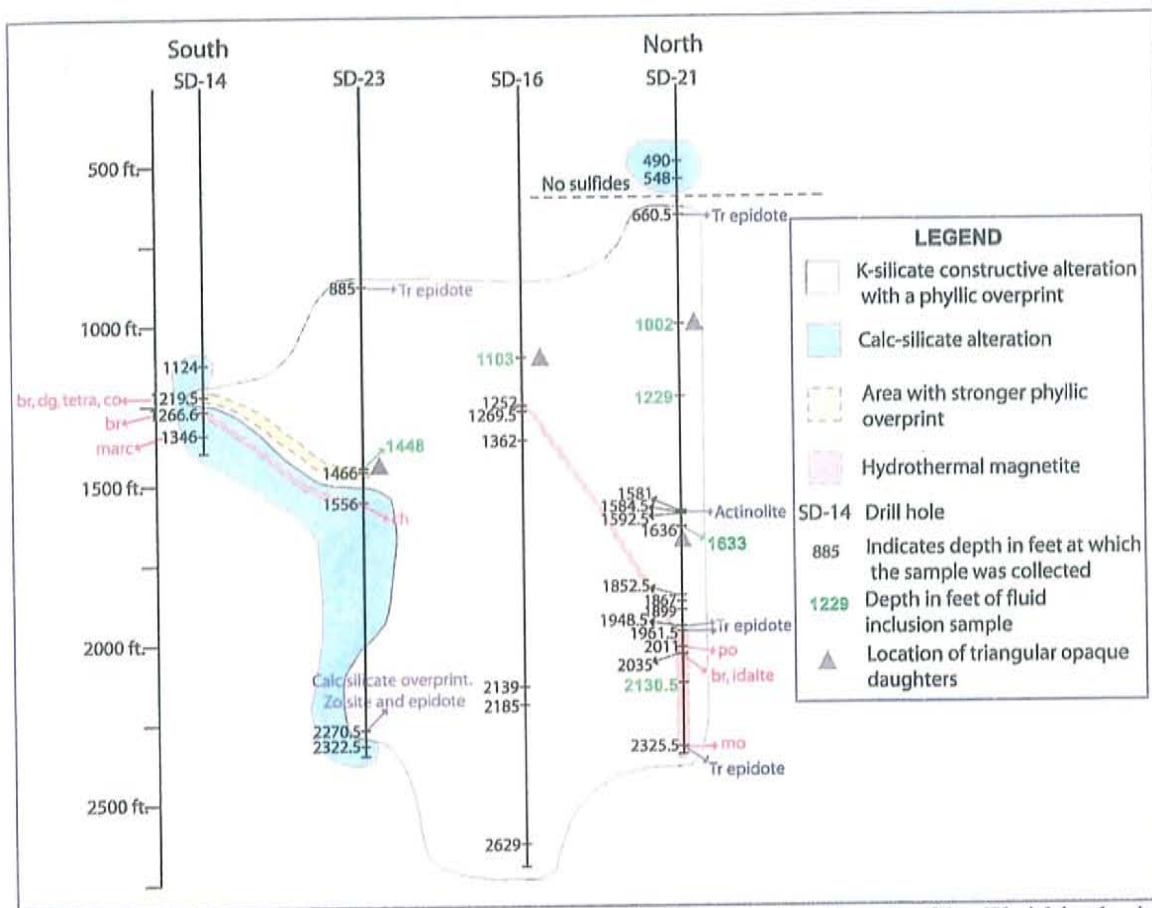


Figure 25: Location of fluid inclusion samples in the alteration profile. Fluid inclusion samples are highlighted in green.

In the Stockton samples it is common to find vapor-rich inclusions occurring together with brine inclusions (Photo 28), which indicates that the fluids that formed them were probably boiling at the time of entrapment; this was also observed in the QMP quartz vein inclusions analyzed from the Bingham orebody (Redmond, et al., 2004).

Vapor-rich inclusions and brine inclusions can be easily identified in the Stockton analyzed samples but microthermometric studies would be necessary to determine the presence of CO₂-rich “critical-type” fluid inclusion.

Analyzed Bingham samples are associated with hydrothermal K-feldspar + biotite, indicating a K-silicate constructive alteration (Redmond, et al., 2004), which is

also the case of most of the studied Stockton samples, excluding the two sedimentary rocks. Copper in Bingham occurs above the critical-type inclusions, grade contours at are shown in figure 26.

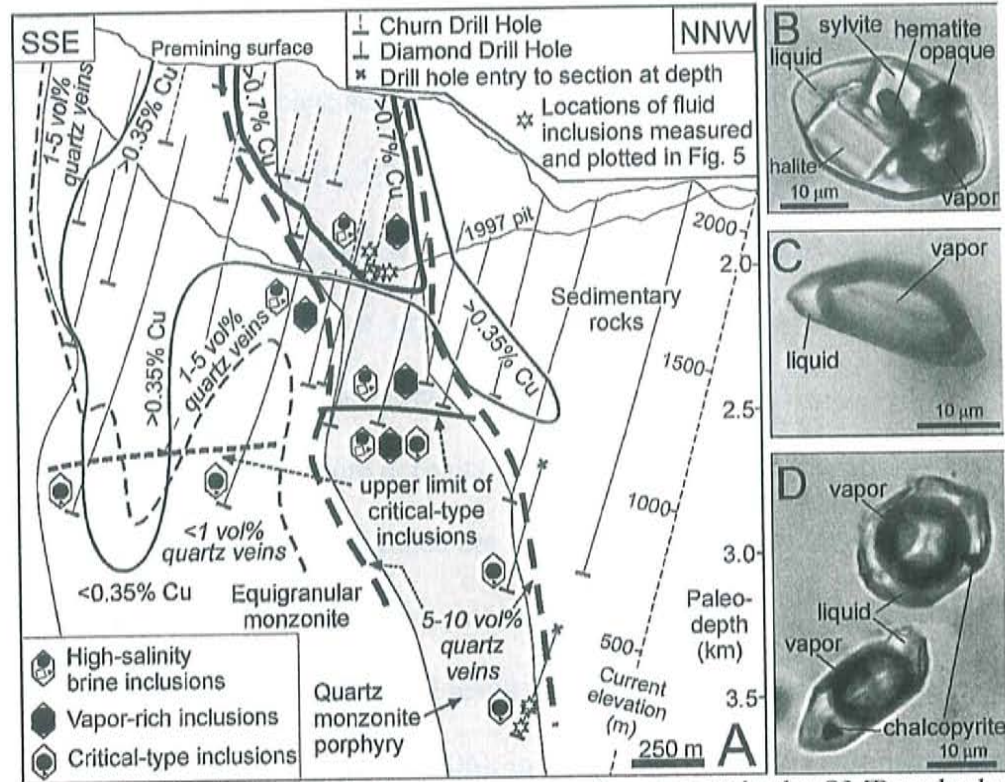


Figure 26: Fluid inclusion study done in quartz veins present in the QMP orebody of the Bingham Canyon deposit (Redmond, et al., 2004).

The presence of these brine inclusions, typical of porphyry Cu systems, is a positive sign for mineral exploration; a more detailed fluid inclusion study could yield important exploration clues.

STABLE ISOTOPES: A VECTOR TOWARDS ORE

Several studies have been done on ore deposits in which stable isotopes are used as an exploration tool. Isotopes are mainly used to identify anomalies or halos which can be used to define drilling targets (Nesbitt, 1996). The formation of these halos is controlled by several variables; such as the original isotopic composition of the rock and the water to rock ratio (Nesbitt, 1996); the temperature and isotopic composition of the fluids will also play a major role. One of the main attractions of stable isotopes is that they can be used to recognize cryptic alteration i.e. that which is not manifest mineralogically in hand specimen (Campbell and Larson, 1998).

The studies focused on ore deposits of hydrothermal origin, because in these there are epigenetic processes in which fluids are involved, and these fluids alter the host rock and change its isotopic composition, sometimes forming halos. Higher fluid flows, meaning, greater water/rock ratios, will result in a bigger shift from the original values of the host rock (Arehart and Donelick, 2006); in the case of oxygen it will usually result in lower $\delta^{18}\text{O}$ values.

Isotope studies around prospect areas can assist in determining zones where major fluid-rock interactions occurred during the formation of the deposit, in other words they can be helpful in delimiting the areas with the highest water/rock ratios; this can be a very useful tool in exploration and can be used as a vector towards ore. Assuming that the ore minerals came with the fluids it would be expected to find the ore zones in areas with the higher water/rock ratios; if more fluids are involved there is a greater possibility for ore deposition. Barren fluids can also alter the isotopic composition of the host rocks, and

because of this, isotopic studies should be carried in conjunction with other types of studies that can help to determine the presence of ore.

Oxygen is the main isotope used since it is a main component of the hydrothermal fluids (water) and is also a major rock forming component. Carbon can be used when the wall rocks are carbonates; such is the case of the area of study. Hydrogen and sulfur are not as abundant in host rocks and thus are not as useful as an exploration tool.

Brief overview of other studies done on hydrothermal deposits

In this review only carbonate hosted deposits will be considered since they can be more relevant to the present study, but it is important to note that stable isotopes have also been used as a vector toward ore in other types of deposits such as epithermal (Criss, et al., 1995) and volcanic massive sulphides (Lerouge, et. al, 2001).

Carlin-Type gold deposits

A study was conducted in Twin Creeks Nevada to determine the presence of oxygen and carbon isotope haloes around the deposit, a total of 108 carbonate rocks were analyzed for oxygen and carbon; the conclusion reached was that low $\delta^{18}\text{O}$ values surround Carlin-Type gold deposits, and that these are a consequence of hydrothermal alteration (Stenger, et al., 1998).

Another study was done in the Pipeline hydrothermal system, with a similar goal, to use carbon and oxygen isotopes as a vector toward ore. Again 108 samples were analyzed for carbon and oxygen. Low $\delta^{13}\text{C}$ and $\delta^{18}\text{O}$ values are center around the pit (Figure 27 and 28). The shift in carbon is smaller, due to the fact that it is less abundant than oxygen in the hydrothermal fluids, so there is a less carbon to react with the carbon of the host rocks. Stable isotope depletions were found to be present up to several

kilometers from the pit, forming a large enough halo that they should be a useful tool in the exploration of similar deposits (Arehart and Donelick, 2006).

Skarn deposits

El Mochito Zn-Pb (Ag) massive skarn was studied to determine whether isotope halos can be used for exploration. The isotopic composition of eighty two limestone and calcite samples was determined (Vazquez et al., 1998). It was found that calcite from skarns has similar $\delta^{18}\text{O}$ values to the surrounding wall rocks but lower $\delta^{13}\text{C}$ values, which is also observed in the samples from Stockton.

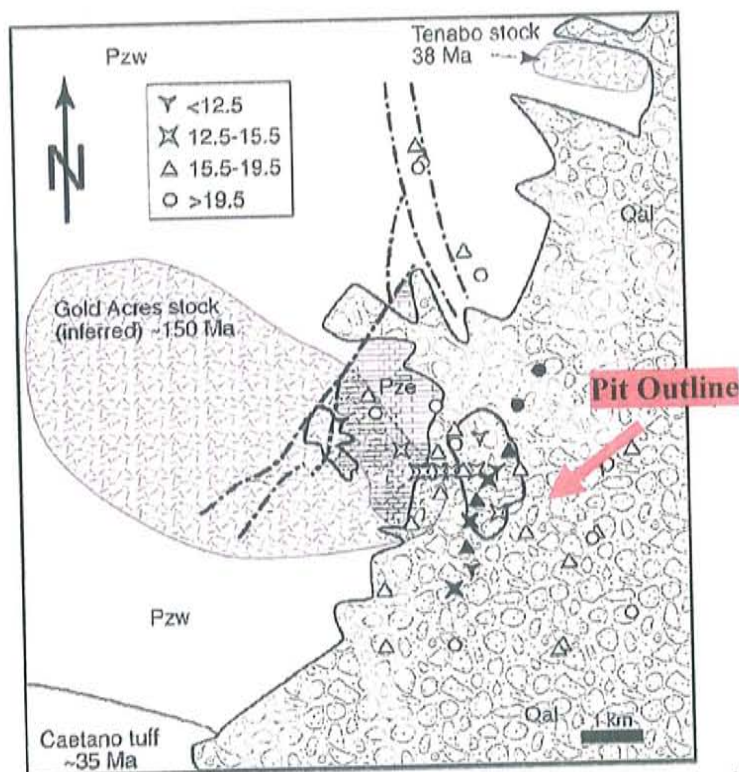


Figure 27: Sample location and oxygen isotope data from carbonate rocks. Heavy line represents the pit outline (After Arehart & Donelick, 2006).

Samples with higher (less altered) carbon and oxygen isotopic values are more abundant with distance from the deposit; these changes are more easily observed in oxygen than in carbon. In chimney-manto deposits, oxygen isotope halos can extend up

to several kilometers from the ore, on the other hand carbon halos are smaller; and almost never reach more than 30 m from the deposit (Vazquez et al., 1998).

Other isotope studies have been done on these types of deposits, such as in Naica (Mexico) and Tsumeb (Namibia) (Kesler, et al., 1995).

These studies were conducted around existing mines which is not the case of Stockton. In all of these the conclusion is similar: higher (less altered) isotopic values occur farther away from the deposit and lower $\delta^{13}\text{C}$ and $\delta^{18}\text{O}$ values are close to the mineralized body, this is mainly observed in the oxygen isotope. The present study correlates well with these observations, low $\delta^{18}\text{O}$ values are believed to have been caused by hydrothermal alteration, and the most depleted samples are interpreted to have been affected by higher water/rock ratios.

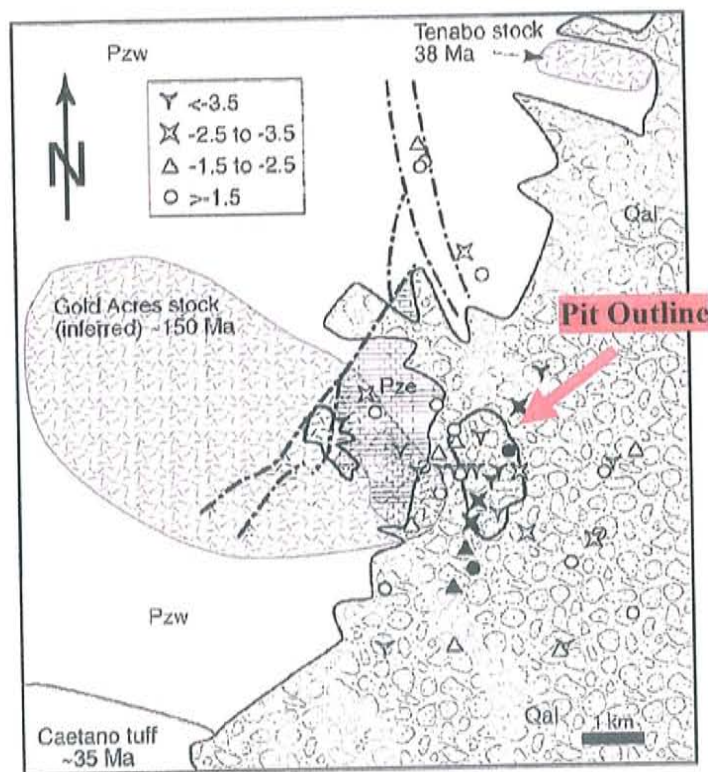


Figure 28: Sample location and carbon isotope data from carbonate rocks. Heavy line represents the pit outline (After Arehart & Donelick, 2006).

In most of these studies haloes could be determined. As mentioned in the stable isotopes chapter at Stockton fluid flow seems to have been largely controlled by structures, and in most cases the alteration is very localized near the structures such that wide spread haloes are not developed. There are however at Stockton two areas that have apparently experienced more pervasive hydrothermal alteration.

If the Stockton area had not been drilled previous to this isotopic analysis the recommendation would have been to drill in the areas that show the pervasive hydrothermal alteration, which is very interesting considering that one of the best holes (SD-16) in the area is located in the middle of one of these zones.

DISSCUSSION

Petrography Analysis and comparison to Bingham

Rock types

Most of the studied Stockton igneous rocks are intrusive in origin; these vary in composition from intermediate to felsic, with monzonites and latites most abundant. This is similar to the intrusive rocks found in the Bingham Canyon mine; which include, from oldest to youngest, monzonite, quartz-monzonite porphyry, latite porphyry dikes and quartz-latite porphyry dikes (Lanier et al., 1978). Volcanic igneous rocks in the Stockton samples include two andesites and one biotite dacite; these are from drill holes SD-18, 04RDYR01 and SD-19 respectively.

Igneous outcrop samples include one monzodiorite, one hornblende monzodiorite and two quartz-latite porphyries. Both the monzodiorite and the hornblende monzodiorite are essentially unaltered, in which clinopyroxene and hornblende are still present.

Stockton area sedimentary rocks are variably altered, except for a single sample collected from drill hole SD-15 at 72 ft. which appears to be a "fresh" limestone. This sample was also analyzed for stable isotopes and shows "cryptic" alteration, which means it was depleted in both carbon and oxygen compared to limestones of Pennsylvanian age. Probable protoliths for the Stockton sedimentary rocks include: limestones, quartz arenites and sandy limestones or limy sandstones.

Alteration

The alteration observed in samples is lithologically controlled (Figure 6 and 7). Igneous rocks present mainly a K-silicate constructive alteration with phyllic overprint; sedimentary rocks exhibit calc-silicate alteration. A few exceptions occur near lithologic

contacts, such as sample SD-23-885 ft., and sample SD-21-490 ft. The former is a quartz arenite in which hydrothermal biotite is the main alteration mineral and the latter is a quartz-lalite porphyry lacking hydrothermal biotite, that has actinolite and carbonate as the most abundant alteration minerals.

Potassium-silicate constructive alteration is characterized by the presence of hydrothermal biotite, which is the most abundant alteration mineral in the Stockton samples studied. K-silicate alteration at Bingham Canyon is characterized by the presence of quartz + K-feldspar + hydrothermal biotite. These occur in veins and as pervasive alteration and, importantly this alteration assemblage is spatially associated with Bingham Canyon copper mineralization (Babcock, et al., 1998). Hydrothermal biotite at Stockton is generally shreddy and usually occurs in clusters, mainly of fine grain biotite (Photo 4). Hydrothermal K-feldspar is not common in the Stockton samples and was only observed in a few samples from drill holes SD-16 and SD-21.

Hydrothermal magnetite is present in igneous rocks from drill holes SD-16, SD-21 and SD-22 and in sedimentary rocks from drill holes SD-14 and SD-23. The presence of hydrothermal magnetite indicates the transition between late magmatic and early hydrothermal processes (Roberts, 1973). In Stockton igneous rocks magnetite occurs spatially associated with the K-silicate constructive alteration, and generally shows variable replacement by specularite, a consequence of late hydrothermal oxidation of the K-silicate + magnetite assemblage (Photo 7).

Phyllic overprint of K-silicate constructive alteration is commonly incipient to weak, and is characterized by white phyllosilicates, muscovite and scarce phengite; these occur altering feldspars, as patches, as veinlets, and in some cases directly replacing both

magmatic and hydrothermal biotite (Photo 8 and 9). Quartz-sericite-pyrite veins occur in sample SD-15-1230 ft. At Bingham Canyon, sericite alteration is spatially associated with, and extends beyond, the hydrothermal biotite, this alteration occurs either as QSP veins or as partial replacement of plagioclase (Phillips et al., 1998). This last mode of occurrence is the most common in the Stockton samples studied.

In general during K-silicate constructive alteration potassium is added to the rocks (Beane, 1982). The ratio of K/H has to be large for biotite and K-feldspar to form and remain stable (Rose, 1970); furthermore, there is a difference in the composition of biotite that forms during K-silicate constructive alteration from that of igneous biotite; hydrothermal biotite has a greater Mg/Fe ratio (Beane, 1974). Phyllic alteration causes a removal of Ca^{++} , Na^+ and Mg^{++} during hydrogen metasomatism; some potassium may also be added to the rocks (Beane, 1982).

Outcrop samples at Stockton also exhibit a K-silicate constructive alteration assemblage. In the monzodiorite and the hornblende monzodiorite samples this alteration is defined by the presence of K-feldspar overgrowths around plagioclase phenocrysts, and in the quartz latite porphyries by the presence of K-feldspar overgrowths around "quartz eyes". Shreddy biotite is also present in the monzo-diorite. White phyllosilicates + muscovite are the most abundant alteration minerals in the outcrop quartz latite porphyries, but the lack of veins and the fact that these alteration minerals occur throughout the sample suggests that these are a consequence of weathering and not hydrothermal alteration.

Carbonate present in the igneous and sedimentary samples is apparently late in origin. In some igneous rocks carbonate is spatially associated with white phyllosilicates and with chlorite. This has been observed in other deposits such as the porphyry copper deposit at El Salvador, Chile, where calcite is associated with sericite that replaces plagioclase and with chlorite that alters biotite (Gustafson and Hunt, 1975).

Calc-silicate alteration minerals present in the Stockton sedimentary rocks include: diopside, actinolite, tremolite, garnet, epidote and zoisite. Sedimentary rocks at Bingham Canyon are also altered to calc-silicate minerals, which include tremolite, diopside, wollastonite, garnet (andradite), actinolite, epidote (Atkinson and Einaudi, 1978). Other alteration minerals observed in the Stockton sedimentary rocks include carbonate, quartz, chlorite, serpentine, magnetite, specularite, smectite and trace chloritoid and K-feldspar.

Sulfides

Pyrite is the most abundant sulfide in the Stockton samples, followed by chalcopyrite. Commonly pyrite and chalcopyrite are spatially associated with hydrothermal biotite (Photo 17). Only in scant samples are sulfides associated with the phyllic overprint.

Detailed sulfide paragenesis could not be determined due to the fact that most sulfides, besides pyrite and chalcopyrite, are not very abundant. Some paragenetic observations are the following. Pyrite was the first mineral to form and is commonly surrounded by chalcopyrite (Photo 19). Bornite replaces pyrite, and locally occurs with chalcopyrite (Photo 20) and rarely with idaite, suggesting that these three sulfides are coeval. Digenite apparently replaces bornite in sample SD-14-1219.5 ft (Appendix A).

Chalcocite was only observed in one sample (SD-23-1556 ft.) where it replaces chalcopyrite (Appendix A). Marcasite surrounds chalcopyrite in sample SD-14-1346 ft. (Appendix A). Covellite, molybdenite and sphalerite are only present in trace amounts, and each one only occurs in one sample, so their paragenetic relation to other sulfides could not be determined.

Copper at the Bingham Canyon mine is of hypogene origin. Chalcopyrite and bornite are the main copper ore minerals, with minor chalcocite. Chalcopyrite in the intrusive rocks is associated with, and constrained to, areas with hydrothermal biotite; greater copper grades and strong biotite alteration are spatially associated (Phillips et al., 1998). Although biotite is the most abundant alteration mineral in the Stockton samples, pyrite, and not chalcopyrite, is the main sulfide associated with biotite.

Sulphosalts present in the Stockton samples studied include trace tetrahedrite and enargite. These occur in samples SD-14-1219.5 ft and 05-STK-034-566.6 meters, respectively. Tetrahedrite occurs spatially associated with digenite-bornite (Appendix A), enargite surrounds pyrite in sample 05-STK-034-566.6 meters.

In general, several similarities exist between the rock types and alteration found in the Stockton area and that described by previous authors in the Bingham Canyon area. Some of the main characteristics that both share are the igneous lithologies, the ages of igneous activity, the presence of strong K-silicate constructive alteration of igneous rocks, the existence of a phyllic overprint, and the fact that adjacent sedimentary rocks have been altered to calc-silicate minerals.

One of the main differences between these two deposits is the quantity of copper sulfides associated with potassium silicate constructive alteration. At Bingham Canyon, high-grade ore is spatially associated with the K-silicate constructive alteration in which chalcopyrite and bornite are the main ore minerals. At Stockton, the overall quantity of copper sulfides is low, even though there is some chalcopyrite associated with hydrothermal biotite.

Stable isotopes

All samples analyzed for carbon and oxygen isotope composition indicate alteration to some extent (Figure 8). The least altered samples, "group one", are the most abundant (Figure 10) and are believed to have been affected mainly by diagenesis, although some of these could also have a superimposed hydrothermal alteration. One factor which supports the hypothesis of diagenetic alteration is the fact that most of the samples analyzed petrographically have been variably recrystallized.

Abundant calcite veins cut Stockton limestones and are generally lighter in both $\delta^{13}\text{C}$ and $\delta^{18}\text{O}$ than their host rocks, with some few exceptions (Figure 9). It was mentioned previously that these veins could have been formed by either diagenesis or hydrothermal alteration. Due to the fact that the superimposed hydrothermal alteration in the area is strongly controlled by structures, it is hard to believe that there was a previous hydrothermal event that caused such homogeneous values, thus the calcite veins are believed to be of diagenetic origin, which can be more pervasive in nature. If this is the case, it is possible that the fluids responsible of forming these veins also lowered the isotopic signature of the rocks in the area, accounting for the general diagenetic depletion observed in all samples. Oxygen values have been more affected than carbon values,

possibly because these diagenetic fluids were richer in oxygen and only had a small amount of carbon to interact with the carbon from the rocks.

Besides diagenesis there are two major processes that have affected the calcareous rocks in the area lowering their isotopic signature even further: hydrothermal alteration and contact metamorphism. Calcite veining precedes these two processes.

Evidence that supports the conclusion that the lowest $\delta^{13}\text{C}$ values found mainly in white limestones (Figure 8 and 10) are a consequence of contact metamorphism, comprises the following:

- 1- Most of these samples are located near areas that have been mapped as having calc-silicate alteration (Figure 24).
- 2- A major intrusion is present in the vicinity of the Calumet Mine, adjacent to where some of these samples were collected (Figure 24).
- 3- The presence of diopside in one the white limestones (Photo 24).

Samples with low $\delta^{13}\text{C}$ are located within the metamorphism-related bleached and recrystallized zones (Figure 24).

Lowest $\delta^{18}\text{O}$ values (Figure 10) are due to hydrothermal alteration. There are two areas at Stockton where these samples are concentrated, indicating a more pervasive fluid flow (higher water/rock ratios); one is centered on drill hole SD-16 and the other is located near the Argent Mine (Figure 24). Petrographic analysis of samples collected from drill hole SD-16 and other drill holes in the vicinity supports the idea that this area has been affected by intense hydrothermal alteration, causing mainly K-silicate constructive alteration.

Fluid flow seems to have been mainly structure-controlled. In some areas the alteration is pervasive, indicating generally more well-developed hydrothermal alteration as a consequence of higher water/rock ratios. The lowest $\delta^{18}\text{O}$ values are concentrated in these areas (Figure 24).

Except for two zones that display pervasive alteration (Figure 24), alteration outside of these areas seems to be constrained to the vicinity of structures. Occasional low $\delta^{13}\text{C}$ and $\delta^{18}\text{O}$ values commonly occur near intrusions, ore bodies (either mantos or veins), or faults.

Regarding exploration at Stockton, a general recommendation would have been to drill test the areas with pervasive hydrothermal alteration or greater water/rock ratios if the area had not been drilled previous to this study. As mentioned above, drill hole SD-16 is located in one of these areas, and interestingly, it is one of the holes with greater copper grades.

Fluid Inclusions

Brine inclusions or inclusions that contain halite or other daughter minerals are present in samples from drill holes SD-16, SD-21 and SD-23, and in one outcrop sample (Photo 29-32). Most of these samples are from quartz veins in igneous rocks, except for sample SD-21-137 ft. and the surface sedimentary sample. Brine inclusions have either one daughter, probably halite as identified by its cubic shape, or two daughters, in which the second crystal is possibly sylvite identified by its more rounded shape. Inclusions with multiple daughters, sometimes including an opaque, were also observed, and are present in samples SD-16-1103 ft., SD-21-1633 ft., and SD-23-1448 ft (Photo 31-32 and Appendix D).

All the inclusions are in vein quartz, except for sample SD-21-2130.5 ft., where they occur in magmatic quartz, the presence of halite-bearing inclusions suggests hydrothermal alteration of the sample.

Opaque daughters are present in inclusions from all the samples, except the one collected at surface (SM-23/05/06-8), some opaques have a triangular shape and a yellow color under reflected light. This matches chalcopyrite which is yellow and forms tetrahedral crystals. This indicates the presence of copper-rich fluids. Triangular opaque inclusions were observed in samples SD-16-1103 ft., SD-21-1002 ft., SD-21-1633 ft. and SD-23-1448 ft.

Vapor-rich inclusions are overall the most abundant type; these sometimes have a halite daughter, an opaque daughter, or both. In the analyzed samples it is common to find these vapor-rich inclusions together with brine inclusion, indicating boiling of the fluids that formed them. The fact that brine inclusions and indication of fluid boiling typical of porphyry Cu deposits are present in the Stockton area is a positive sign for mineral exploration.

Hydrothermal alteration and sulfide zonation based on petrographic analysis

Although alteration of outcropping igneous rocks at Stockton is also K-silicate constructive, it is not as well-developed as the K-silicate observed in the igneous rocks at depth. In the drill hole samples it is characterized by the presence of abundant hydrothermal biotite, while in the outcrop samples only scarce hydrothermal K-feldspar, in the form of overgrowths, is present. Phyllic overprint is also weaker in outcrop samples, and was only observed in sample SM15/06/06-4, in which there is scant alteration of feldspars to white phyllosilicates. All of this indicates that the alteration

weakens towards shallow or surface levels. Regional sampling of petrographic samples would be necessary to better define zoning and determine the limits of K-silicate constructive alteration.

Pyrite ghosts, now consisting of hematite and goethite, were the only indication of sulfides observed in outcrop samples, suggesting that copper bearing fluids did not reach surface levels. Fluid inclusion study from outcrop sample (SM-23/05/06-8), showed that no opaque daughters were observed, in contrast to the ones collected from drill holes.

Exploration conclusions

In the mineralized core of porphyry systems is it common to find halite-bearing inclusions coexisting with vapor-rich inclusions; another common feature is the presence of chalcopyrite daughters in the halite-bearing inclusions (Beane and Bodnar, 1995). After comparing the analyzed fluid inclusion samples with previous inclusions studies done in the Bingham Canyon area, it is clear that there are important similarities in both areas. At Bingham Canyon brine inclusions and vapor-rich inclusions are more abundant at higher elevations (Figure 26), in the area which also coincides with the greatest copper grade. At Stockton both inclusion types are present in all the analyzed samples, indicating that the samples represent a well-developed hydrothermal system.

High copper grades at Bingham Canyon are spatially associated with strong biotite alteration, similar to other deposits in which elevated metal grades coincide with the K-silicate constructive alteration, such as Yerington, Bagdad, Esperanza, Safford and El Teniente (Rose, 1970). In porphyry copper deposits of southwestern North America, it is common to find K-silicate constructive alteration spatially associated with hypogene ore minerals (Beane, 1982). There are other deposits, such as Santa Rita, were greatest

copper grades are located at the contact between K-silicate constructive alteration and phyllic alteration, or as at San Manuel, where enhanced copper grades extend into the phyllic or "quartz-sericite" alteration (Rose, 1970).

In the studied Stockton samples the main alteration type is a K-silicate constructive assemblage; pyrite is the most volumetrically important sulfide mineral associated with this assemblage, and chalcopyrite is volumetrically minor. In a few cases there are sulfides associated with phyllic overprint but most of the sulfides are associated spatially with K-silicate constructive alteration.

The Stockton prospect area has many lithological and alteration characteristics which are common to porphyry Cu-Mo deposits, such as strong K-silicate constructive alteration, phyllic overprint, and the presence of halite daughter minerals within fluid inclusions. As such, it is concluded that exploration tools used in this study suggest that exploration is being executed in the right place, and that there is no zonation of alteration or mineralization assemblages to indicate that alteration is more well-developed or potentially economic at depth.

REFERENCES

- Arehart, G.B., and Donelick, R.A., 2006, Thermal and isotopic profiling of the Pipeline hydrothermal system: application to exploration for Carlin-type gold deposit: *Journal of Geochemical Exploration*, 91, p. 27-40.
- Atkison, W.W. Jr., and Einaudi, M.T., 1978, Skarn formation and mineralization in the contact aureole at Carr Fork, Bingham, Utah: *Economic Geology*, v. 73, p. 1326-1365.
- Babcock, R.C. Jr., Ballantyne, G.H., and Phillips, C.H., 1998, Summary of the Geology of the Bingham District, Utah (reprint), *in* John, D.A., and Ballantyne, G.H., eds., *Geology and ore deposits of the Oquirrh and Wasatch mountains, Utah: Society of Economic Geologist, Guidebook series*, v. 29, p. 113-132.
- Beane, R.E., 1974, Biotite stability in the porphyry copper environment: *Economic Geology*, v. 69, p. 241-256.
- Beane, R.E., 1982, Hydrothermal alteration in silicate rocks, southwestern North America, *in* Titley, S.R., ed., *Advances in geology of the porphyry copper deposits, southwestern North America: Tucson, University Press*, 560 p.
- Beane, R. E., and Bodnar, R. J., 1995, Hydrothermal fluids and hydrothermal alteration in porphyry copper deposits, *in* Pierce, F.W., and Bohm, J.G, eds., *Porphyry copper deposits of the American Cordillera: Arizona Geological Society. Digest 2*, p. 83-93.
- Campbell, A.R., and Larson, P. B., 1998, Introduction to stable isotope applications in hydrothermal systems, *in* Richardson, J., and Larson, P., eds., *Techniques in hydrothermal ore deposit geology: Reviews in Economic Geology*, v. 10, p. 173-193.
- Creasey, S.C., 1959, Some phase relations in the hydrothermally altered rocks of porphyry copper deposits: *Economic Geology*, v. 54, p. 351-373.
- Criss, R.E., Champion, D.E., and McIntyre, D.H., 1985, Oxygen isotope, aeromagnetic, and gravity anomalies associated with hydrothermally altered zones in the Yankee Fork mining district, Custer County, Idaho: *Economic Geology*, v. 80, p. 1277-1296.
- Davis, I., 1996, The host rock alteration associated with a porphyry copper prospect in the Oquirrh Mountains, Utah, USA: Unpublished MS Dissertation, University of Leicester, 79 p.

- Dunham, R.J., 1962, Classification of carbonate rocks according to their depositional texture, *in* Ham W.E., ed., Classification of Carbonate Rocks-a symposium: Tulsa, OK, American Association of Petroleum Geologists, Memoir 1, p. 108-121.
- Folk, R.L., 1962, Spectral subdivision of limestone types, *in* Ham W.E., ed., Classification of Carbonate Rocks-a symposium: Tulsa, OK, American Association of Petroleum Geologists, Memoir 1, p. 62-84.
- Gilluly, J., 1932, Geology and ore deposits of the Stockton and Fairfield quadrangles, Utah: U.S. Geological Survey Professional Paper 173, 171 p.
- Grossman, E.L., Zhang, C., and Yancey, T.E., 1991, Stable-isotope stratigraphy of brachiopods from Pennsylvanian shales in Texas: Geological Society of America Bulletin, v. 103, p. 953-965.
- Grossman, E.L., Mii, H-S., and Yancey, T.E., 1993, Stable isotope in late Pennsylvanian brachiopods from the United States: Implications for Carboniferous paleoceanography: Geological Society of America Bulletin, v. 105, p. 1284-1296.
- Guilbert J.M., and Parks, C.F., Jr., 2007, The Geology of Ore Deposits: Waveland Press, Inc., Illinois, 985 p.
- Gustafson, L.B., and Hunt, J.P., 1975: The porphyry copper deposit at El Salvador, Chile: Economic Geology, v.70, p. 857-912.
- Gustafson, L.B., and Quiroga, J., 1995, Patterns of mineralization and alteration below the porphyry copper orebody at El Salvador, Chile: Economic Geology, v. 90, p. 2-16.
- Hintze, L.F., 1988, Geologic History of Utah: Brigham Young University Geology studies, 202 p.
- Hughes, C.J., 1982, Igneous petrology: Elsevier scientific publishing company, The Netherlands, 551 p.
- Kesler, S.E., Vennemann, T.W., Vazquez, R., Stenger, D.P., and Frederickson, G.C., 1996, Application of large-scale oxygen isotope haloes to exploration for chimney-manto Pb-Zn-Cu-Ag deposits: Geology and Ore Deposits of the American Cordillera, Geological Society of Nevada Symposium, Reno/Sparks, NV, April 1995, Proceedings, p. 1383-1396.
- Lanier, G., John, E.C., Swense, A.J., Reid, J., Bard, C.E., Caddey, S.W., and Wilson, J.C., 1978, General geology of the Bingham mine, Bingham Canyon, Utah: Economic Geology, v. 73, p. 1223-1241.

- Lerouge, C., Deschamps, Y., Joubert, M., Bechu, E., Fouillac, A.-M., and Castro, J.A., 2001, Regional oxygen isotope systematics of felsic volcanics: a potential exploration tool for volcanogenic massive sulphide deposits in the Iberian Pyrite Belt: *Journal of Geochemical Exploration*, 72, p. 193-210.
- Meyer, C., 1965, An early potassic type of wall-rock alteration at Butte, Montana: *The American Mineralogist*, v. 50, p. 1717-1722.
- Moore, W.J., Curtin, G.C., Roberts, R.J., and Tooker, E.W., 1966, Distribution of selected metals in the Stockton district, Utah: U.S. Geological Survey Professional Paper 550, p. 197-205.
- Nesbitt, B.E., 1996, Application of oxygen and hydrogen isotopes to exploration for hydrothermal mineralization. *SEG Newsletter*, number 27, p. 1-13.
- Phillips, C.H., Smith, T.W., and Harrison, E.D., 1998, Alteration, metal zoning, and ore controls in the Bingham Canyon porphyry copper deposits, Utah, in John, D.A., and Ballantyne, G.H., eds., *Geology and ore deposits of the Oquirrh and Wasatch mountains, Utah*: Society of Economic Geologists, Guidebook series, v. 29, p. 133-145.
- Redmond, P.B., Einaudi, M.T., Inan, E.E., Landtwing, M.R., and Heinrich, C.A., 2004, Copper deposition by fluid cooling in intrusion-centered systems: new insights from the Bingham porphyry ore deposit, Utah: *Geology*, v. 32., no. 3, p. 217-220.
- Roberts, S.A., 1973, Pervasive early alteration in the Butte District, Montana, in Miller, R.D., ed., *Guidebook for the Butte District Montana*, p. HH-1 to HH-8.
- Rose, A.W., 1970, Zonal relations of wall rocks alteration and sulfide distribution at porphyry copper deposits: *Economic Geology*, v. 65, p. 920-936.
- Shieh, Y.N., and Taylor, H.P., 1969, Oxygen and carbon isotope studies on contact metamorphism of carbonate rocks: *Journal of Petrology*, v. 10, p. 307-331.
- Stenger, D.P., Kesler, S.E., and Vennemann, T., 1998, Carbon and oxygen isotope zoning around Carlin-type gold deposits: a reconnaissance survey at Twin Creeks, Nevada: *Journal of Geochemical Exploration*, 63, p. 105-121.
- Stokes, W.L., 1988, *The geology of Utah*: Utah Museum of Natural History and Utah Geological and Mineral Survey, 280 p.
- Valley, J. W., 1986, Stable isotope geochemistry of metamorphic rocks, in Valley, J.W., Taylor, H.P., O'Neil, J.R., eds., *Stable isotopes in high temperature geological processes: Reviews in Mineralogy*, v. 16, p. 445-489.

- Vazques, R., Vennemann, T.W., and Kesler, S.E., 1998, Carbon and oxygen isotope halos in the host limestone, El Mochito Zn-Pb-(Ag) skarn massive sulfide-oxide deposit, Honduras: *Economic Geology*, v. 93, p. 15-31.
- Warnaars, F.W., Smith, W.H., Bray, R.E., Lanier, G., and Shafiqullah, M., 1978, Geochronology of igneous intrusions and porphyry copper mineralization at Bingham, Utah: *Economic Geology*, v. 73, p. 1242-1249.

APENDIX A
PETROGAPHY OF DRILL CORE SAMPLES

DRILL HOLE SD-14

SD-14-1219.5 ft. Protolith: Igneous rock?

Note: This rock was originally logged as skarn, but the presences of biotite phenocrysts, magmatic in appearance, suggests a probable igneous protolith.

This sample presents a strong alteration to white phyllosilicates (and scarce muscovite) with total white phyllosilicates comprising approximately 50-55 vol-% of the rock (phyllitic alteration). Other alteration minerals include hydrothermal biotite, quartz, cinnamon rutile, smectite and carbonate. Phenocrysts are biotite, quartz and trace zircon.

Two types of biotite are present in the rock with total biotite being approximately 5-6 vol-%:

1- Biotite phenocrysts, possibly magmatic. These sometimes show strong alteration to smectite.

2- Fine to coarse grain shreddy biotite (hydrothermal). Usually occurs in clusters. The color varies from light and dark brown sometimes with a green tint. It also shows alteration to smectite. This second type of biotite is the most abundant.

Both types of biotite have cinnamon rutile associated with them, total cinnamon rutile in the sample is <1 vol-%.

Some of the biotite is being altered to white phyllosilicates (phyllitic overprint, Photo A.1). It is possible that the amount of biotite was larger originally but is has now been replaced by white phyllosilicates.

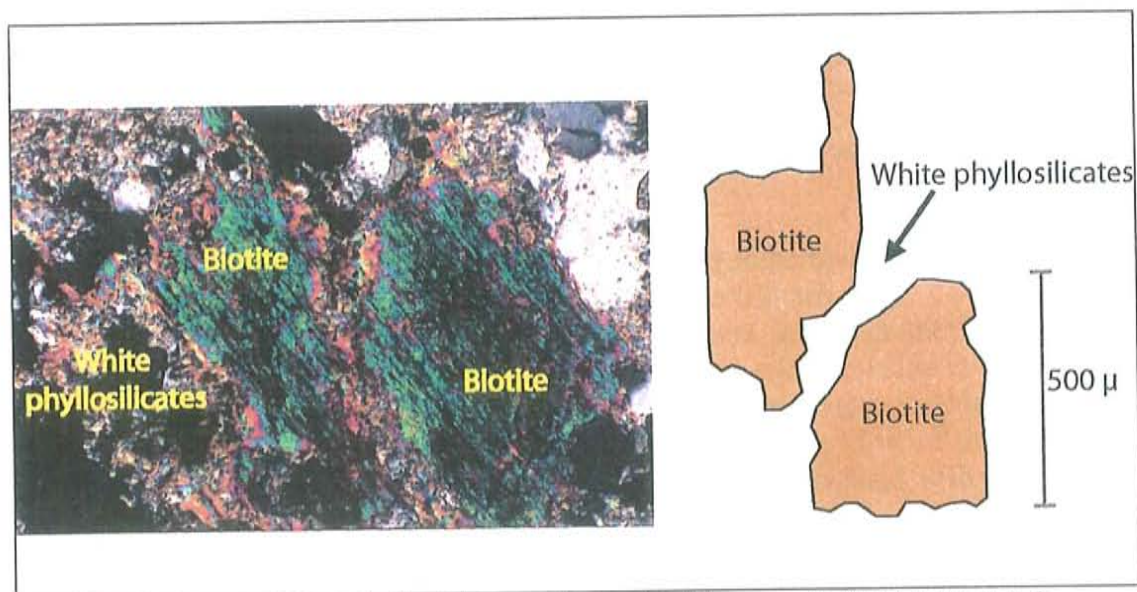


Photo A.1 : White phyllosilicates altering biotite, sample SD-14-1219.5 ft.

Abundant fine grain quartz (approximately 30 vol-%) is present in the matrix together with the white phyllosilicates. (Introduced or primary?). Quartz phenocrysts are mainly subeuhedral with some having a rounded shape. They sometimes seem to show

alteration to white phyllosilicates (Figure A.1), it could also be that the white phyllosilicates are altering inclusions that were inside the quartz.

Carbonate occurs as random patches across the sample, and it comprises less than 1 vol-% of the sample.

Abundant submillimeter scale and scarce millimeter scale quartz veinlets are present throughout the sample.

Ore minerals comprise approximately 4-5 vol-% of the sample. They include: pyrite, chalcopyrite, bornite, digenite, a sulphosalt (tetrahedrite?) and trace covellite. Pyrite is the most abundant mineral and it appears to be the first sulfide to have formed, it is followed by chalcopyrite and bornite with sub-equal amounts and then by the less abundant digenite. Bornite occurs mainly at the edges of pyrite suggesting that it is probably replacing it, in some cases together with chalcopyrite (Photo A.2).

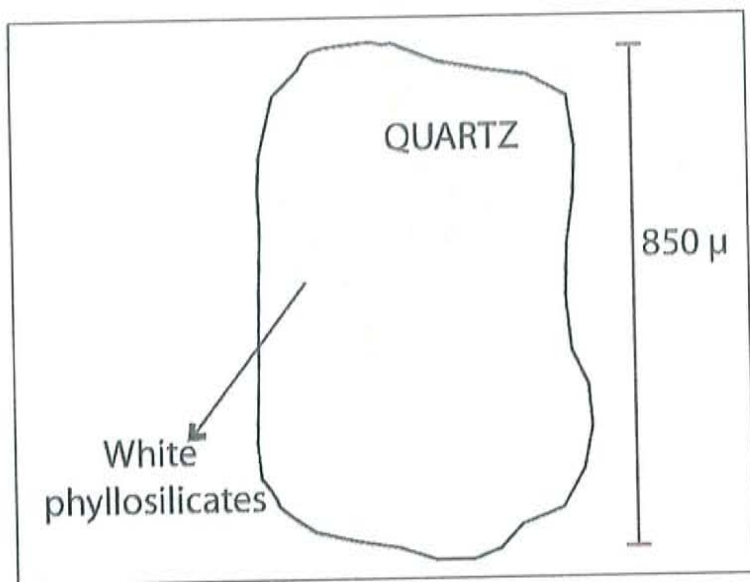


Figure A.1: Quartz phenocryst being replaced by white phyllosilicates?, sample SD-14-1219.5 ft.

Chalcopyrite and bornite appear to be coeval, in some cases chalcopyrite cuts and surrounds bornite and in others bornite cuts chalcopyrite (Photos A.3).

Digenite and tetrahedrite seem to have formed last, and they appear to be replacing bornite (Photo A.4). Given that there is only trace covellite it is difficult to determine its paragenetic relationship to the other ore minerals. Sulfides are mainly disseminated although some appear to be in stringer veinlets. Most of the sulfides are associated with white phyllosilicates and only scarce are associated with hydrothermal biotite.

Ore minerals paragenesis:

Pyrite \longrightarrow Bornite/Chalcopyrite \longrightarrow Digenite/Tetrahedrite/Covellite?

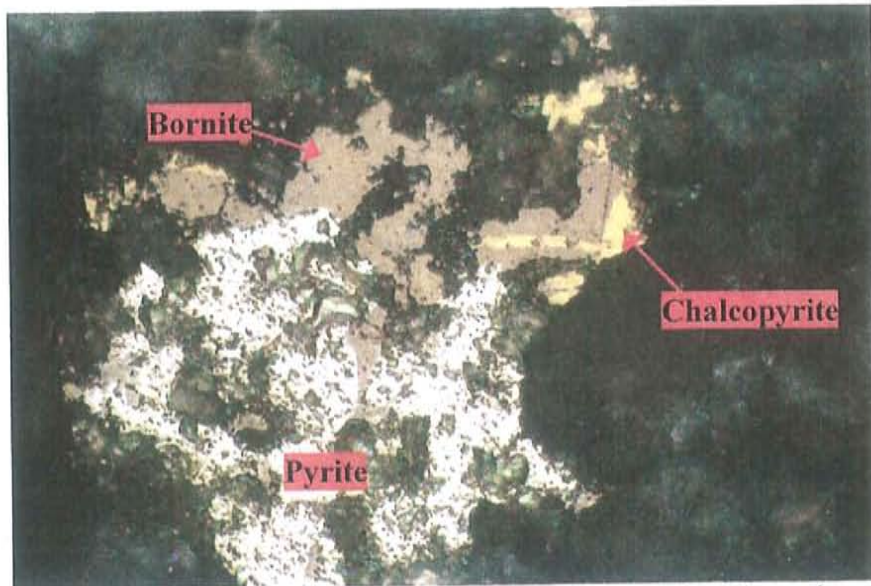


Photo A.2: Bornite and chalcopyrite replace pyrite (f.o.v. = 0.225 mm long). Sample SD-14-1219.5 ft.

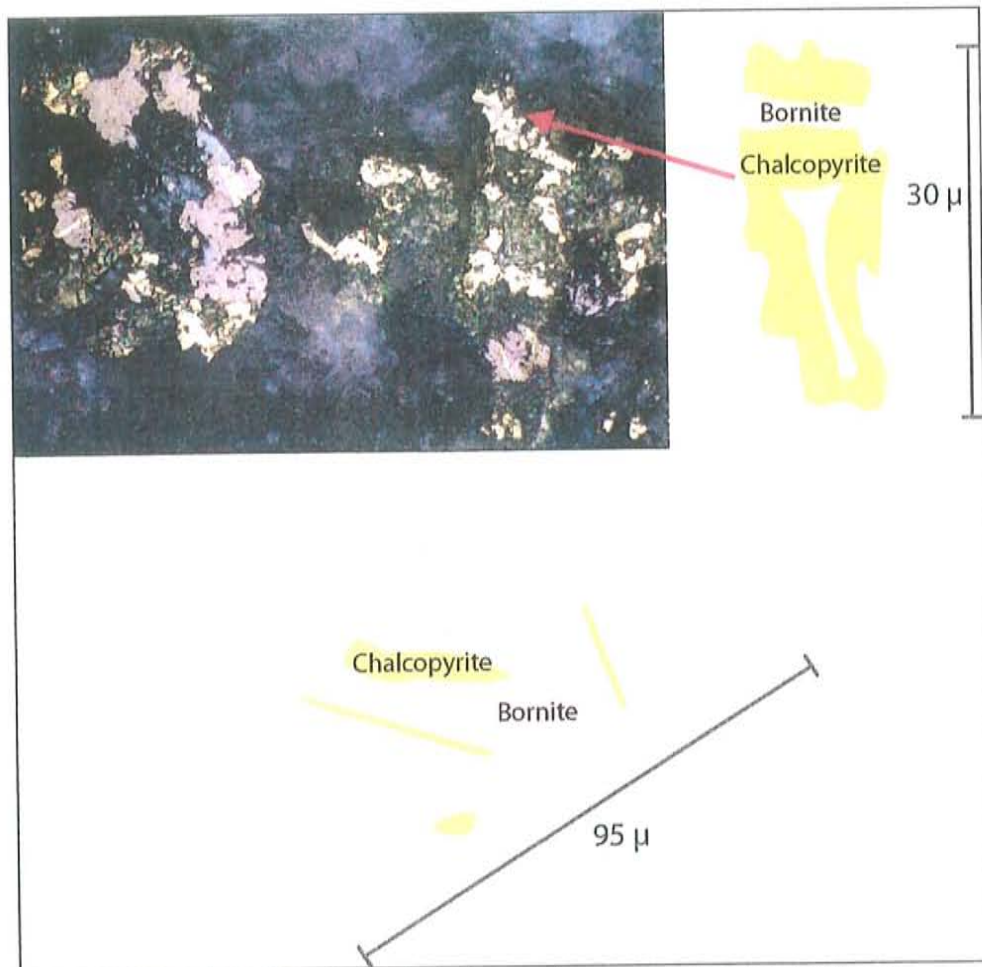


Photo A.3: Bornite and chalcopyrite, sample SD-14-1219.5 ft

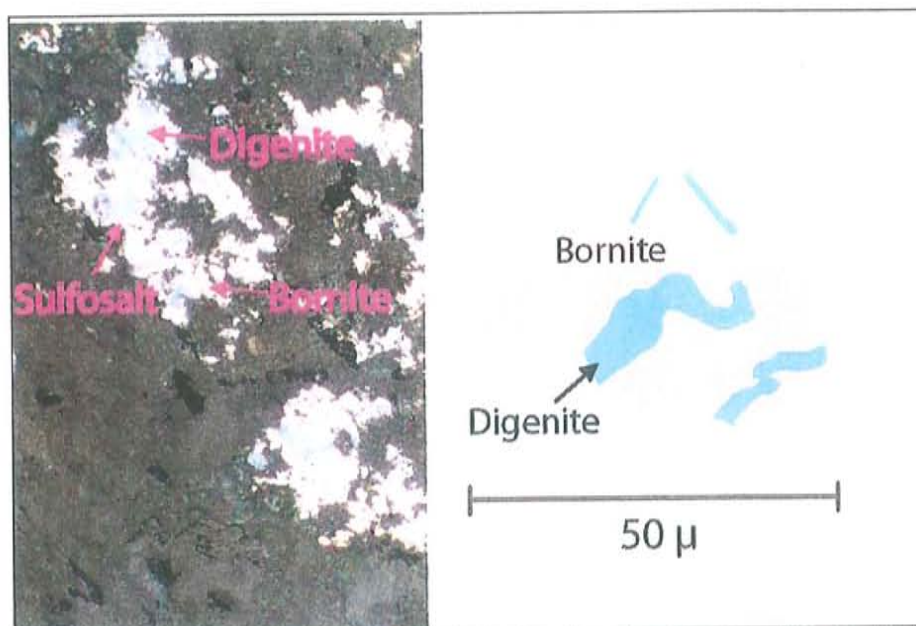


Photo A.4: Digenite and tetrahedrite replacing bornite. Sample SD-14-1219.5 ft

SD-14-1266.6 ft. Protolith: Quartz arenite

The protolith corresponds to a quartzarenite composed mainly of well sorted, angular quartz. Quartz still comprises approximately 35 vol-% of the sample.

Several alteration minerals are present, these are: actinolitic amphibole, epidote, smectite, carbonate, chlorite and trace garnet. Actinolite is the most abundant (Photo A.5) and it occurs everywhere in the sample (possibly replacing the original matrix of the rock), total actinolite is approximately 30 vol-%. Sub-equal amounts of smectite and carbonate are present with approximately 10 vol-% of each; smectite replaces actinolite. Epidote follows in abundance comprising < 5vol-% of the rock. Chlorite occurs together with actinolite and sulfides (replacing?) and it comprises < 1vol-%. Hydrous minerals are present in the thin section but their relationship to anhydrous minerals is yet to be determined.

Pyrite, chalcopyrite and trace bornite are the sulfides present in the rock, together these comprise approximately 8 vol-% (pyrite > chalcopyrite). Chalcopyrite surrounds pyrite indicating that it formed later. Bornite occurs with chalcopyrite, possibly coeval.

Specular hematite and hydrothermal magnetite are also present in the. Due to the fact that it is a thin section and not a polished thin section, the relationship between hydrothermal magnetite and specular hematite can not be determined, and it is also difficult to estimate the percentage of these minerals.

Specularite formed before the sulfides, evidence for this is the fact that pyrite surrounds specular hematite. Specular hematite, magnetite, and most sulfides occur concentrated in one area (in veins).

Pyrite and chalcopyrite are apparently being altered to hematite (not specular).

Veins present in the rock are:

- 1- Veinlets of carbonate.
- 2- Veins of carbonate + smectite (probably originally actinolite).

- 3- Veins of pyrite + epidote + carbonate + garnet + specular hematite
 - 4- Veins of carbonate + actinolite + smectite + epidote + quartz (inherited?) + pyrite + specular hematite + trace chalcopyrite.
 - 5- Stringer veinlets of pyrite and of chalcopyrite.
 - 6- Veinlets of smectite + actinolite.
 - 7- Veins of actinolite + epidote + scarce chlorite.
- All these veins are submillimeter scale.

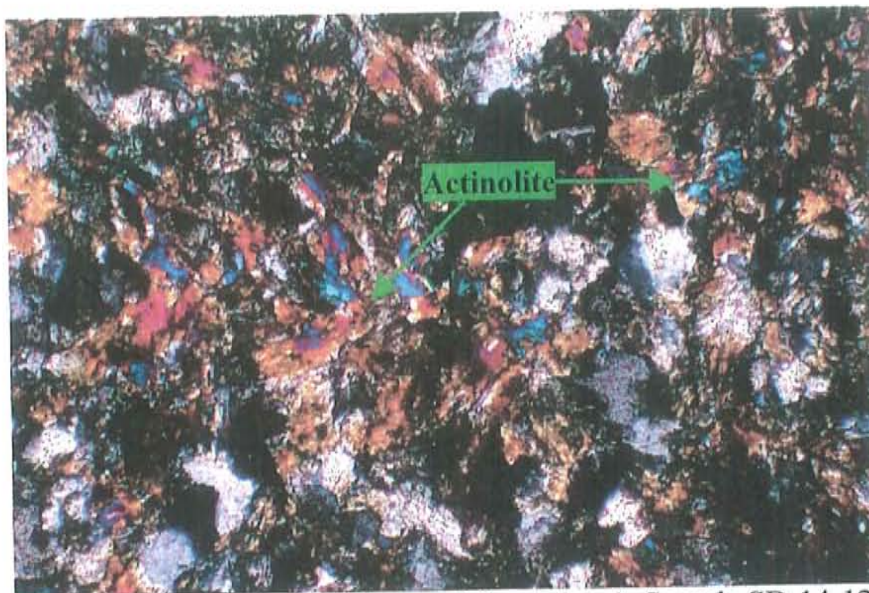


Photo A.5: Abundant actinolite (f.o.v. = 0.9 mm long). Sample SD-14-1266.6 ft.

SD-14-1346 ft. Silicified Limestone

The two main minerals in the sample are quartz and carbonate (calcite) with sub-equal amounts. No original rock forming components seem to be present in the rock. Protolith was probably a limestone that got silicified. The carbonate present in the sample seems to have formed by recrystallization, and it came after the quartz since it surrounds quartz crystals in several areas of the sample (Photo A.6).

All the silica appears to be introduced (alteration mineral) based on the fact that it is all irregular shaped and patchy.

Pyrite, marcasite and chalcopyrite are the three sulfides present in the sample. Total percentage of sulfides is approximately 7-8 vol-%. Trace euhedral pyrite crystals are present in the sample.

Pyrite seems to be the least abundant and it appears to only occur in a vein and as trace euhedral crystals, although it is sometimes difficult to differentiate it from marcasite. Marcasite and chalcopyrite are disseminated and forming stringer veinlets throughout the sample, some of these have carbonate in them. There is sub-equal amount of each. Marcasite surrounds chalcopyrite in some areas (Photo A.7), suggesting that it probably was the last sulfide to form. Its shape varies from blebs to acicular and usually occurs with carbonate. Some of the marcasite is really fine grain.

There are several veins present in the sample:

- 1- Millimeter scale carbonate + pyrite + marcasite + scarce quartz.

- 2- Submillimeter scale barren carbonate veinlets.
- 3- Submillimeter scale quartz veinlets.
- 4- Sulfide stringer veinlets mentioned above.

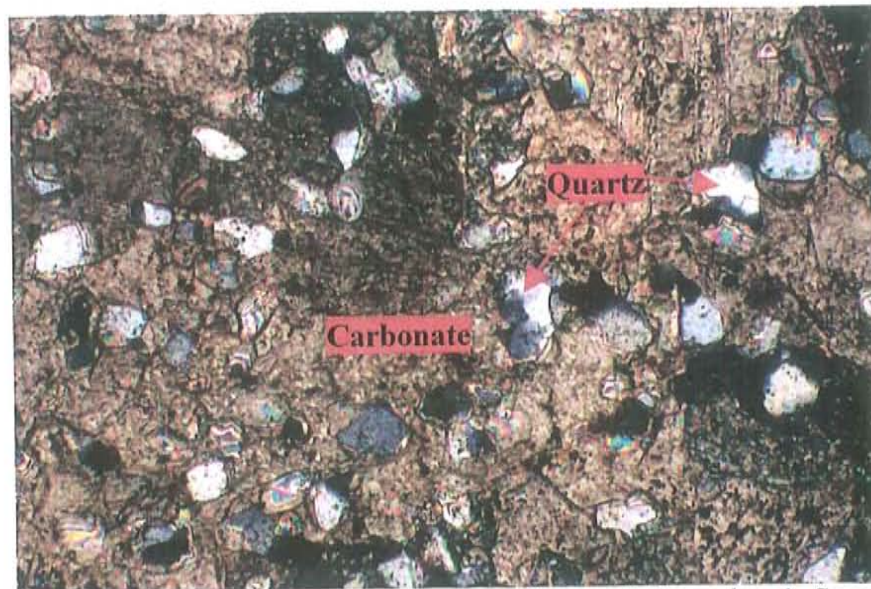


Photo A.6: Poikilotopic calcite surrounds quartz (f.o.v = 0.9 mm long). Sample SD-14-1346 ft.

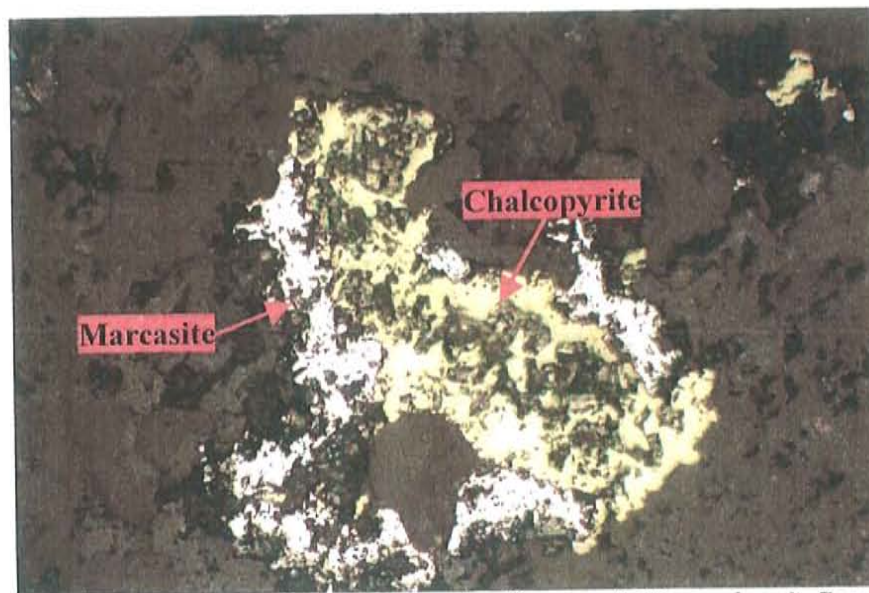


Photo A.7: Marcasite surrounding chalcopyrite (f.o.v. = 0.45 mm long). Sample SD-14-1346 ft.

DRILL HOLE SD-15

SD-15-1230 ft. Biotite Quartz-Diorite

Original rock forming phenocrysts include plagioclase, quartz, magnetite, biotite, scarce K-feldspar and trace apatite and zircon, of these plagioclase is the most abundant (Photo A.8), and it shows alteration to smectite and white phyllosilicates. Most of the plagioclase is subeuhedral in shape. Quartz and biotite follow plagioclase in abundance. Some of the quartz is patchy and irregular shaped suggesting that it might be introduced.

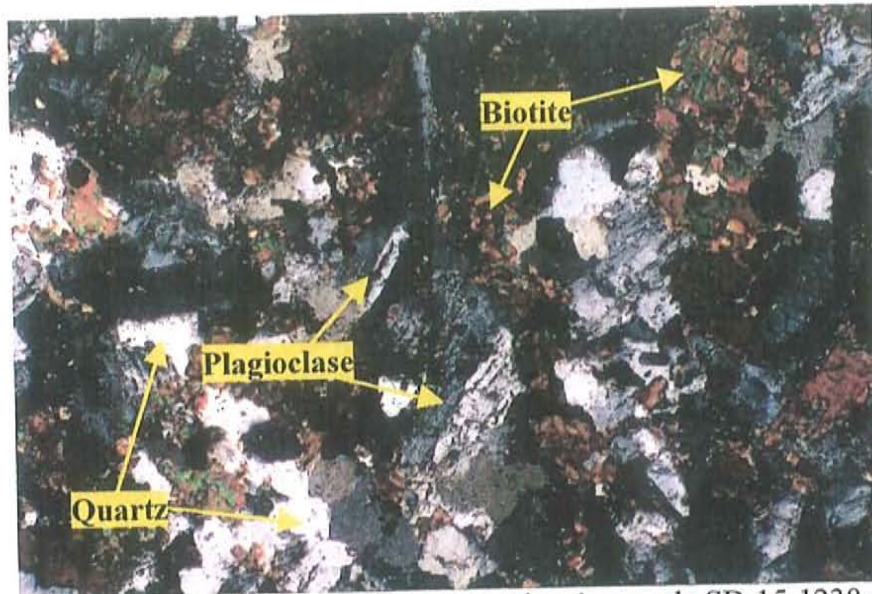


Photo A.8: Monzonite (f.o.v. = 1.8 mm long), sample SD-15-1230 ft.

Because of the strong K-silicate constructive alteration of the rock it is hard to determine which percentage of the biotite is magmatic and which one corresponds to alteration.

Magnetite comprises approximately 5-6 vol-% of the rock and it all appears to be magmatic in origin.

There appears to be some scarce K-spar in the rock although it is hard to determine the exact amount because of the strong biotite alteration present in the rock. It is only differentiated from quartz because of its dirtier appearance under plane light. The alteration of feldspars to white phyllosilicates varies from none to less than 5 vol-%.

Magmatic biotite usually presents mineral inclusions (Photo A.9).

Hydrothermal biotite is the main alteration mineral; it is mainly shreddy and fine grain (Photo A.11). Its color varies from brown to olive green.

Total biotite in the sample is approximately 40 vol-% with most being hydrothermal.

Trace chlorite is present altering biotite (Photo A.10).

Cinnamon rutile comprises <1 vol-% of the sample and it is associated with both magmatic and hydrothermal biotite

Tree types of veins are recognized in the rock:

1- Submillimeter stringer scale veinlets of biotite.

2- Submillimeter scale quartz veins with biotite occurring along the edges and sometimes in the centerline. Biotite seems to have come later and it followed the same path as the quartz. Note: This vein has very good fluid inclusions sometimes with a halite daughter.

3- Two millimeter scale quartz + sericite + pyrite (QSP) veins cross cut each other. The thickest one has a centerline composed of quartz, pyrite, carbonate and scarce chalcopyrite and a halo made of fine grain white phyllosilicates, scarce muscovite and sulfides (sub-equal amounts of pyrite and chalcopyrite). The thinner vein has a centerline composed of pyrite and quartz (no carbonate) and a halo that consists of white phyllosilicates and sulfides (mainly chalcopyrite). Based on the mineralogy and the characteristics this vein can be classified as a "D" vein (Gustafson & Hunt, 1975).

The D vein cuts the quartz vein.

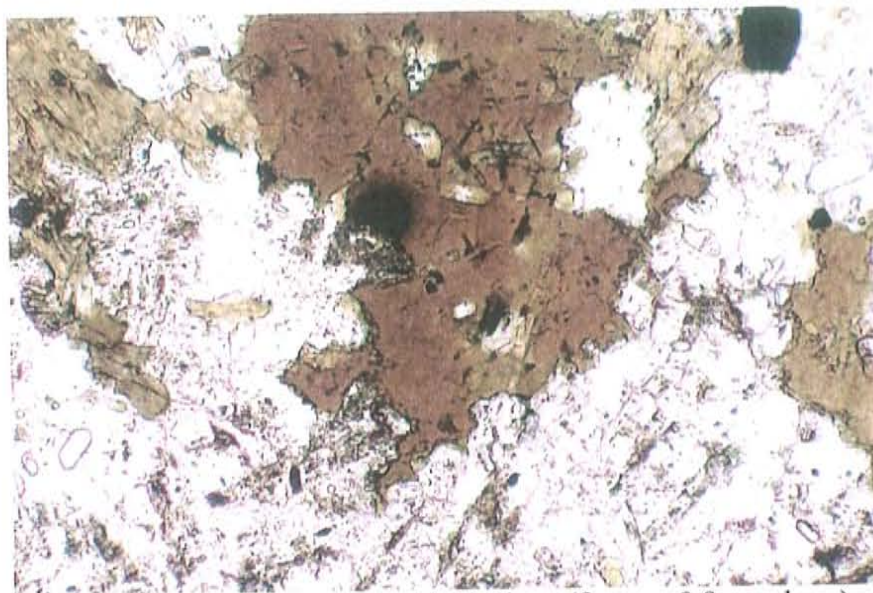


Photo A.9: Magmatic biotite with mineral inclusions (f.o.v. = 0.9 mm long), sample SD-15-1230 ft.

Trace chalcopyrite (less than 1 vol-%) also occurs disseminated in the rock, outside of the veins. It also occurs associated with cinnamon rutile and magmatic biotite (chalcopyrite could be replacing the biotite, Figure A.2). Chalcopyrite also appears to be replacing some magnetite.

The alteration type can be classified as K-silicate constructive with a phyllic overprint as it is evidenced by the presence of a D vein with white phyllosilicate halo. Patchy white phyllosilicates not associated with the veins are also present in some areas of the rock.

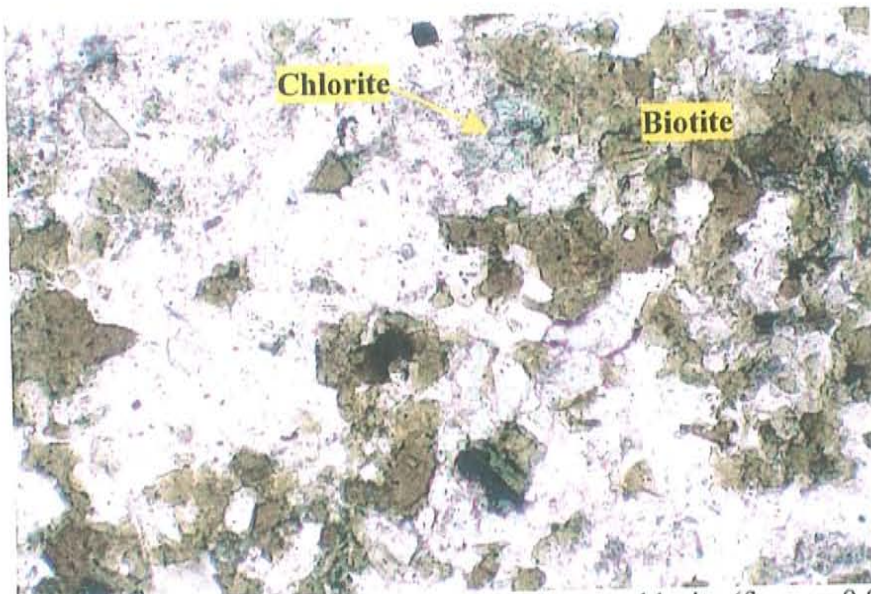


Photo A.10: Hydrothermal biotite with some alteration to chlorite (f.o.v. = 0.9 mm long).
Sample SD-15-1230 ft.

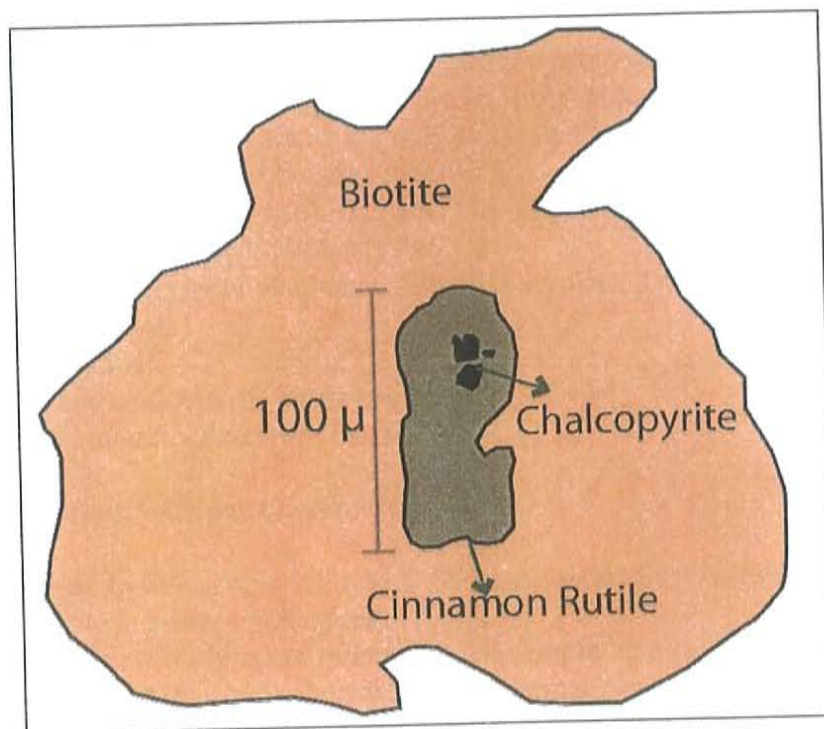


Figure A.2: Cinnamon rutile replacing biotite. Chalcopyrite replacing? Cinnamon rutile,
sample SD-15-1230 ft.

SD-15-1237 ft. Biotite Quartz-Diorite

This sample shares many similarities with the previous sample, but it lacks D vein and it seems to have more K-feldspar, although it is hard to tell because of the abundant biotite alteration.

Plagioclase is the most abundant feldspar, showing very distinctive polysynthetic twinning. Plagioclase and K-feldspar show scarce alteration to white phyllosilicates, varying from none to less than 5 vol-%. Fine grain biotite is also present altering feldspars.

Trace zircon and apatite are present.

Biotite is the most abundant mineral in the sample comprising approximately 50 vol-%; there are two types of biotite present:

- 1- Phenocrysts with some mineral inclusions (magmatic).
- 2- Olive to brown shreddy biotite (hydrothermal).

Scarce chlorite is present altering biotite.

The alteration type can be classified as K-silicate constructive.

Total quartz comprises approximately 15 vol-% of the sample; some grains have irregular boundaries suggesting that there it was probably introduced as an alteration mineral.

Magnetite is present throughout the sample (approximately 2-3 vol-%), it all appears to be magmatic in origin and it is sometimes associated with hydrothermal biotite (being replaced?).

Cinnamon rutile is present as an alteration mineral with total rutile comprising <1 vol-%, this mineral occurs associated with biotite and sometimes with chalcopyrite.

Ore minerals comprise pyrite and chalcopyrite with total sulfide content approximately 3 vol-% and chalcopyrite > pyrite. They occur disseminated, in veinlets and in stringer veinlets. Sulfides are sometimes associated with biotite.

Five different types of veinlets are identified:

1- Biotite submillimeter scale veinlets. They sometimes cross cut each other and some are present cutting feldspar phenocrysts.

2- Pyrite \pm chalcopyrite veinlets. Cut biotite veinlets. There is some biotite along the edges of these veinlets

3- Quartz veinlet.

4- Pyrite and chalcopyrite stringer veinlets.

Biotite and quartz veinlets are barren.

SD-15-1534 ft. Alkali feldspar Quartz-Syenite.

Phenocrysts in the sample include K-feldspar, plagioclase, biotite, magnetite and quartz. Trace apatite is present in the rock.

Biotite is the most abundant mineral in the sample, comprising approximately 40 vol-%; most of this biotite is hydrothermal. Hydrothermal biotite is usually fine grain and sometimes shows olive green color. Magmatic biotite varies from subeuhedral to xenomorphic and has mineral inclusions. Biotite shows scarce alteration to chlorite. Abundant submillimeter scale biotite veinlets are present cutting the rock.

Alteration of K-feldspar to white phyllosilicates seems to vary from none to strong but most show very weak alteration. There are areas where feldspars show strong

alteration to white phyllosilicates (up to 60 vol-%) and scarce carbonate (difficult to determine whether it was originally plagioclase or K-feldspar). Trace muscovite is also present altering feldspars.

The lack of K-feldspar in veins makes it hard to determine whether all the K-feldspar is magmatic; some is probably late magmatic-early hydrothermal (part of the K-silicate constructive alteration).

Plagioclase phenocrysts show strong alteration to smectite and white phyllosilicates. Some phenocrysts that have been strongly altered to smectite were probably originally plagioclase.

Total magnetite is approximately 3 vol-%; all seems to be magmatic in origin.

White phyllosilicates are also present as patches and not only altering feldspars.

Trace cinnamon rutile shows a strong association to biotite.

Millimeter scale quartz veins are present in the rock; some have pyrite and chalcopyrite along the edge of the vein (probably the sulfides came later); scarce chalcopyrite is also present in the center of the veins. The coarser quartz vein also has carbonate following one of the edges. Magnetite is also present in the edges of some of these veins but it seems to have been inherited meaning that it did not come with the vein but that it was part of the original rock (magmatic). These quartz veins are cut by the thin submillimeter scale biotite veinlets.

Barren submillimeter scale quartz veins are also present in the rock.

In some areas there is chalcopyrite surrounding magnetite (replacing? Photo A.11)

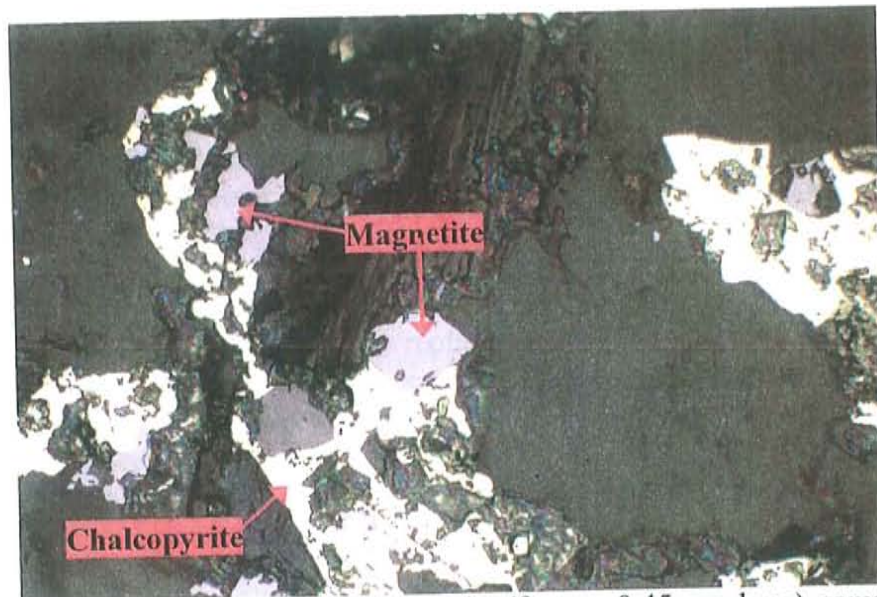


Photo A.11. Chalcopyrite surrounds magnetite (f.o.v. = 0.45 mm long), sample SD-15-1534 ft.

Sulfides are also present in stringer veinlets of pyrite, chalcopyrite and pyrite + chalcopyrite. Total percentage of sulfides is approximately 3 vol-% (taking into consideration the one in the quartz veins) with sub-equal amounts of pyrite and chalcopyrite. Sulfides show close association to biotite (outside of the quartz veins), some sulfide stringer veinlets seem to follow the same path as biotite veinlets.

The alteration assemblage is classified as K-silicate constructive with a weak phyllic overprint.

DRILL HOLE SD-16

SD-16-1252 ft. Quartz-Monzonite

Phenocrysts present in the sample are: K-feldspar, quartz, biotite and plagioclase. Phenocrysts in the rock vary from subeuhedral to anhedral, and submillimeter to millimeter scale.

K-feldspars show alteration to patchy carbonate, patchy quartz, fine grain biotite and white phyllosilicates (as patches and veinlets). Total alteration of K-feldspar to white phyllosilicates varies substantially from trace to very strong, although most of the phenocrysts only show scarce alteration.

Plagioclase phenocrysts are strongly altered to white phyllosilicates (usually >75 vol-%). Other minerals altering plagioclase are smectite and fine grain biotite. There are some phenocrysts (possibly feldspars) that have been almost completely altered to white phyllosilicates up to 90 to 95 vol-%.

Zircon is present as microcrysts.

Total biotite comprises approximately 5-10 vol-% of the rock; most seems to be of hydrothermal origin which is characterized by being shreddy and usually occurring in clusters; hydrothermal biotite replaces magmatic biotite. Trace muscovite is present altering hydrothermal biotite. Biotite also shows incipient alteration to chlorite (total chlorite in the rock is <1 vol-%). Total percentage of white phyllosilicates + muscovite in the rock (including the ones altering feldspars) is <2 vol-%.

Carbonate is present in patches altering K-feldspar (mentioned above) and in veinlets; total carbonate in the sample is <2 vol-%.

Cinnamon rutile comprises <2 vol-% of the rock and occurs as granular grain aggregates associated with biotite.

Hydrothermal magnetite is also present in the form of veinlets; apparently this magnetite occurs contemporaneously with the hydrothermal biotite; total percentage of magnetite is <2 vol-%. Specular hematite replaces magnetite.

Sulfide minerals present are chalcopyrite and pyrite; the total percentage of both is approximately <4 vol-%, with chalcopyrite > pyrite. They occur in veins and veinlets.

Several veins cut the rock:

- 1- Millimeter scale veins of quartz + K-feldspar + biotite + carbonate + chlorite + chalcopyrite + magnetite + trace pyrite.
- 2- Submillimeter scale veinlet of pyrite + chalcopyrite + carbonate + biotite + chlorite + muscovite + white phyllosilicates.
- 3- Submillimeter scale veinlets of carbonate.
- 4- Submillimeter scale veinlet of magnetite + biotite + scarce chalcopyrite.
- 5- Biotite veinlets
- 6- Stringer veinlets of chalcopyrite.

Based on the assemblage of minerals the alteration is defined as K-silicate constructive (characterized by the presence of hydrothermal biotite and magnetite) with a very weak phyllic overprint.

SD-16-1269.5 ft. Quartz-Monzonite Porphyry

This sample is very similar to SD-16-2629 ft.

The matrix comprises 50-55 vol-% of the rock and it is composed mainly of quartz and K-feldspar; scarce plagioclase is also present. Phenocrysts include K-feldspar, plagioclase, quartz and biotite.

K-feldspars show alteration to fine grain biotite, patchy carbonate and white phyllosilicates (as patches and veins). Alteration to white phyllosilicates varies from <5 vol-% to 70 vol-%. Plagioclase phenocrysts have been strongly altered to white phyllosilicates + scarce biotite; alteration to white phyllosilicates is >80 vol-%.

Some phenocrysts have been so strongly altered to white phyllosilicates + trace muscovite that it can not be determine what they were (possibly feldspars, most likely plagioclase considering that they usually show strong alteration). Kaolinite, scarce biotite and patchy carbonate are also sometimes present altering these phenocrysts.

Quartz phenocrysts are unaltered and are usually irregular shaped.

Zircon is present as trace microcrysts.

Magmatic and hydrothermal biotite both present; together they comprise approximately 10 vol-% of the rock, most of this corresponds to hydrothermal biotite. Some biotite phenocrysts that have abundant mineral inclusions are most likely to be of magmatic origin. Hydrothermal biotite usually occurs in clusters and is shreddy looking. Biotite replaces magmatic biotite and possibly hornblende (based on shape). Biotite that occurs in clusters is sometimes being replaced by scarce muscovite + phengite and by scarce patchy carbonate. It also shows incipient replacement by chlorite.

Total percentage of white phyllosilicates + muscovite is <4 vol-%.

Carbonate occurs as patches (altering phenocrysts and in the matrix) and in veins; total percentage of carbonate is approximately 2 vol-%.

Cinnamon rutile occurs associated with biotite and comprises <1 vol-% of the rock.

Sulfides are chalcopyrite and pyrite and comprise <4 vol-% of the rock, chalcopyrite is the most abundant with only trace pyrite present in the rock. There is trace muscovite associated with chalcopyrite.

Four types of veins are present in the rocks:

- 1- Quartz + biotite + chalcopyrite + scarce carbonate.
- 2- Quartz + K-spar + biotite + chalcopyrite + scarce carbonate.
- 3- Chalcopyrite + biotite.
- 4- Chalcopyrite stringer veinlets.

All of the veinlets present in this sample are of submillimeter scale.

Alteration assemblage is K-silicate constructive with a weak phyllic overprint; also weakly overprinted by carbonate.

SD-16-1362 ft. Breccia

This sample corresponds with a breccia. Phenocrysts present include: plagioclase, K-feldspar, quartz eyes, biotite and trace zircon.

Abundant carbonate veins (most coarsely crystalline, Photo A.12) are present cutting the rock, with total carbonate being approximately 15 vol-% of the sample. Some of the carbonate has a rhombic shape suggesting that it is probably dolomitic.

Magmatic biotite is scarce throughout the sample. It is characterized by the presence of abundant mineral inclusions (zircon/apatite/rutile) and its shape goes from subeuhedral to euhedral.

Hydrothermal biotite comprises approximately 7-8 vol-% of the sample. It is usually shreddy, it mainly occurs in clusters and it varies from fine grain to coarse grain. This biotite sometimes has a green tint.

Smectite is present altering feldspars and biotite.

Cinnamon rutile is an abundant mineral (2-3 vol-%) that is usually but not always associated with biotite.

Irregular shaped patchy quartz in the matrix suggests that it was probably introduced corresponding with an alteration mineral.

White phyllosilicates are also present as an alteration mineral. Alteration of feldspars to white phyllosilicates varies from 30 to less than 5 vol-% on K-feldspar and from 10 to 15 vol-% average on plagioclase, with a few plagioclase phenocrysts having less than 5 vol-%. White phyllosilicates sometimes occur as patches associated with hydrothermal biotite (overprinting). Some feldspars show alteration to fine grain shreddy biotite.

Based on the mineralogy the alteration can be classified as K-silicate constructive with a weak phyllic overprint.

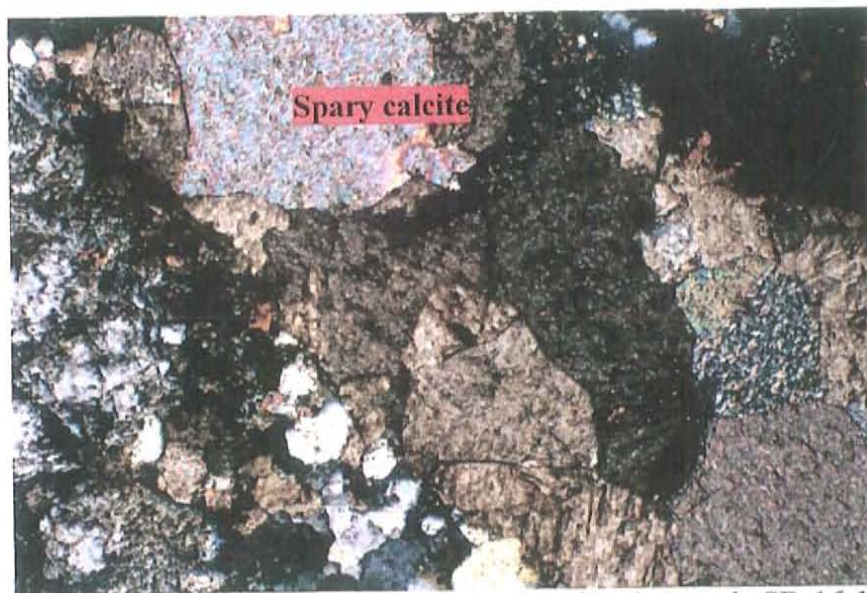


Photo A.12: Coarse calcite vein (f.o.v. = 1.8 mm long), sample SD-16-1362 ft.

Veinlets of white phyllosilicates and carbonate cut K-feldspar phenocryst.

Ore minerals comprise less than 2 vol-% of the rock, with sub-equal amounts of pyrite and chalcopyrite. They occur disseminated and in stringer veinlets and they are sometimes associated with hydrothermal biotite.

SD-16-2139 ft. Quartz-Monzonite Porphyry

This sample is very similar to SD-16-2629 ft.

Phenocrysts include: K-feldspar, plagioclase, quartz, and biotite.

K-feldspar phenocrysts are the biggest phenocrysts in the sample; they are cut by thin submillimeter scale white phyllosilicate veinlets, quartz stringer veinlets and sulfide stringer veinlets. K-feldspars are being altered to white phyllosilicates (varying from trace to less than 5 vol-%) and sometimes to scarce patchy carbonate. Mineral inclusions (plagioclase and quartz) are common in the K-feldspar phenocryst.

Plagioclase phenocrysts are altered to white phyllosilicates and smectite (the alteration to smectite is strong). Some feldspars show very strong alteration to white phyllosilicates (up to 70 vol-%), because of the strong alteration it is hard to determine whether it was originally plagioclase or K-feldspar. Scarce muscovite is also present altering feldspars.

Quartz phenocrysts are not as rounded as in QLP. Magmatic biotite varies from subeuhedral to euhedral and it is characterized by the presence of mineral inclusions like zircons. Total percentage of biotite and quartz phenocryst is approximately 5 vol-% each.

The groundmass is composed of quartz and K-feldspar and it comprises approximately 30 vol-% of the sample. It is very hard to determine whether all the quartz and K-feldspar present in the matrix are original early magmatic minerals. Some of the quartz looks patchy and irregular (introduced?). Some of the K-feldspar could be late magmatic-early hydrothermal (part of the K-silicate constructive alteration).

Hydrothermal biotite is the main alteration mineral; its total percentage is approximately 6 vol-%. It is fine grain biotite and usually occurs in clusters. There are some areas where hydrothermal biotite is replacing magmatic biotite (Photo A.13).

Patchy carbonate and white phyllosilicates are present as alteration minerals in the matrix. There are white phyllosilicates that seem to be replacing magmatic biotite. Total percentage of carbonate is <1 vol-% and of white phyllosilicates is approximately 1-2 vol-% (not taking into account the white phyllosilicates that are altering the feldspars mentioned above).

The alteration assemblage can be classified as K-silicate constructive with a weak phyllic overprint.

Cinnamon rutile is present in the sample and it is mainly associated with magmatic and hydrothermal biotite. There is scarce rutile that occurs alone in the matrix and some scarce occurs with white phyllosilicates (was it originally biotite that got replaced?). Total percentage of cinnamon rutile is < 1 vol-%.

Sulfides (pyrite and chalcopyrite) occur in stringer veinlets and disseminated, there is also a thin discontinuous pyrite veinlet. They show a strong association to biotite both magmatic and hydrothermal. Scarce sulfides also occur with white phyllosilicates (was it originally biotite that got replaced?). Total percentage of ore minerals is approximately 3 vol-% with sub-equal amounts of pyrite and chalcopyrite. Pyrite is sometimes present along the cleavage of biotite (replacing? Photo A.14)

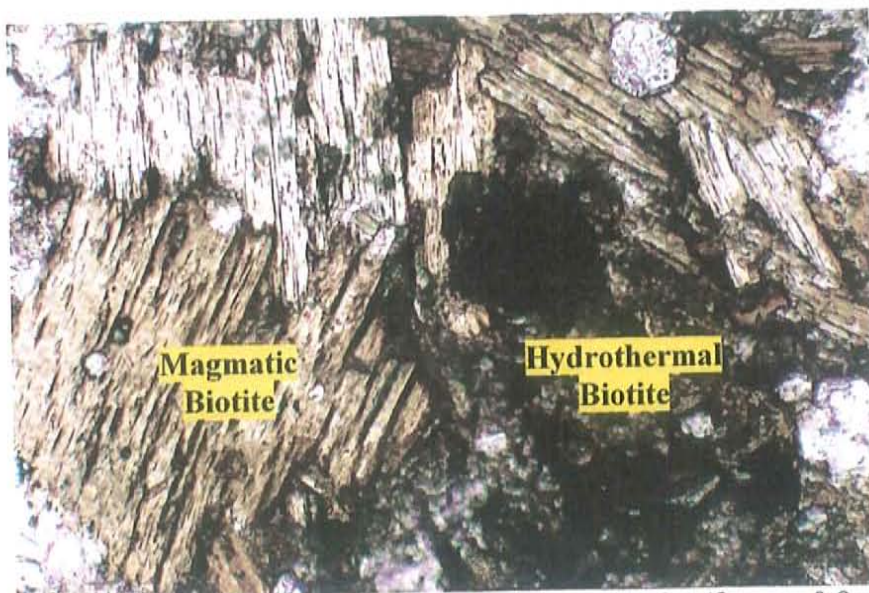


Photo A.13: Hydrothermal biotite replacing magmatic biotite (f.o.v. = 0.9 mm long).
Sample SD-16-2139 ft.

There is one-submillimeter scale pyrite + chalcopyrite + white phyllosilicate + carbonate veinlet in the sample. Paragenesis of the vein: it seems that the white phyllosilicates formed first, followed by pyrite, then chalcopyrite and that carbonate was the last minerals to form in the vein.



Photo A.14: Pyrite on the cleavage of biotite (f.o.v. = 0.9 mm long). Sample SD-16-2139 ft.

SD-16- 2185 ft. Quartz-Latite Porphyry

Feldspars are the most abundant phenocrysts with sub equal amounts of plagioclase and K-feldspar; they are followed by quartz and then biotite in abundance.

Some scarce altered phenocrysts are also present (possibly hornblende) these have been replaced by hydrothermal biotite, pyrite and scarce chalcopyrite.

Big K-feldspar phenocrysts usually present mineral inclusions (euhedral plagioclase, biotite, quartz and scarce sphene). Thin sub-millimeter scale white phyllosilicates veinlets and carbonate veinlets cut some of the K-feldspars.

Plagioclase phenocrysts show alteration to smectite and are sometimes cut by abundant white phyllosilicate veins. Total alteration of feldspars to white phyllosilicates varies from weak to moderate; this alteration is stronger in plagioclase, in some cases reaching 45 vol-%.

Besides white phyllosilicates there also seems to be fine grain biotite altering plagioclase as veins and patches (brown pleochroism), because it is so fine grain it is hard to differentiate it from the white phyllosilicates.

Quartz phenocrysts present a very distinctive rounded shape (quartz eyes), and they constitute less than 10 vol-% of the rock; some of these quartz eyes are shattered.

Magmatic biotite is characterized by the presence of mineral inclusions, which are usually very fine grained (Photo A.15).

Groundmass percentage is approximately 50 to 55 vol-% and it is composed mainly of fine grain quartz. Fine grain biotite is present in the matrix (Photo A.16), this biotite is probably either late magmatic or early hydrothermal.

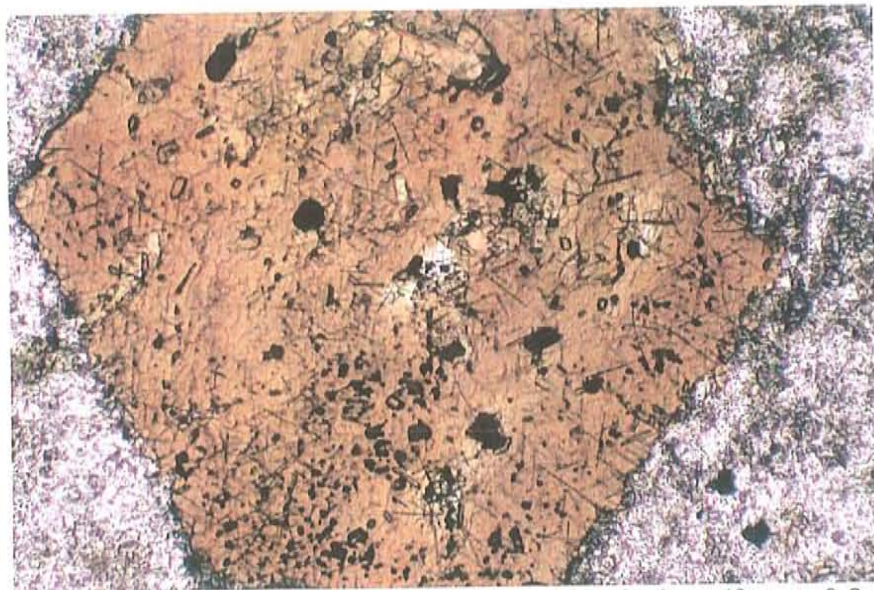


Photo A.15: Magmatic biotite with abundant mineral inclusions (f.o.v = 0.9 mm long).
Sample SD-16-2185 ft.

Hydrothermal biotite is fine grain, shreddy and it usually occurs in clusters (sometimes with sulfides, Photo A.17), total percentage of hydrothermal biotite is approximately 7-10 vol-% (taking into account the fine grain biotite present in the matrix). Some of the hydrothermal biotite has olive green pleochroism.

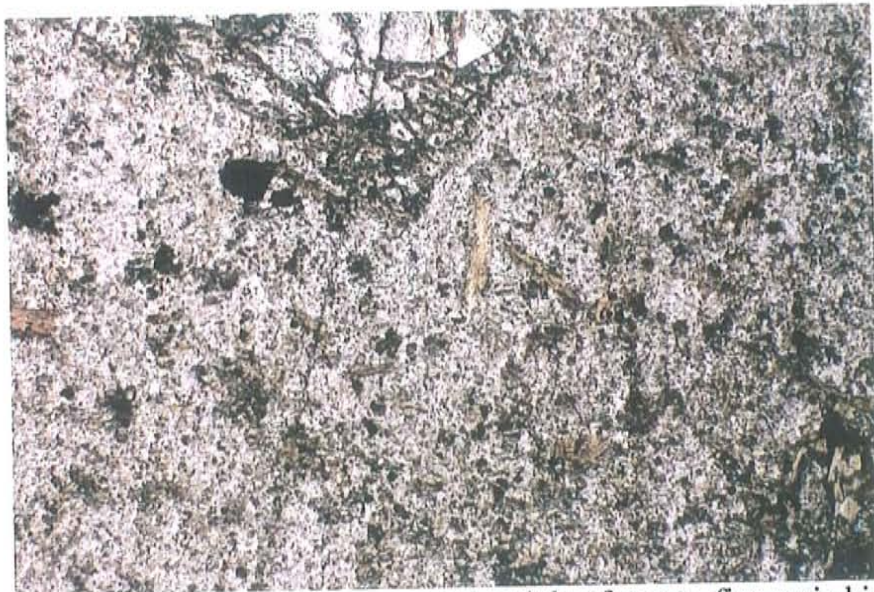


Photo A.16: QLP, fine grain matrix composed mainly of quartz, fine grain biotite is also present (f.o.v. = 1.8 mm long). Sample SD-16-2185 ft.

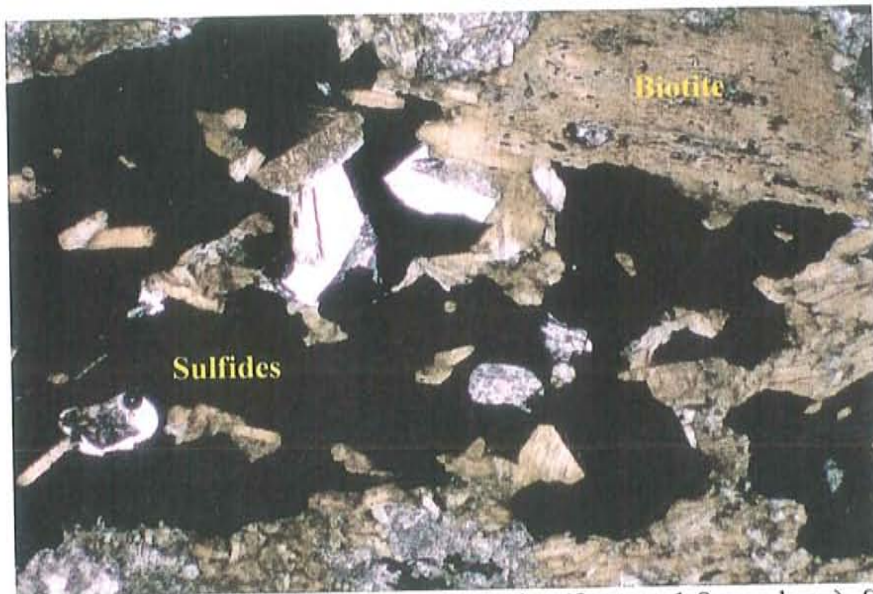


Photo A.17: Abundant biotite together with sulfides (f.o.v. = 1.8 mm long). Sample SD-16-2185 ft.

The alteration assemblage can be classified as K-silicate constructive characterized by the presence of hydrothermal biotite and it has been weakly overprinted by white phyllosilicates (phyllitic overprint). There does not seem to be introduced K-feldspar present.

White phyllosilicates are present in two ways: altering feldspar and as patches throughout the sample (together with muscovite), the total percentage of patchy white phyllosilicates is approximately 2-3 vol-%. They sometimes occur together with carbonate and sulfides.

Magmatic biotite phenocrysts are sometimes being altered to white phyllosilicates (Photo A.18), white phyllosilicates are also sometimes associated with hydrothermal biotite (replacing?).

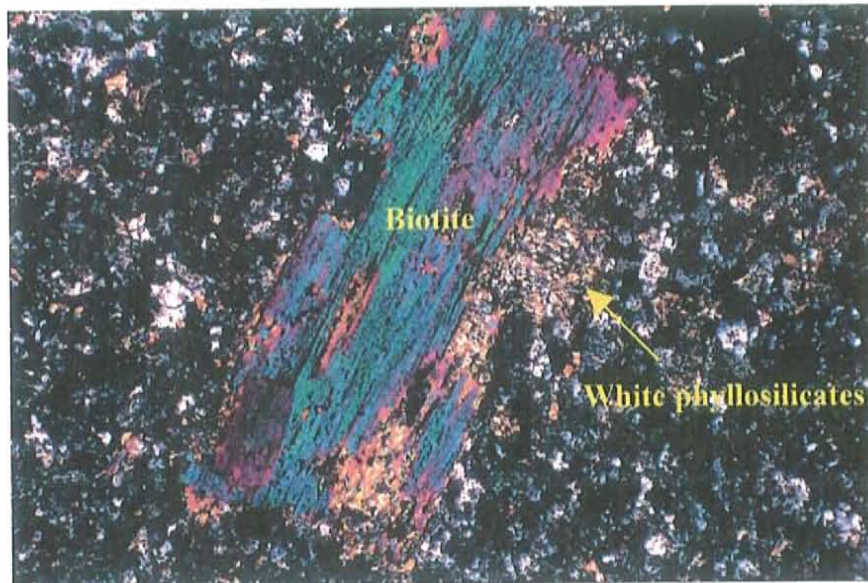


Photo A.18; White phyllosilicates altering biotite (f.o.v. = 1.8 mm long). Sample SD-16-2185 ft.

Other alteration minerals besides hydrothermal biotite and white phyllosilicates include: carbonate, cinnamon rutile and chlorite (Photo A.19). Carbonate occurs as scarce patches in the matrix and in veins. Patchy carbonate sometimes occurs with hydrothermal biotite (possibly replacing?), white phyllosilicates and sulfides; total carbonate in the sample is approximately 2 vol-%. Cinnamon rutile comprises <1 vol-% of the sample and it mainly occurs with hydrothermal biotite and sulfides, it also sometimes occurs with carbonate or close to carbonate veins and scarce occurs with white phyllosilicates (was it originally biotite?). Some rutile inclusions are present in magmatic biotite phenocrysts. Chlorite is present in trace amounts and it is altering hydrothermal biotite.

Trace phenocrysts that were probably sphene (based on their shape) have now been altered to cinnamon rutile (Photo A.20); total percentage of these is <1 vol-%.

Pyrite and chalcopyrite are the only two ore minerals present and they constitute approximately 3-4 vol-% of the sample with pyrite > chalcopyrite. The total amount of chalcopyrite is approximately 1 vol-%. They mainly occur with hydrothermal biotite; scarce occur with white phyllosilicates (originally biotite?).

Veins present in the sample:

1- Carbonate veins

2- Thin smectite veinlets that cut the rock.

3- White phyllosilicates veinlets cutting feldspar, quartz phenocrysts and the matrix.

All these veins are sub-millimeter scale.

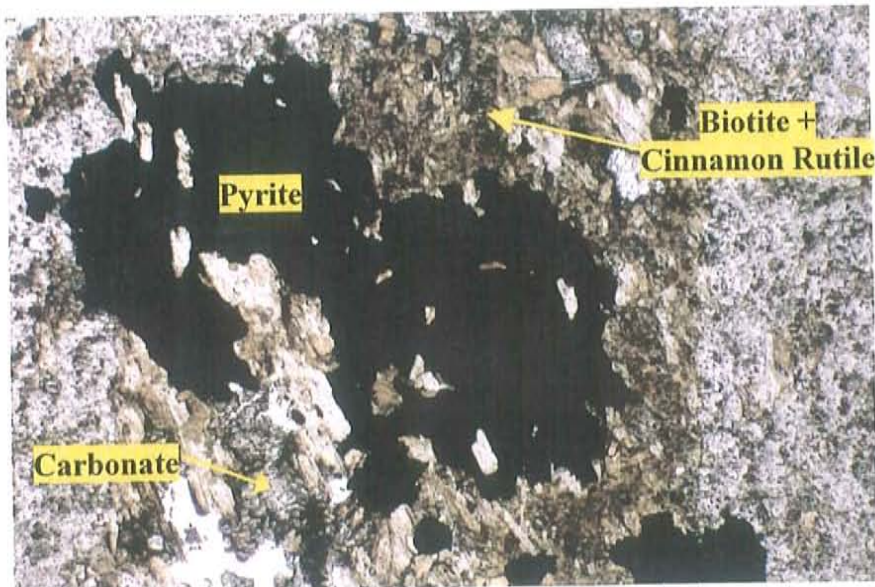


Photo A.19: Biotite + pyrite + carbonate + cinnamon rutile altering a phenocryst (f.o.v. = 1.8 mm long). Sample SD-16-2185 ft.

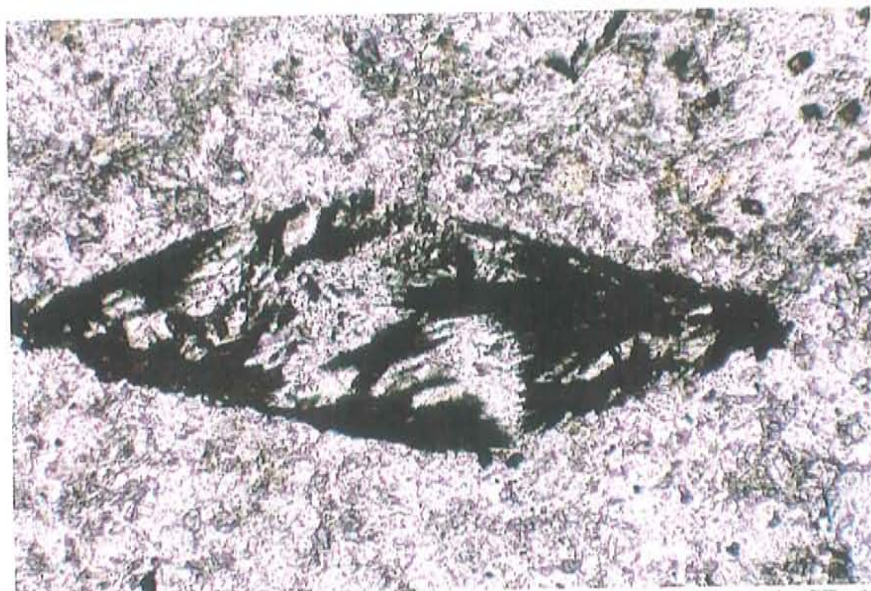


Photo A.20: Sphenes replaced by rutile (f.o.v. = 0.9 mm long). Sample SD-16-2185 ft.

SD-16-2629 ft. Quartz-Monzonite Porphyry

Alteration minerals include secondary biotite (late magmatic-early hydrothermal), smectite, cinnamon rutile, carbonate and white phyllosilicates; with biotite being the most abundant. The alteration can be classified as K-silicate constructive with a weak phyllic overprint. Some of the K-feldspar found in the matrix and surrounding the phenocrysts could be late magmatic early hydrothermal, but the lack of veins makes it hard to determine for sure the presence of hydrothermal K-feldspar.

Quartz phenocrysts comprise less than 10 vol-% of the rock; their shape goes from anhedral to subeuhedral, with a few presenting a rounded form (quartz eyes).

There are sub equal amounts of plagioclase and K-feldspar phenocrysts in the sample with both comprising approximately 40-45 vol-%.

Plagioclase is subeuhedral to euhedral in shape. It has been altered to smectite (sometimes as selective overgrowths, Photo A.21) and white phyllosilicates (Photo A.22); the degree of alteration to white phyllosilicates varies from less than 5 to 40 vol-% in some few cases. Patchy carbonate is also present altering plagioclase (Photo A.23).

Some K-feldspars have been strongly altered to white phyllosilicates, up to 70 vol-%, but these are very scarce and they are located near the edge of the thin section (close to a vein?). On average the alteration of K-feldspar to white phyllosilicates varies from 5 to 10 vol-%.

Two types of biotite are present in the sample:

1- Magmatic biotite, comprising approximately 4 vol-% of the rock. This biotite has a shape that varies from subeuhedral to anhedral, and it has mineral inclusions (mainly zircon, rutile and apatite).

2- Hydrothermal-late magmatic biotite. Occurs as fine grain shreddy clusters, its color varies from brown to light green. Hydrothermal biotite sometimes surrounds magmatic phenocrysts (replacing?). This type of biotite comprises approximately 6-8 vol-% of sample. Hydrothermal biotite replaces magmatic biotite (Photo A.24).

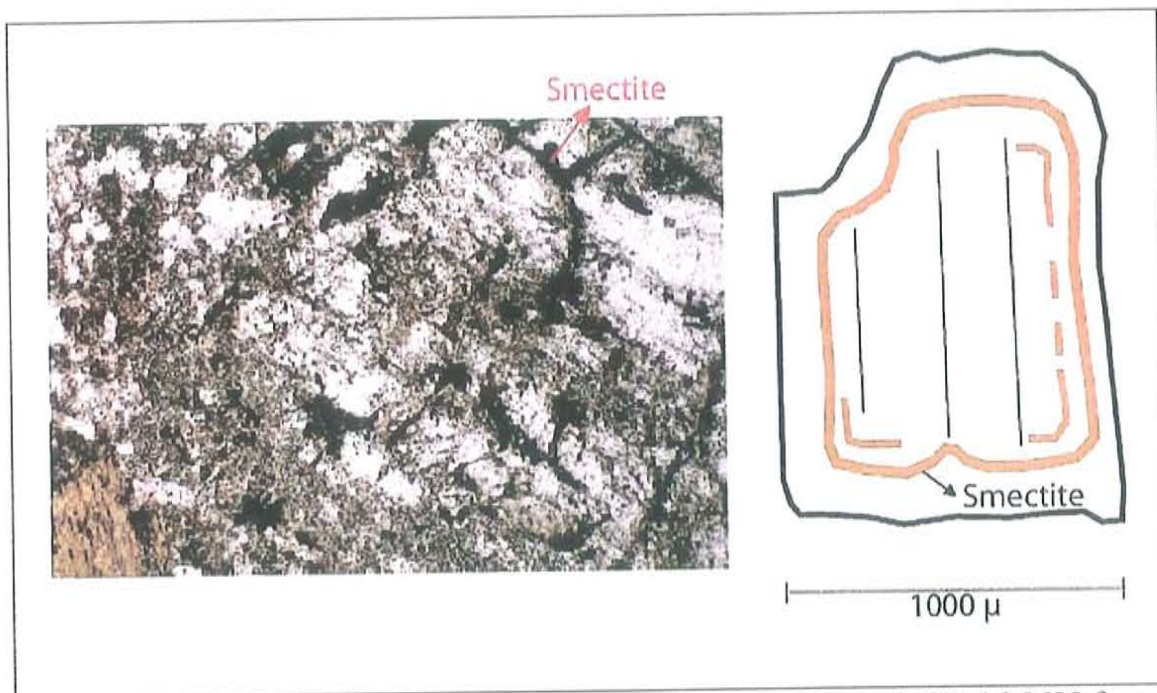


Photo A.21: Selective smectite overgrowths in plagioclase, sample SD-16-2629 ft.



Photo A.22: Fine grain white phyllosilicates altering plagioclase (f.o.v. = 0.9 mm long).
Sample SD-16-2629 ft.

There is a moderate to strong alteration of hydrothermal biotite to chlorite, and only a scarce alteration of magmatic biotite to chlorite (Photo A.25).

Cinnamon rutile comprises approximately 2 vol-% of the sample and it occurs as an alteration mineral that is mainly but not always associated with biotite (Photo A.26). In magmatic biotite is usually occurs as inclusions.

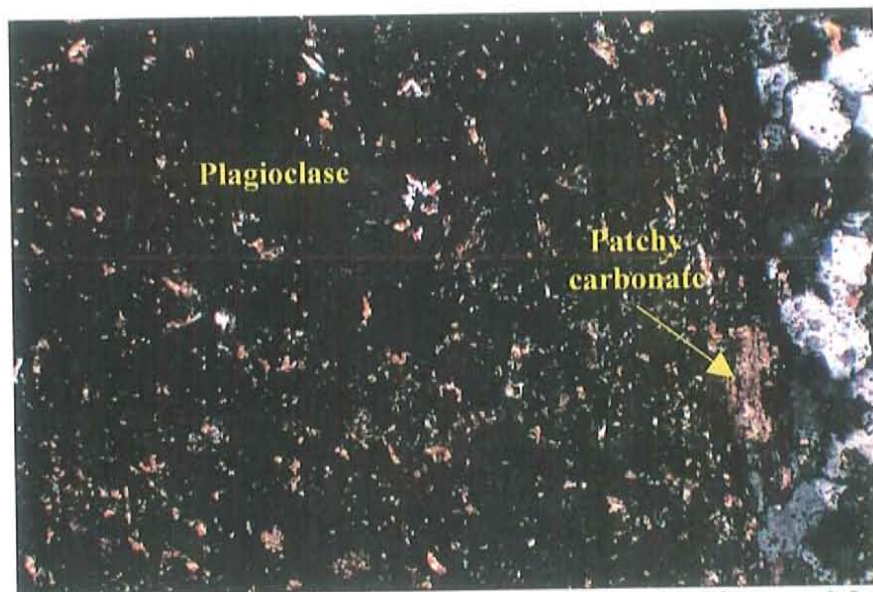


Photo A.23: Patchy carbonate altering plagioclase on the edge (f.o.v. = 0.9 mm long).
Sample SD-16-2629 ft.

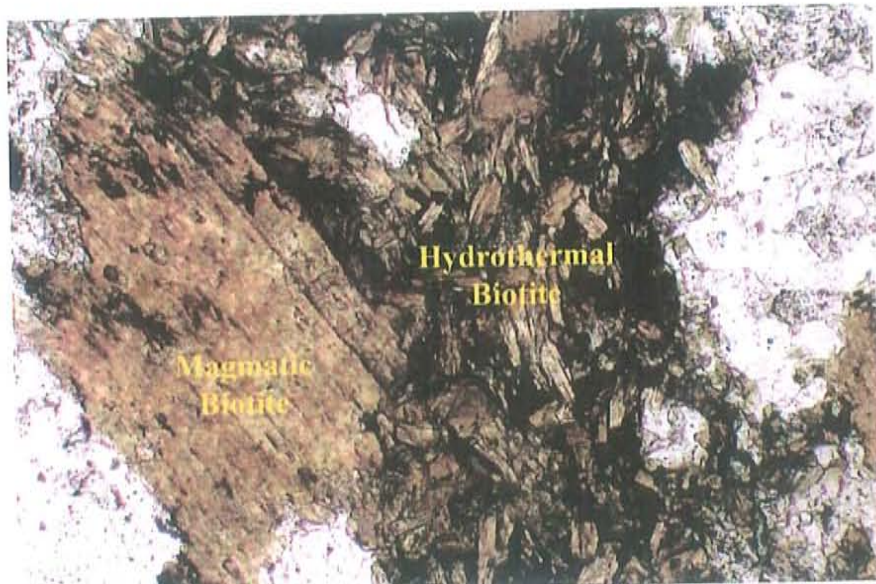


Photo A.24: Hydrothermal biotite replacing magmatic biotite (f.o.v. = 0.9 mm long).
Sample SD-16-2629 ft.

Trace zircon is also present in the rock as part of the rock forming minerals.

The matrix of the rock comprises approximately 35-40 vol-% of the rock and it is composed of mainly quartz and K-feldspar. Some of the quartz could have been introduced as an alteration mineral and not correspond with the original rock forming components. Some trace carbonate is present in the matrix, and there is also some together with hydrothermal biotite possibly replacing it.

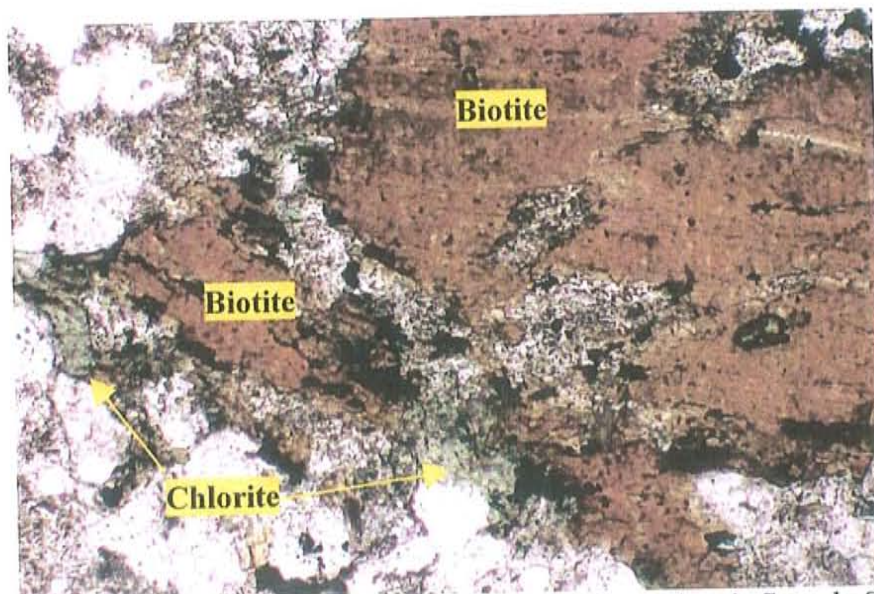


Photo A.25: Biotite being altered to chlorite (f.o.v. = 0.9 mm long). Sample SD-16-2629 ft.

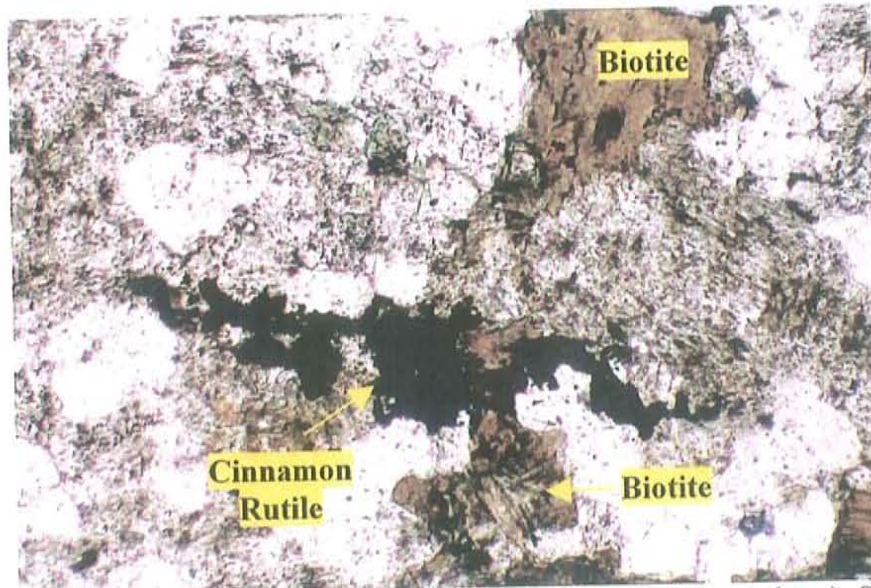


Photo A.26: Cinnamon rutile associated with biotite (f.o.v = 0.9 mm long). Sample SD-16-2629 ft.

Three different types of veins are recognized in this sample and they are all barren:

- 1- Quartz stringer veinlets cutting K-feldspar phenocrysts.
- 2- Submillimeter scale veinlets of white phyllosilicates that cut plagioclase and K-feldspar phenocrysts.
- 3- Carbonate vein? It is located near the edge of the sample.

Pyrite and chalcopyrite represent the only two ore minerals present with pyrite being the most abundant. They sometimes are associated with hydrothermal biotite (replacing?). Total sulfide percentage in the sample is less than 1 vol-%. Sulfides are disseminated.

DRILL HOLE SD-18

SD-18-1108 ft. Andesite

This sample corresponds to a porphyritic rock apparently of volcanic origin. The matrix is very fine grain and its main component seems to be plagioclase. Smectite is also present in the matrix giving it a dirty aspect.

Plagioclase phenocrysts are the most abundant, they have been altered to white phyllosilicates and smectite; the alteration to white phyllosilicates varies from note to scarce.

K-feldspar phenocrysts are scarce; the total alteration of K-feldspars to white phyllosilicates is weak.

All the quartz is fine grain (no big phenocrysts are present); some is patchy and irregular shaped (introduced?).

Total biotite in the sample is <4 vol-%. Phenocrysts with abundant mineral inclusions are more likely of magmatic origin. Shreddy biotite is possibly late magmatic-early hydrothermal.

There are clusters where white phyllosilicates have replaced biotite (still some residual biotite left); also in these clusters there is the greatest concentration of pyrite. The total amount of white phyllosilicates in the rock is <4 vol-%.

There are also clusters of smectite quartz and pyrite (was it a phenocryst that got replaced?).

Cinnamon rutile occurs associated with biotite and to white phyllosilicates (possibly originally biotite), the total amount of rutile in the samples is <2 vol-%.

Holes are present throughout the sample, some have mineral shapes suggesting that they might have formed by dissolution; but most are irregular.

The total amount of pyrite in the rock is 4-5 vol-%. Only trace chalcopyrite is present.

Alteration assemblage is K-silicate constructive with a weak phyllic overprint.

DRILL HOLE SD-19

SD-19-1548 ft. Biotite-Dacite, Volcanic Rock

This sample has been strongly altered to hydrothermal biotite and smectite (Photo A.27). Smectite is present altering phenocrysts (some have been completely altered) and as patches throughout the sample. Hydrothermal biotite is very fine grain and it occurs in clusters, its color varies from brown to olive green. Total percentage of hydrothermal biotite is approximately 15-20 vol-% and the percentage of smectite is approximately 10-15 vol-%. Some phenocrysts have been altered to biotite (probably mafics). Based on the amount of secondary biotite the alteration assemblage is classified as K-silicate constructive.

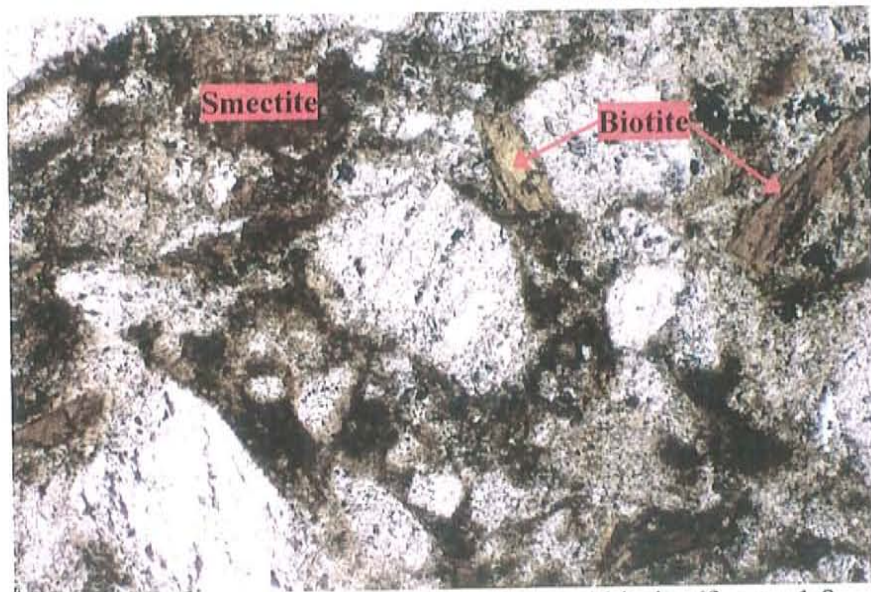


Photo A.27: Alteration to smectite and hydrothermal biotite (f.o.v = 1.8 mm long), sample SD-19-1548 ft.

Phenocrysts include plagioclase, K-feldspar, quartz, biotite and trace zircon. Plagioclase is the most abundant phenocryst, these show trace alteration to white

phyllosilicates and usually have holes (dissolution?). Plagioclase and biotite phenocryst both vary from euhedral to subeuhedral. Some biotite phenocrysts have been altered to smectite.

Scarce thin sub millimeter scale veinlets of white phyllosilicates are present cutting some phenocrysts; possibly K-feldspar (hard to determine because of the strong alteration present in the sample).

The matrix is composed of really fine grain quartz. The strong alteration to biotite and smectite makes it hard to determine the percentage of matrix present in the rock; an estimate would be around 15-20 vol-%.

There is an area of the sample that has less density of phenocrysts and also shows less alteration, possibly a xenolith.

Scarce patchy irregular quartz suggests that it is probably an alteration mineral and not part of the original rock forming quartz.

No ore minerals were observed. Disseminated iron oxides or hydroxides (possibly hematite) comprise approximately 3-4 vol-% of the sample, and they occur mainly with hydrothermal biotite.

Holes are present throughout the sample, some occur in plagioclase phenocrysts (mentioned before) and some in the matrix (dissolution?), their lack of regular rounded shape suggest that they are probably not a magmatic feature; these holes are also visible in hand specimen. No cinnamon rutile

DRILL HOLE SD-21

SD-21-490 ft. Quartz-Latite Porphyry

Matrix comprises approximately 30 to 40 vol-% and it is mainly composed of fine grain irregular quartz. Phenocrysts include K-feldspar, plagioclase, quartz and hornblende; trace zircon and fresh sphene are also present.

K-feldspars show moderate alteration to epidote + carbonate (Photo A.28). White phyllosilicates are also present altering K-feldspars, which occur as patches and thin submillimeter scale veinlets, total alteration to white phyllosilicates is <5 vol-%.

Plagioclase phenocrysts have been altered to white phyllosilicates, carbonate and silica (with carbonate as the most abundant), all of these occur as veinlets and patches; total alteration of plagioclase to white phyllosilicates is scarce (<5 vol-%).

Quartz phenocrysts are rounded. A few have an iron oxide rim.

A fibrous amphibole (actinolite/tremolite) replaces biotite and hornblende phenocrysts (Photo A.29), and also occurs in the matrix indicating hydration of the rock. Residual hornblende is still present but there does not seem to be any biotite left. This amphibole comprises <5 vol-% of the rock.

Epidote and carbonate also occur in the matrix and not just replacing phenocrysts. Total carbonate in the rock is <5 vol-% and epidote comprises <2 vol-%.

No sulfides were found. Iron oxides and hydroxides comprise <2 vol-% of the rock.

Besides the veinlets mentioned above there are also carbonate + silica submillimeter scale veinlets

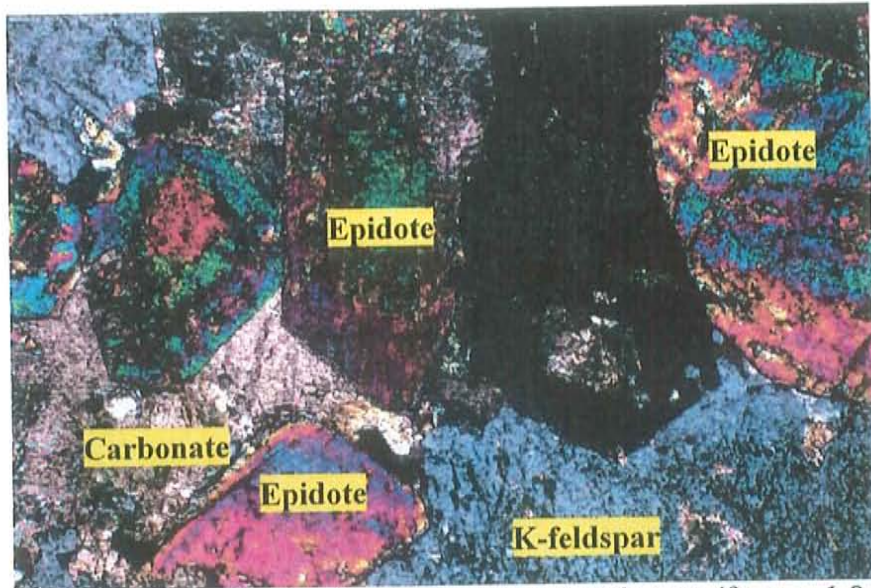


Photo A.28: K-feldspar with alteration to epidote and carbonate (f.o.v. = 1.8 mm long), sample SD-21-490 ft.

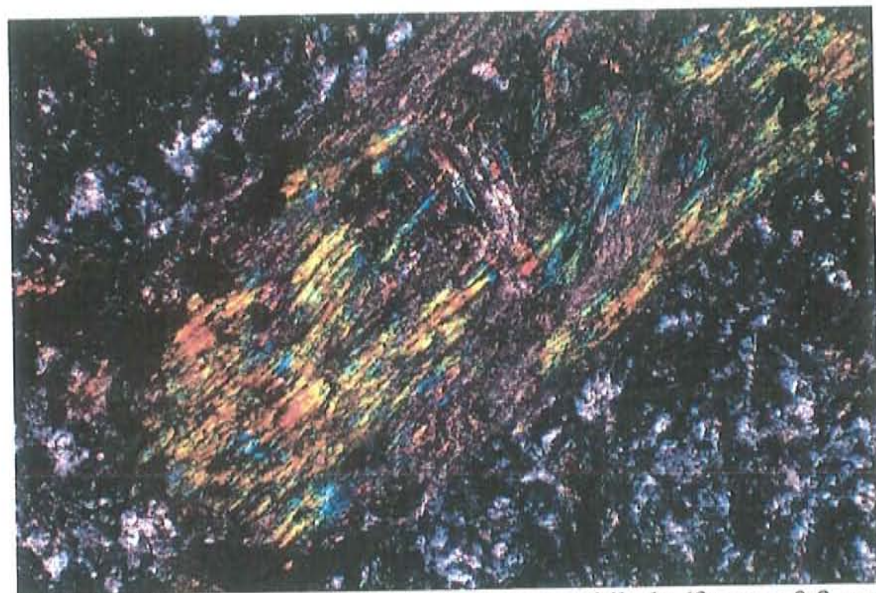


Photo A.29: Mafic mineral replaced by fibrous amphibole (f.o.v. = 0.9 mm long). Sample SD-21-490 ft.

SD-21-548 ft. Protolith: Limestone?

This rock has been completely replaced by alteration minerals (replacement body). The two main minerals are tremolite and diopside; tremolite is the most abundant comprising approximately 40-45 vol-% and total diopside is approximately 35 vol-% (Photo A.30). Other minerals present include: carbonate comprising approximately 15 vol-%, a silicate mineral (apparently serpentine) which comprises <5 vol-% and silica (sometimes as chalcedony) with a percentage of <2 vol-%.

Carbonate occurs localized only in one area of the sample together with silica and serpentine; in this area carbonate replaces tremolite and to a lesser degree diopside (Photo A.31), although some parts have completely been replaced by carbonate.

Two different types of veins are present in the rock:

1- Carbonate (spary) + chalcedony; this vein occurs in the area where the carbonate is concentrated.

2- Diopside vein.

Both are submillimeter scale.

Protolith was probably a carbonate.

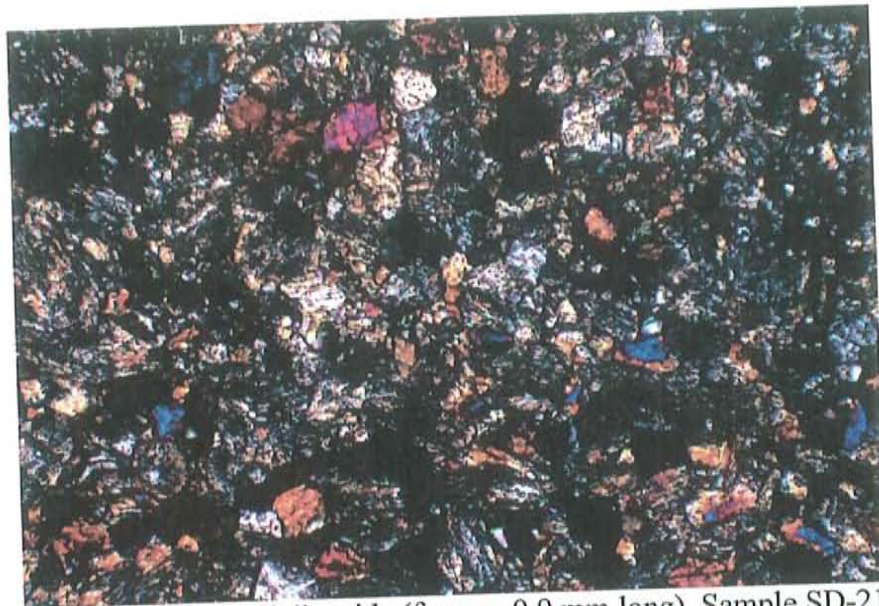


Photo A.30: Tremolite and diopside (f.o.v. = 0.9 mm long). Sample SD-21-548 ft.



Photo A.31: Tremolite replaced by carbonate (f.o.v. = 0.9 mm long). Sample SD-21-548 ft.

SD-21-660.5 ft. Biotite Quartz-Latite Porphyry

This rock presents a strong alteration to hydrothermal biotite (biotitized, Photo A.32). Only scarce phenocrysts are present, these include: K-feldspar, plagioclase, biotite, hornblende and trace quartz. Trace apatite is present.

Matrix is composed of fine grain quartz, plagioclase and K-feldspar; it is difficult to estimate the matrix percentage because of the strong alteration to biotite. Trace epidote is present in the matrix.

K-feldspar phenocrysts sometimes have mineral inclusions of plagioclase and hornblende. These feldspars show alteration to biotite, sulfides, and white phyllosilicates (total alteration to white phyllosilicates is scarce). A stringer chalcopyrite + pyrite veinlet cuts a K-feldspar phenocryst.

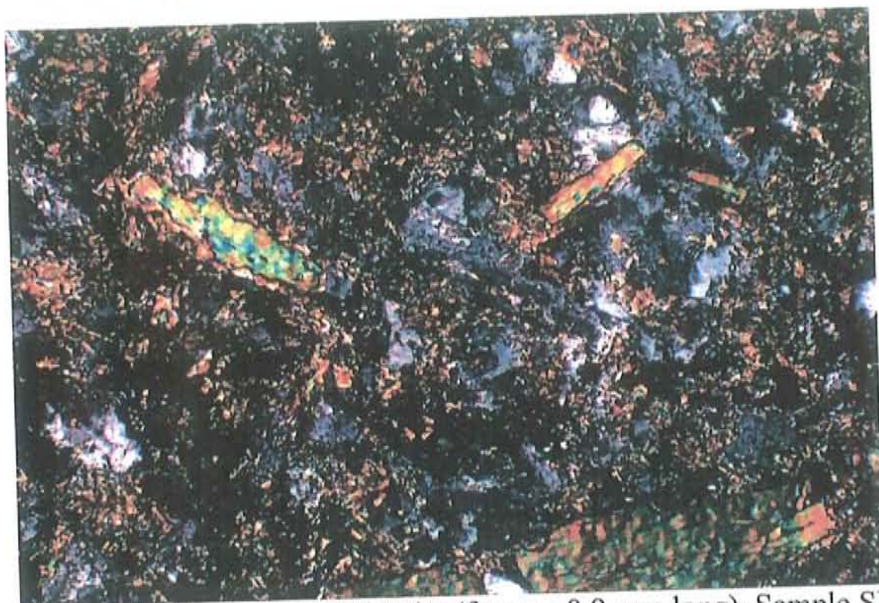


Photo A.32: Abundant hydrothermal biotite (f.o.v. = 0.9 mm long). Sample SD-21-660.5 ft.

Plagioclase phenocrysts have been altered to fine grain biotite which occurs as patches and veinlets.

Scarce hornblende is present in the sample comprising <2 vol-% of the rock, it is closely associated with sulfides (mainly pyrite and some chalcopyrite) to hornblende (replacing it?). There is a hornblende phenocryst that has been completely replaced by biotite + pyrite + chalcopyrite.

Most of the biotite seems to be of hydrothermal origin (total amount of biotite in the sample is approximately 50-55 vol-%), it is usually very fine grain and shreddy, it sometimes occurs in clusters (possibly replacing mafic minerals); in some cases these clusters have sulfides associated with them (Photo A.33). Hydrothermal biotite varies from brown to olive green. Biotite phenocrysts with mineral inclusions are possibly magmatic in origin. Trace chlorite is present altering biotite. Biotite also occurs as veinlets.

Sulfides are pyrite and chalcopyrite and together they comprise approximately 5-10 vol-% of the rock, of these <2 vol-% corresponds to chalcopyrite. Chalcopyrite surrounds pyrite in some cases suggesting that it formed later (Photo A.34). Sulfides occur disseminated and in stringer veinlets.

Cinnamon rutile is scarce in the sample, with total amount <1 vol-%. It sometimes occurs together with chalcopyrite (Photo A.35).

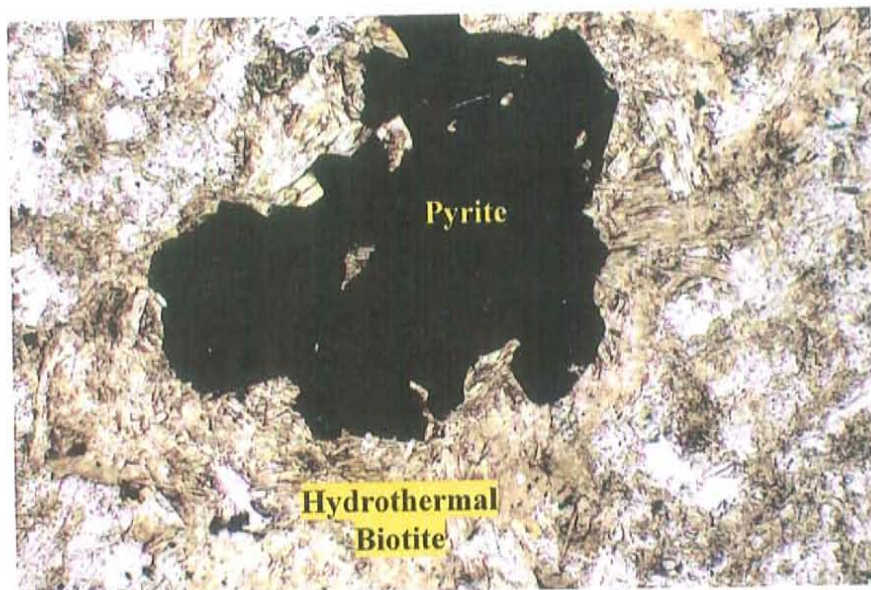


Photo A.33: Cluster of hydrothermal biotite and pyrite (f.o.v. = 0.9 mm long). Sample SD-21-660.5 ft.

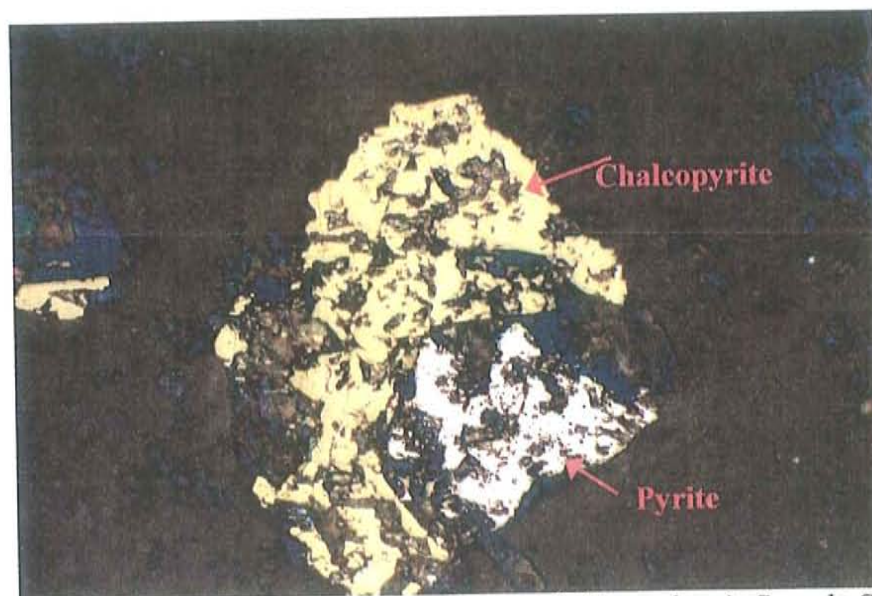


Photo A.34: Chalcopyrite surrounds pyrite (f.o.v. = 0.45 mm long). Sample SD-21-660.5 ft.

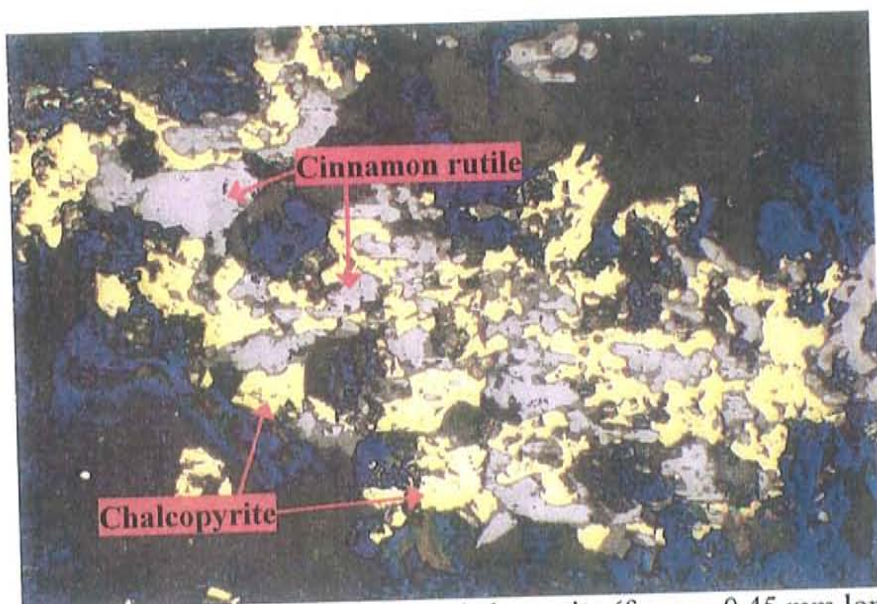


Photo A.35: Cinnamon rutile together with chalcopyrite (f.o.v. = 0.45 mm long). Sample SD-21-660.5 ft.

SD-21-1581 ft. Quartz-Latite Porphyry

Phenocrysts include: plagioclase (the most abundant), K-feldspar, biotite and quartz. Trace zircon is present in the rock.

K-feldspars have been altered to patchy chlorite + carbonate, biotite, patchy silica, and white phyllosilicates (total alteration to white phyllosilicates <5 vol-%). These phenocrysts are cut by veinlets of carbonate and by silica veinlets; both submillimeter scale.

Plagioclase phenocrysts show alteration to white phyllosilicates, carbonate, biotite (most abundant, up to 40 vol-% in some cases) and kaolinite and in some cases are cut by abundant biotite veinlets. Alteration to white phyllosilicates varies from <10 vol-% to 30 vol-% approximately.

Quartz phenocrysts vary from well rounded to irregular shaped; some have been altered to carbonate and chlorite.

Matrix comprises approximately 35-40 vol-% of the rock and it is made of fine grain irregular quartz.

Biotite phenocrysts with mineral inclusions are possibly of magmatic origin.

Some phenocrysts have been completely replaced by alteration minerals, these include: hydrothermal biotite, chlorite, carbonate, cinnamon rutile, quartz and white phyllosilicates (with scarce muscovite); these alteration minerals usually occur together, but biotite, silica and muscovite are not always present. Some of these altered phenocrysts were once hornblende based on shape (Photo A.36), others might have been plagioclase.

Hydrothermal biotite is fine grain and shreddy, it occurs everywhere in the rock and it comprises approximately 5-10 vol-% of the rock. It is followed in abundance by carbonate and chlorite with approximately 5 vol-% of each; there is a close association between these two minerals in the rock.

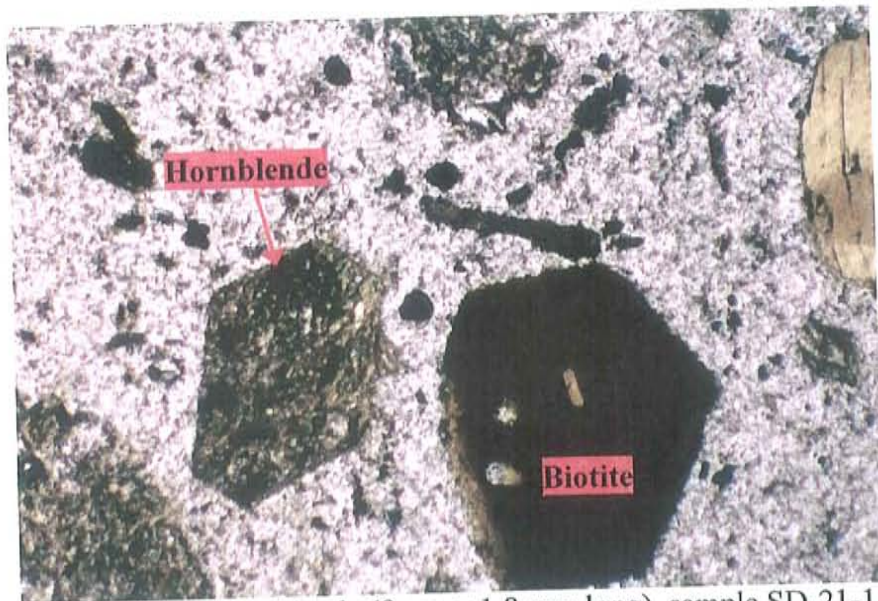


Photo A.36: Altered hornblende (f.o.v. = 1.8 mm long), sample SD-21-1581 ft.

Cinnamon rutile comprises 2-3 vol-% of the rock and it has a close association to biotite; in some cases rutile is also occurs with chlorite and carbonate (was it originally biotite that got replaced?).

White phyllosilicates comprise <3 vol-% of the rock, besides altering feldspars there is trace patchy white phyllosilicates + trace muscovite in the matrix.

Sulfides are pyrite and chalcopyrite and occur disseminated with no close relationship to any other mineral; the total percentage is approximately 5-7 vol-% (pyrite > chalcopyrite). Difficult to estimate sulfides, not a polishes thin section.

Alteration assemblage can be classified as K-silicate constructive overprinted by carbonate + chlorite and white phyllosilicates.

SD-21-1584.5 ft. Hornblende Dacite Porphyry

Based on texture this rock is probably a shallow hypabyssal intrusion.

Biotite is the most abundant phenocryst followed by hornblende (which sometimes occurs in clusters). Plagioclase and quartz are the least abundant with only scarce amount of each. Trace zircon and sphene are present in the rock. Fine grain magnetite apparently of magmatic origin comprises <3 vol-% of the rock.

Quartz phenocrysts are very rounded and in some cases appear to be shattered. These sometimes have been altered by scarce carbonate and white phyllosilicates.

Plagioclase phenocrysts are cut by white phyllosilicate veinlets and by carbonate veinlets (both submillimeter scale). Alteration of plagioclase to white phyllosilicates is <5 vol-%.

Biotite phenocrysts with mineral inclusions are possibly of magmatic origin. Most of the biotite is shreddy suggesting that it might be late magmatic-early hydrothermal. Total biotite in the sample is approximately 20 vol-%.

Matrix comprises approximately 30 vol-% of the rock and it is made of smectite, K-feldspar and fine grain quartz (some of the quartz is irregular shaped, introduced?).

Carbonate occurs as abundant submillimeter to millimeter scale veins and as scarce patches. The veins are made of coarse carbonate (spary). Total percentage of carbonate in the sample is approximately 15-20 vol-%.

Actinolite comprises 5-10 vol-% of the rock; it sometimes occurs with fine grain biotite altering phenocrysts, some also seems to be replacing biotite.

Chlorite is present altering biotite and hornblende. Some phenocrysts have been altered to carbonate + chlorite. Total chlorite in the sample is <3 vol-%.

Thin submillimeter scale quartz veins cut the rock.

No ore minerals seem to be present in the rock.

SD-21-1592.5 ft. Quartz-Monzonite Porphyry

Alteration of K-feldspar to white phyllosilicates (as patches and submillimeter scale veinlets) varies from <5 to 75 vol-%. Other alteration minerals that are sometimes present altering K-feldspar include: biotite (abundant in some cases), patchy carbonate, patchy silica + K-feldspar and cinnamon rutile.

Plagioclase phenocrysts have all been strongly altered. Alteration minerals in order of abundance are: white phyllosilicates + muscovite, carbonate and fine grain biotite. Total alteration varies from 70-90 vol-%.

There are feldspars that have been so strongly altered that it can not be determined whether they are plagioclase or K-feldspar.

Quartz phenocrysts sometimes have holes that have been filled with K-feldspar (possibly introduced).

There is trace zircon present in the rock.

Biotite phenocrysts with abundant mineral inclusions (such as: zircon and cinnamon rutile) are possibly of magmatic origin, most of the mineral inclusions are very fine grain.

The matrix comprises 25-30 vol-% of the rock and it is composed of quartz and K-feldspar; both are very irregular shaped (introduced?). Graphic texture was seen in the matrix.

Hydrothermal biotite is fine grain and shreddy, pleochroism varies from olive green to brown. It sometimes occurs in clusters together with cinnamon rutile. Total percentage of biotite in the sample is approximately 15 vol-%, with half corresponding to hydrothermal and half to magmatic. There is hydrothermal biotite replacing magmatic biotite. Hydrothermal biotite also replaces hornblende (Photo A.37); trace hornblende is still present in the sample.

Total carbonate in the rock <5 vol-%, it occurs as patches in the matrix and altering phenocrysts.

White phyllosilicates + muscovite + phengite comprise 10 vol-% of the rock; these alter feldspars (mentioned above) and sometimes occur as patches in the matrix. There is one area where there is a cluster of biotite + carbonate + white phyllosilicates + sulfides + cinnamon rutile.

Cinnamon rutile comprises 3-4 vol-% of the rock and is usually associated with biotite.

Sulfides are pyrite and chalcopyrite and occur disseminated; together these comprise <2 vol-% with sub-equal amounts of each. They sometimes occur with fine

grain biotite and there are some cases where they grew on magmatic biotite (replacing?). Scarce sulfides also occur with white phyllosilicates (possibly originally biotite).

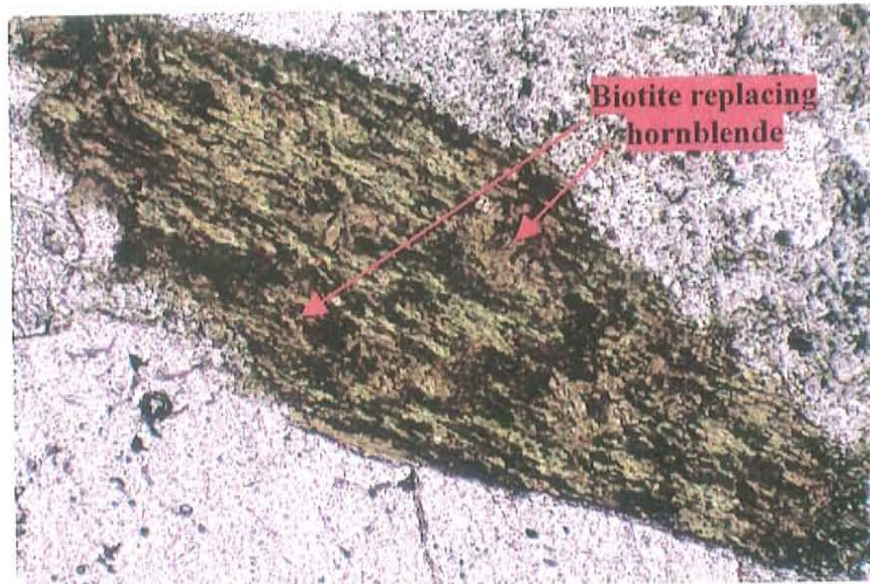


Photo A.37: Biotite (brown) replacing hornblende (green) (f.o.v = 0.9 mm long). Sample SD-21-1592.5 ft.

The alteration can be classified as K-silicate constructive weakly overprinted by white phyllosilicates and scarce carbonate.

SD-21-1636 ft. Quartz -Monzonite

K-feldspar phenocrysts have been altered to patchy carbonate, patchy biotite and white phyllosilicates (as patches and veinlets); total alteration to white phyllosilicates varies from 10-25 vol-%.

Quartz is abundant and is characterized by having an irregular shape. Magmatic biotite has abundant mineral inclusions, usually very fine grain.

Trace zircon is present.

Plagioclase was probably originally present even though there is none left.

There are some phenocrysts that have been completely altered to biotite and by biotite + muscovite (sometimes with phengite).

In some cases muscovite is surrounded by sulfides (like in SD-23-1466 ft.), indicating they formed after.

Hydrothermal biotite is shreddy and occurs in clusters (off fine and coarse grain biotite). There are also some clusters of biotite + phengite + sulfides + scarce carbonate (possibly replacing the biotite). Biotite pleochroism varies from brown to green. Total percentage of biotite in the sample is approximately 20-25 vol-%, most of hydrothermal origin. Scarce chlorite alters biotite.

Carbonate occurs in veins and as patches, total carbonate in the sample is <5 vol-%. White phyllosilicates together with muscovite and phengite comprise approximately 10 vol-% of the rock. There are some areas with abundant patchy carbonate + white phyllosilicates + muscovite.

Cinnamon rutile comprises 1-2 vol-% of the rock and is closely associated with biotite.

Several veins cut the rock; all of these are submillimeter scale:

1- Quartz + K-spar.

2- Pyrite + chalcopyrite + quartz + carbonate, this vein has a biotite halo and is cut by a chalcopyrite veinlet.

3- Stringers of chalcopyrite and of pyrite + chalcopyrite.

4- Chalcopyrite + white phyllosilicates.

5- White phyllosilicate.

Sulfides are pyrite and chalcopyrite and they occur in veins, veinlets and in clusters with biotite. Total percentage of sulfides is approximately 3 vol-%, with chalcopyrite as the most abundant. Apparently there is no magnetite present (hard to say not a polished thin section), but there seems to be some hematite present, possibly originally magnetite.

Based on the mineralogy the alteration can be classified as K-silicate constructive with a weak phyllic overprint.

SD-21-1852.5 Hornblende Quartz-Latite Porphyry

This rock has a fine grain matrix which comprises approximately 50-60 vol-% of the rock and is composed mainly of irregular quartz (K-feldspar is also present).

Phenocrysts include: K-feldspar, plagioclase, hornblende, quartz and biotite. Trace zircon is present.

K-feldspars are big phenocryst with mineral inclusions (plagioclase). Alteration of K-feldspar to white phyllosilicates (as patches and veinlets) is scarce usually <5 vol-%. Some have also been altered to scarce patchy carbonate. Plagioclase is the most abundant feldspar; these phenocrysts have been strongly altered to smectite. Alteration to white phyllosilicates is usually very weak to none, although there are some scant phenocrysts that show strong alteration (up to 40 vol-%).

Hornblende has been altered by several minerals: smectite (Photo A.38), carbonate, biotite and quartz.

Quartz phenocrysts vary from well rounded to irregular.

Magmatic biotite is characterized by having mineral inclusions. Hydrothermal biotite is fine grain and shreddy, and is being replaced by smectite and scarce chlorite. Total biotite in the sample is approximately 5 vol-%, most of magmatic origin. Hydrothermal biotite sometimes forms clusters together with: quartz + cinnamon rutile + carbonate (possibly replacing the biotite).

There are some phenocrysts that have been completely replaced by chlorite (total chlorite in the sample <2 vol-%). Other phenocrysts have been replaced by smectite + biotite + rutile + carbonate + chlorite. And some have been replaced by smectite + carbonate + silica + biotite + cinnamon rutile + pyrite.

Alteration minerals (carbonate, quartz, cinnamon rutile and biotite) usually occur in clusters, although not all of them are always present, these clusters sometimes have pyrite.

Carbonate occurs associated with other alteration minerals and also occurs alone in the matrix, total percentage of carbonate in the sample is <5 vol-%. Smectite alters

phenocryst and occurs in veinlets (originally biotite?); total smectite is approximately 8-10 vol-%. Total cinnamon rutile in the rock is <2 vol-%.



Photo A.38: Hornblende altered to smectite (f.o.v. = 0.9 mm long), sample SD-21-1852.5 ft.

White phyllosilicate veinlets also cut the rock.

Pyrite is the main sulfide comprising approximately 5 vol-% of the rock. Only trace chalcopyrite is present. Pyrite occurs in veinlets (discontinuous and stringers) and associated with alteration minerals.

Alteration is classified as K-silicate constructive weakly overprinted by white phyllosilicates, carbonate and chlorite.

SD-21-1867 ft. Quartz-Monzonite

Phenocrysts include K-feldspar, plagioclase, quartz and biotite. Trace zircon is present.

K-feldspars have been altered to patchy carbonate, hydrothermal biotite, white phyllosilicates, and patchy silica. Total alteration to white phyllosilicates varies from 10-20 vol-%. Three types of veinlets cut these phenocrysts: white phyllosilicate, carbonate and silica.

Plagioclase has been altered by fine grain biotite, smectite and white phyllosilicates. Biotite occur as patches and veins (sometimes very abundant); smectite usually occurs as veins (was it biotite that got replaced by smectite?). Total alteration to white phyllosilicate is usually <10 vol-%, although in some cases it reaches 30 vol-%. There is a pyrite + biotite + smectite veinlet that cuts a plagioclase phenocryst.

Quartz is sometimes very irregular shaped and patchy (introduced?).

Magmatic biotite is characterized by having mineral inclusions. Hydrothermal biotite is shreddy, it varies from fine grain to coarse and usually occurs in clusters, sometimes with carbonate (replacing?), sulfides and cinnamon rutile (total percentage of cinnamon rutile in the rock is <2 vol-%). Biotite color varies from brown to green.

Smectite alters hydrothermal biotite (total smectite in the rock is approximately 10 vol-%). Total percentage of biotite in the sample is approximately 20 vol-%, most of hydrothermal origin.

Carbonate comprises <2 vol-% of the rock, as mentioned above it alters K-spar and sometimes occurs in clusters with biotite.

Pyrite and chalcopyrite are the only two sulfides present, together these comprise <5 vol-%, of this <1 vol-% corresponds to chalcopyrite. Pyrite forms stringers and thin discontinuous veinlets. Some pyrite occurs in clusters with biotite, and there is some that grew along the cleavage of biotite (replacing?).

Alteration assemblage is K-silicate constructive with a very weak phyllic overprint.

SD-21-1899 ft. Biotitized igneous rock

The protolith of this rock can not be determined due to the strong alteration to hydrothermal biotite ("biotitized"). Total percentage of biotite in the rock is approximately 75-80 vol-% and most seems to be either late magmatic or early hydrothermal. Biotite varies from fine to coarse grain (Photo A.39), and in cases has olive green pleochroism. Some biotite has been altered to smectite.

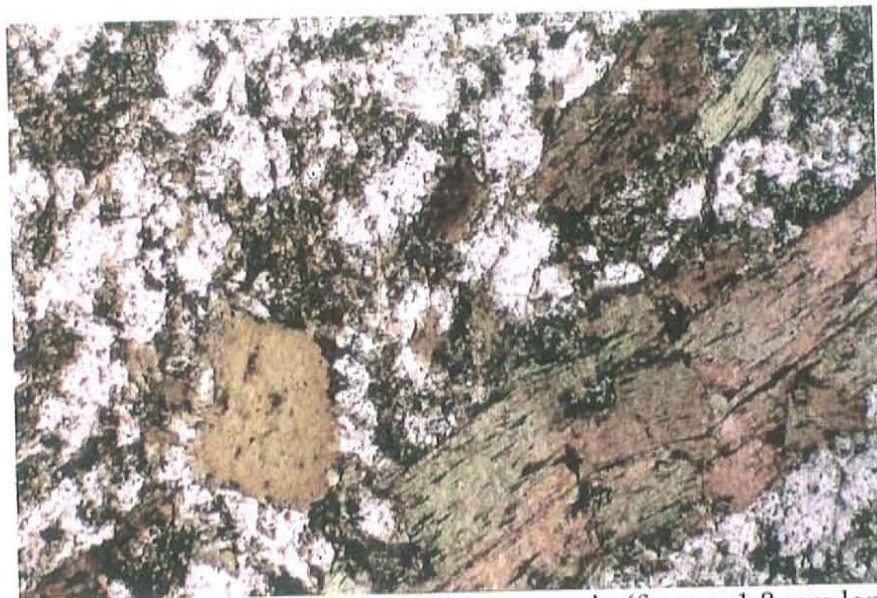


Photo A.39: Abundant biotite both fine and coarse grain (f.o.v. = 1.8 mm long), sample SD-21 1899 ft.

Biotite phenocrysts are the most abundant, these sometimes have pyrite associated with them (replacing?). Biotite replaces both biotite and hornblende.

Besides biotite there are only scarce phenocrysts of plagioclase and quartz in the rock. Plagioclase has been altered to white phyllosilicates (as veins and patches); total alteration varies from 10-20 vol-%. Trace zircon is also present.

Patchy carbonate and patchy white phyllosilicates both replace biotite. White phyllosilicates comprise <2 vol-% of the rock and the total percentage of carbonate is <1 vol-%.

Quartz is the main component of the matrix; K-feldspar is also present.

Cinnamon rutile is closely associated with biotite, the total amount of rutile in the rock is <1 vol-%.

Pyrite and chalcopyrite are the only two sulfides present; together these comprise <5 vol-%, with pyrite > chalcopyrite. They occur as stringers of pyrite + chalcopyrite and in clusters with biotite.

Alteration type is strong K-silicate constructive with a very weak overprint by white phyllosilicates and carbonate.

SD-21-1948.5 ft. Quartz-Monzonite (weakly porphyritic)

Alteration of K-feldspar to white phyllosilicates (as patches and veinlets) varies from <5 vol-% to 60 vol-% (in some cases), but it is usually <10 vol-%. Patchy biotite also alters K-feldspar.

Plagioclase phenocrysts have been altered to smectite (abundant), patchy biotite and white phyllosilicates. Total alteration to white phyllosilicates varies from none to <10 vol-%. Thin submillimeter scale veinlets of white phyllosilicates and veinlets of biotite cut plagioclase phenocrysts.

The total amount of white phyllosilicates in the rock is <2 vol-%.

One feldspar has been so strongly altered to biotite that it can not be determined whether it was plagioclase or K-feldspar. There is trace epidote altering a feldspar.

Quartz phenocrysts are abundant, these are irregular shaped. There is also some fine grain, patchy, irregular shaped quartz (introduced).

Magnetite comprises <1 vol-% of the rock. It seems to be of magmatic origin. There is some fine grain magnetite that occurs in a cluster with biotite.

Biotite with mineral inclusions is possibly of magmatic origin, sometimes there is fine grain pyrite and cinnamon rutile that grew on biotite phenocrysts. Total biotite in the sample is approximately 5-10 vol-%, most of hydrothermal origin, some with olive green pleochroism. Biotite is being altered by chlorite, the percentage of chlorite in the rock is <1 vol-%, smectite and trace muscovite. There is also some patchy carbonate that occurs with biotite, possibly replacing it (total carbonate in the rock is <2 vol-%).

Cinnamon rutile comprises approximately 1 vol-% of the rock and occurs associated with biotite.

Total percentage of smectite in the rock is approximately 7-8 vol-%.

Several veins are present in the rock:

- 1- Carbonate + pyrite.
- 2- White phyllosilicate.
- 3- Biotite.
- 4- Biotite + smectite + pyrite + chalcopyrite.
- 5- Quartz + biotite + pyrite + chalcopyrite.
- 6- Pyrite and chalcopyrite stringers.

All of these are submillimeter scale.

Pyrite and chalcopyrite are the only two sulfides present, the total percentage is <4 vol-% (pyrite > chalcopyrite). Besides occurring in veins they sometimes occur in clusters with biotite.

Alteration assemblage can be classified as K-silicate constructive with a very weak phyllic overprint.

SD-21-1961.5 ft. Quartz-Monzonite

Phenocrysts include K-feldspar, plagioclase, quartz and biotite. Trace zircon is also present. Alteration minerals include: white phyllosilicates, biotite, cinnamon rutile, patchy carbonate, scarce quartz and trace epidote. Alteration assemblage is K-silicate constructive with a weak phyllic overprint.

Several minerals alter K-feldspars, these include: white phyllosilicates, fine grain biotite, patchy carbonate and patchy quartz, these do not necessarily occur together. Alteration to white phyllosilicates varies from <5 vol-% to very strong, reaching up to 80 vol-% in some cases. Thin white phyllosilicate veinlets and biotite veinlets cut K-feldspar phenocrysts.

Plagioclase phenocrysts show alteration to smectite, patchy carbonate and white phyllosilicates and are cut by veinlets of smectite, of biotite and white phyllosilicate veinlets. Alteration of plagioclase to white phyllosilicates is weaker than K-feldspar, it varies from scarce to approximately 40 vol-%, but is usually <5 vol-%. The total amount of white phyllosilicates in the rock is approximately 5-8 vol-%.

There are some feldspars that have been strongly altered (total alteration 90 vol-%) to white phyllosilicates + scarce carbonate + scarce muscovite, it can not be determined if they were plagioclase or K-feldspar.

Quartz is very irregular shaped, suggesting that some could have been introduced.

Magmatic and hydrothermal biotite usually occurs in clusters; the total amount of biotite in the rock is approximately 10 vol-% (mostly hydrothermal). Magmatic biotite has mineral inclusions, some of which are really fine grain. Hydrothermal biotite varies from fine to coarse grain, is shreddy and sometimes has olive green pleochroism. Chlorite and smectite alter biotite. Total percentage of smectite in the rock is <3 vol-% and the total amount of chlorite is <1 vol-%.

Cinnamon rutile comprises <2 vol-% of the rock and is closely associated with biotite.

Besides hydrothermal biotite there is also hydrothermal magnetite; the total amount is <2 vol-%. Magnetite is being replaced by specular hematite (Photo A.40).

The percentage of patchy carbonate in the rock is approximately <2 vol-%. Trace epidote occurs together in a cluster with carbonate.

Pyrite and chalcopyrite are the only two sulfides present; these comprise approximately <3 vol-% of the rock, with pyrite > chalcopyrite. Sulfides occur in veins and in clusters with biotite. Magnetite also occurs associated with biotite. Scarce specular hematite seems to be replacing chalcopyrite. There is no close association between magnetite and chalcopyrite.

Veins present in the rock are:

1- Submillimeter to millimeter scale quartz + magnetite (being replaced by specularite) + pyrite + carbonate + scarce cinnamon rutile. This vein seems to have a halo made of biotite + smectite.

2- Submillimeter scale biotite + pyrite

3- Submillimeter scale carbonate + magnetite.

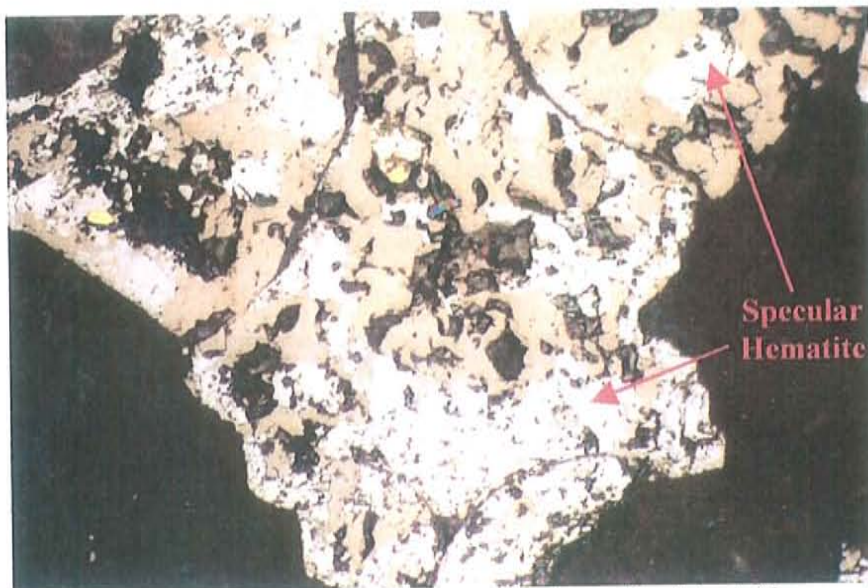


Photo A.40: Magnetite being replaced by specular hematite (blue) (f.o.v. = 0.225 mm long), sample SD-21-1961.5 ft.

SD-21-2011 ft. Quartz-Diorite Porphyry

This sample has been strongly altered by hydrothermal biotite (biotitized). Total percentage of biotite in the rock is approximately 40 vol-%, most of hydrothermal origin. Hydrothermal biotite is usually fine grain, shreddy and sometimes occurs in clusters. Magmatic biotite has mineral inclusions; and sometimes has magnetite associated with it.

Besides biotite other phenocrysts include plagioclase and quartz. Trace zircon is also present.

Plagioclase phenocrysts have been altered to white phyllosilicates (mainly on the edges). White phyllosilicates occur as patches and veinlets and the total amount varies from <5 vol-% up to 20 vol-% approximately. Other alteration minerals include: patchy carbonate, smectite, fine grain silica and fine grain biotite.

There does not seem to be any K-feldspar phenocrysts present, it could be that they were some originally but they have been altered.

Quartz phenocrysts in some cases seem to have quartz overgrowths, suggesting introduced silica. Some quartz phenocrysts are surrounded by hydrothermal biotite.

Plagioclase and quartz are present in the matrix; total matrix percentage was probably originally around 50 vol-% (difficult to estimate due to the strong alteration).

Magnetite comprises approximately 4 vol-% of the rock; it commonly occurs in clusters together with biotite and sulfides. Magnetite is being replaced by specular hematite. Most magnetite seems to be hydrothermal, although some euhedral grains could be of magmatic origin.

Patchy carbonate and patchy white phyllosilicates are sometimes present in the matrix, these minerals each comprise <1 vol-% of the rock.

Some phenocrysts have been completely replaced by alteration minerals. A possibly hornblende (based on shape) was altered to: hydrothermal biotite + magnetite + scarce chlorite + trace pyrite. Another possible hornblende was replaced by:

hydrothermal biotite + magnetite. Hydrothermal biotite + magnetite + chalcopyrite alter another phenocryst.

Chlorite replaces biotite; the total amount in the sample is approximately 2 vol-%.

Cinnamon rutile is present in the rock, comprising <1 vol-%.

Sulfides are pyrite, chalcopyrite and trace pyrrhotite; together these comprise <1.5 vol-% of the rock (chalcopyrite > pyrite). Chalcopyrite surrounds pyrite in some cases indicating that pyrite formed first (Photo A.41). Sulfides are closely associated with biotite.

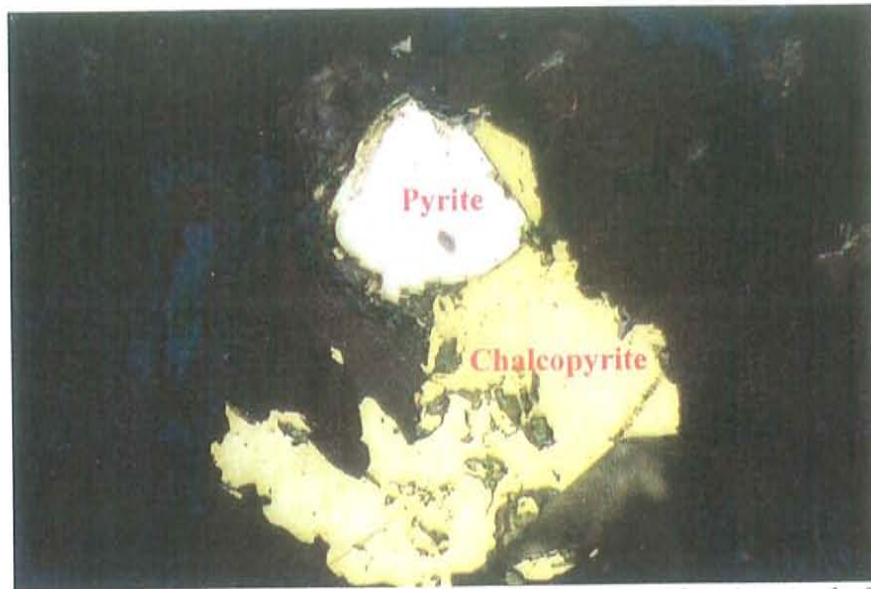


Photo A.41: Chalcopyrite surrounds pyrite (f.o.v. = 0.225 mm long), sample SD-21-2011 ft.

Pyrrhotite and chalcopyrite have a close relationship to magnetite (Photo A.42); these three metals are possibly coeval, pyrrhotite and chalcopyrite probably formed by exsolution.

Magnetite stringer veinlets cut the rock.

Alteration assemblage is defined as K-silicate constructive, based on the presence of abundant hydrothermal biotite and the presence of hydrothermal magnetite; with a very weak overprint.

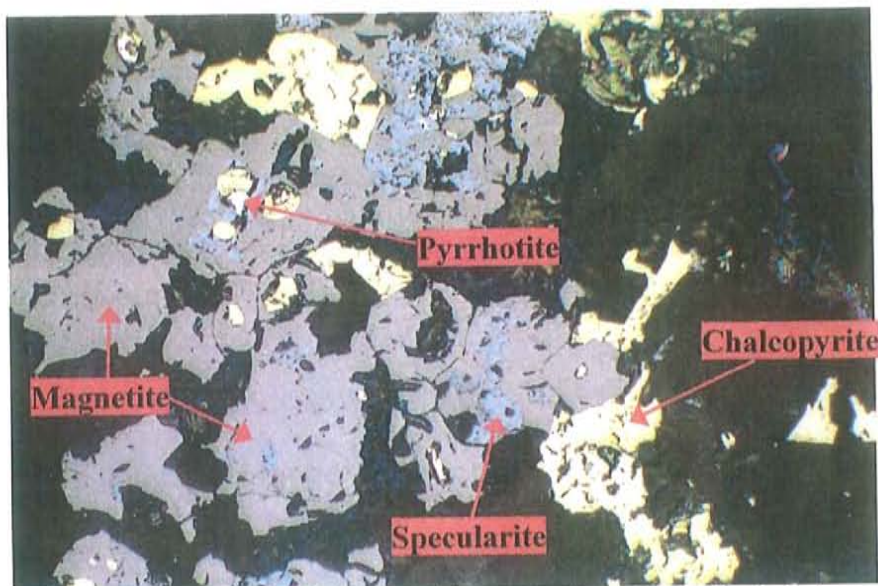


Photo A.42: Chalcopyrite and pyrrhotite with magnetite. Magnetite is being replaced by specularite (blue) (f.o.v. = 0.45 mm long), sample SD-21-2011 ft.

SD-21-2035 ft. Quartz-Latite Porphyry

The matrix is made of quartz, K-feldspar and scarce plagioclase, with quartz as the most abundant. Feldspars in the matrix have been altered to white phyllosilicates.

Phenocrysts include plagioclase, K-feldspar, quartz and biotite. Trace zircon is also present.

Alteration of feldspars to white phyllosilicates is usually weak to none, but in some cases it reaches 20 vol-%. Plagioclase phenocrysts have also been altered to smectite and patchy carbonate; in some cases the alteration to these two minerals is strong. Patchy carbonate also alters K-feldspar; the total amount of carbonate in the sample is <1 vol-% and it is all altering feldspars. White phyllosilicate veinlets and biotite veinlets cut K-feldspar phenocryst.

Quartz phenocrysts vary from well rounded to irregular.

The total amount of biotite in the rock is approximately 7-8 vol-%, most of hydrothermal origin. Biotite phenocrysts with mineral inclusions (some really fine, like needles) are possibly of magmatic origin. Hydrothermal biotite is shreddy and usually occurs in clusters. Fine grain biotite in the matrix is possibly late magmatic-early hydrothermal.

Biotite is being altered to smectite and chlorite, the total amount of chlorite in the rock is approximately 1 vol-%. Hydrothermal biotite replaces phenocrysts, some of these were possibly hornblende. White phyllosilicates sometimes occur in clusters with biotite (possibly replacing it), the total amount of white phyllosilicates in the rock, including the ones altering feldspars is <2 vol-%.

Magnetite comprises approximately 2 vol-%, and it is closely associate to hydrothermal biotite (is the magnetite also of hydrothermal origin?). Specular hematite replaces magnetite.

Cinnamon rutile usually occurs in clusters with hydrothermal biotite, the total amount of rutile in the rock is <1 vol-%.

Pyrite and chalcopyrite comprise <4 vol-% of the rock, with sub-equal amounts of each. Trace bornite and idaite are also present and they occur together with chalcopyrite, these three minerals are possibly coeval. Chalcopyrite in some cases surrounds pyrite indicating that pyrite was the first sulfide to form. Some sulfides grew within biotite phenocrysts (replacing?). Sulfides in the rock occur in veins and in clusters with biotite.

Trace chalcopyrite occurs within magnetite (formed by exsolution?).

Three types of veins cut the rock (all submillimeter scale):

- ✕ White phyllosilicate veinlets.
- ✕ Biotite veinlets.
- ✕ Sulfide stringers.

Alteration type is K-silicate constructive with a very weak phyllic overprint.

SD-21-2325.5 ft. Quart-Monzonite

There are several minerals that alter K-feldspars, these include: patchy biotite, patchy quartz, trace epidote and white phyllosilicates; the total alteration to white phyllosilicates varies from scarce (<5 vol-%) to 15 vol-%, in some cases it reaches 30 vol-%. White phyllosilicate veinlets cut K-feldspar phenocrysts.

Some phenocrysts have been completely altered to smectite, biotite and white phyllosilicates (with some phengite); some of these could have been originally plagioclase. The total amount of smectite in the rock is approximately 5 vol-%.

Quartz varies in size, some is very fine grain and patchy (introduced?).

Trace zircon is present in the rock.

Most of the biotite in the sample is of hydrothermal origin, the total amount of biotite is approximately 10 vol-%. Hydrothermal biotite is shreddy and usually occurs in clusters, some biotite has olive green pleochroism. Chlorite alters biotite, the total amount in the rock is <0.5 vol-%. There is some trace phengite (apparently) that occurs in clusters with biotite, possibly replacing it, the total amount of phengite and white phyllosilicates in the rock is <2 vol-%.

Magnetite comprises approximately 5 vol-% of the rock, it all seems to be of hydrothermal origin; it is closely associated with biotite and sometimes occurs veins. Specularite replaces magnetite.

Cinnamon rutile is present in the rock, the total amount is <1 vol-%; some is associated with biotite.

Chalcopyrite is the most abundant sulfide comprising <3 vol-% of the rock, it is followed by pyrite with approximately 1 vol-%. Trace molybdenite is also present. Chalcopyrite surrounds pyrite indicating that it formed later. Sulfides occur in veins and in clusters with biotite. Trace chalcopyrite inside of magnetite (little blebs) possibly formed by exsolution.

Besides the trace epidote altering K-feldspars there is trace amounts that occurs in clusters with biotite, magnetite and chalcopyrite. The total amount of epidote in the rock is <1 vol-%.

Several veins cut the rock:

- 1- Barren submillimeter scale quartz veins.
- 2- Carbonate veinlets. The total amount of carbonate in the rock is <1 vol-%.
- 3- Biotite veinlets

4- Millimeter scale veins of quartz + biotite + magnetite + chalcopyrite + trace molybdenite. In these biotite and magnetite surround quartz grains indicating that they formed after (Photo A.43).

5- Pyrite + chalcopyrite + biotite.

Based on the presence of hydrothermal magnetite and hydrothermal biotite the alteration assemblage is classified as K-silicate constructive with a weak phyllic overprint.

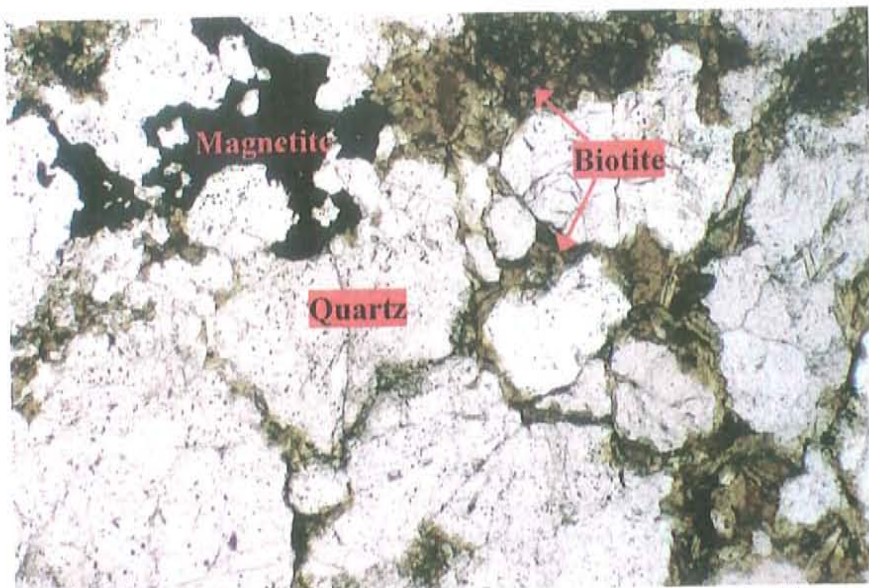


Photo A.43: Magnetite and biotite surround quartz grains in a vein (f.o.v. = 1.8 mm long), sample SD-21-2325.5 ft.

DRILL HOLE SD-22

SD-22-724 ft. Biotite Monzonite

Total alteration of feldspars to white phyllosilicates varies from none to 5 vol-% (in K-feldspar). Scarce patchy carbonate replaces feldspars.

Plagioclase is sometimes altered by biotite; both as patches and veinlets and in some cases grew along preferential overgrowths.

Biotite comprises approximately 20 vol-% of the rock and seems to be mainly of hydrothermal origin; which is shreddy, sometimes has olive green pleochroism and usually occurs in clusters. Hydrothermal biotite varies from fine to coarse grain. Smectite alters biotite (mainly hydrothermal biotite). Biotite replaces phenocrysts, in some cases possibly hornblende (based on shape).

Patchy carbonate sometimes occurs associated with biotite (replacing it?); total amount of carbonate in the rock is approximately 1 vol-%.

Cinnamon rutile comprises approximately 1 vol-% of the rock and is closely related to biotite.

White phyllosilicates together with muscovite comprise <2 vol-% of the rock.

Alteration assemblage is classified as K-silicate constructive weakly overprinted by white phyllosilicates + muscovite and carbonate.

The total amount of sulfides in the rock is <2 vol-%; these are apparently pyrite and chalcopyrite (not a polished thin section). Sulfides occur associated with biotite, in some cases they grew along the cleavage of biotite.

Veins present in the rock are:

- 1- Sulfide + biotite veinlets. Now mainly smectite.
- 2- Sulfide + biotite + muscovite veinlet.
- 3- Smectite veinlets (originally biotite?).
- 4- Sulfide stringers.
- 5- Sulfide discontinuous veinlets.

SD-22-1240 ft. Quartz-Latite Porphyry

This sample corresponds to a porphyritic rock, phenocrysts include: plagioclase, K-feldspar, biotite, quartz and scarce hornblende. Trace zircon and sphene are also present. The matrix is composed of quartz (main mineral) and K-feldspar, and it comprises approximately 50 vol-% of the rock.

Total alteration of feldspars to white phyllosilicates varies from scarce to none and it is weaker in K-feldspar. Plagioclase phenocrysts have also been altered to smectite and are sometimes cut by carbonate veinlets. There are several veinlets that cut K-feldspar phenocrysts: carbonate veinlets, silica + biotite veinlets, carbonate + biotite veinlets and biotite veinlets; K-feldspars also show scarce alteration to patchy carbonate.

Quartz phenocrysts are irregular shaped and are sometimes cut by carbonate veinlets.

Residual hornblende is still present in the rock; it has been strongly altered to smectite. There is a possible hornblende, based on shape, that has been completely altered to biotite + magnetite + smectite.

There are phenocrysts that have been completely replaced by smectite (based on shape some could have been hornblende).

Biotite comprises approximately 5-10 vol-% of the rock; most is of hydrothermal origin. Magnetite sometimes occurs together with magmatic biotite, it either surrounds it or it grew along the cleavage of biotite (replacing it?). Hydrothermal biotite is shreddy, sometimes has olive green pleochroism and usually occurs in clusters. Biotite has incipient replacement by chlorite, the total amount of chlorite in the rock is <1 vol-%.

Total amount of magnetite in the rock is approximately 4-6 vol-%, and it all seems to be of hydrothermal origin. specularite replaces magnetite.

Chalcopyrite and pyrite are the only two sulfides present in the rock. The total amount of chalcopyrite is approximately 1 vol-% and the amount of pyrite present is <1 vol-%. Chalcopyrite sometimes occurs in clusters with magnetite and in some cases it surrounds it, suggesting it probably formed after (Photo A.44). There is trace chalcopyrite in magnetite (formed by exsolution?). Sulfides and magnetite occur in veins and in clusters with biotite.

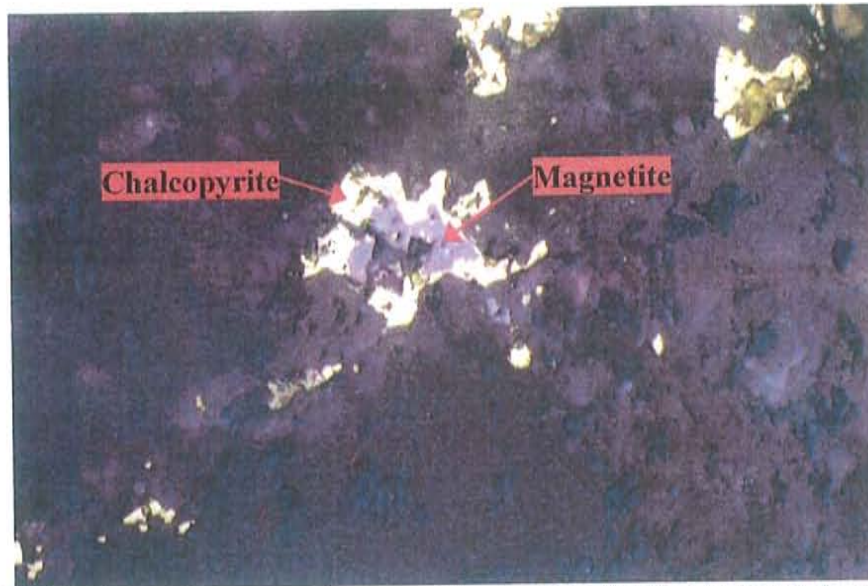


Photo A.44: Chalcopyrite surrounds magnetite (f.o.v. = 0.225 mm long). Sample SD-22-1240 ft.

Abundant veins cut this rock:

- 1- Carbonate + biotite + chalcopyrite + trace pyrite. Biotite, chalcopyrite and trace pyrite occur along the edges
- 2- Carbonate + biotite + magnetite
- 3- Magnetite + biotite. These are cut and displaced by late carbonate veins.
- 4- Biotite + chalcopyrite + pyrite + magnetite.
- 5- Magnetite veins. Cut and displaced by later carbonate + biotite veins (Photo A.45).
- 6- Magnetite + chalcopyrite + biotite.
- 7- Chalcopyrite + carbonate.
- 8- Magnetite + carbonate.
- 9- Carbonate + biotite. Biotite occurs along the edges.
- 10- Quartz + magnetite + scarce chalcopyrite. Cut and displaced by later carbonate + biotite (Photo A.46).
- 11- Chalcopyrite and pyrite stringers.
- 12- Thin barren carbonate veinlets.
- 13- Smectite veinlets (possibly originally biotite).

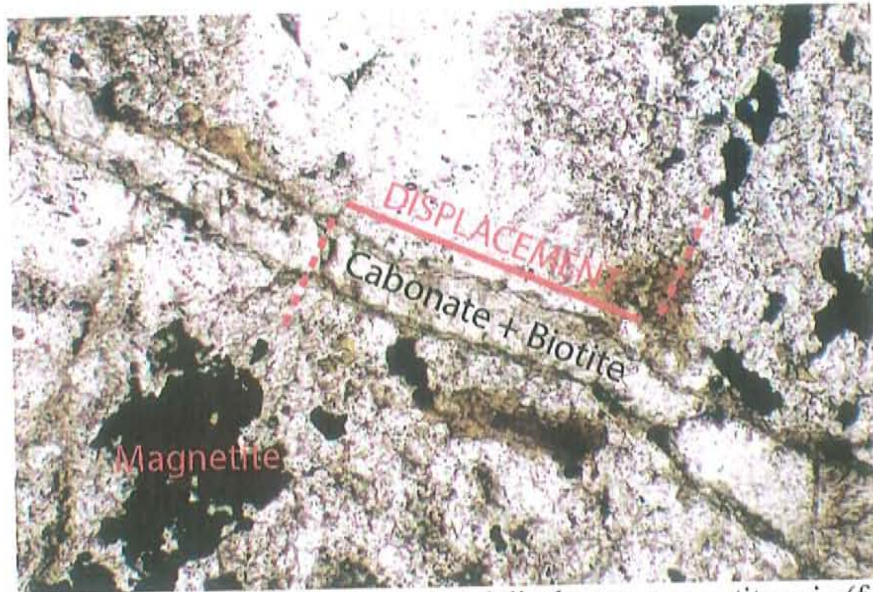


Photo A.45: Carbonate + biotite vein cuts and displaces a magnetite vein (f.o.v. = 0.9 mm long). Sample SD-22-1240 ft.

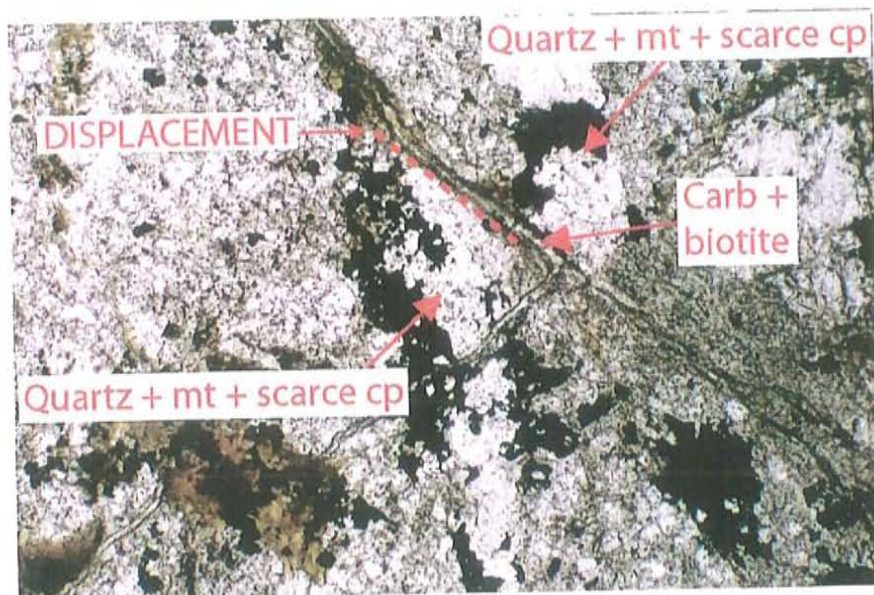


Photo A.46: Carbonate + biotite veinlets cuts and displaces a quartz + magnetite + scarce chalcopyrite vein (f.o.v = 1.8 mm long), sample SD-22-1240 ft.

Carbonate and it is the most abundant alteration mineral in the rock, comprising 15-20 vol-%. Base on cross cutting relationships observed it can be determined that most magnetite veins are early compared to carbonate veins.

Alteration assemblage is K-silicate constructive.

SD-22-1270 ft. Quartz-Monzonite (weakly porphyritic)

Magmatic minerals in this rock are equigranular, these are: plagioclase, K-feldspar, quartz, biotite and trace zircon. Alteration minerals include: biotite, magnetite, white phyllosilicates, carbonate, chlorite and smectite.

K-feldspars have been altered to patchy carbonate, smectite and white phyllosilicates, the total alteration to white phyllosilicates is scarce <5 vol-%.

Plagioclase have been altered to smectite, patchy biotite, and white phyllosilicates (total alteration to white phyllosilicates varies from trace to 5 vol-%, and it is stronger than in K-feldspar). Biotite veinlets cut plagioclase.

Quartz is very abundant, it characterized by having an irregular shape. A great part of the quartz seems to be introduced, occurring in veins.

Magmatic biotite is scarce (most seems to of hydrothermal origin). The total amount of biotite in the sample is 5-8 vol-%. Hydrothermal biotite is fine grain shreddy and usually occurs in clusters. Chlorite replaces both magmatic and hydrothermal biotite, total chlorite in the rock is <1 vol-%.

Magnetite comprises approximately 10-15 vol-% of the rock and seems to be all of hydrothermal origin. It sometimes occurs together with magmatic biotite (replacing?). Specular hematite replaces magnetite.

Magnetite veins are very abundant; these usually have quartz and sometimes have scarce carbonate. Most off these veins are parallel (Photo A.47).

Other veins present in the rock are:

- ✖ Biotite veinlets.
- ✖ Pyrite + chalcopyrite + carbonate + biotite. This vein apparently formed after the magnetite veins (cuts through them?).

Total carbonate in the rock is approximately 2vol-%, it occurs in veins and as patches. It is possibly that carbonate in the sample is late and it just follows the path of previous veins.



Photo A.47: Parallel magnetite veins (f.o.v. = 1.8 mm long), sample SD-22-1270 ft.

Pyrite and chalcopyrite are the only two sulfides present; together they comprise approximately 1 vol-% of the rock (with sub-equal amounts of each), and they are all present in the vein mentioned above.

Alteration assemblage is classified as K-silicate constructive, based on the abundance of hydrothermal magnetite and hydrothermal biotite.

SD-22-1321 ft. Quartz-Monzonite

K-feldspars have been altered to patchy carbonate, biotite and white phyllosilicates; alteration to white phyllosilicates is usually weak (trace to <3 vol-%) but in some few cases reaches up to 85 vol-%. Carbonate veinlets cut K-feldspars.

Plagioclase shows alteration to smectite (in some cases strongly altered), patchy carbonate, biotite and white phyllosilicates (and scarce muscovite). Alteration to white phyllosilicates is stronger than in K-feldspar (varies from <5 to 80 vol-%). White phyllosilicate veinlets cut plagioclase grains.

Trace zircon is present in the rock.

Quartz is abundant in the rock, it is mostly irregular shaped.

Biotite with abundant fine grain mineral inclusions (possibly rutile) is most likely of magmatic origin. The total amount of biotite in the rock is approximately 6-10 vol-%; most is of hydrothermal origin. Hydrothermal biotite is mostly fine grain and usually occurs in clusters (some of these clusters have shapes suggesting that they might have been minerals, possibly mafic that got replaced). Magmatic biotite is sometimes being replaced by hydrothermal biotite. Chlorite replaces biotite, the total amount of chlorite in the rock is <1 vol-%. Muscovite and trace phengite also replaces biotite (Photo A.48); white phyllosilicates together with muscovite comprise approximately 5 vol-% of the rock.

Some grains have been completely replaced by biotite; others have been replaced by white phyllosilicates (sometimes with muscovite) + biotite (possibly originally feldspars). There is one mineral that was completely altered to biotite + carbonate + pyrite + chalcopyrite.

Carbonate occurs in patches and veins, the total amount of carbonate in the rock is approximately 1 vol-%. There is some carbonate that occurs together with biotite in clusters (overprinting?).

Cinnamon rutile is closely associated with biotite, the total amount is <1.5 vol-%

Sulfides present are pyrite and chalcopyrite; chalcopyrite is more abundant, comprising approximately 2-3 vol-% of the rock, the total amount of pyrite is approximately 1 vol-%. Chalcopyrite in some cases surrounds pyrite indicating that it formed later (Photo A.49). Sulfides occur in veins and they sometimes occur in clusters with biotite.

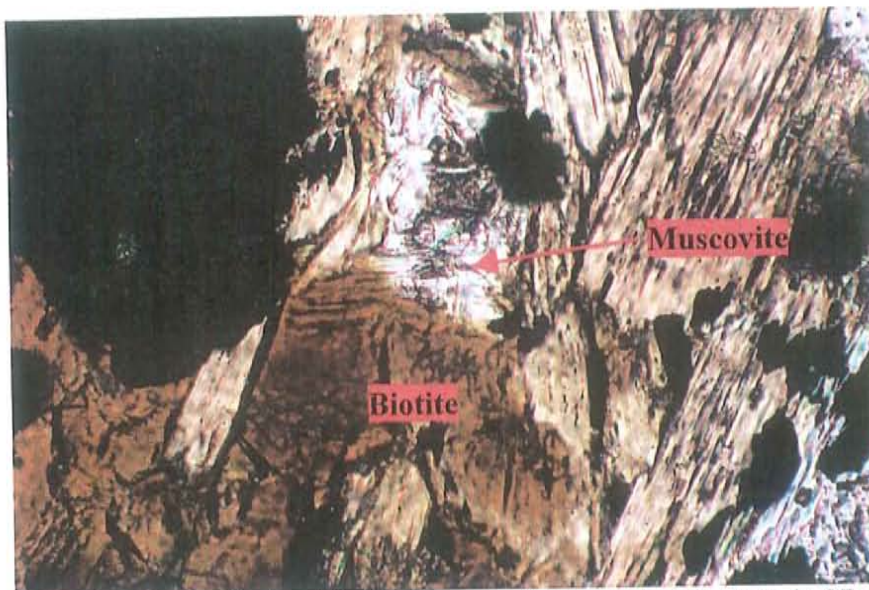


Photo A.48: Muscovite replacing biotite (f.o.v. = 0.45 mm long), sample SD-22-1321 ft.

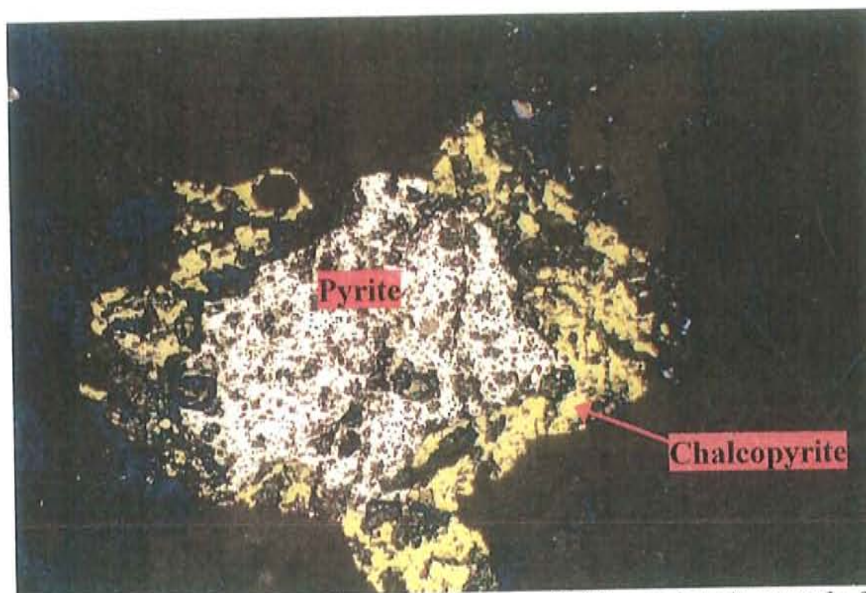


Photo A.49: Chalcopyrite surrounds pyrite (f.o.v. = 0.45 mm long), sample SD-22-1321 ft.

Based on mineralogy the alteration assemblage of this rock can be classified as K-silicate constructive with a weak phyllic overprint.

Several veinlets cut the rock:

- 1- Chalcopyrite + pyrite + carbonate.
- 2- Biotite veinlets.
- 3- Quartz + biotite.
- 4- Quartz + chalcopyrite + scarce biotite. In these veins chalcopyrite formed after quartz, since it sometimes surrounds quartz grains.
- 5- Pyrite + chalcopyrite + muscovite + carbonate.
- 6- Chalcopyrite stringers.

7- Chalcopyrite + trace pyrite stringers.
All of these are submillimeter scale.

DRILL HOLE SD-23

SD-23-885 ft. Protolith: Quartz arenite

Note: this rock was originally logged as a monzonite.

Abundant quartz grains are present in the sample; most of them seem to be primary suggesting that the protolith was probably a quartzarenite. Trace zircon is present in the rock.

Alteration minerals present in the rock include biotite (the most abundant), white phyllosilicates + muscovite, carbonate, quartz, cinnamon rutile and trace epidote. Most of the alteration minerals seem to filling the spaces between the quartz grains.

There are areas where there is a greater concentration of biotite (Photo A.50); total biotite in the sample is approximately 15 vol-%. Hydrothermal biotite and carbonate are the main minerals altering the quartzarenite.



Photo A.50: Abundant biotite (f.o.v. = 1.8 mm long), sample SD-23-885 ft.

Total carbonate present in the sample is approximately 5-10 vol-%, taking into consideration the carbonate that is present in the veins.

Cinnamon rutile occurs with carbonate, biotite (Photo A.51) and scarce with white phyllosilicates (these were probably originally biotite that got replaced); total cinnamon rutile in the sample is < 2 vol-%.

As mentioned above quartz is also present as an alteration mineral; it differs from primary quartz because it is fine grain, irregular and patchy. Introduced silica occurs together with white phyllosilicates and the total amount is approximately 5-10 vol-%. In some areas of the sample fine grain white phyllosilicates (Photo A.52), scarce muscovite and patchy quartz are the main minerals present, these areas occur only in the edges of the sample and sometimes have straight contacts with the rest of the rock (related to

veins or just zoning in the alteration?). Although white phyllosilicates are present throughout the sample their biggest concentration occurs in these areas together with the introduced silica, the total amount of white phyllosilicates + muscovite in the rock is < 7 vol-%.

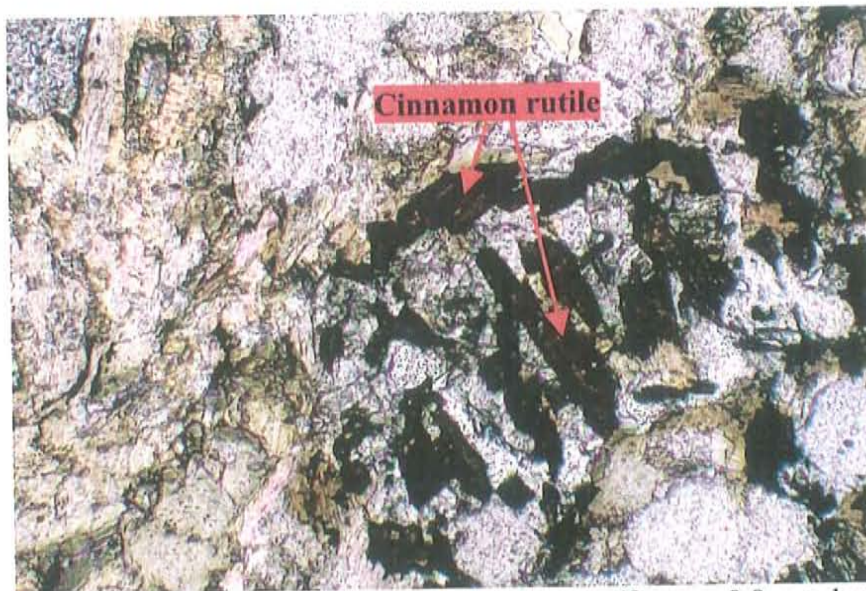


Photo A.51: Cinnamon rutile with biotite and carbonate (f.o.v. = 0.9 mm long), sample SD-23 -885 ft.

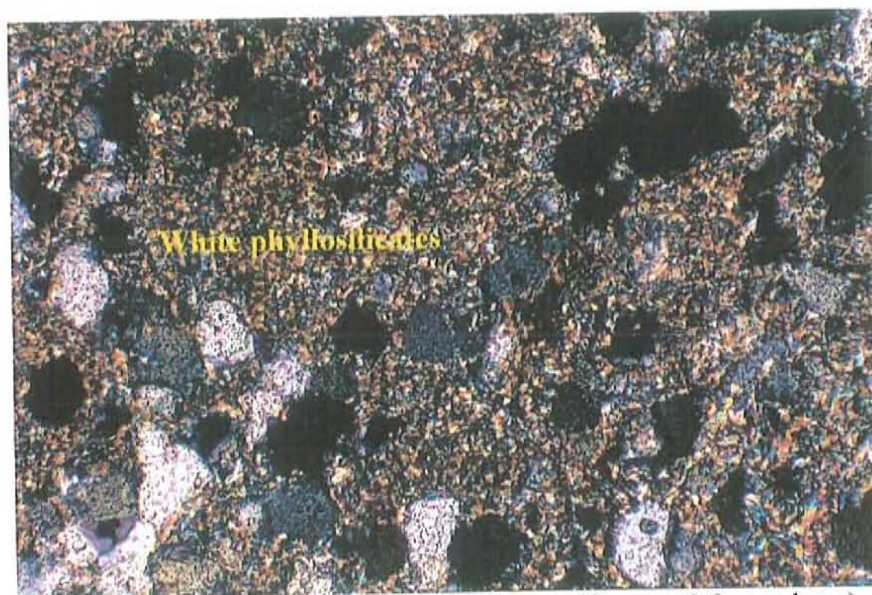


Photo A.52: Area with abundant white phyllosilicates (f.o.v. = 0.9 mm long), sample SD-23-885 ft.

Based the protolith and the alteration minerals this rock can be classified as a biotitized quartzarenite overprinted by carbonate and white phyllosilicates.

Pyrite seems to be the only sulfide present with a total percentage of approximately 5 vol-% (it is a thin section and not a polished thin section which makes it hard to identify ore minerals), it mainly occurs with carbonate and biotite, only scarce to

trace sulfides are present in the areas with abundant introduced silica and white phyllosilicates.

Several veins are present in the sample:

- 1- Carbonate + pyrite.
- 2- Barren carbonate veins.
- 3- Muscovite veinlets.
- 4- Thin biotite veins.

All these veins are submillimeter scale.

SD-23-1466 ft. Alkali feldspar Quartz-Syenite.

Phenocrysts include quartz, K-feldspar and biotite. There are also some phenocrysts that have been completely altered to white phyllosilicates (Photo A.53) and white phyllosilicate + carbonate, in some cases kaolinite is also present (Were some of them originally plagioclase?).

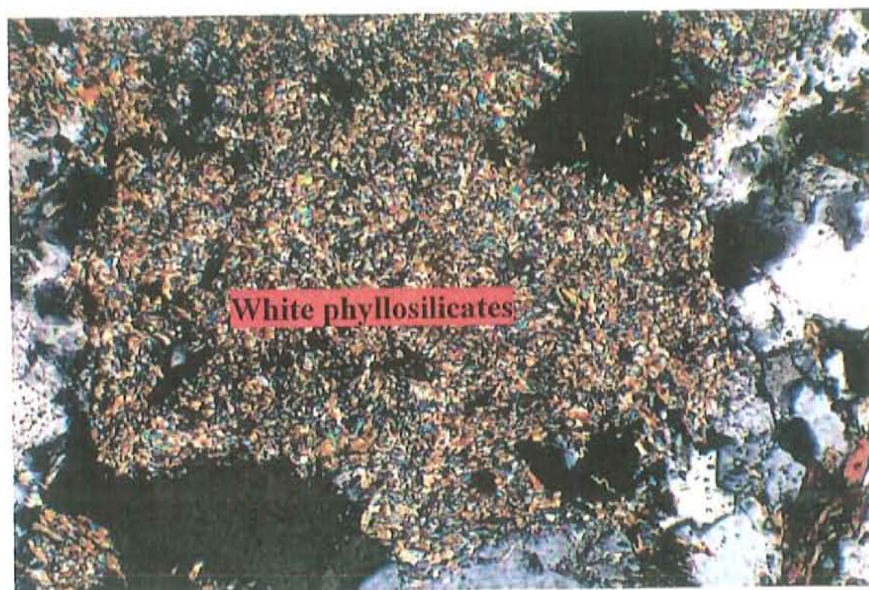


Photo A.53: Phenocryst replaced by white phyllosilicates (f.o.v. = 0.9 mm long), sample SD-23-1466 ft.

Quartz is very abundant, most is irregular shaped and patchy suggesting that it might be introduced (alteration mineral) and not part of the original rock forming components.

Alteration of K-feldspars to white phyllosilicates varies from none to very strong (up to 75 vol-%).

Magmatic biotite has mineral inclusions, including rutile. Most biotite seems to be hydrothermal, it is shreddy usually fine grain and occurs in clusters (Photo A.54); some has olive green pleochroism. Thin irregular submillimeter scale biotite veinlets are cutting the rock. Total biotite is approximately 10-15 vol-%. White phyllosilicates sometimes surround hydrothermal biotite (overprinting).

Trace zircon and apatite are present.

Muscovite is usually associated with chalcopyrite; the chalcopyrite surrounds euhedral muscovite crystals, indicating that it formed after (Photo A.55).

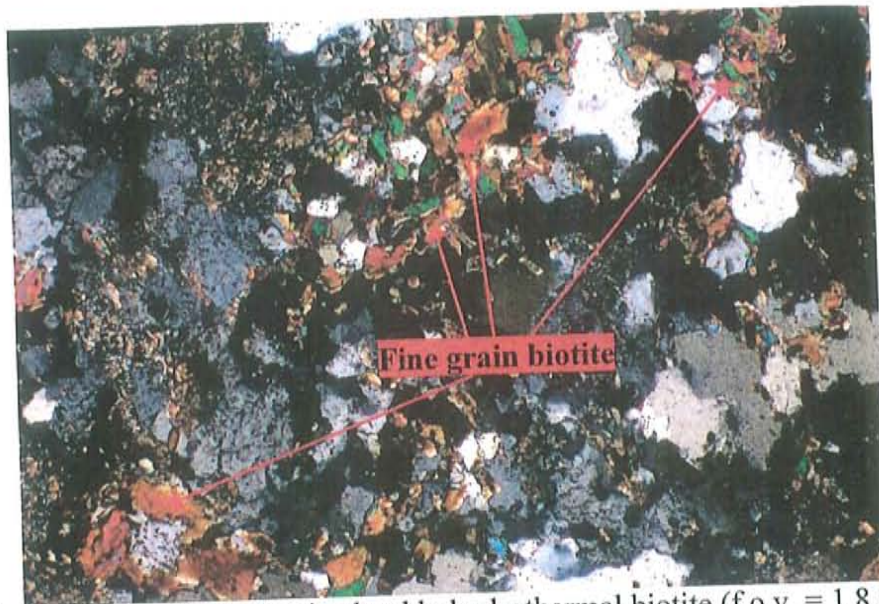


Photo A.54: Rock with fine grain shreddy hydrothermal biotite (f.o.v. = 1.8 mm long), sample SD-23-1466 ft.

Cinnamon rutile comprises approximately 1-2 vol-% of the sample and it occurs associated with biotite (Photo A.56) and with white phyllosilicates (was it originally biotite?).

There is an area in the sample (next to a centimeter scale quartz vein) where everything has been completely altered to white phyllosilicates + carbonate + silica + cinnamon rutile + muscovite. This area also has the greatest concentration of sulfides (mainly chalcopyrite) and cinnamon rutile in the sample. Some pyrite is also present. Total white phyllosilicates and muscovite comprise approximately 18 vol-% of the sample. The carbonate percentage is approximately 5-8 vol-%.

Chalcopyrite and pyrite are the only two sulfides present and they comprise less than 10 vol-% of the sample; with chalcopyrite as the most abundant, total pyrite is <2 vol-%. Chalcopyrite surrounds pyrite indicating that it formed after. Sulfides occur mainly as stringer veinlets, some are disseminated. Some sulfides occur together with biotite but the greatest concentration occurs with white phyllosilicates. In this sample there were two pulses in which copper was introduced, one associated with the K-silicate constructive alteration and one to the phyllic alteration.

Centimeter scale and millimeter scale quartz veins cut the rock (salty fluid inclusions are present in the quartz crystals). The centimeter scale quartz vein is cut by different types of submillimeter scale veinlets:

- 1- Carbonate veinlets
- 2- Carbonate + chalcopyrite ± pyrite veinlets
- 3- Sulfide stringer veinlets (mainly chalcopyrite)
- 4- White phyllosilicate veinlets

Patchy white phyllosilicates and scarce muscovite are present in the centimeter scale quartz vein. Also present are clusters of fine grain biotite surrounding the quartz grains and scarce chalcopyrite surrounding euhedral muscovite crystals.

The smaller quartz vein (millimeter scale) is also cut by submillimeter scale veinlets:

- 1- Carbonate veinlets
- 2- Sulfide stringer veinlets.

Patchy white phyllosilicates are also present in this vein and they occur in clusters with sulfides (mainly chalcopyrite). Muscovite euhedral crystals are surrounded by sulfides.



Photo A.55: Chalcopyrite surrounds muscovite (A: f.o.v. = 0.45 mm long. B: f.o.v. = 0.9 mm long). Sample SD-23-1466 ft.

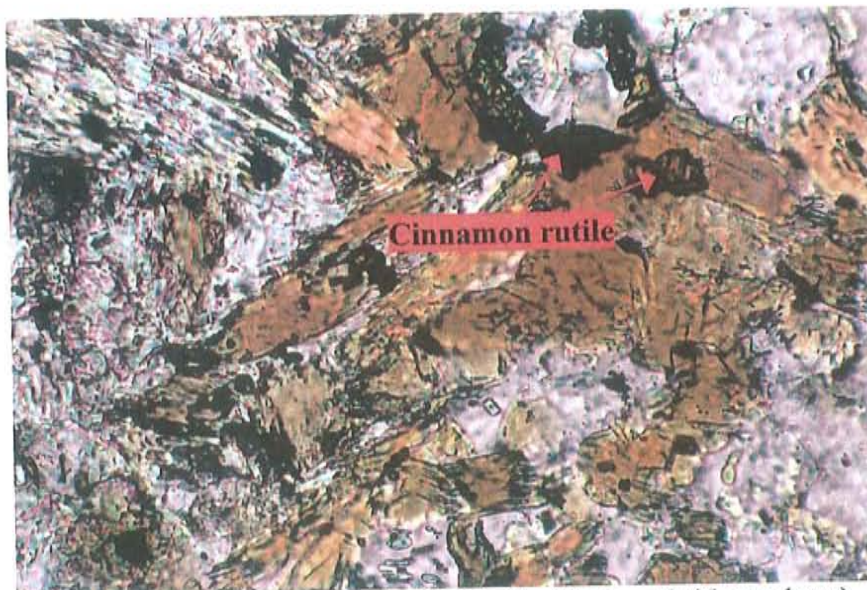


Photo A.56: Cinnamon rutile associated with biotite (f.o.v. = 0.45 mm long). Sample SD-23-1466 ft.

The alteration assemblage is classified as K-silicate constructive overprinted by white phyllosilicates, muscovite and carbonate.

SD-23-1556 ft. Protolith: Limestone?

This sample has been strongly altered. Protolith was probably a carbonate.

Quartz is one of the most abundant minerals comprising approximately 35 vol-% of the sample; it seems to be an alteration mineral (irregular shaped and patchy), indicating that the rock has been silicified.

Carbonate follows quartz in abundance comprising approximately 15-20 vol-% of the rock, it occurs as patches and in veins. Clinopyroxenes (augite?) and amphiboles (tremolite?) are also present as alteration minerals, the approximate percentage of each is <10 vol-% for clinopyroxene and 5 vol-% for amphiboles. Chloritoid alters both clinopyroxenes and amphiboles; total percentage of chloritoid is approximately 1-2 vol-%.

Clays (apparently smectite) are present in the rock comprising approximately 8-10 vol-%. Trace muscovite is present in the rock.

A silicate, possibly serpentine is one of the least abundant minerals comprising <2 vol-%.

Specular hematite is being replaced by magnetite (Photo A.57); both together comprise approximately <6 vol-% of the sample. Specular hematite and magnetite show a close association to sulfides.

Sulfides are pyrite, chalcopyrite and chalcocite; pyrite is the most abundant comprising <10 vol-% of the sample. The percentage of chalcopyrite is approximately 2-3 vol-% and chalcocite is the least abundant with <1 vol-%. Sulfides are present in veins, stringer veinlets (of pyrite, chalcopyrite and pyrite + chalcopyrite) and disseminated. Sometimes magnetite and specularite are also present in the stringer veinlets. Pyrite was the first sulfide to form and it is followed by chalcopyrite. Magnetite is apparently late

since it replaces specularite and it surrounds pyrite and chalcopyrite (apparently also replacing) (Photo A.58). Magnetite is of hydrothermal origin.

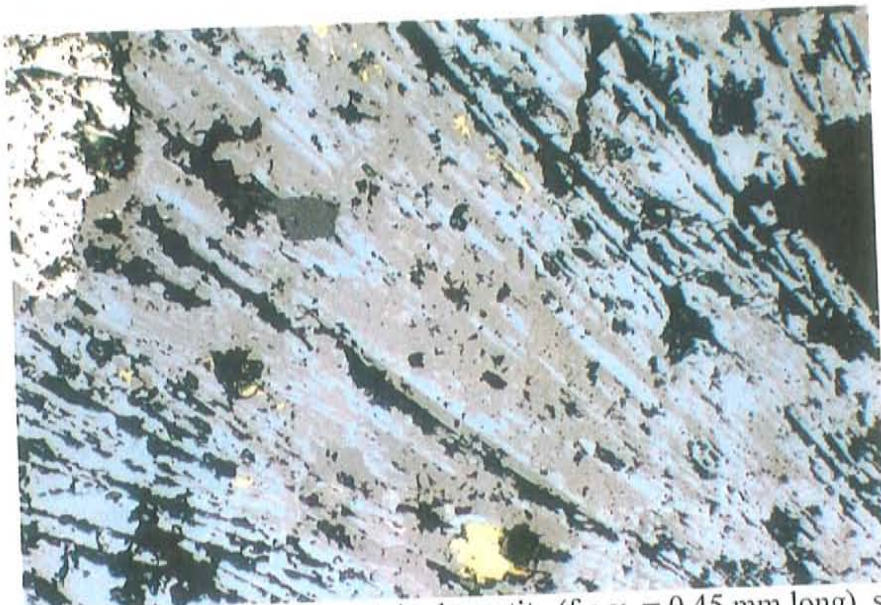


Photo A.57: Magnetite replacing specular hematite (f.o.v. = 0.45 mm long), sample SD-23-1556 ft.

Chalcocite surrounds (replaces?) chalcopyrite (Photo A.59).

Two millimeter scale pyrite + carbonate + magnetite + specularite + chalcopyrite + epidote veins are present in the sample. Total epidote in the sample is approximately <5 vol-%.

Submillimeter scale carbonate veins cut the rock.



Photo A.58: Chalcopyrite surrounds pyrite, magnetite surrounds chalcopyrite (f.o.v. = 0.45 mm long). Sample SD-23-1556 ft.

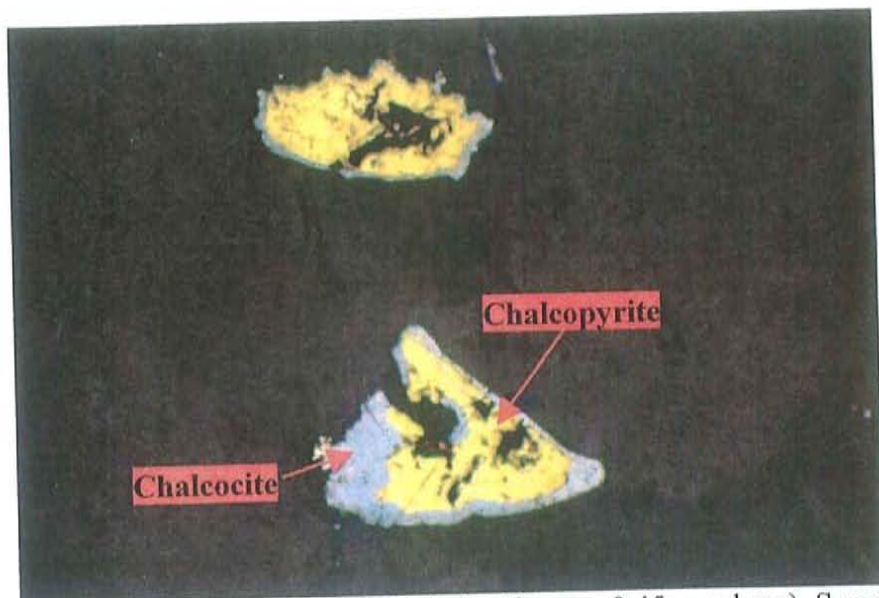


Photo A.59: Chalcocite replacing chalcopyrite (f.o.v. = 0.45 mm long). Sample SD-23-1556 ft.

SD-23-2270.5 ft. Quartz-Latite Porphyry

Phenocrysts include quartz, plagioclase, K-feldspar, biotite and trace hornblende.

Quartz phenocrysts present subrounded shapes and they are usually cut by white phyllosilicate veinlets. Calcite submillimeter scale veinlets also cut quartz phenocrysts (Photo A.60).

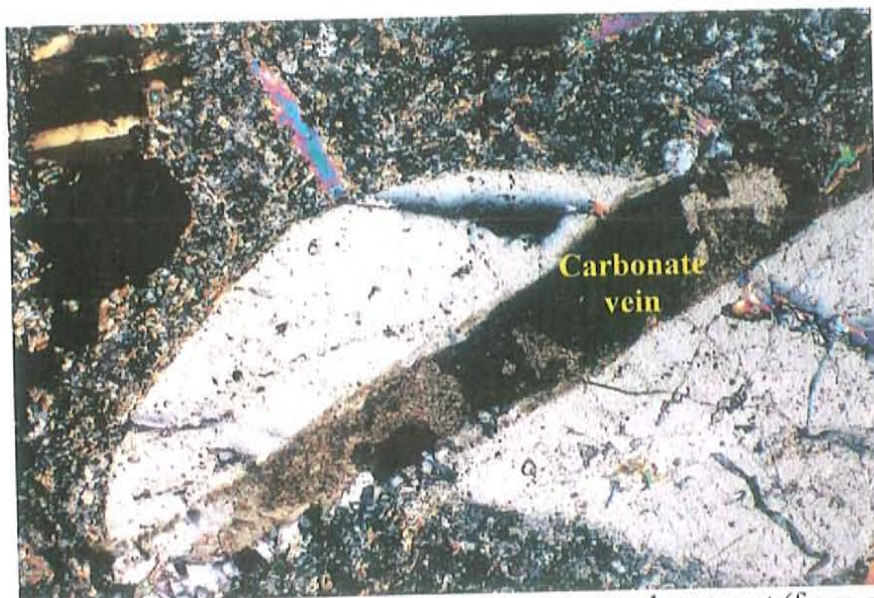


Photo A.60: Carbonate vein cuts and displaces a quartz phenocryst (f.o.v. = 1.8 mm long). Sample SD-23-2270.5 ft.

Plagioclase phenocrysts show alteration to white phyllosilicates (as patches and veinlets) this alteration varies from 5 vol-% up to 30 vol-% in a few cases. Patchy biotite

also alters some plagioclase phenocrysts. Scarce epidote is also present altering plagioclase (Photo A.61). Carbonate submillimeter scale veins cut plagioclase.

K-feldspar phenocrysts are the biggest ones in the sample; they contain plagioclase as mineral inclusions. These phenocrysts are cut by three different types of submillimeter scale veinlets: carbonate, white phyllosilicate and quartz. Patchy quartz and white phyllosilicates are also present. Total alteration of K-feldspars to white phyllosilicates varies from 10-20 vol-%.

Trace zircon is present in the sample.

The matrix comprises approximately 40 vol-% of the sample and it is made mainly of anhedral quartz.

Most of the biotite in the sample seems to be hydrothermal. It is usually fine grain and shreddy; some bigger phenocrysts are also present but the lack of mineral inclusions suggests that they might be either late magmatic or early hydrothermal. Biotite pleochroism varies from olive green to brown. Some mafic minerals, including biotite have been altered to fine grain biotite.

Alteration minerals that are present in the matrix include: biotite, white phyllosilicates, carbonate and scarce epidote (<2 vol-%). Carbonate occurs as veinlets and in patches, comprising approximately 10-15 vol-% of the sample. Thin white phyllosilicate veins are also present cutting the rock and not only the phenocrysts.

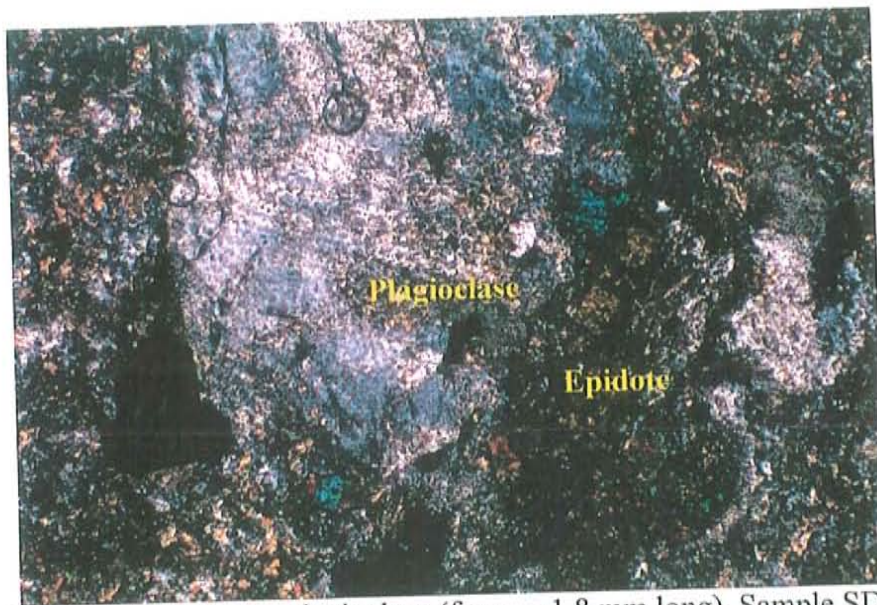


Photo A.61: Epidote replacing plagioclase (f.o.v. = 1.8 mm long). Sample SD-23-2270.5 ft.

The fact that the white phyllosilicates and biotite are so fine grain and that they occur together in the matrix makes it hard to estimate their percentage. Estimation for the total biotite would be approximately 10-15 vol-%.

Trace (<1 vol-%) sphene is present in the rock (Photo A.62).

Veins present in the sample:

1-Millimeter scale vein made of pyrite + carbonate + quartz + trace chalcocopyrite. The halo is made of zoisite, scarce epidote and sulfides (pyrite + chalcocopyrite in sub equal amounts).

2-Submillimeter scale barren carbonate veins. These veins formed later since they cut the first type of vein described.

3-Submillimeter scale white phyllosilicate veinlets.



Photo A.62: Sphene (f.o.v. = 0.9 mm long). Sample SD-23-2270.5 ft.

Pyrite and chalcopyrite are the only two sulfides present; total percentage is approximately 5-7 vol-%; only trace corresponds to chalcopyrite. They occur together with biotite and with carbonate.

Some of the quartz is patchy and irregular shaped suggesting that it might have been introduced.

Trace cinnamon rutile occurs in association with biotite.

Based on the mineralogy present the alteration can be classified as K-silicate constructive with phyllic overprint and calc-silicate overprint.

SD-23-2322.5 ft. Protolith: Limestone?

This sample corresponds to a garnet-diopside replacement body. Other minerals present are: carbonate, quartz, serpentine and sulfides.

Diopside and garnet are the two most abundant minerals each one comprising approximately 40-45 vol-% of the sample.

Serpentine is present altering the garnet; nearly one half of the garnet has been replaced by serpentine. The serpentine shows growth zoning (Photo A.63).

Carbonate comprises <5 vol-% of the sample and it seems to be poikilotopic (big crystals surrounding quartz and diopside, Photo A.64); suggesting that it might have been of the last minerals to form. Quartz also comprises <5 vol-% and it is irregular shaped and patchy (Photo A.65), it seems to be an alteration mineral and not part of the original rock.

The total percentage of sulfides is approximately 3-4 vol-%; chalcopyrite and pyrite seem to be the only two sulfides present (hard to say not a P.T.S).

Two types of submillimeter scale veinlets are cutting the rock:

- 1- Diopside veinlet
 - 2- Serpentine veinlet
- Protolith was probably a carbonate.



Photo A.63: Diopside-garnet replacement body; garnet is being replaced by serpentine (f.o.v. = 1.8 mm long). Sample SD-23-2322.5 ft.

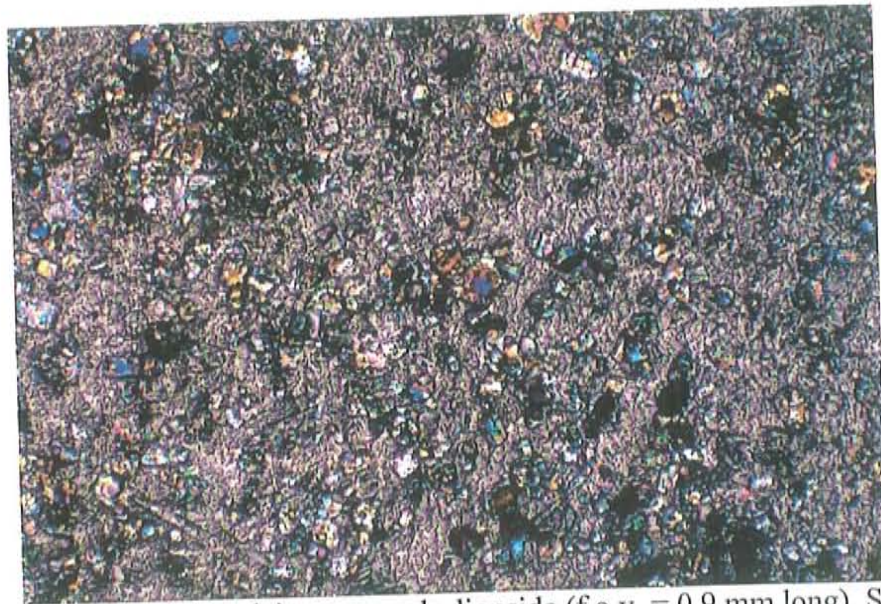


Photo A.64: Poikilotopic calcite surrounds diopside (f.o.v. = 0.9 mm long). Sample SD-23-2322.5 ft.



Photo A.65: Patchy quartz (f.o.v. = 0.9 mm long). Sample SD-23-2322.5 ft.

DRILL HOLE SD-26

SD-26-1167 ft. Quartz-Monzonite

Phenocrysts include K-feldspar, plagioclase, quartz and biotite. Trace zircon is present.

Alteration of feldspars to white phyllosilicates (as patches and in some cases veinlets) varies greatly from <10 vol-% to 80 vol-%, it seems to be stronger in plagioclase. Some feldspars have been so strongly altered that it can no be determined if were plagioclase or K-feldspar. Plagioclase also shows alteration to muscovite, smectite and patchy carbonate. K-feldspars also have been altered by scarce patchy carbonate and trace phenocrysts are cut by carbonate veinlets.

Quartz phenocrysts are very irregular. Quartz sometimes grew together with K-feldspar (graphic texture).

Magmatic biotite has abundant fine grain mineral inclusions (zircon, cinnamon rutile). Hydrothermal biotite is shreddy and sometimes occurs in clusters. Total percentage of biotite is approximately 8-10 vol-% (hydrothermal biotite is the most abundant). Smectite is present altering biotite.

White phyllosilicates + muscovite and carbonate sometimes occur in clusters with biotite, possibly replacing it, there is a close association between carbonate and muscovite. Total percentage of carbonate in the rock <2 vol-% and the percentage of white phyllosilicates + muscovite is approximately 5-7 vol-%.

Scarce irregular shaped silica (introduced?) sometimes occurs in clusters with biotite.

There are some clusters where there is just white phyllosilicates + muscovite, these are possibly replacing a phenocryst.

Cinnamon rutile comprises approximately 1-2 vol-% and is closely associated with biotite.

Pyrite and chalcopyrite are the only two sulfides present, these comprise <3 vol-% (pyrite > chalcopyrite). Sulfides are closely associated with biotite, usually occurring in clusters.

Besides white phyllosilicates and carbonate veinlets that cut feldspars only two other types of veins were observed in the rock:

- 1- Pyrite discontinuous veinlets.
- 2- Muscovite veinlets.

Alteration is K-silicate constructive, weakly overprinted by white phyllosilicates, muscovite and scarce carbonate.

SD-26-1352 ft. Biotite Quartz-Diorite

This rock is very similar to samples SD-15-1230 ft. and SD-15-1237 ft.

Plagioclase is very abundant, it is altered to smectite, fine grain biotite, and white phyllosilicates (total alteration to white phyllosilicates varies from none to <5 vol-%). Some smectite veins cut plagioclase (originally biotite?).

Quartz is fine grained and irregular shaped. Trace zircon and apatite are present in the rock. There appears to be K-feldspar, only differentiated from quartz by its dirty appearance.

Magnetite is present in the rock, the total amount is approximately 3 vol-%; it occurs everywhere in the rock and is apparently of magmatic origin. specularite replaces magnetite.

Biotite comprises approximately 5-10 vol-% of the rock, most seems to be of magmatic origin (has mineral inclusions). Hydrothermal biotite sometimes has olive green pleochroism. Magmatic biotite is being replaced by hydrothermal biotite in some areas. Hydrothermal biotite has been altered to chlorite and smectite; chlorite comprises <1 vol-% of the rock and the total amount of smectite in the rock is approximately 5 vol-%. Biotite veinlets cut the rock.

There are clusters of biotite with carbonate; carbonate possibly replaces biotite. Total amount of carbonate in the rock is approximately 6 vol-%.

The only ore mineral present in the rock corresponds to trace chalcopyrite.

Alteration assemblage can be classified as K-silicate constructive weakly overprinted by carbonate.

DRILL HOLE SD-31

SD-31-1430 ft. Protolith: Sandy limestone or lime sandstone?

Carbonate is the most abundant mineral in the rock, none seems to be original, it apparently all formed by recrystallization. Most of the carbonate is sparry, and there are some areas where it is poikilotopic (big crystals that surround other minerals).

Quartz is the second most abundant mineral comprising approximately 20 vol-% of the rock. Most quartz seems to be introduced (an alteration mineral), it is usually irregular shaped and patchy. Some quartz appears to be detrital. The protolith was probably either a sandy limestone or a limy sandstone.

Diopside comprises approximately 5 vol-% of the rock. There is an area of the rock that is composed mainly of dirty carbonate; this area does not have diopside. Quartz is present throughout the sample.

Quartz veinlets cut the rock; the fact that these veins have no diopside in them suggests that the introduced quartz possibly formed after the diopside. Carbonate was possibly the last mineral to form.

Pyrite and chalcopyrite were the only two sulfides identified, together these comprise <3 vol-% (chalcopyrite > pyrite). Sulfides occur in veins; there are sulfide stinger veinlets and veins of carbonate + sulfides. The greater concentration of sulfides occurs together with the dirty carbonate in the area where there is no diopside.

Besides the carbonate + sulfide veins there are also carbonate barren veins that cut the rock.

SD-31-1760 ft. Protolith: Sandy limestone or lime sandstone?

Garnet and clinopyroxene (possibly diopside) are the two most abundant minerals in the rock. Garnet is the most with a percentage of >60 vol-%. It is apparently being replaced by serpentine. Clinopyroxene comprises approximately 15 vol-%. Trace patchy carbonate replaces clinopyroxenes.

Quartz varies from fine to coarse grain, its total percentage is approximately 10 vol-%; some of the quartz is irregular shaped and patchy (possibly introduced), there is also bladed quartz. Part of the quartz appears to be detrital.

Epidote is present in veins, the total amount is <3 vol-%.

There are some areas of the rock which are pretty dirty (apparently smectite).

The protolith was probably either a sandy limestone or a limy sandstone; possibly with some clay content.

Sulfides present are pyrite, chalcopyrite, bornite, and idaite. Together pyrite and chalcopyrite comprise approximately 5-7 vol-% of the rock (pyrite > chalcopyrite). Bornite and idaite are only present in trace amount, and are closely associated with chalcopyrite (Photo A.66); these three minerals are possibly coeval. Pyrite is in some cases surrounded by chalcopyrite indicating that it was the first sulfide to form.

Hematite is present throughout the sample; the total amount is approximately 1-2 vol-%.

Parallel veins cut the rock:

✕ Chalcopyrite + pyrite + trace bornite and idaite.

✕ Pyrite + epidote + chalcopyrite + trace bornite and idaite.

Bornite and idaite are not always present in the veins.

There is another mineral present it is very fine grain and has strong internal reflections (possibly ruby silvers).

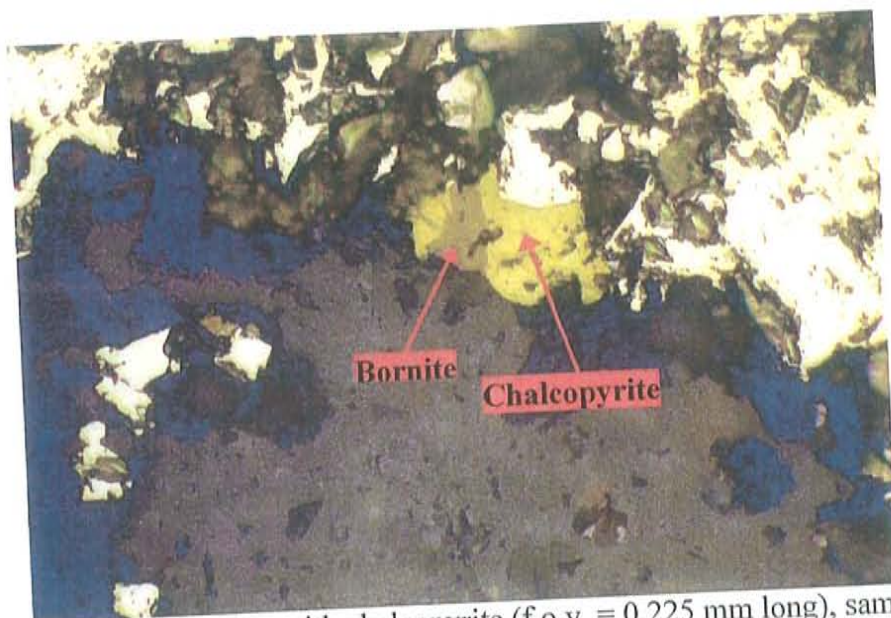


Photo A.66: Bornite together with chalcopyrite (f.o.v. = 0.225 mm long), sample SD-31-1760 ft.

SD-31-2178 ft. Protolith: Sandy limestone or lime sandstone?

Carbonate and quartz are the two most abundant minerals in the rock, with sub-equal amounts of each (approximately 30 vol-%); they are followed in abundance by epidote and diopside also with sub-equal amounts (approximately 15 vol-%).

K-feldspar is present in the sample (<1 vol-%), it is very clean and has apatite inclusions.

Some of the quartz has been introduced (it occurs in veins), but the abundant quartz in the matrix is possibly detrital. All the carbonate formed by recrystallization. Protolith is possibly a limy sandstone or a sandy limestone.

Some of the carbonate is poikilotopic (big crystals that surround other minerals). Chlorite comprises approximately 5 vol-% of the rock; part of it seems to be replacing an amphibole (tremolite/actinolite?). Carbonate replaces both: chlorite and the amphibole. Only scarce amount of the amphibole remains.

The total amount of sulfides (pyrite and chalcopyrite) in the rock is approximately 6 vol-%; most of this corresponds to pyrite. Pyrite occurs in veins a disseminated.

Some of the pyrite is euhedral.

Different vein types cut the rock:

- 1- Submillimeter scale epidote veinlets.
- 2- Submillimeter scale carbonate + epidote.
- 3- Millimeter scale epidote + diopside, which turns into a carbonate + chlorite + diopside + scarce epidote vein.
- 4- Millimeter scale quartz + carbonate + epidote + chlorite + scarce diopside.
- 5- Pyrite veins.

SD-31-2205 ft. Hornblende Quartz-Monzonite

Plagioclase is very abundant, several minerals alter plagioclase grains: fine grain biotite, white phyllosilicates, patchy carbonate, and epidote. Some have been strongly altered to carbonate (up to 40 vol-%). Alteration to white phyllosilicates varies from none to 10 vol-%. Carbonate veinlets cut plagioclase.

K-feldspars have been altered to white phyllosilicates and trace epidote. Alteration to white phyllosilicates is usually <5 vol-%, but in some cases reaches 15 vol-%.

Quartz is usually very irregular shaped; some seem to be filling spaces between grains (introduced?).

Trace amounts of zircon and sphene are present in the rock.

Biotite comprises approximately 10 vol-% of the rock; most seems to be of magmatic origin, usually has abundant mineral inclusions. There is scarce hydrothermal biotite (fine grain and shreddy) replacing magmatic biotite.

The main alteration minerals are actinolite, chlorite and carbonate, and they usually occur together. Actinolite comprises <5 vol-% of the rock, it replaces biotite (Photo A.67) and hornblende (scarce residual hornblende is still present in the rock). The total amount of carbonate in the rock is <4 vol-%. Chlorite comprises approximately 2-3 vol-% of the rock. It could be that there was a greater amount of hydrothermal biotite originally but it got replaced by actinolite, chlorite and carbonate.

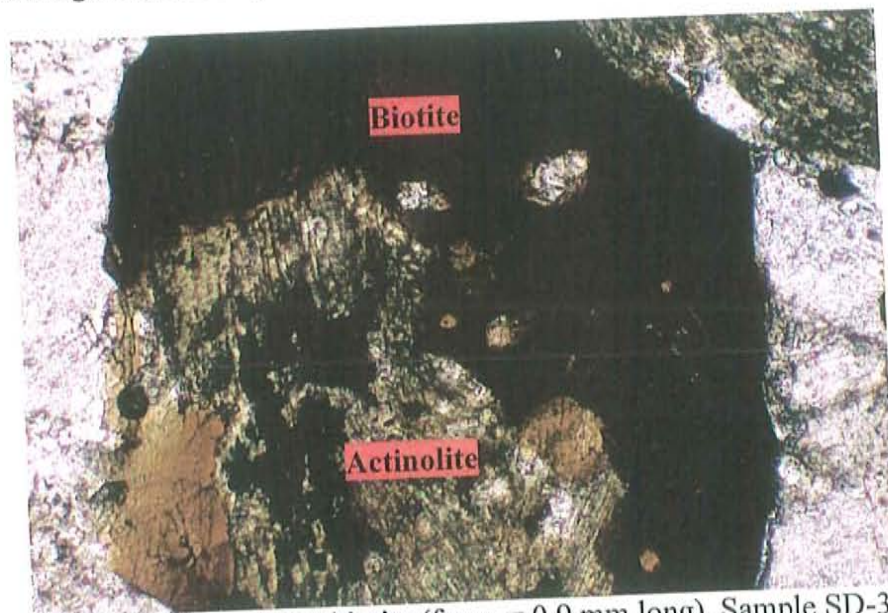


Photo A.67: Actinolite replaces biotite (f.o.v. = 0.9 mm long). Sample SD-31-2205 ft.

Some phenocrysts have been completely replaced by alteration minerals, for example, there is a hornblende phenocryst (based on shape) that has been completely altered to carbonate + actinolite; another example is actinolite + carbonate + scarce epidote altering what appears to have been a magmatic biotite. The total amount of epidote in the rock is <1 vol-%.

There are some clusters of biotite + actinolite + hornblende + carbonate + magnetite.

Besides altering feldspars, white phyllosilicates sometimes occur together with carbonate, the total amount of white phyllosilicates in the sample is <2 vol-%.

Cinnamon rutile is only present in trace amounts.

Magnetite occurs disseminated throughout the sample, the total amount is <1.5 vol-%, it all seems to be of magmatic origin. Some magnetite is associated with biotite and some to actinolite.

Sulfides are pyrite and chalcopyrite, the total amount of these is <1.5 vol-% (mainly pyrite, only trace chalcopyrite). There is some pyrite that occurs together with actinolite.

Veins that cut the rock are:

- 1- Quartz + plagioclase + biotite + scarce K-feldspar + pyrite.
- 2- Chlorite + carbonate veinlets. This vein cuts the previous type.
- 3- Pyrite stringers.

DRILL HOLE 05 STK 034

05-STK 034-566.6 m.

Note: this sample was made into a polished slab so silicates were not described.

Based on texture, the host rock appears to be an intrusive igneous rock? White phyllosilicates are the only alteration mineral visible. Sulfides and sulphosalts are also present.

Enargite is the most abundant opaque mineral followed by pyrite, marcasite and trace sphalerite. Pyrite is surrounded by enargite indicating that it had to form first.

Only trace sphalerite is present in the rock and it is not in contact with the other opaque minerals so its paragenesis can not be determined.

Pyrite varies from euhedral to sub-euhedral and it occurs disseminated and as stringer veinlets.

Based on the abundance of enargite this sample could be classified as a copper ore, if the copper from the enargite can be recovered.

05-STK-034-609 m. Protolith: Quartz arenite

Quartz is the most abundant minerals, comprising approximately 90 vol-% of the rock; this quartz seems to be detrital, which makes the rock a quartz arenite. Detrital quartz grains are anhedral in shape and show overgrowth textures.

Tremolite, diopside and patchy carbonate fill the spaces between the quartz grains. One area of the sample, possibly more susceptible to alteration, has completely been altered to tremolite + diopside + carbonate + scarce epidote and zoisite, there is also trace amount of another mineral present (possibly gypsum). Tremolite and diopside are the two most abundant alteration minerals (Photo A.68).

A sub-millimeter scale veinlet of quartz + carbonate is present cutting the rock, this vein also cuts through the completely altered area.



Photo A.68: Alteration minerals, abundant diopside (f.o.v.= 0.9 mm long), sample 05-STK-034-609 m.

DRILL HOLE 04RDYR01 (Youngs Ranch)

04RDYR01-1896.5 ft. Andesite

Based on texture this rock appears to be of volcanic origin (Photo A.69). The matrix comprises approximately 55vol-% of the rock and it is composed mainly of plagioclase microcrysts.



Photo A.69: Volcanic rock with abundant plagioclase phenocrysts (f.o.v. = 1.8 mm long), sample 04RDYR01-1896.5 ft.

Plagioclase are the most abundant phenocrysts, this are usually unaltered, only some have been altered to smectite. Clinopyroxenes, possibly augite follow plagioclase in abundance, scarce smectite also alters these phenocrysts, the total percentage of clinopyroxenes in the rock is approximately 8 vol-%, some clinopyroxenes occur in clusters.

Biotite is usually euhedral and comprises approximately 5 vol-% of the rock, like clinopyroxenes biotite sometimes occurs in clusters, in some cases associated with euhedral magnetite. Some fine grain biotite is shreddy (late magmatic-early hydrothermal?).

Hornblende comprises <3 vol-% of the rock. There is scarce smectite altering hornblende.

Trace apatite is present as microcrysts.

There are some phenocrysts that have been completely altered to smectite; the total percentage of smectite in the rock is approximately 2 vol-%.

Magnetite is present throughout the sample comprising <3 vol-% of the rock, as mentioned before some occurs in clusters with biotite. There is also some magnetite that grew inside biotite phenocrysts. All the magnetite appears to be of magmatic origin. Specular hematite replaces magnetite.

Holes are present in the sample, these could have formed due to dissolution or could be a magmatic feature; they vary from rounded to irregular shaped.

Pyrite is the only sulfide present in the rock and it is only present in trace amounts.

No veins were observed in the rock.

APENDIX B PETROGAPHY OF FIELD SAMPLES

SM-29/05/06-1. Monzodiorite (Coordinates 387263mE / 4478421mN)

This is a very fresh rock. Clinopyroxenes (possibly augite) and hornblende are still present, with sub-equal amounts of each (<4 vol-%). Some clinopyroxenes are being replaced by hornblende (hydration of the rock).

Biotite is usually irregular shaped; the total amount of biotite in the rock is approximately 6-8 vol-%. Some of the biotite is shreddy, possibly late-magmatic-early hydrothermal. Fine grain biotite alters phenocrysts (clinopyroxene and hornblende).

Chlorite alters hornblende and biotite, the total amount of chlorite in the rock is <1.5 vol-%.

Quartz is fine grain and irregular (is some introduced?)

Trace zircon is present in the rock.

Plagioclase and K-feldspars are abundant; unlike in most drill hole samples, these have not been altered to white phyllosilicates. There are K-feldspar overgrowths around plagioclase phenocryst.

Magnetite comprises approximately 3-4 vol-% of the rock (apparently all of magmatic origin), it occurs disseminated throughout the sample, although the greatest concentration usually occurs in clusters with clinopyroxene, hornblende and biotite.

Actinolitic amphibole occurs as an alteration mineral replacing mafic minerals (biotite, hornblende and clinopyroxenes); the total amount of actinolite in the rock is approximately 1 vol-%.

Smectite veinlets are the only type of veins that cut the rock (originally biotite?).

The alteration assemblage is classified as K-silicate constructive due to the presence of K-feldspar overgrowths and hydrothermal biotite.

No sulfides seem to be present in the rock.

SM-29/05/06-11. Quartz-Latite Porphyry (Coordinates 387107mE / 4478564mN)

White phyllosilicates and muscovite are the main alteration minerals, followed by chlorite. The total alteration to white phyllosilicates is approximately 10 vol-%. The lack of white phyllosilicate or chlorite veins, suggests that these minerals possibly formed due to weathering and are not a consequence of hydrothermal alteration. The total amount of chlorite in the sample is <5 vol-%.

Iron oxides and hydroxides are abundant, comprising approximately 10 vol-% of the rock; they seem to be hematite and goethite.

Plagioclase phenocrysts have been strongly altered to white phyllosilicates + muscovite; alteration of phenocrysts is usually >30 vol-%. There are some plagioclase smaller crystals that show scarce to no alteration.

Trace patchy carbonate alters K-feldspars. Some big K-feldspar phenocrysts have white phyllosilicates and muscovite, but they seem to be mainly altering mineral inclusions (possibly plagioclase) and not the actual K-feldspar. There is only trace alteration of K-feldspars to white phyllosilicates. Some smaller K-feldspars also show alteration to chlorite.

Quartz phenocrysts are rounded. These are the least altered of all the phenocrysts in the rock. There are K-feldspar overgrowths around quartz eyes.

Plagioclase, quartz and K-feldspar microcrysts are present in the matrix.

There is a big cluster where everything has been altered to muscovite + goethite or hematite + carbonate + white phyllosilicates.

No mafic minerals are present in the rock; they have all been altered by goethite or hematite, chlorite, white phyllosilicates and muscovite.

Pyrite comprised approximately 1 vol-% of the rock but it has now been replaced by goethite and hematite.

The alteration assemblage is classified as K-silicate constructive due to the K-feldspar overgrowths.

SM-15/06/06-4. Hornblende Monzodiorite (Coordinates 390232mE / 4477240mN)

This rock is very similar to sample SM-29/05/06-1. Magmatic minerals include: plagioclase, K-feldspar, quartz, biotite, magnetite, hornblende and clinopyroxenes (possibly augite). Trace apatite, rutile and zircon are also present.

Clinopyroxenes are less abundant than in SM-29/05/06-1, comprising <1 vol-% of the rock and hornblende phenocrysts are more abundant with a total percentage of approximately 7-10 vol-%. In some cases clinopyroxenes are being replaced by hornblende (Photo B.1) and by hornblende + biotite, there is also some actinolite altering clinopyroxenes. Biotite replaces hornblende.

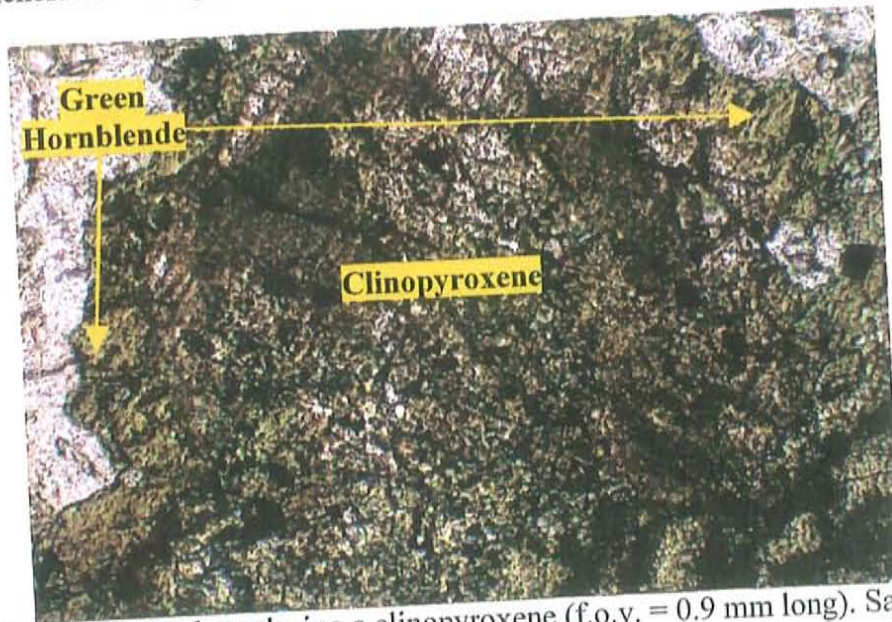


Photo B.1: Hornblende replacing a clinopyroxene (f.o.v. = 0.9 mm long). Sample SM-15/06/06-4.

Biotite comprises approximately 5 vol-% of the rock, most have abundant mineral inclusions and are possibly of magmatic origin. Trace muscovite replaces biotite.

There are K-feldspar overgrowths around plagioclase phenocrysts. The alteration of plagioclase to white phyllosilicates varies from none to <5 vol-% and in some cases white phyllosilicate veinlets cut plagioclase.

K-feldspar phenocrysts have also been cut by white phyllosilicate veinlets. The total alteration of K-feldspar to white phyllosilicates is weaker than in plagioclase (varies from none to trace).

Quartz is irregular shaped; some seems to be filling spaces between other minerals.

Magnetite comprises approximately 3 vol-% of the rock and it occurs everywhere in the sample (apparently magmatic), the biggest concentrations occur associated to biotite and hornblende. No sulfides in the rock.

Chlorite and actinolite are present in small amounts (<1 vol-% for each).

The presence of K-feldspar overgrowths allows for the alteration assemblage to be classified as weak K-silicate constructive with a weak phyllic overprint.

SM-15/06/06-5. Quartz -Latite Porphyry (Coordinates 390260mE / 4477290mN)

This sample is very similar to SM-29/05/06-11.

There is only trace alteration of K-feldspars to white phyllosilicates. Mineral inclusions inside K-feldspar phenocrysts (possibly plagioclase), have been altered to white phyllosilicates + muscovite + scarce chlorite. Some K-feldspar phenocrysts are cut by white phyllosilicate veinlets (these are probably just fractures that got filled by white phyllosilicates).

Plagioclase phenocrysts have usually been strongly altered to white phyllosilicates, hematite or goethite and scarce patchy carbonate. Some scarce plagioclase phenocrysts show no alteration to white phyllosilicates but only to hematite or goethite, patchy carbonate and muscovite.

Quartz phenocrysts are rounded and seem to have K-feldspar overgrowths (K-silicate constructive alteration).

Trace zircon is present in the rock.

Sphene was originally present (based on shape) but has now been altered to muscovite + iron hydroxides (possibly goethite).

Unlike in sample SM-29/05/06-11, chlorite is only present in trace amounts. Some phenocrysts have been completely replaced by alteration minerals, which include: goethite, hematite, muscovite, white phyllosilicates and carbonate. White phyllosilicates + muscovite comprise approximately 7-9 vol-% of the rock. The total amount of carbonate in the sample is <1 vol-%.

The matrix is fine grain; quartz seems to be the main component.

Iron oxides and hydroxides are abundant in the rock (apparently hematite and goethite) the total amount is approximately 10 vol-%. Some of these are replacing pyrite, based on cubic shape.

The alteration to white phyllosilicate is possibly a weathering consequence and not related to hydrothermal fluids.

SM-18/07/06-2. Chert (Coordinates 391682mE / 4471576mN)

Rock is very similar to SM-06/06/06-13 (see limestone descriptions in Appendix C). This rock also corresponds to a chert (which might also be replacing the limestone,

although evidence is not as clear). Unlike in SM-06/06/06-13 no fabric is observed. This sample contains malachite and azurite, and it was collected to determine host rock. Abundant really fine grain opaque minerals are present (apparently pyrite). Submillimeter scale carbonate veinlets cut the rock.

APENDIX C LIMESTONE DESCRIPTIONS

SM-13/01/06-9 (SD-14-1124 ft). Protolith: Probable limestone.

Alteration minerals include: quartz, garnet and carbonate. Quartz is the most abundant, followed closely by sub-equal amounts of carbonate and garnet. Trace epidote is also present and it occurs together with the garnet.

Based on cross cutting relationships garnet appears to be the first one to have formed, since it is cut by quartz and carbonate veins (Photo C.1). Carbonate surrounds quartz grains indicating that it was the last of these minerals to form (recrystallization).

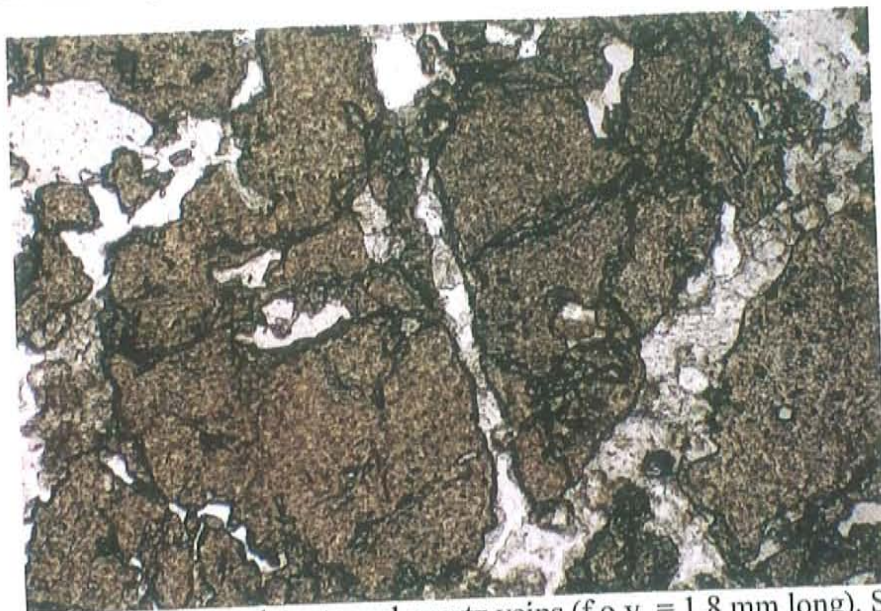


Photo C.1: Garnet cut by carbonate and quartz veins (f.o.v. = 1.8 mm long). Sample SM-13/01/06-9.

Analyses would be necessary to determine garnet composition.

Quartz varies in size (some is really fine grain); all the quartz is patchy suggesting that corresponds to an alteration mineral (introduced).

Chalcedony is present as overgrowths around quartz grains and filling spaces, total percentage of chalcedony is <2 vol-%.

Sulfide minerals are chalcopyrite and pyrite and comprise approximately 5 vol-% of the rock with pyrite >> chalcopyrite. Most of the pyrite is present in a millimeter scale veinlet. Chalcopyrite occurs in stringer veinlets and disseminated.

Several types of veins are present cutting the rock:

- 1- Millimeter scale vein of pyrite.
- 2- Submillimeter scale carbonate veinlets.
- 3- Submillimeter scale carbonate + quartz veinlets.
- 4- Chalcopyrite stringer veinlets.

SM-29/05/06-4. Packstone-Wackstone/Biomicroite

This specific sample was collected on the hanging wall of a mined manto located near the Argent mine. It corresponds with a dark micritic limestone (organic material gives it the dark color). As with the previous sample SD-15-72 ft. this rock has not been recrystallized.

Abundant millimeter and submillimeter scale veins of coarsely crystalline calcite (spary) cut the rock and in some cases cross cut each other.

Sulfides have now been replaced by iron oxides, (not as many as in SD-15-72 ft.); these oxides are mostly in veins. Stable isotope values for this sample are $\delta^{13}\text{C} = 4.1\text{‰}$ and $\delta^{18}\text{O} = 22.1\text{‰}$. This rock can be classified as a packstone-wackstone/biomicroite (Dunham, 1962 and Folk, 1962).

SM-30/05/06-1. Packstone/Biomicroite

This rock has been completely recrystallized to poikilotopic calcite cement; original cement was probably micritic. Fossils were possibly present (based on some visible outlines) but there is no good preservation to determine what they might have been.

Trace thin submillimeter scale calcite veins are present cutting the rock. Chert is present in scarce amount replacing the rock.

Based on the classifications schemes by Dunham (1962) and Folk (1962) this rock can be classified as a packstone/biomicroite.

When analyzed for stable isotopes this rock was characterized by having a low $\delta^{13}\text{C}$ value of -3.9‰ and a $\delta^{18}\text{O}$ value of 15.5‰ .

SM-03/06/06-3 II. Protolith: Sandy limestone or calcareous sandstone

Minerals present in the sample include: carbonate, quartz, diopside (Photo C.2) and fine grain silica. Of these carbonate is the most abundant comprising approximately 35 vol-% of the rock, it is closely followed by quartz which comprises approximately 30 vol-%, total amount of diopside is approximately 25 vol-% and the least abundant is fine grain silica, comprising <10 vol-%. Quartz overgrowths around detrital quartz grains are abundant; these are difficult to spot but they are mainly identified by the fact that most quartz grains have abundant inclusions in the middle (corresponding to the detrital quartz) and are very clean in the edges (overgrowths).

This rock corresponds to a sandy limestone or calcareous sandstone.

Two areas are defined in the sample based on differences in mineralogy (related to layering? or differences in alteration?) the first one has a tabular mineral, possibly an amphibole (tremolite or actinolite) which has been completely replaced by carbonate and fine grain silica (Photo C.3); only scarce sand (quartz grains) is present in this area. The other corresponds mainly to quartz and carbonate. Diopside is present everywhere throughout the sample. Possibly originally a tremolite/actinolite-diopside replacement body, in which late carbonate has replaced mainly the amphibole; diopside shows scarce alteration to carbonate.

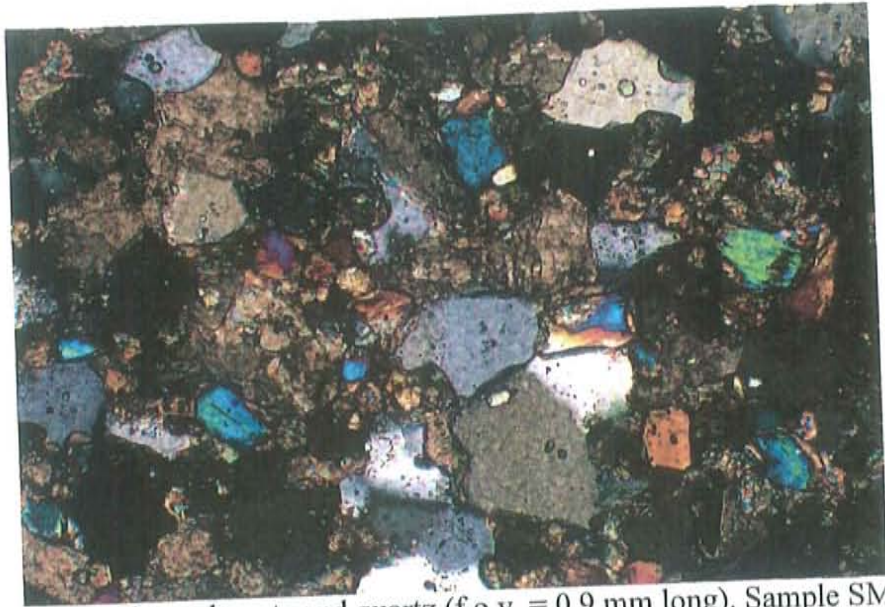


Photo C.2: Diopside, carbonate and quartz (f.o.v. = 0.9 mm long). Sample SM-03/06/06-3.



Photo C.3: Tabular mineral (tremolite/actinolite?) replaces by carbonate and fine grain silica (f.o.v. = 0.9 mm long). Sample SM-03/06/06-3.

Isotope analysis yielded low carbon and oxygen values: $\delta^{13}\text{C} = -5.7\text{‰}$ and $\delta^{18}\text{O} = 10.4$; this low carbon value is due to the decarbonation process that took place during contact metamorphism, evidenced by the presence of diopside.

SM-05/06/06-5. Packstone-Grainstone/Biosparite

This sample corresponds to a sandy limestone. As in the previous sample (SM-30/05/06-1), this rock has also been recrystallized (mainly the cement) but in this case fossils are still present.

The lack of mud (micrite) could be due to recrystallization, there is the possibility that there was micrite present as part of the original cement but it became recrystallized to coarser calcite crystals; since this can not be determined for sure the rock it was classified as a packstone-grainstone, (Dunham 1962), and as a sandy biosparite when using the Folk (1962) classification scheme.

Calcite and quartz are the two main minerals with sub-equal amounts of each. Scarce plagioclase grains are also present in the rock. Quartz grains vary in shape from rounded to angular.

As mentioned before fossils have been preserved in the sample, these include: echinoderms (Photo C.4), braquiopods and bryozoans (possibly fenestrate), of these echinoderms (mainly crinoids) are the most abundant and they sometimes have syntaxial overgrowths (early cement). Also present are pelloids.

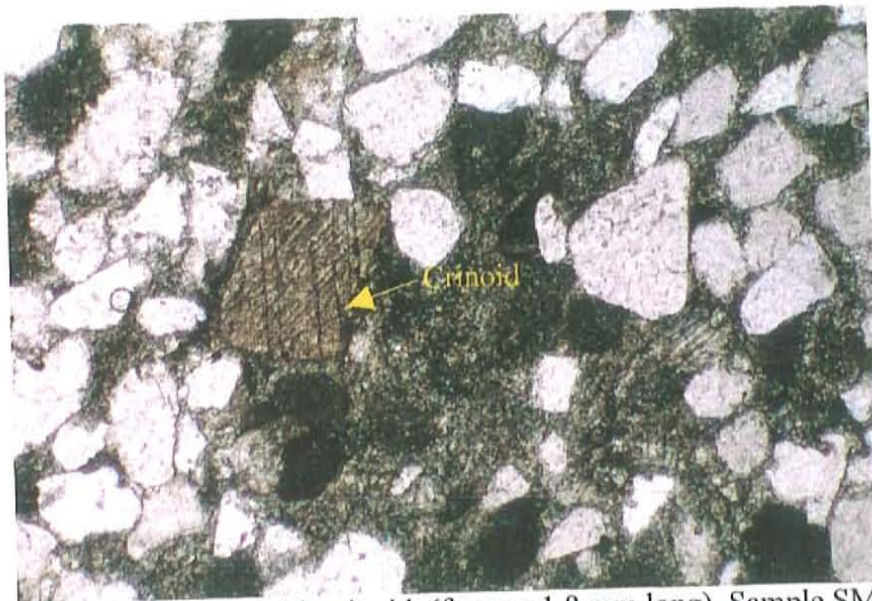


Photo C.4: Sandy limestone with crinoid. (f.o.v. = 1.8 mm long). Sample SM-05/06/06-5.

Scarce fine grain silica (chert) is present and it seems to be either replacing grains or filling spaces.

Iron oxides are present in scant amounts.

Stable isotope analysis for this sample gave the following values: $\delta^{13}\text{C} = 2.7\text{‰}$ and $\delta^{18}\text{O} = 22.6\text{‰}$.

SM-05/06/06-10. Packstone/Biomicrite

As with the previous sample (SM-05/06/06-5) this rock also corresponds to a sandy limestone, although it is finer grain (Photo C.5). Quartz and calcite are the two main minerals with sub-equal amounts of each. Scarce muscovite is present in the sample.

Sparite is the main cement but most if not all was probably originally micrite that became recrystallized, based on this the rock can be classified as a packstone/biomicrite (Dunham, 1962 and Folk, 1962).



Photo C.5: Finer grain sandy limestone (f.o.v. = 0.9 mm long). Sample SM-05/06/06-10.

This sample is layered and it contains abundant iron oxides, clay and organic material. Hematite is present replacing pyrite (based on cubic shape). Chert occurs in scarce (either filling spaces or replacing grains).

Thin submillimeter scale calcite veins cut the rock.

Pressure solution features are present due to compaction of the rock.

Some fossils are still present, these include: echinoderms and bones (phosphate), both present in scarce amounts. Other fossils are also present which based on morphology might correspond to either syringopora tubular coral or poorly preserved siliceous sponges.

Stable isotope analysis gave the following values: $\delta^{13}\text{C} = 3.4\text{‰}$ and $\delta^{18}\text{O} = 20.0\text{‰}$.

SM-06/06/06-13. Protolith: Probable sandy limestone

This rock corresponds to a layered chert. Original detrital quartz is still present. Possible fossils (based on outlines) have been replaced by chert, there is one in particular that looks like it might have been an echinoderm (Photo C.6). Protolith was probably a sandy limestone, in which the carbonate was replaced by chert.

Very fine grain pyrite seems to have been replaced by hematite.

Submillimeter scale carbonate veins are present; they sometimes cross cut each other.

This sample yielded the lowest carbon value of all the samples analyzed for stable isotopes with a $\delta^{13}\text{C}$ of -10.9‰ , believed to have been caused by contact metamorphism. $\delta^{18}\text{O}$ has a value of 18.5‰ .



Photo C.6: Possible echinoderm replaced by chert (f.o.v. = 1.8 mm long). Sample SM-06/06/06-13.

SM-14/06/06-15. Packstone-Wackstone/Biomicrite

This sample corresponds to a recrystallized dark micritic limestone very similar to SM-29/5/06-4 and it is also classified as a packstone-wackestone/biomicrite (Dunham, 1962 and Folk, 1962). Dark color of the rock is due to the amount of organic material.

Several submillimeter scale calcite veins (spary) cut they rock and cross cut and displace each other.

Hematite is present replacing pyrite (cubic shape). Echinoderms are the only type of fossil identified in the sample.

Stable isotope values for this sample are: $\delta^{13}\text{C} = 1.7\text{‰}$ and $\delta^{18}\text{O} = 20.6\text{‰}$.

SM-07/08/06-1 (SD-15-72 ft.). Boundstone/Biolithite

This limestone corresponds to a dark fine grain micritic limestone (which has not been recrystallized); organic material is present giving it the dark color. Laminations in the sample were possibly caused by microbial interactions, based on this it was classified as a boundstone/biolithite, under the classifications of Dunham (1962) and Folk (1962) respectively.

Abundant submillimeter scale veinlets are present; these are made of clean coarse calcite (sparite). Some of these veins cross cut and displace each other.

On the hand sample this dark grey limestone seems to be cut by millimeter scale white calcite veins, but when seen under the microscope these white areas are very

similar to the rest of the rock (dark and micritic) and the contact between the supposed veins and the rest of the rock seems to be transitional suggesting that they are not really veins but differences in the same rock, they might correspond to areas that became bleached possibly by oxidizing fluids. When analyzing for stable isotopes, these white areas (bleached?) were sampled separately from the rest of the rock.

For stable isotope analysis, one sample was taken from the dark gray part of the rock which gave the following values: $\delta^{13}\text{C} = 1.7\text{‰}$ and $\delta^{18}\text{O} = 10.9\text{‰}$ and two samples were taken from the white areas, these gave similar $\delta^{18}\text{O}$ values as the dark part of the rock (10.5 and 11.4‰ respectively) but were lighter in $\delta^{13}\text{C}$, with values of: 0.3 and 0.0‰.

Hematite replaces pyrite in the sample based on the cubic shape of the crystals, with a total amount of approximately 2 vol-%. Pyrite replaced crystals are disseminated and they occur everywhere except for in the submillimeter scale sparite veins.

NOTE: this one is called a biolithite/boundsonte because it has laminations suggesting microbial interactions. The other dark limestones (SM-29/5/06-4 and SM-14/06/06-15) don't have such clear laminations. Dark limestones are rich in organic material and in iron. Only one of the dark rocks has been recrystallized.

APPENDIX D
FLUID INCLUSION DESCRIPTIONS

SD-16-1103 ft.

Fluid inclusions in this sample are present in vein quartz.
Types of fluid inclusions present include:

- * Liquid + vapor + halite + opaque (Photo D.1).

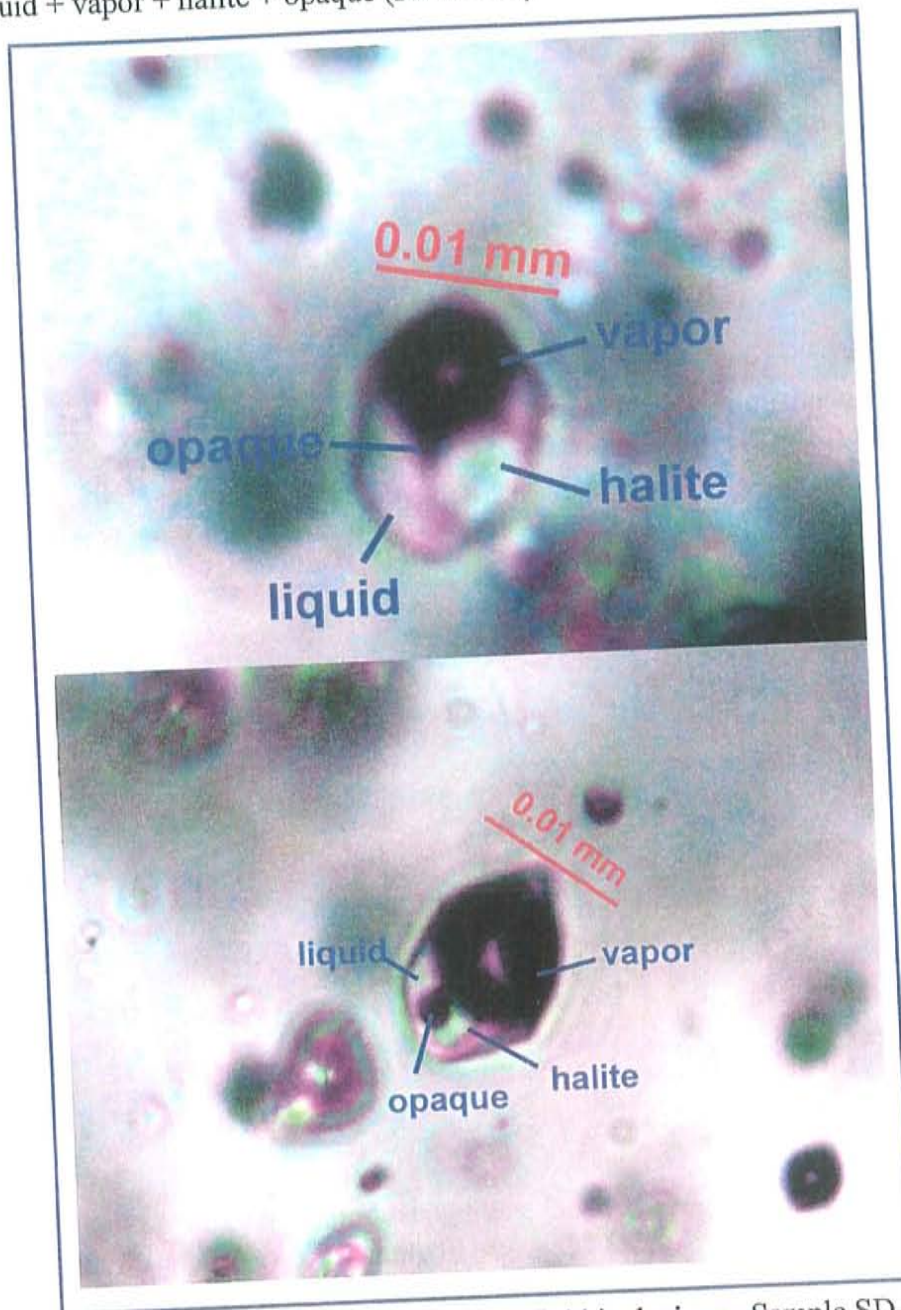


Photo D.1: Liquid + vapor + halite + opaque fluid inclusions. Sample SD-6-1103 ft.

- * Liquid + vapor + two daughters: possibly halite and sylvite, sometimes with also with an opaque daughter (Photo D.2).

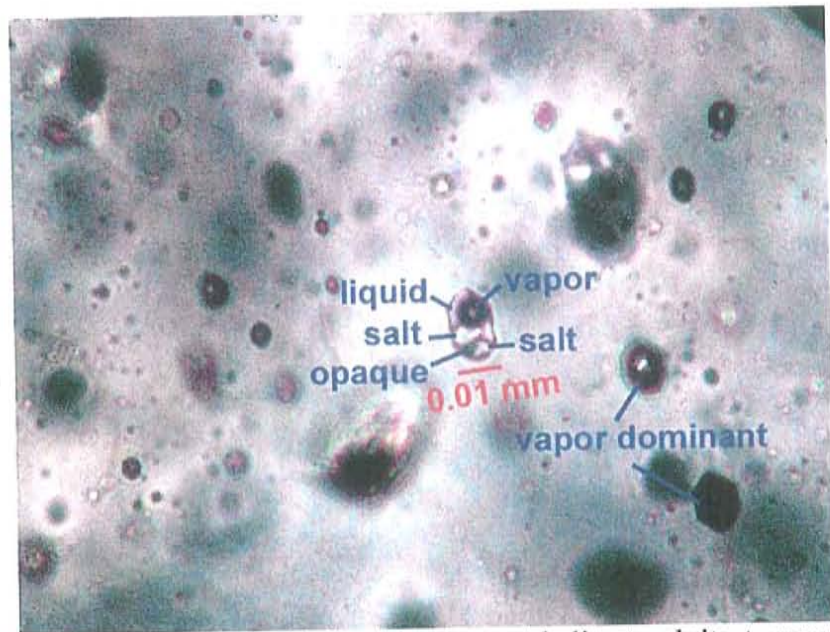


Photo D.2: Fluid inclusion with liquid + vapor + halite + sylvite + opaque occurs together with abundant vapor-rich fluid inclusions. Sample SD-16-1103 ft.

✘ Liquid + vapor + multiple daughters, including an opaque (Photo D.3).

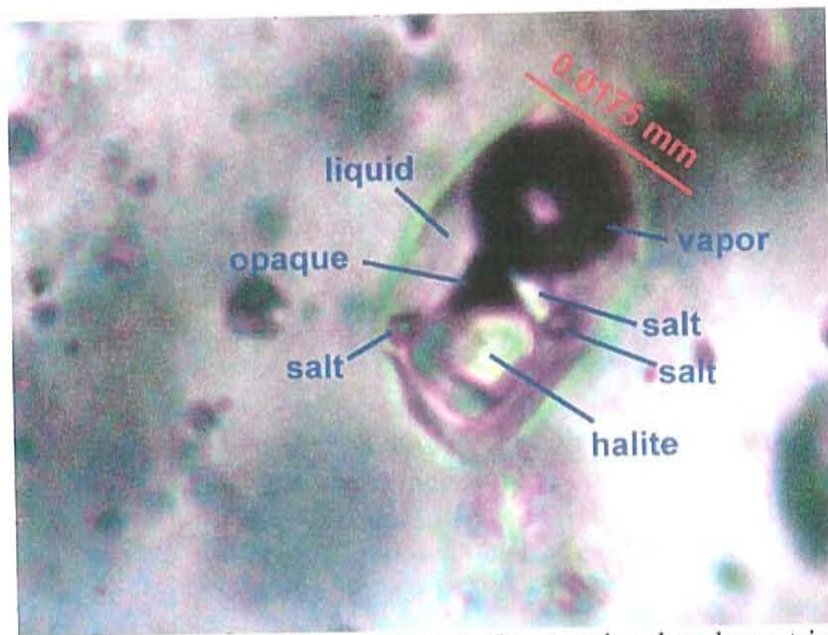


Photo D.3: Liquid + vapor + multiple daughters. Opaque daughter has a triangular shape. Sample SD-16-1103 ft.

- ✘ Vapor-rich (Photo 2).
- ✘ Vapor-rich + halite (Photo 4), sometimes also with an opaque daughter.

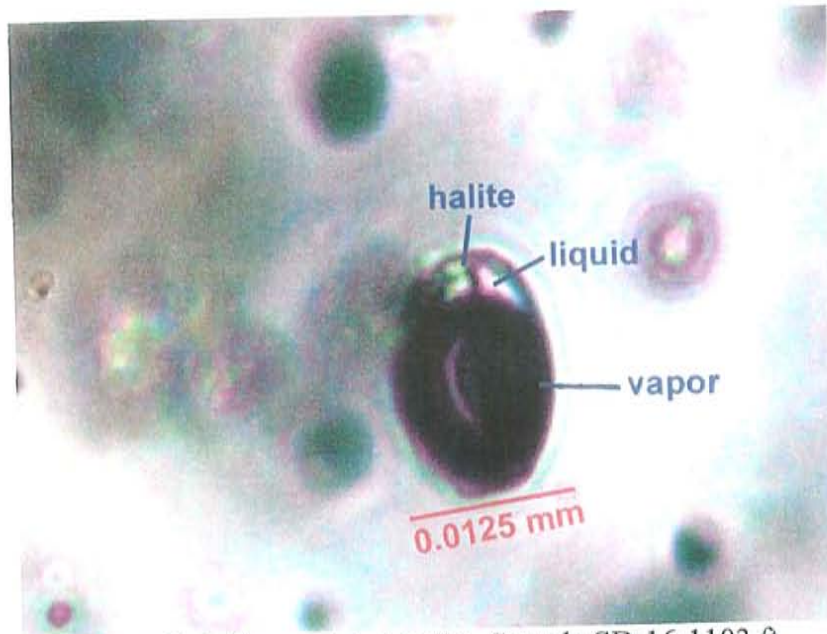


Photo D.4: Vapor-rich + halite. Sample SD-16-1103 ft.

Opaque daughters sometimes have a triangular shape, which is characteristic of chalcopyrite (Photo D.3).

Vapor-rich seem to be the most abundant type; these sometimes occur together with inclusions that have: liquid + vapor + halite + opaque and with liquid + vapor + halite + sylvite + opaque (Photo D.2); this assemblage indicates possible boiling of the fluids.

Ratios of vapor to liquid in this sample are not always constant (Photo D.1).

SD-21-137 ft.

Fluid inclusions present in this sample include:

- ✘ Liquid + vapor.
- ✘ Liquid + vapor + halite, some of these also have an opaque daughter.
- ✘ Liquid + vapor + two daughters, possibly halite and sylvite.
- ✘ Vapor-rich.

Vapor-rich inclusions are characterized by having a crystal shape, and sometimes occur in clusters with inclusions that have two daughters and with two phase inclusions (liquid + vapor). In other cases vapor-rich inclusions occur together with liquid + vapor + halite + opaque inclusions. The coexistence of vapor-rich inclusions together with these other types of inclusions is probably a consequence of boiling of the fluids that formed them.

The ratio of liquid to vapor is not constant throughout the sample.
All these inclusions are present in a quartz vein.

SD-21-1002 ft.

Fluid inclusions are in quartz that forms part of a centimeter quartz + calcite + pyrite + molybdenite vein.

Several inclusions are present in this sample, these include:

- ✘ Vapor-rich.
- ✘ Vapor-rich + opaque.
- ✘ Vapor-rich + halite (Photo D.5).

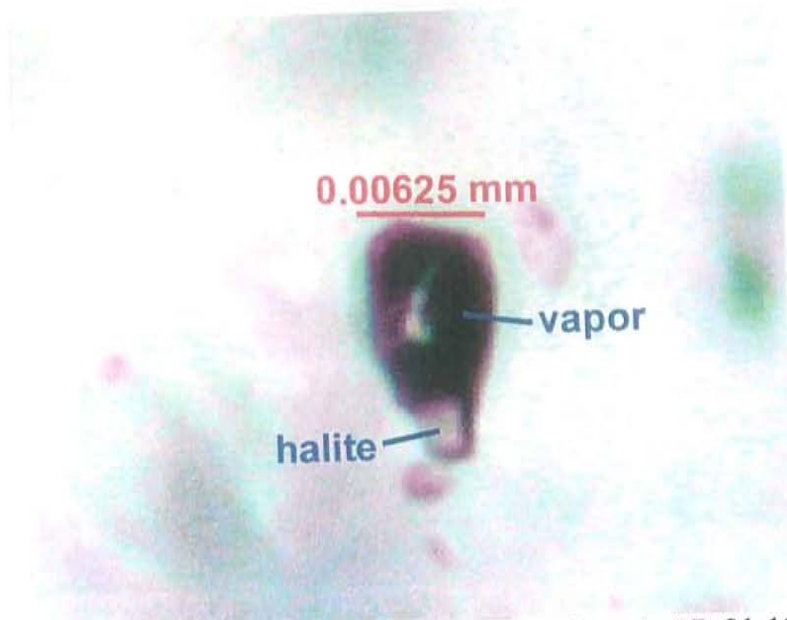


Photo D.5: Vapor-rich fluid inclusion + halite. Sample SD-21-1002 ft.

- ✘ Liquid + vapor + halite, sometimes also with an opaque or dark daughter. This opaque daughter sometimes has a triangular shape, suggesting it could be chalcopyrite (Photo D.6).

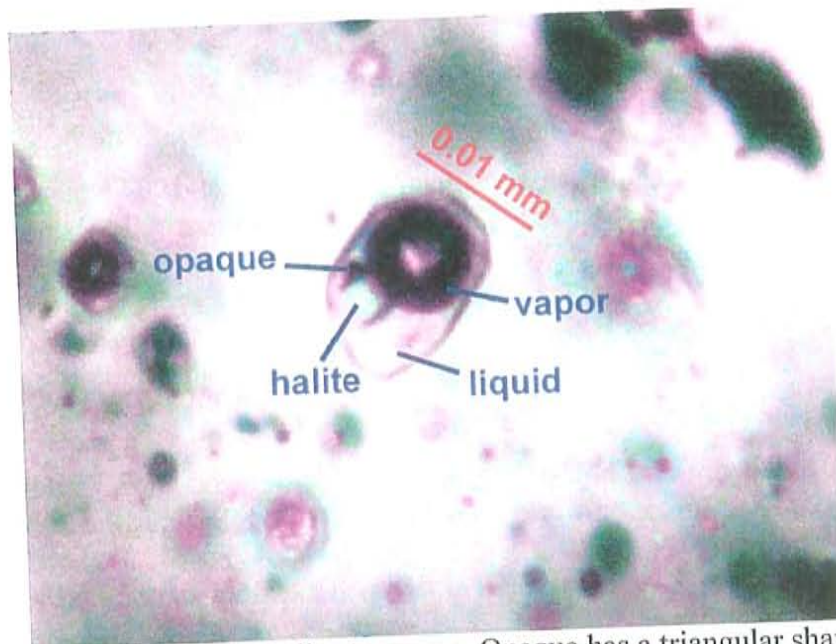


Photo D.6: Liquid + vapor + halite + opaque. Opaque has a triangular shape (possibly chalcopyrite). Sample SD-21-1002 ft.

- ✗ Liquid + vapor + two daughters: possibly halite and sylvite (Photo D.7). These inclusions seem to be scarce.

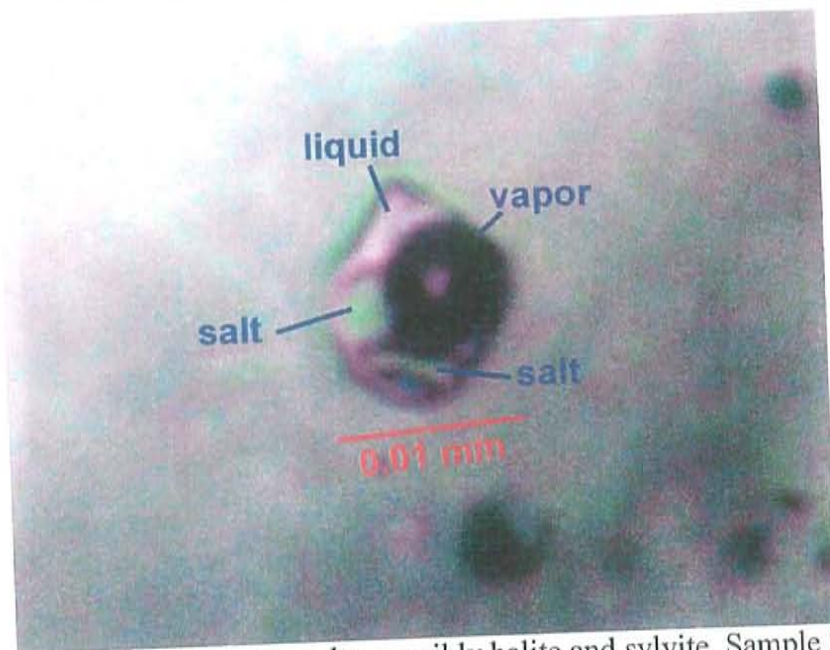


Photo D.7: Liquid + vapor + two salts, possibly halite and sylvite. Sample SD-21-1002 ft.

Vapor-rich inclusions are sometimes associated to other inclusions, such as: liquid + vapor + halite and in some cases liquid + vapor + halite + opaque. These assemblages are probably due to boiling.

Overall the ratio of liquid to vapor and halite seems to be similar throughout the sample.

SD-21-1229 ft.

Like in sample SD-21-1002 ft., fluid inclusions described in this case also are in quartz that is present in a centimeter scale quartz + calcite + pyrite + molybdenite vein; these fluid inclusions include:

- ✗ Vapor-rich.
- ✗ Vapor-rich + opaque.
- ✗ Liquid + vapor (Photo D.8).
- ✗ Liquid + vapor + halite (Photo D.8).
- ✗ Liquid + vapor + halite + opaque.

Vapor-rich inclusions are the most abundant type and sometimes occur in clusters with two phase inclusions (liquid + vapor), possibly a consequence of boiling of the hydrothermal fluids.

The ratio of liquid to vapor is not constant in the sample.

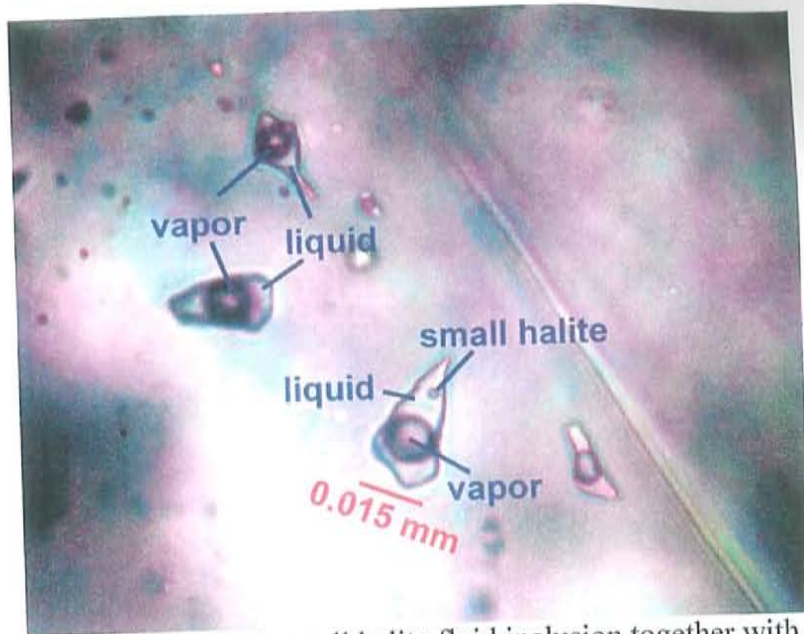


Photo D.8: Liquid + vapor + small halite fluid inclusion together with two phase inclusions (liquid + vapor). Sample SD-21-1229 ft. SD-21-1633 ft.

Fluid inclusions include:
 ✖ Vapor-rich (Photo D.9).

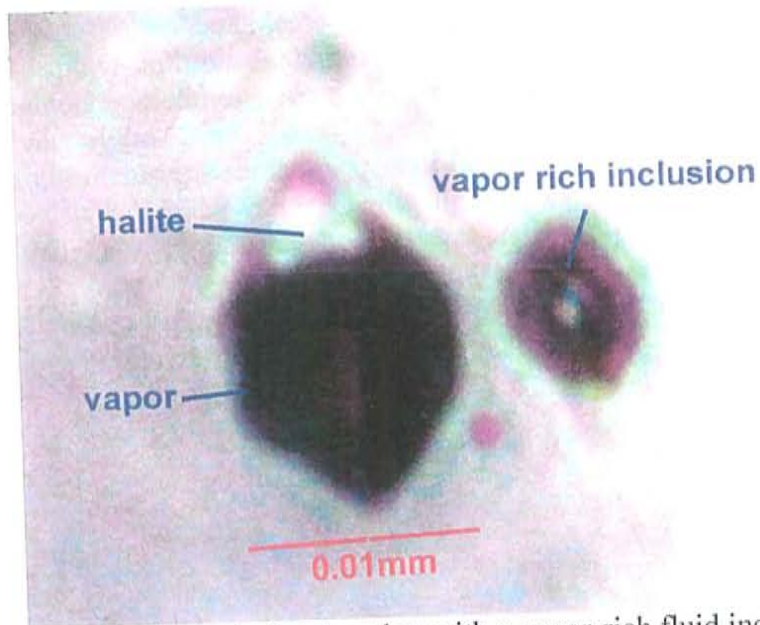


Photo D.9: Vapor + halite inclusion together with a vapor-rich fluid inclusion. Sample SD-21-1633 ft.

- ✖ Vapor-rich + opaque.
- ✖ Vapor-rich + halite daughter (Photo D.9).
- ✖ Vapor-rich + halite + opaque (Photo D.10).

✖ Liquid + vapor.

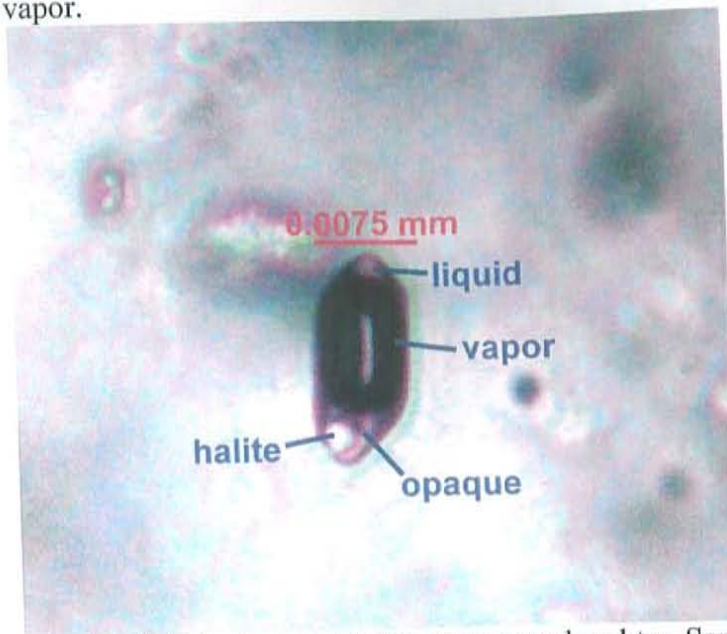


Photo D.10: Vapor-rich fluid inclusion + halite + opaque daughter. Sample SD-21-1633 ft.

- ✖ Liquid + vapor + halite, sometimes also with an opaque (Photo D.11), or in trace cases two opaque daughters.
- ✖ Liquid + vapor + two daughters, possibly halite and sylvite.
- ✖ Liquid + vapor + two daughters + opaque.
- ✖ Liquid + vapor + multiple daughters.

Opaque daughters sometimes have a triangular shape (Photo D.11), suggesting that they might be chalcopyrite.

Vapor-rich fluid inclusions sometimes occur in clusters with other types of inclusion such as: liquid + vapor, liquid + vapor + halite, liquid + vapor + two daughters and liquid + vapor + two daughters + opaque. These assemblages are probably a consequence of boiling.

The ratio of liquid to vapor to halite in this sample is not constant. Fluid inclusions in this sample are present in a quartz vein.

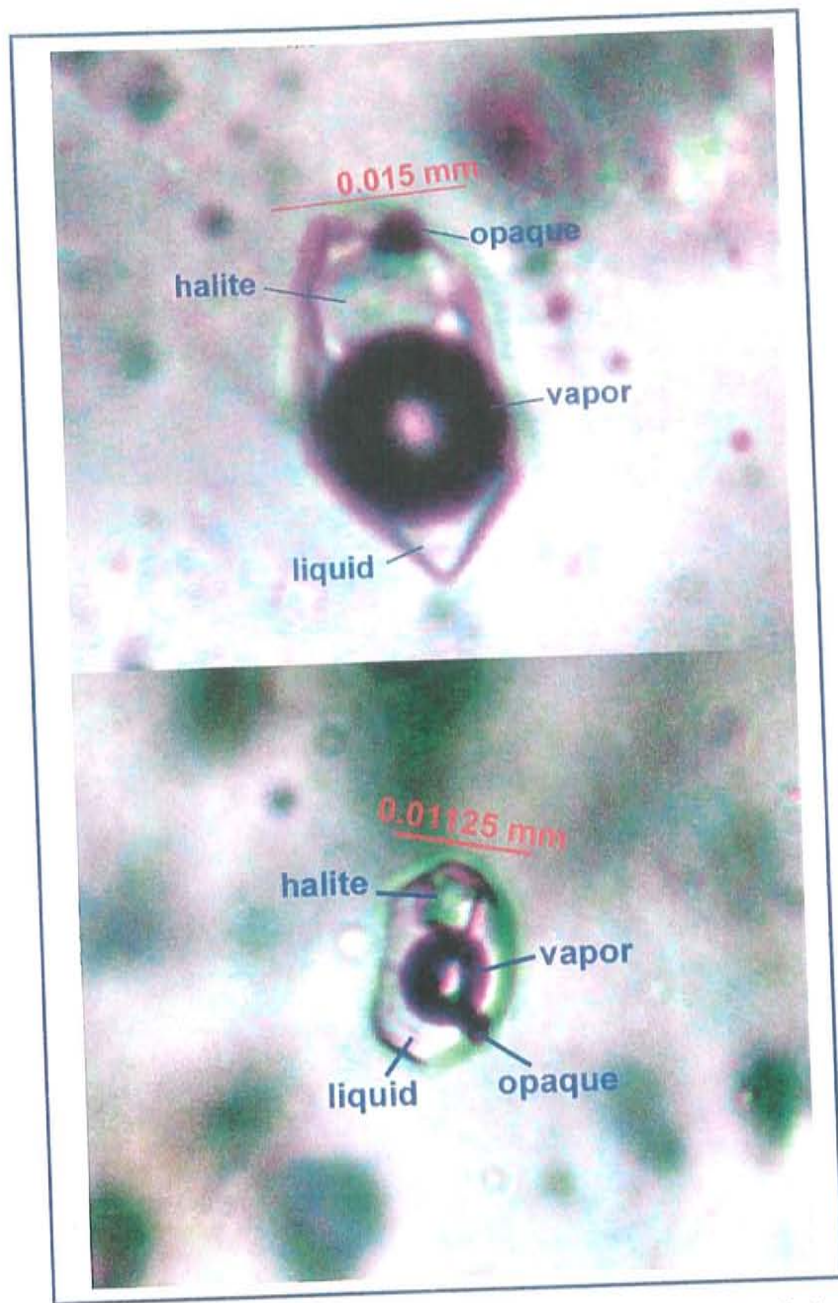


Photo D.11: Liquid + vapor + halite + opaque fluid inclusions. Dark daughter has a triangular shape, possibly chalcopyrite. Sample SD-21-1633 ft.

SD-21-2130.5 ft.

Fluid inclusions described in this sample are from magmatic quartz, the presence of halite bearing inclusions suggest that the rock has been affected by hydrothermal fluids.

Inclusions observed include:

- ✘ Vapor-rich. These inclusions usually have a euhedral shape (Photo D.12).
- ✘ Vapor-rich + halite.
- ✘ Vapor-rich +opaque (Photo D.13).



Photo D.12: Vapor-rich with euhedral inclusion. Sample SD-21-2130.5 ft.

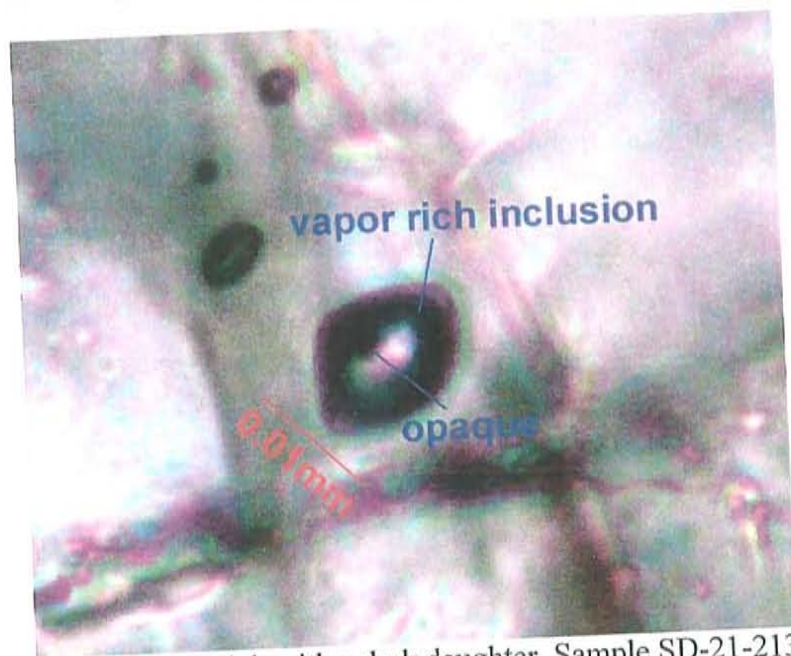


Photo D.13: Vapor-rich with a dark daughter. Sample SD-21-2130.5 ft.

- ✕ Liquid + vapor.
- ✕ Liquid + vapor + halite.
- ✕ Liquid + vapor + opaque.
- ✕ Liquid + vapor + two daughters (Photo D.14), possibly halite and sylvite.

In some cases vapor-rich inclusions occur in clusters with liquid + vapor and liquid + vapor + halite + sylvite (Photo D.14); this assemblage suggests that the fluid was probably boiling when these inclusions formed.

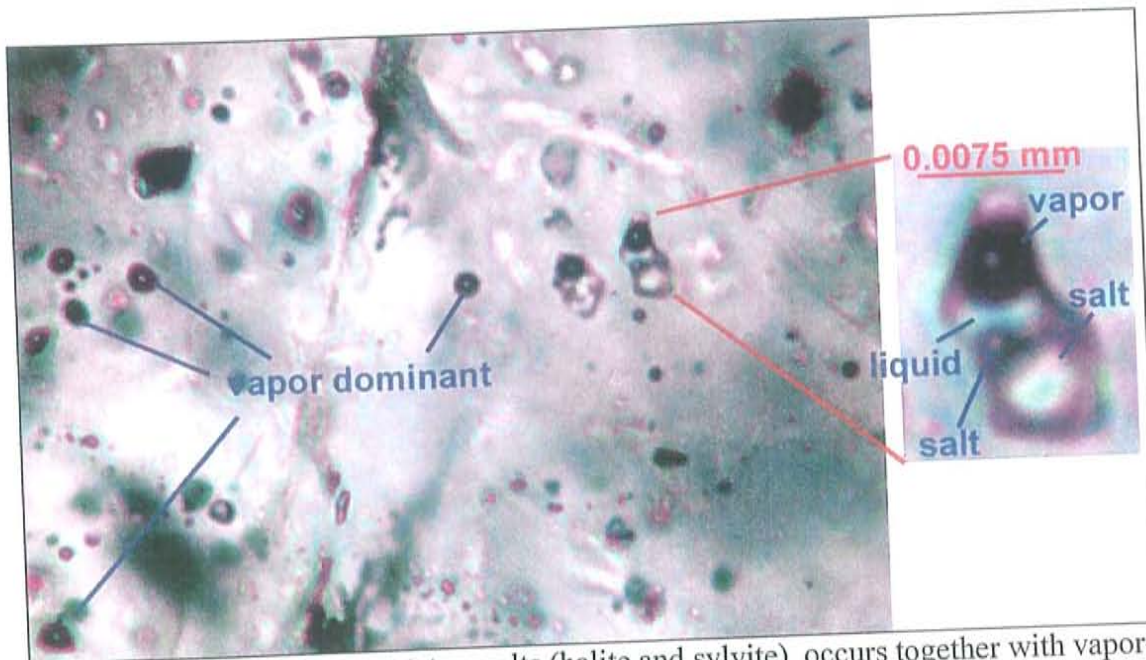


Photo D.14: Liquid + vapor + two salts (halite and sylvite), occurs together with vapor-rich fluid inclusions. Sample SD-21-2130.5 ft.

SD-23-1448 ft.

This sample is characterized by having abundant fluid inclusion, which are present in a quartz vein.

Types of inclusions present include:

- ✗ Vapor-rich.
- ✗ Vapor-rich + halite (Photo D.15).

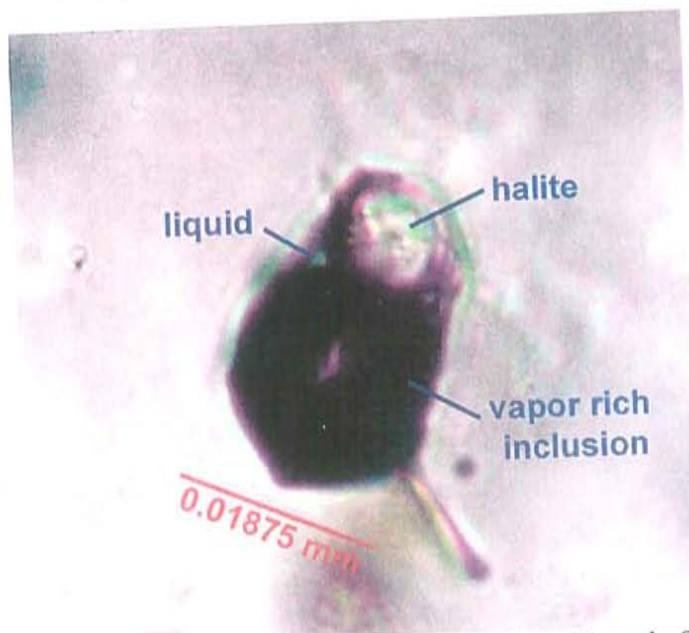


Photo D.15: Vapor-rich inclusion with halite daughter. Sample SD-23-1448 ft.

- ✘ Vapor-rich + opaque (Photo D.16).

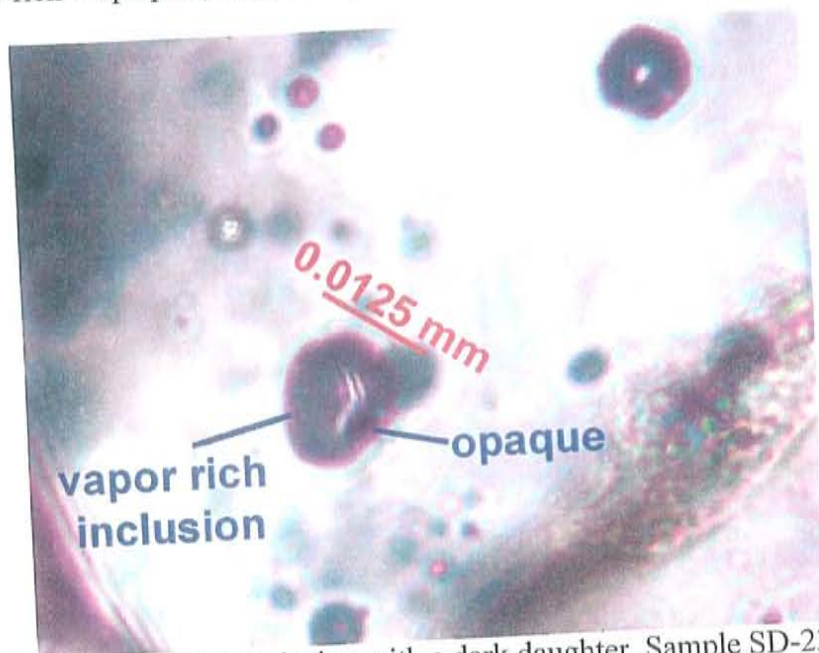


Photo D.16: Vapor-rich inclusion with a dark daughter. Sample SD-23-1448 ft.

- ✘ Vapor-rich + halite + opaque.
- ✘ Liquid + vapor + halite + opaque.
- ✘ Liquid + vapor + two daughters, possibly halite and sylvite. These sometimes have an opaque daughter (Photo D.17).

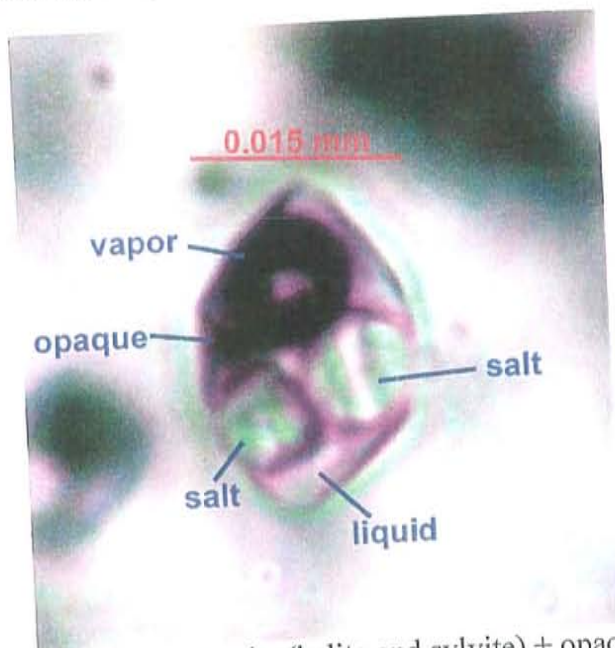


Photo D.17: Liquid + vapor + two salts (halite and sylvite) + opaque daughter. Sample SD-23-1448 ft.

- ✘ Liquid + vapor + multiple daughters (Photo D.18).

* Scarce: liquid + vapor.

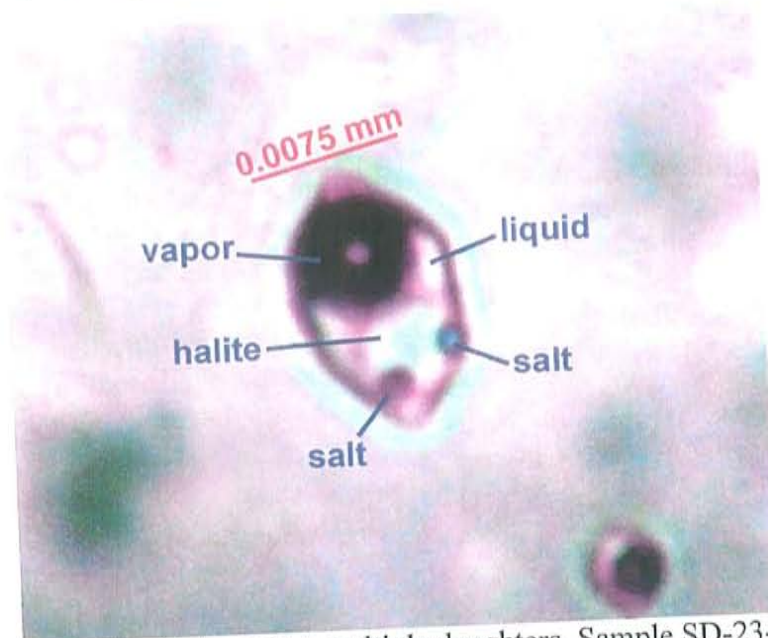


Photo D.18: Liquid + vapor + multiple daughters. Sample SD-23-1448 ft.

Vapor-rich are the most abundant type, these occur everywhere in the quartz veins and are sometimes associated to salty inclusions that are liquid dominated ("boiling") (Photo D.19).

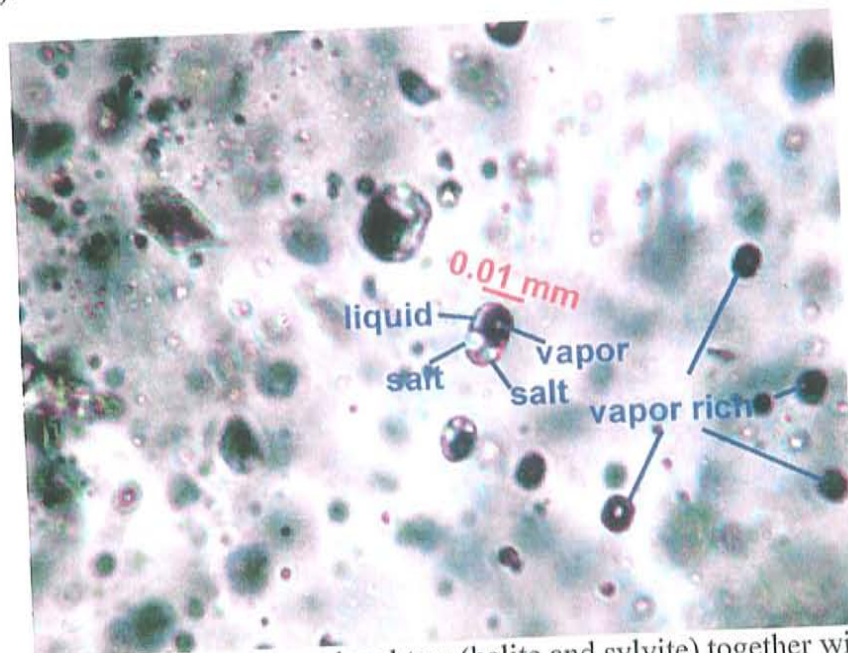


Photo D.19: Liquid + vapor + two daughters (halite and sylvite) together with vapor-rich inclusions. Sample SD-23-1448 ft.

Opaque daughters present in vapor-rich inclusions are sometimes triangular in shape, suggesting that they might be chalcopyrite.

SM-23/05/06-8 (Coordinates 366577mE / 4479258mN)

This sample was collected from a quartz vein in an outcrop. Fluid inclusions present include:

- ✘ Liquid + vapor.
- ✘ Vapor-rich.

These two types of inclusions sometimes occur in clusters ("boiling"). Two phase fluid inclusions (liquid + vapor) seem to be the most abundant.

The ratio of vapor to liquid in the fluid inclusions throughout the sample seems to be constant.

Scarce inclusions with halite daughters are also present, indicating the presence of salty fluids. Trace of these have a second daughter, possibly sylvite (Photo D.20).



Photo D.20: Liquid + vapor + two daughters (possibly halite and sylvite). Sample SM-23/05/06-8.

Appendix E Stable Isotope Data

#	Easting	Northing	Sample	$\delta^{13}\text{C} \text{‰}$	$\delta^{18}\text{O} \text{‰}$	Vein Density ¹	Comments
1			SM-13/01/06-9	-0.1	10.4	ND	Skarn with garnet. Taken from drill holes SD-14 at 1124 ft. Thin section was made (Appendix C). This sample was not plotted on the maps.
2	386208	4479357	SM-23/05/06-2 (A)	3.2	18.2	ND	Sample is from dump, coordinates are from adit.
3	386208	4479357	SM-23/05/06-2 (B)	3.4	22.3	ND	Sample is from dump, coordinates are from adit.
4	386208	4479357	SM-23/05/06-2 (VEIN)	3.0	18.9	NA	From sample SM-23/05/02- (A)
5	386304	4479333	SM-23/05/06-3	2.5	19.1	35	
6	386304	4479333	SM-23/05/06-3 (VEIN A)	-1.0	17.9	NA	
7	386304	4479333	SM-23/05/06-3 (VEIN B)	-1.0	17.9	NA	
8	386547	4479253	SM-23/05/06-4	2.8	21.1	29	There is a shaft 10 to the S75W.
9	386552	4479252	SM-23/05/06-5	3.4	22.2	25	
10	386560	4479248	SM-23/05/06-6 (A)	4.0	21.8	21	
11	386560	4479248	SM-23/05/06-6 (B)	4.2	21.5	21	
12	386566	4479244	SM-23/05/06-7	4.1	16.8	17	
13	386726	4479232	SM-23/05/06-9	2.9	15.3	36	Near dump were there is bladed calcite.
14	386726	4479236	SM-23/05/06-10	3.2	19.0	25	Near dump were there is bladed calcite.
15	386858	4479237	SM-23/05/06-11	2.7	14.9	25	
16	387002	4479228	SM-23/05/06-12	3.4	24.4	7	Approximately 40 m from shaft.
17	385805	4479163	SM-24/05/06-1	1.4	3.7	5	Has trilobites. Geochemistry in this area has high gold. Coarse.
18	385791	4479170	SM-24/05/06-2	2.0	11.8	29	Abundant thin discontinuous veins.
19	387703	4478555	SM-27/05/06-2	1.8	7.7	5	
20	387691	4478537	SM-27/05/06-3	1.0	11.5	11	
21	387823	4478504	SM-27/05/06-4	2.3	13.4	7	
22	387904	4478332	SM-27/05/06-5	-2.3	17.1	Nominal	Very weathered difficult to count veins.
23	388061	4478313	SM-27/05/06-6	1.8	24.1	13	
24	388103	4478324	SM-27/05/06-7	2.0	25.5	16	Has crinoids.
25	388120	4478424	SM-27/05/06-8	1.4	20.0	26	
26	388089	4478445	SM-27/05/06-9	2.5	22.5	44	
27	387845	4478627	SM-27/05/06-10	2.3	19.9	30	
28	387834	4478988	SM-27/05/06-11	0.6	14.2	6	Really close to shaft. Argent mine.
29	387823	4478988	SM-27/05/06-12	3.9	22.6	33	

30	387823	4478988	SM-27/05/06-12 (VEIN)	-0.5	12.4	NA	
31	387812	4478994	SM-27/05/06-13	3.6	20.8	35	
32	387801	4478993	SM-27/05/06-14	3.8	24.7	34	
33	387790	4478997	SM-27/05/06-15	4.5	25.3	25	
34	387771	4479004	SM-27/05/06-16	4.2	24.8	33	
35	387756	4479005	SM-27/05/06-17	3.5	22.2	35	
36	387756	4479005	SM-27/05/06-17 (VEIN)	-1.2	16.7	NA	
37	387740	4479007	SM-27/05/06-18 (A)	3.1	21.3	25	
38	387740	4479007	SM-27/05/06-18 (B)	3.4	22.6	25	
39	387897	4478992	SM-29/05/06-2	3.1	23.0	13	
40	387904	4478989	SM-29/05/06-3	4.0	21.7	13	
41	387927	4478972	SM-29/05/06-4	4.1	22.1	41	On hanging wall of mined manto. Thin section was made (Appendix C).
42	387927	4478972	SM-29/05/06-4 (VEIN)	-2.5	10.2	NA	
43	387962	4478947	SM-29/05/06-5 (A)	4.2	24.8	32	
44	387962	4478947	SM-29/05/06-5 (B)	3.8	23.6	32	
45	387723	4479017	SM-29/05/06-6	1.4	19.5	22	
46	387671	4479072	SM-29/05/06-7	4.1	23.2	24	
47	387652	4479069	SM-29/05/06-8	-0.1	16.4	25	
48	387652	4479069	SM-29/05/06-8 (VEIN)	1.2	13.9	NA	
49	387649	4479074	SM-29/05/06-9	4.1	26.1	8	
50	387656	4478777	SM-29/05/06-10	2.6	23.6	8	
51	387859	4478311	SM-30/05/06-1	-3.9	15.5	None visible	Clean white limestone. Thin section was made (Appendix C).
52	387913	4478448	SM-30/05/06-2	1.5	21.9	7	
53	387951	4478420	SM-30/05/06-3	2.0	20.6	Nominal	Not a good place to count veins.
54	387867	4478213	SM-30/05/06-4	-1.5	13.4	6	Clean white limestone.
55	387082	4478216	SM-03/06/06-1	-3.5	19.2	20	From outcrop in shaft. Gray with white rim.
56	387082	4478216	SM-03/06/06-2	-7.8	17.0	ND	2 m away from previous. White.
57			SM-03/06/06-3 (I)	-8.4	20.9	ND	Really weathered white limestone. Not plotted in maps.
58			SM-03/06/06-3 (II)	-5.7	10.4	ND	Really weathered white limestone. Has diopside. Not plotted in maps.
59	387231	4478074	SM-03/06/06-4	-1.4	17.6	ND	Thin section was made (Appendix C).
60	387277	4478027	SM-03/06/06-5	0.3	19.7	6	Very coarse limestone (recrystallized?).
							Very coarse limestone.

61	387298	4478030	SM-03/06/06-6		-7.3	15.9	13	White limestone.
62	387298	4478030	SM-03/06/06-6 (VEIN)		-5.8	14.8	NA	
63	387399	4477983	SM-03/06/06-9 (A)		0.7	21.9	8	Sample comes from shaft.
64	387399	4477983	SM-03/06/06-9 (B)		1.2	21.6	8	Sample comes from shaft. Coarsely crystalline.
65	387676	4477344	SM-03/06/06-10		-2.5	16.7	1	Almost no veins, 1 in a meter. Coarse limestone.
66	387748	4477414	SM-03/06/06-11		2.2	21.9	17	
67	387732	4477522	SM-03/06/06-12		-4.2	16.8	8	Very white limestone. Weathered.
68	387746	4477561	SM-03/06/06-13		1.5	23.0	32	
69	387184	4480075	SM-04/06/06-1		3.5	23.6	28	
70	387188	4480076	SM-04/06/06-2		2.9	23.1	32	
71	387198	4480081	SM-04/06/06-3		3.8	25.1	10	
72	387197	4480079	SM-04/06/06-4		3.0	21.1	26	
73	387217	4480082	SM-04/06/06-5		3.0	2.5	40	
74	387230	4480084	SM-04/06/06-6		3.4	22.5	44	Really close to vein or replacement body.
75	387234	4480080	SM-04/06/06-7		3.7	22.5	26	Other side of vein from SM-04/06/06-6.
76	387284	4480088	SM-04/06/06-8		3.0	18.5	29	50 cm from mined vein.
77	387284	4480088	SM-04/06/06-8 (VEIN)		2.8	25.3	NA	
78	387257	4480081	SM-04/06/06-9		2.9	23.8	17	
79	387269	4480079	SM-04/06/06-10		1.6	23.2	19	
80	387269	4480079	SM-04/06/06-10 (VEIN)		-0.1	16.4	NA	
81	387267	4480075	SM-04/06/06-11		2.9	20.0	18	
82	387266	4480073	SM-04/06/06-12		2.0	21.5	21	
83	387280	4480010	SM-04/06/06-13		2.2	20.5	13	
84	387333	4480088	SM-04/06/06-14		3.3	24.8	30	
85	387428	4480007	SM-04/06/06-15		2.5	20.5	6	
86	387434	4480010	SM-04/06/06-16		2.2	20.7	13	
87	387459	4480013	SM-04/06/06-17		1.5	18.6	13	
88	387474	4480017	SM-04/06/06-18		2.0	19.1	ND	
89	387497	4480020	SM-04/06/06-19		1.2	20.6	19	
90	387529	4480022	SM-04/06/06-20		1.5	16.7	13	
91	387702	4479970	SM-04/06/06-21		3.4	21.7	17	Weathered surface.
92	387697	4479972	SM-04/06/06-22		2.5	22.2	19	
93	387479	4479637	SM-04/06/06-23		3.2	22.7	17	
94	387990	4480025	SM-05/06/06-1		3.7	25.2	19	

95	387963	4480050	SM-05/06/06-2	3.5	23.9	24	
96	387963	4480050	SM-05/06/06-2 (VEIN)	3.1	24.0	NA	
97	387944	4480040	SM-05/06/06-3	-0.9	19.8	14	
98	387918	4480039	SM-05/06/06-4	3.6	24.2	18	Coarse, Recrystallized? Thin section was made (Appendix C).
99	387903	4480029	SM-05/06/06-5	2.7	22.6	12	It has abundant thin veins.
100	387873	4480021	SM-05/06/06-6	1.7	19.8	38	
101	387873	4480021	SM-05/06/06-6 (VEIN)	1.0	14.5	NA	
102	387786	4480039	SM-05/06/06-7	2.9	20.2	22	It's probably a sandy limestone. Coarse.
103	387764	4480048	SM-05/06/06-8	2.4	22.5	12	
104	387750	4480045	SM-05/06/06-9	3.3	24.6	32	Thin section was made (Appendix C).
105	387418	4479318	SM-05/06/06-10	3.4	20.0	3	
106	387405	4479312	SM-05/06/06-11	4.2	22.1	8	
107	387413	4479286	SM-05/06/06-12	3.0	15.1	10	
108	387429	4479277	SM-05/06/06-13	5.0	17.9	14	Thin calcite veins.
109	387214	4479229	SM-05/06/06-14	2.5	13.0	10	Shaft 7 m to the S60E (120)
110	387221	4479226	SM-05/06/06-15	2.4	16.8	9	Close to replacemente body (manto).
111	387211	4479220	SM-05/06/06-16 (A)	0.1	6.5	13	Close to replacemente body (manto).
112	387211	4479220	SM-05/06/06-16 (B)	0.1	6.6	13	
113	387167	4479178	SM-05/06/06-17	1.7	20.7	3	50 cm from vein in shaft. Abundant fractures.
114	387476	4479131	SM-05/06/06-18	4.4	18.8	13	
115	387797	4479237	SM-05/06/06-19	3.1	17.4	12	
116	387793	4479238	SM-05/06/06-20	3.2	17.9	22	Contact with quartzite that has vein (SWP-131661)
117	387788	4479286	SM-05/06/06-21	0.4	18.1	12	
118	388340	4479366	SM-05/06/06-22	3.2	24.5	34	
119	388331	4479373	SM-05/06/06-23	2.8	23.4	38	Coarser (possibly sandier) different bed.
120	388318	4479386	SM-05/06/06-24	3.3	22.7	6	
121	388307	4479375	SM-05/06/06-25	2.9	21.7	27	In a shaft.
122	386789	4478911	SM-06/06/06-1	1.1	16.2	40	In a shaft.
123	386815	4478900	SM-06/06/06-2	2.8	17.7	9	Surface to weathered to count veins.
124	386464	4478635	SM-06/06/06-3	1.2	15.2	ND	
125	386510	4478609	SM-06/06/06-4	2.3	11.0	12	
126	386539	4478595	SM-06/06/06-5	2.0	16.3	38	
127	386582	4478555	SM-06/06/06-6	2.0	10.1	47	Looks brecciated in parts. Abundant thin veins.
128	386587	4478538	SM-06/06/06-7	2.6	8.5	47	Abundant thin veins.

129	386601	4478536	SM-06/06/06-8	0.2	14.1	34	Abundant thin veins.
130	386618	4478530	SM-06/06/06-9	1.1	16.5	ND	Coarse limestone.
131	386628	4478539	SM-06/06/06-10	-1.3	11.6	35	
132	386456	4478536	SM-06/06/06-11	-0.5	14.1	40	
133	386456	4478536	SM-06/06/06-11 (VEIN)	-0.4	14.1	NA	Coarse limestone.
134	386361	4478524	SM-06/06/06-12	0.9	15.0	13	White. 4 m on top of SM-06/06/06-12. Fractured. Thin section was made (Appendix C).
135	386363	4478531	SM-06/06/06-13	-10.9	18.5	5	White and gray together. Bleached.
136	387208	4478718	SM-14/06/06-1	-0.3	18.7	15	Bleached.
137	387197	4478700	SM-14/06/06-2	1.1	16.9	19	
138	387194	4478808	SM-14/06/06-3	2.3	23.3	32	
139	387416	4478965	SM-14/06/06-4	2.6	13.1	37	Abundant thin veins.
140	387541	4478938	SM-14/06/06-5	2.7	17.7	52	
141	387561	4478939	SM-14/06/06-6	2.5	18.1	15	To weathered to count veins Close to mineralized vein (6 m).
142	387485	4478894	SM-14/06/06-7	-1.4	10.0	Nominal	Close to mineralized vein (altered).
143	387414	4478912	SM-14/06/06-8	2.8	17.0	25	Has sandy lenses. Marbelized.
144	387439	4478859	SM-14/06/06-9	-0.3	11.6	7	
145	387439	4478846	SM-14/06/06-10	2.8	22.3	26	
146	387425	4478855	SM-14/06/06-11	1.5	16.4	20	
147	387409	4478859	SM-14/06/06-12	2.5	17.7	17	Top Elizabeth. Close mayor fault. Calc-silicate alt? White.
148	387317	4478719	SM-14/06/06-13	-3.1	13.8	10	Close to fault allows mineralization.
149	387162	4478809	SM-14/06/06-14	2.3	20.5	60	2.5 m to the E of contact w/ dike (QLP?). Thin section was made (Appendix C).
150	387064	4478847	SM-14/06/06-15	1.7	20.6	70	
151	387172	4478924	SM-14/06/06-16	2.4	19.1	24	
152	387205	4478901	SM-14/06/06-17	1.4	17.1	19	Just below a monzonite sill (50 cm -1 m). Not plotted in maps.
153	389521	4476694	SM-15/06/06-1	1.7	15.9	19	
154	386217	4478925	SM-28/06/06-1	1.7	13.8	37	
155	386196	4478938	SM-28/06/06-2	2.7	12.6	30	It has been brecciated.
156	385853	4479384	SM-13/07/06-2	3.3	8.8	17	
157	385806	4479422	SM-13/07/06-3	-1.0	1.9	11	Thick limestone bed.
158	385789	4479448	SM-13/07/06-4	2.9	8.3	22	
159	385693	4479239	SM-13/07/06-5	2.3	8.5	24	Has silica. Can't see veins (weathered).Sandy?
160	385609	4479299	SM-13/07/06-6	-1.4	1.7	ND	

161	385928	4479353	SM-14/07/06-1	2.6	23.0	9	Difficult to count veins. Near N-S fault. Coarse.
162	385975	4479414	SM-14/07/06-2	4.3	4.8	13	Near mine.
163	385975	4479414	SM-14/07/06-2 (VEIN)	4.0	21.7	NA	
164	386006	4478946	SM-15/07/06-1	2.0	9.0	38	Becciated. Bleached.
165	386052	4478806	SM-15/07/06-2	2.2	14.6	35	
166	386057	4478799	SM-15/07/06-3	1.3	13.7	21	
167	386287	4478715	SM-15/07/06-4	-2.8	10.3	13	Difficult place to count veins. Sandy?. It's bleached. White.
168	386846	4478816	SM-15/07/06-5	-6.3	15.3	24	Difficult place to count veins. Has copper. Bleached. White.
169	386674	4478701	SM-15/07/06-6 (A)	-2.7	22.1	30	White.
170	386674	4478701	SM-15/07/06-6 (B)	-0.4	23.0	30	
171			SM-07/08/06-1	1.7	10.9	ND	From drill hole SD-15 at 72 ft. Not plotted in maps.
172			SM-07/08/06-1 (White A)	0.3	10.5	NA	From drill hole SD-15 at 72 ft. Not plotted in maps.
173			SM-07/08/06-1 (White B)	0.0	11.4	NA	From drill hole SD-15 at 72 ft. Not plotted in maps.

1. Vein density was determined by counting how many veins intersected a meter long line.